UNIVERSIDADE FEDERAL DO CEARÁ

CENTRO DE CIÊNCIAS

PROGRAMA DE PÓS-GRADUAÇÃO EM QUÍMICA

FRANCISCO AFRÂNIO CUNHA

GREEN SYNTHESIS OF SILVER NANOPARTICLES: FOCUS ON MONOSACCHARIDES AND FUNGI ISOLATED FROM BRAZILIAN SOIL

FORTALEZA

2016

FRANCISCO AFRÂNIO CUNHA

GREEN SYNTHESIS OF SILVER NANOPARTICLES: FOCUS ON MONOSACCHARIDES AND FUNGI ISOLATED FROM BRAZILIAN SOIL

Tese de Doutorado apresentada à Coordenação do Curso de Pós-Graduação em Química da Universidade Federal do Ceará, como parte dos requisitos para obtenção do Título de Doutor em Química. Área de Concentração: Química.

Orientador: Prof. Dr. Pierre Basílio Almeida Fechine

FORTALEZA

2016

Dados Internacionais de Catalogação na Publicação
Universidade Federal do Ceará
Biblioteca Universitária
Gerada automaticamente pelo módulo Catalog, mediante os dados fornecidos pelo(a) autor(a)

C978g Cunha, Francisco Afrânio.
Green synthesis of silver nanoparticles : focus on monosaccharides and fungi isolated from brazilian soil / Francisco Afrânio Cunha. – 2016.
170 f. : il. color.

Tese (doutorado) – Universidade Federal do Ceará, Centro de Ciências, Programa de Pós-Graduação em Química, Fortaleza, 2016.
Orientação: Prof. Dr. Pierre Basílio Almeida Fechine.
Coorientação: Prof. Dr. Everardo Albuquerque Menezes.

1. Green synthesis. 2. Silver nanoparticles. 3. Monosaccharides. 4. Rhodotorula glutinis. 5. Rhodotorula mucilaginosa. I. Título.

CDD 540

Esta Tese foi apresentada como parte dos requisitos necessários à obtenção do Grau de Doutor em Química, área de concentração Química, outorgado pela Universidade Federal do Ceará, e em cuja Biblioteca Central encontra-se à disposição dos interessados.

Francisco Afranio Cunha

Francisco Afranio Cunha

Tese aprovada em: **18/10/2016.**

Dr. Pierre Basílio Almeida Fechine
(Orientador-UFC)

Dr. Adonay Rodrigues Loiola
(UFC)

Dr. Amauri de Paula Jardim
(UFC)

Dr. Everardo Albuquerque Menezes
(UFC)

Dr. Francisco Walber Ferreira da Silva
(UECE)

Nada, absolutamente nada, resiste ao trabalho.

(Euryclides de Jesus Zerbini)

AGRADECIMENTOS

A Deus por ter me permitido chegar até aqui e me protegeu em um mundo tão insano e violento.

À minha querida família, meus pais, minhas irmãs, que me criaram e me deram condições para que eu estudasse.

À Conceição Cunha, minha companheira de uma vida, meus esforços são por ela compreendidos e incentivados.

As minhas duas filhas Yasmin e Cecília, nas quais a alegria é contagiante.

A todos os meus amigos do Departamento de Análises Clínicas da Universidade Federal do Ceará que sempre me incentivaram, em destaque para: João Rodrigues Coelho, Lúcia Cutrim, Adalgisa Torquato, Ieda Pereira de Souza e Francisca Maria.

Ao meu Amigo, Orientador e Irmão Professor Everardo Albuquerque Menezes que desde de tempos imemoriais me incentivou a estudar e crescer pessoal e profissionalmente.

Ao meu Orientador e Amigo Professor Pierre Basílio Almeida Fechine que confiou em mim e me ajudou imensamente, sem sua colaboração esse trabalho seria infinitamente menor.

A todos os Professores do Departamento de Química e em especial aos Professores do Departamento de Física: Amauri Jardim de Paula, Odair Pastor, Emílio Castro Miguel e Josué Souza Filho, professores que me ensinaram muito e que tive o prazer de conviver nesse intervalo de tempo.

Ao meu amigo Professor Eduardo Mallman ao qual fiz uma promessa há tempos e que hoje se realiza, meu muito obrigado.

A todos os amigos e alunos que de alguma forma me ajudaram nessa empreitada, cabendo destacar: Janaina, Auberson, Bruno, Tiago, José Gadelha, e muitos outros pelos quais tenho imensa gratidão.

RESUMO

Nanopartículas de prata (AgNPs) são estruturas com tamanho até 100 nm e que exibem propriedades diferentes daquelas encontradas no material de origem. AgNPs possuem diversas aplicações tecnológicas e podem ser sintetizadas por métodos físicos, químicos e biológicos. O uso de micro-organismos, açúcares e plantas para biossíntese de AgNPs é considerado como tecnologia verde, pois não envolve substâncias químicas tóxicas. Entre os açúcares, os monossacarídeos (glicose) são promissores devido a sua disponibilidade, custos baixos e atoxicidade. Já as leveduras possuem uma grande variedade de enzimas e são fáceis de manusear. Entretanto, existem poucos trabalhos explorando a capacidade biossintética de AgNPs por leveduras. Os resíduos da produção de AgNPs, gerados por fungos, podem ser usados com finalidade catalítica, desde que suportado em matrizes poliméricas como o alginato. Os objetivos desse estudo foram usar glicose e leveduras para produzir AgNPs, caracterizar essas estruturas e avaliar as atividades antibacterianas, antifúngicas, citotóxica e catalíticas. Além disso, os resíduos gerados pelos fungos foram usados para a produção de esferas de alginato que foram utilizadas com objetivos catalíticos. A síntese de AgNPs foi realizada com glicose e duodecil sulfato de sódio (SDS) foi usado com estabilizador. As AgNPs de origem química foram associadas com o antibiótico ciprofloxacina e testadas contra *Escherichia coli*. As AgNPs elevaram a atividade da ciprofloxacina em 40%. A ação sinérgica de AgNPs e anfotericina B e nistatina foram avaliadas contra *C. parapsilosis*. AgNPs quando combinadas com anfotericina B e nistatina mostraram potente ação antifúngica e aumentaram a zona de inibição em torno dos discos antifúngicos em 222,6 e 319,3%, respectivamente. A combinação de AgNPs e anfotericina B ou Nistatina pode apresentar uma vantagem tecnológica contra fungos resistentes. Em outra vertente, duas leveduras *Rhodotorula glutinis* e *Rhodotorula mucilaginosa* foram isoladas do solo cearense e avaliadas quanto a sua capacidade de produzir AgNPs. As AgNPs foram caracterizadas pelas técnicas UV–vis, DLS, FTIR (Infra-vermelho com transformada de Fourier), XRD (difração de Raios-X), EDX, MEV (Microscopia Eletrônica de Varredura), MET (Microscopia Eletrônica de Transmissão) e MFA (Microscopia de Força Atômica). AgNPs produzidas pelas leveduras mostraram atividades antifúngicas e catalíticas. AgNPs produzidas por *R. glutinis* e *R. mucilaginosa* mediram 15,45 nm ± 7,94 e 13,70 nm ± 8,21 (média ± DP), respectivamente, quando analisada por MET. As AgNPs mostraram alta atividade catalítica na degradação de 4-nitrofenol e azul de metileno. As 35 cepas de *C. parapsilosis* mostraram grande sensibilidade as AgNPs e essas partículas também aumentaram as propriedades antifúngicas do fluconazol (42,2% *R. glutinis* e 29,7 % *R. mucilaginosa*). A atividade citotóxica das AgNPs foi detectada em concentrações acima daquelas que exerceram atividade biológica, mostrando a segurança dessas partículas. As esferas de alginato produzidas com AgNPs de origem fúngica foram capazes de degradar o 4-nitrofenol e o antibiótico ceftazidima eliminando sua atividade microbiológica. Finalmente, duas leveduras com habilidade de produzir AgNPs foram isoladas do solo brasileiro (Ceará) e apresentaram multifuncionalidades que podem representar uma alternativa tecnológica com potenciais aplicações em diferentes áreas. O uso de monossacarídeos e leveduras na síntese de AgNPs pode representar uma alternativa a síntese convencional e reduzir o impacto ambiental que essas substâncias causam.

Palavras-Chaves: Síntese Verde; Nanopartículas de prata; Monossacarídeos; *Rhodotorula glutinis*; *Rhodotorula mucilaginosa*; atividade catalítica; atividade antifúngica.

ABSTRACT

Silver nanoparticles (AgNPs) are structures with sizes up to 100 nm and exhibit properties that are different from those found in the bulk material. AgNPs are structures with several technological applications and can be synthetized by chemical, physical and biological methods. Use of microorganisms, sugars, and plants for the biosynthesis of silver nanoparticles is considered a green technology, as it does not involve any harmful chemicals. Among the sugars, monosaccharides (glucose) are promising because they are readily available, inexpensive, and non-toxic. Yeasts have a wide enzymatic range and are easy to handle. However, there are few reports of yeasts with biosynthetic ability to produce stable AgNPs. The waste generated by fungi in AgNP production can be used for catalytic purposes, provided that it is supported on polymer matrices, such as alginate. The objectives of this study were to use glucose and yeasts to produce AgNPs, characterize these structures, and evaluate their antibacterial, antifungal, cytotoxic and catalytic activities. Additionally the waste generated by fungi was used for the production of alginate beads that were used for catalytic purposes. The synthesis of AgNPs was performed with glucose, and sodium dodecyl sulfate (SDS) was used as a stabilizer. The AgNPs of synthetic origin were associated with the antibiotic ciprofloxacin and tested against *Escherichia coli*. The AgNPs increased the action of ciprofloxacin by 40%. The synergistic action of AgNPs produced with amphotericin B and nystatin against *C. parapsilosis* was evaluated. *Candida spp.* were isolated from candidemia of patients admitted to public hospitals in Ceará. AgNPs, when combined with amphotericin B and nystatin, showed potent antifungal activity and increased the zone around the antifungal disk by 222.6 and 319.3%, respectively. The combination of substances AgNPs and amphotericin B or nystatin can potentiate their effects, therefore showing a large zone of growth inhibition. Two yeasts – *Rhodotorula glutinis* and *Rhodotorula mucilaginosa* – were isolated from Brazilian soil and their ability to produce AgNPs was evaluated. AgNPs were characterized by UV–vis, DLS, FTIR, XRD, EDX, SEM, TEM and AFM. AgNPs produced by yeasts showed catalytic and antifungal activities. The AgNPs produced by *R. glutinis* and *R. mucilaginosa* measured 15.45 nm ± 7.94 and 13.70 nm ± 8.21 (average ± SD), respectively, when analyzed by TEM. The AgNPs showed high catalytic capacity in the degradation of 4-nitrophenol and methylene blue. *C. parapsilosis* showed high sensitivity to AgNPs and also enhanced the antifungal property of fluconazole (42.2% for *R. glutinis* and 29.7 % for *R. mucilaginosa*). Cytotoxic activity of AgNPs was above the concentrations that exerted biological activity, showing the safety of these particles. The alginate spheres produced with these AgNPs of fungal origin were able to degrade 4-nitrophenol and antibiotic ceftazidime, eliminating microbiological action of ceftazidime. Finally, two yeasts isolated from brazilian soil (Ceará), with the ability to produce AgNPs, were described. These particles (AgNPs) showed multifunctionality and can represent a technological alternative in many different areas with potential applications. The use of monosaccharides and yeasts for AgNP synthesis may be an alternative to orthodox synthesis and reduce the environmental impact that these substances cause.

Keywords: Green synthesis; Silver nanoparticles; Monosaccharides; *Rhodotorula glutinis*; *Rhodotorula mucilaginosa*; catalytic activity; antifungal activity.

FIGURES

CHAPTER ONE

SUPPORTING INFORMATION CHAPTER ONE

CHAPTER TWO

SUPPORTING INFORMATION CHAPTER TWO

CHAPTER THREE

SUPPORTING INFORMATION CHAPTER THREE

CHAPTER FOUR

SUPPORTING INFORMATION CHAPTER FOUR

CHAPTER FIVE

SUPPORTING INFORMATION CHAPTER FIVE

TABLES

CHAPTER ONE

CHAPTER TWO

CHAPTER THREE

CHAPTER FOUR

ACRONYMS AND ABBREVIATIONS

AFM= Atomic Force Microscopy
AgNP=Rm= Silver nanoparticles synthesized by *Rhodotorulla mucilaginosa*
AgNP-G= Silver nanoparticles synthesized based on glucose
AgNP-R= Silver nanoparticles synthesized based on ribose
AgNP-Rg= Silver nanoparticles synthesized by *Rhodotorulla glutinis*
AgNPs= Silver nanoparticles
C. parapsilosis= Candida parapsilosis
C. tropicalis = Candida tropicalis
DLS= Dynamic light scattering
EDX= Energy-dispersive X-ray spectroscopy
FEG= Field-emission gun
FT-IR= Fourier Transform Infrared Spectroscopy
PDI- Polydispersity index
Rg= *Rhodotorulla glutinis*
Rm= *Rhodotorulla mucilaginosa*
SDS= Sodium dodecyl sulfate
SEM= Scanning Electron Microscopy
TEM= Transmission Eletronic Microscopy
XRPD= X-ray powder diffraction

SUMMARY

CHAPTER ONE

Introduction

ABSTRACT

Nanotechnology is a rising science that studies the properties of materials with sizes ranging from 1 to 100 nm. Nanoparticles have several applications, among which we can highlight medical and industrial applications. Metal nanoparticles – especially gold, silver, platinum, zinc and copper – are the most widely studied, and new protocols for obtaining nanoparticles have been developed to improve and enhance the synthesis of these structures. Chemical, physical and biological methods are described. Some of these methods can be considered as green methods, because aggression to the environment and human health is minimal. Among these particles, silver nanoparticles (AgNPs) are the ones that exhibit well documented antimicrobial activity against fungi, bacteria and viruses. The green synthesis of AgNPs is a current issue, and living organisms are being used in the production thereof. It is noteworthy that fungi stand out due to the synthesis of AgNPs quickly, easily and cheaply. However, with fungal diversity, the number of test organisms is still small. In this Dissertation, we describe biological and chemical processes considered as green processes, whereby we use fungi and sugars. The AgNPs produced are characterized and their various applications are evaluated.

Keywords: Nanotecnology; Metallic nanoparticles; Silver nanoparticles.

INTRODUCTION

The last two decades have witnessed breakthroughs in the development of nanoparticles, especially metal nanoparticles. With the emergence of this new material, it has been necessary to find techniques, instruments, obtainment protocols, and means of safe disposal for these structures. All such knowledge has given rise to a new scientific field: Nanotechnology. This science involves knowledge of several others, such as physics, mathematics, biology, engineering, and materials science, among others. Nanotechnology researches particle sizes ranging from 1 to 100 nm and that have properties different from the source material (CHEN AND SCHLUESENER, 2008; HULKOTI et al., 2014). In FIGURE 1 we can see various structures ranging from 10^{-1} nm to 10^{8} nm, separated by size. The nanoparticles represented here and highlighted are equivalent to the size of various cellular components, such as proteins, DNA and organelles.

FIGURE 1. Different sizes of materials in nanometers, and highlighted the size of nanoparticles (1-100 nm).

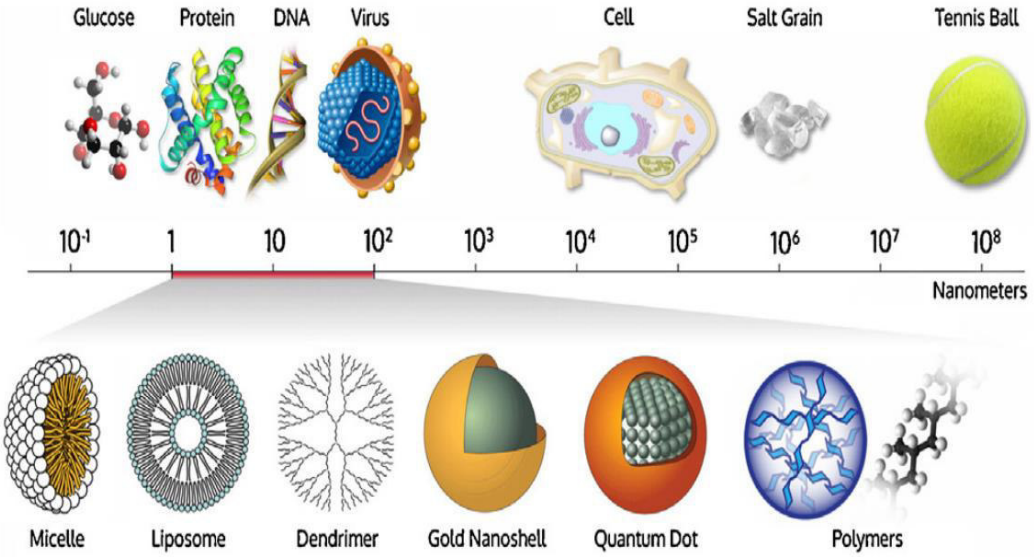

Source: Reprinted with permission from HULKOTI et al., 2014.

These new materials developed and studied by nanotechnology may provide solutions for important areas such as: Medicine (PELGRIFT, FRIEDMAN 2013), catalysis (DHAKSHINAMOORTHY, GARCIA 2012), solar energy production (LINIC et al., 2011; THOMANN et al. 2011) and water treatment (LI et al., 2008; QU et al., 2013).

Metal nanoparticles are the most commonly studied, and the most widely known ones are gold (Au), silver (Ag), copper (Cu), zinc (Zn), and platinum (Pt) nanoparticles (ARVIZO et al., 2008; HAU et al., 2008; JIA et al., 2008; RUPARELIA et al., 2007). A peculiar property of metal nanoparticles is Localized Surface Plasmon Resonance (LSPR). This characteristic matches the oscillation of the electric field on the surface of the nanoparticles and is influenced by the constitution of the material, the geometry of the nanoparticle, and the environment in which it is immersed (DYKMAN, KHLEBTSOV, 2012; WILLETS, VAN DUYNE, 2007). We can observe this peculiar activity in FIGURE 2 (DYKMAN, KHLEBTSOV, 2012; WILLETS, VAN DUYNE, 2007).

Metal nanoparticles have been the subject of various studies. The biological activities of these structures may revolutionize certain fields such as pharmacology and cancerology (EL-SAYED, HUANG, EL-SAYED, 2005). The various biological utilities can be synthesized in FIGURE 3 (SAPSFORD et al., 2011). These particles may serve as a

mainstay for drugs, proteins, hormones and radiological contrasts that can help fight various diseases, including diseases caused by fungi, viruses and bacteria.

SILVER NANOPARTICLES (AgNPs)

Of the metal nanoparticles, those made of silver (AgNPs) have antimicrobial and catalytic properties (GAJBHIYE et al., 2009; NARAYANAN et al., 2013). The antimicrobial activity of silver has been known since ancient times, and this activity is maintained in AgNPs. Moreover, AgNPs have been described as effective catalysts with applications in the pharmaceutical and chemical industries (BARUAH et al., 2013; JIANG, LIU, SUN, 2005; SARINA, WACLAWIK, ZHU, 2013; ZHANG, TANG, VLAHOVIC, 2016). Catalysis of aromatic compounds and antibiotics are recent examples of the versatility of these new compounds (DU et al., 2015; JUNEJO, GÜNER, BAYKAL, 2014). To meet this demand for AgNPs, methods of synthesis have to be developed and optimized.

FIGURE 2: Localized Surface Plasmon Ressonance (LSPR).

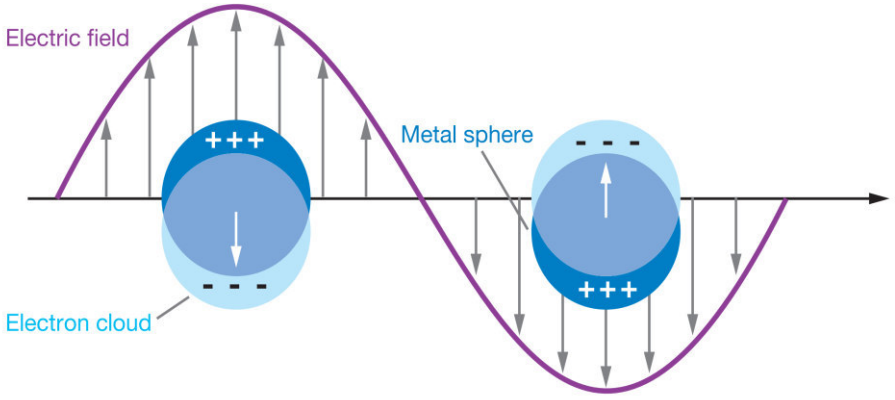

Source: Reprinted with permission from WILLETS, VAN DUYNE, 2007.

FIGURE 3- Multifarious activities of metal nanoparticles.

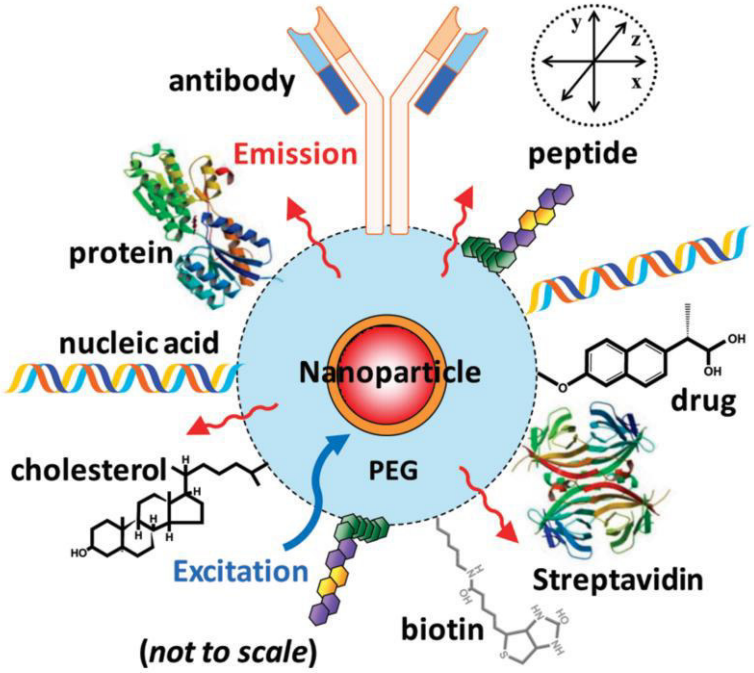

Source: Reprinted with permission from SAPSFORD et al., 2011.

SYNTHESIS OF AgNPs

Synthesis of AgNPs can be done by various processes: chemical, physical and biological. Chemical processes use reducing agents such as sodium borohydride ($NaBH_4$), hydrazine (N_2H_4), reducing sugars ($C_{n(}H_2O)_n$) and stabilizers, which can be: citrate ($Na_3C_6H_5O_7$), sodium dodecyl sulfate (SDS) ($NaC_{12}H_{25}SO_4$) and others (CUNHA et al., 2016; MALLMANN et al., 2015) (FIGURE S1 Supporting Information Chapter 1). Among AgNP production processes are those that are considered as green; these include methods in which three principles are important: (1) selection of solvent (the most appropriate one is water); (2) selection of a reducing agent that does not harm the environment; and (3) the AgNP stabilizing agents must not show any toxicity (SHARMA et al., 2009). Many other requirements are necessary in order for the method to be considered green, but those mentioned above are the most relevant. Synthesis using sugars is the AgNP obtainment process considered as green, because it meets these three basic principles and waste generation is minimal. Various sugars have been used successfully in AgNP synthesis, of which we can highlight the following: glucose, ribose, fructose, sorbose, xylose, galactose,

starch, maltose, sucrose, and honey (FILLIPO et al., 2010; PETTEGREW et al., 2014; PHILLIP, 2010; VIGNESHWARAN et al., 2005; WANG et al., 2005). However, the use of SDS as a stabilizer of these AgNPs is still under-reported in the literature and the activity of these AgNPs against bacteria and fungi has been scarcely explored (PANÁČEK et al., 2009).

Physical processes for the synthesizing AgNPs, in some cases, may also be considered as green. However, these processes require specialized equipment and trained personnel, and the implementation of such processes usually involves the use of a considerable amount of electricity (MAFUNÉ et al. 2000; THUC et al., 2016).

Another recent development is AgNP synthesis using biological structures, in this case bacteria, plants, fungi and yeasts are used (HULKOTI, TARANATH, 2014; MASHWANI et al., 2016). This method is currently expanding; as it is a green method, it does not use toxic reagents and the waste products generated are biodegradable. A summary of the main mechanisms of synthesis is shown in FIGURE 4.

In mechanisms A, B, C and D of FIGURE 4, the general procedures are shown, which utilize the noble metal salts (Ag, Au, Pt), the reducing agent, and sometimes a stabilizing agent (SDS, citrate) (DERAEDT et al., 2014; ZHANG et al., 2011). In mechanism E, we describe the process used in this Dissertation in which monosaccharides (glucose) are used as a reducing agent and an ionic surfactant (SDS) is used as a stabilizer. This mechanism is described in Chapter 2 and Chapter 3. In Mechanism F, yeast (fungi) extracts are used (*Rhodotorula glutinis* and *Rhodotorula mucilaginosa*) in the reduction and stabilization of the nanoparticles. This mechanism is described in Chapter 4. Both processes E and F are considered green.

FIGURE 4: Representative chemical and biological reduction, schematics for nanoparticle synthesis.

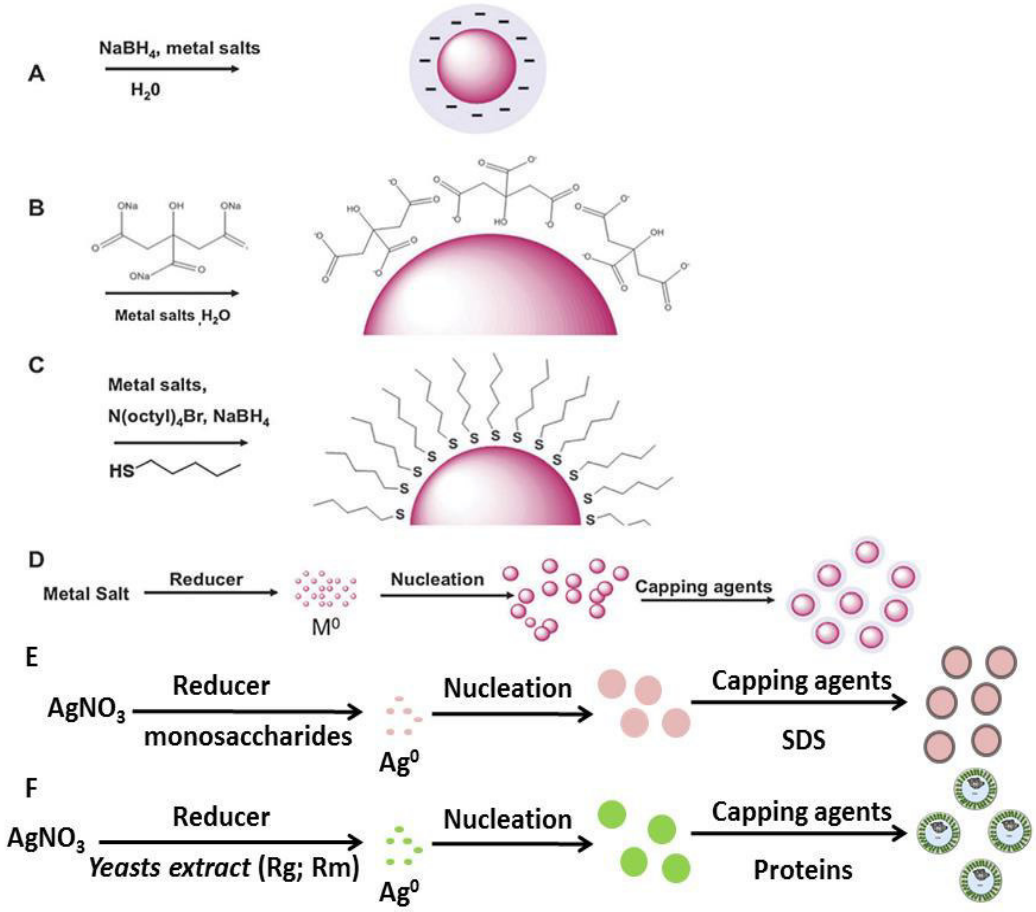

Source: Reprinted with permission from ARVIZO et al., 2012, with modifications.

We have on this planet a wide variety of fungal organisms, around 5.1 million species, and only 70,000 have been adequately described. Of these, around 100 have been used in the production of AgNPs (BLACKWELL, 2011). The usefulness of these AgNPs generated by fungi is multivariate, but the antimicrobial activity is noteworthy. In Table 1, we seek to describe the main fungi used in the production of AgNPs in a 13-year time span. One can see that Table 1 was organized taking into account the species of fungus, and filamentous fungi are generally predominant. Rare AgNP-producing yeasts are also described.

Table 1- Silver nanoparticles produced by fungi.

Fungi	Source	AgNPs size (nm)	Shape	Activity	Reference
Agaricus bisporus	ND	8-20	spherical	antitumor	EL-SONBATY 2013
Alternaria alternata	collection	20-60	spherical	antimicrobial	GAJBHIYE et al., 2009
Alternaria solani	plant	5-20		antimicrobial	DEVI et al,. 2014
Arthroderma fulvum	soil	13-18	spherical	antifungal	XUE, et al. 2016
Aspergillus clavatus	stem tissues	10-25	spherical or hexagonal	antimicrobial	VERMA et al., 2010
Aspergillus clavatus	soil	ND	ND	antimicrobial	SARAVANANA, NANDA, 2010
Aspergillus flavus	soil	10-35	spherical	ND	JAIN et al., 2011
Aspergillus flavus	collection	7.3-10.5	spherical	ND	VIGNESHWARAN et al., 2007
Aspergillus flavus	collection	5-30	spherical	antimicrobial	NAQVI et al., 2013
Aspergillus flavus, Trichoderma gamsii, Talaromyces flavus, Aspergillus oryzae	marine sediment	20–60	spherical	anti-cancer, antimicrobial. antioxidant	ANAND et al., 2015
Aspergillus fumigatus	collection	5-25	spherical	ND	BHAINSA, SOUZA, 2006.
Aspergillus fumigatus	compost	15-45	spherical	ND	ALANI et al., 2012
Aspergillus orizae, Penicillium chrysogenhum	collection	70-100.6	spherical	antimicrobial	PEREIRA et al., 2014
Aspergillus niger	soil	20	spherical	antimicrobial	GADE et al., 2008
Aspergillus tamarii	enviroment	25-50	spherical	ND	KUMAR *et al*., 2012
Aspergillus tamarii PFL2, Aspergillus niger PFR6, Penicllium ochrochloron PFR8	plant	3.5, 8.7, 7.7	spherical	ND	DEVI, JOSHI, 2015
Aspergillus terreus SP5, Paecilomyces lilacinus SF1 and Fusarium sp. MP5	soil	5-50	distinct shape	antimicrobial	DEVI, JOSHI, 2012
Aspergillus terreus	soil	1-20	spherical	antimicrobial	LI et al., 2012
Cladosporium cladosporioides	collection	10-100	spherical	ND	BALAJI et al., 2009
Cochliobolus lunatus	ND	3-21	spherical	larvicide	SALUNKHE et al., 2011b
Cordyceps militaris	collection	15	spherical	antimicrobial	
Cordyceps sinensis	ND	50	spherical	antimicrobial cytotoxicity	CHEN et al., 2016
Coriolus versicolor	soil	10	spherical	ND	SANGUI, VERMA 2009.
Cylindrocladium floridanum	collection	7.7-58.3	spherical	catalytic	NARAYANAN et al., 2013
Chrysosporium keratinophilum, Verticillium lecanii, and Fusarium oxysporum	collection	24–51 20–50 20–40	spherical	larvicide	SONI, PRAKASH 2012
Chrysosporium tropicum	collection	20-50	spherical	larvicide	SONI, PRAKASH 2012b
Cryphonectria sp	stems chestnut tree	30-70	ND	antimicrobial	DAR et al., 2013
Epicoccum nigrum	collection	10–15	spherical	antimicrobial	QUIAN et al., 2013
Fusarium oxysporum	collection	20–50	spherical	ND	DÚRAN et al., 2005
Fusarium oxysporum	collection		spherical	ND	SUNITA et al., 2013

Fungi	Source	AgNPs size (nm)	Shape	Activity	Reference
Fusarium oxysporum	banana fruit	10–20	spherical	ND	BIRLA et al., 2013
Fusarium oxysporum	ND	5–50	spherical	ND	AHMAD et al., 2003
Fusarium semitectum	collection	10-60	spherical	ND	BASAVARAJA et al., 2008.
Fusarium solani	garlic	5-35	spherical	ND	INGLE et al., 2009.
Fusarium solani	collection	3-8	ND	antimicrobial	EL-RAFIE et al., 2010.
Guignardia mangiferae	plant	5–30	spherical	antimicrobial, cytotoxicity	BALAKUMARAN et al., 2015
Isaria fumosorosea	soil	51.31-111.02	spherical	larvicide	BANU, BALASUBRAMANIAN, 2014.
Metarhizium anisopliae	collection	28–38	rod-like	larvicide	AMERASAN et al., 2016
Neurospora crassa	ND	11	spherical	ND	CASTRO-LONGORIA et al., 2011
Penicillium sp	environment	10-100	spherical	ND	MALISZEWSKA et al., 2008
Penicillium brevicompactum	collection	58.35	ND	ND	SHALIGRAM et al., 2009
Penicillium diversum	collection	5-45	spherical	antimicrobial	GANACHARI et al., 2012
Penicillium funiculosum	plant	5-10	spherical	antimicrobial	DEVI et al,. 2014
Penicillium oxalicum	ND	4-6	spherical	catalytic	DU et al., 2015
Pestalotia sp	leaves	10-40	spherical	antimicrobial	RAHEMAN et al., 2011
Phoma sp	collection	71.06 ± 3.46	ND	ND	CHEN et al., 2003
Phoma glomerata	collection	19	spherical	ND	GADE et al., 2014
Phoma glomerata	collection	60–80	spherical	antimicrobial	BIRLA et al., 2009
Phaenerochaete chrysosporium	collection	50-200	pyramidal	ND	VIGNESHWARAN et al., 2006.
Pleurotus djamor var. roseus	forest	5-50	spherical	anti-cancer	RAMAN et al., 2015
Pleurotus florida	forest	15-25	spherical	antimicrobial	BHAT et al., 2012
Pycnoporus sanguineus	forest	52.8-103.3	spherical	antimicrobial	CHAN, DON 2013.
Puccinia graminis	soil	30-120	spherical, oval	ND	KIRTHI et al., 2012
Rhizopus stolonifer	soil	3-20	spherical	antimicrobial	BANU et al., 2011
Schizophyllum commune	collection	54-99	spherical	antimicrobial. cytotoxicity	ARUN et al., 2015
Trichoderma asperellum	ND	13-18	ND	ND	MUKHERJEE et al., 2008.
Trichoderma reesei	ND	5-50	spherical	ND	VAHABI et al., 2011
Trichoderma harzianum	collection	51.1	spherical	antibacterial	AHLUWALIA et al., 2014
Tricholoma matsutake	forest	10-20	spherical	antimicrobial	ANTHONY et al., *2014*
Yarrowia lipolytica	collection	15	spherical	antimicrobial, antibiofilm	APTE, et al., 2013
Rhodotorula glutinis	soil	7.6-23	spherical	antimicrobial, catalytic cytotoxicity	***This work***
Rhodotorula mucilaginosa	soil	5.5-22	spherical	antimicrobial, catalytic cytotoxicity	***This work***

Notes: ND- not determined.

Source : Author

Some fungi are repeated several times, such as *Fusarium oxysporum* (SUNITA et al., 2013). This fungus was one of the first ones to produce AgNPs, which were characterized, and the process of extracellular formation of AgNPs began to be understood (AHMAD et al., 2003). Brazil is a pioneer in this type of synthesis, where *F. oxysporum* has been used successfully in the production of extracellular AgNPs for roughly 10 years (DURÁN et al., 2005).

This Dissertation was divided into six independent chapters, in which the central theme was silver nanoparticles, their properties and practical applications. In Chapter 1, the general aspects of the properties of metal nanoparticles were discussed, as well as synthesis methods and the main AgNP-producing fungi. In chapter 2, AgNP synthesis by monosaccharides, characterization of the AgNPs, and use of these nanoparticles against bacteria were addressed. In Chapter 3, use of AgNPs associated with antifungals to combat pathogenic fungi was discussed. In Chapter 4, two fungi isolated and identified in Ceará, Brazil were challenged to produce AgNPs; these nanoparticles were characterized and several properties and applications were explored. In Chapter 5, AgNP solutions produced by the fungi identified in the previous chapter were used to produce alginate spheres; with these AgNPs impregnated, such spheres were characterized by physical–chemical techniques and their catalytic capacity was put to the test in the degradation of pollutants and antibiotics. In Chapter 6, the final chapter, the closing considerations are addressed, as well as the directions that the study indicates and possible lines of research that may arise from this Dissertation.

REFERENCES

1. AHLUWALIA, V. *et al*. Green synthesis of silver nanoparticles by *Trichoderma harzianum* and their bio-efficacy evaluation against *Staphylococcus aureus* and *Klebsiella pneumoniae*. **Industrial Crops and Products**, v. 55, p. 202–206, 2014. Disponível em: http://linkinghub.elsevier.com/retrieve/pii/S0926669014000338 Acesso em: 2 jul. 2016.
2. AHMAD, A. *et al*. Extracellular biosynthesis of silver nanoparticles using the fungus *Fusarium oxysporum*. **Colloids and Surfaces B: Biointerfaces**, v. 28, n. 4, p. 313–318, 2003. Disponível em: http://linkinghub.elsevier.com/retrieve/pii/S0927776502001741 . Acesso em: 3 ago. 2016.

3. ALANI, F.; MOO-YOUNG, M.; ANDERSON, W. Biosynthesis of silver nanoparticles by a new strain of *Streptomyces* sp. compared with *Aspergillus fumigatus*. **World Journal of Microbiology and Biotechnology**, v. 28, n. 3, p. 1081–1086, 2012. Disponível em: http://link.springer.com/10.1007/s11274-011-0906-0 . Acesso em: 1 jul. 2016.
4. AMERASAN, D. *et al*. Myco-synthesis of silver nanoparticles using *Metarhizium anisopliae* against the rural malaria vector *Anopheles culicifacies* Giles (Diptera: Culicidae). **Journal of Pest Science**, 2016. Disponível em: http://link.springer.com/10.1007/s10340-015-0675-x . Acesso em: 1 jul. 2016.
5. ANAND, B. G. *et al*. Biosynthesis of silver nano-particles by marine sediment fungi for a dose dependent cytotoxicity against HEp2 cell lines. **Biocatalysis and Agricultural Biotechnology**, v. 4, n. 2, p. 1–8, 2015. Disponível em: http://linkinghub.elsevier.com/retrieve/pii/S1878818115000031 Acesso em: 1 jul. 2016..
6. ANTHONY, K. J. P. *et al*. Synthesis of silver nanoparticles using pine mushroom extract: A potential antimicrobial agent against *E. coli* and *B. subtilis*. **Journal of Industrial and Engineering Chemistry**, v. 20, n. 4, p. 2325–2331, 2014. Disponível em: http://linkinghub.elsevier.com/retrieve/pii/S1226086X13004887 Acesso em: 1 abr. 2016.
7. APTE, M. *et al*. Psychrotrophic yeast *Yarrowia lipolytica* NCYC 789 mediates the synthesis of antimicrobial silver nanoparticles via cell-associated melanin. **AMB Express**, v. 3, n. 1, p. 32, 2013. Disponível em: http://www.pubmedcentral.nih.gov/articlerender.fcgi?artid=3702394&tool=pmcentrez&rendertype=abstract . Acesso em: 1 dez. 2014.
8. ARUN, G.; EYINI, M.; GUNASEKARAN, P. Green synthesis of silver nanoparticles using the mushroom fungus *Schizophyllum commune* and its biomedical applications. **Biotechnology and Bioprocess Engineering**, v. 19, n. 6, p. 1083–1090, 2014. Disponível em: http://link.springer.com/10.1007/s12257-014-0071-z . Acesso em: 3 abr. 2016
9. ARVIZO, R.R. *et al*. Intrinsic therapeutic applications of noble metal nanoparticles: past, present and future. **Chem Soc Rev**, v. 41, n. 7, p. 2943–2970, 2012. Disponível em: http://www.ncbi.nlm.nih.gov/pubmed/22388295 . Acesso em: 4 abr. 2015

10. BAFFOU, G.; QUIDANT, R. Nanoplasmonics for chemistry. **Chemical Society reviews**, v. 43, n. 11, p. 3898–907, 2014. Disponível em: http://www.ncbi.nlm.nih.gov/pubmed/24549257 . Acesso em: 12 dez. 2015
11. BALAJI, D. S. *et al*. Extracellular biosynthesis of functionalized silver nanoparticles by strains of *Cladosporium cladosporioides* fungus. **Colloids and surfaces. B, Biointerfaces**, v. 68, n. 1, p. 88–92, 2009. Disponível em: http://www.ncbi.nlm.nih.gov/pubmed/18995994 . Acesso em: 29 nov. 2014.
12. BALAKUMARAN, M.D.; RAMACHANDRAN, R.; KALAICHELVAN, P.T. Exploitation of endophytic fungus, *Guignardia mangiferae* for extracellular synthesis of silver nanoparticles and their in vitro biological activities. **Microbiological Research**, v. 178, p. 9–17, 2015. Disponível em: http://linkinghub.elsevier.com/retrieve/pii/S0944501315001068 . Acesso em: 5 jan. 2016
13. BANU, A.; RATHOD, V.; RANGANATH, E. Silver nanoparticle production by *Rhizopus stolonifer* and its antibacterial activity against extended spectrum β-lactamase producing (ESBL) strains of *Enterobacteriaceae*. **Materials Research Bulletin**, v. 46, n. 9, p. 1417–1423, 2011. Disponível em: http://linkinghub.elsevier.com/retrieve/pii/S0025540811002108 . Acesso em: 1 abr. 2016
14. BANU, A.N.; BALASUBRAMANIAN, C. Optimization and synthesis of silver nanoparticles using *Isaria fumosorosea* against human vector mosquitoes. **Parasitology research**, v. 113, n. 10, p. 3843–51, 2014. Disponível em: http://www.ncbi.nlm.nih.gov/pubmed/25085201 . Acesso em: 29 nov. 2015.
15. BARUAH, B. *et al*. Facile Synthesis of Silver Nanoparticles Stabilized by Cationic Polynorbornenes and Their Catalytic Activity in 4-Nitrophenol Reduction. **Langmuir**, v. 29, n. 13, p. 4225–4234, 2013. Disponível em: http://pubs.acs.org/doi/abs/10.1021/la305068p .Acesso em: 11 ago. 2016.
16. BASAVARAJA, S. *et al*. Extracellular biosynthesis of silver nanoparticles using the fungus *Fusarium semitectum*. **Materials Research Bulletin**, v. 43, n. 5, p. 1164–1170, 2008. Disponível em: http://linkinghub.elsevier.com/retrieve/pii/S0025540807002358 . Acesso em: 29 nov. 2014.
17. BHAINSA, K. C; D'SOUZA, S. F. Extracellular biosynthesis of silver nanoparticles using the fungus *Aspergillus fumigatus*. **Colloids and surfaces. B, Biointerfaces**,

v. 47, n. 2, p. 160–4, 2006. Disponível em: http://www.ncbi.nlm.nih.gov/pubmed/16420977 . Acesso em: 22 nov. 2014.

18. BHAT, R. *et al*. Photo-irradiated biosynthesis of silver nanoparticles using edible mushroom *Pleurotus florida* and their antibacterial activity studies. **Bioinorganic chemistry and applications**, v. 2011, p. 650979, 2011. Disponível em:http://www.pubmedcentral.nih.gov/articlerender.fcgi?artid=3235432&tool=pmcentrez&rendertype=abstract . Acesso em: 29 nov. 2014.
19. BIRLA, S. S. *et al*. Fabrication of silver nanoparticles by *Phoma glomerata* and its combined effect against *Escherichia coli*, *Pseudomonas aeruginosa* and *Staphylococcus aureus*. **Letters in applied microbiology**, v. 48, n. 2, p. 173–9, 2009. Disponível em: http://www.ncbi.nlm.nih.gov/pubmed/19141039 . Acesso em: 28 nov. 2014.
20. BIRLA, S. S. *et al*. Rapid synthesis of silver nanoparticles from Fusarium oxysporum by optimizing physicocultural conditions. **The Scientific World Journal**, v. 2013, p. 796018, 2013. Disponível em: http://www.pubmedcentral.nih.gov/articlerender.fcgi?artid=3810422&tool=pmcentrez&rendertype=abstract . Acesso em: 17 jun. 2015
21. BLACKWELL, M. The Fungi: 1, 2, 3 ... 5.1 million species? **American Journal of Botany**, v. 98, n. 3, p. 426–438, 2011. Disponível em: http://www.amjbot.org/cgi/doi/10.3732/ajb.1000298 . Acesso em: 7 fev. 2014.
22. CASTRO-LONGORIA, E; VILCHIS-NESTOR, A. R; AVALOS-BORJA, M. Biosynthesis of silver, gold and bimetallic nanoparticles using the filamentous fungus *Neurospora crassa*. **Colloids and surfaces. B, Biointerfaces**, v. 83, n. 1, p. 42–8, 2011. Disponível em: http://www.ncbi.nlm.nih.gov/pubmed/21087843 . Acesso em: 22 nov. 2014.
23. CHAN, Y. S; MAT DON, M. Biosynthesis and structural characterization of Ag nanoparticles from white rot fungi. **Materials Science and Engineering: C**, v. 33, n. 1, p. 282–288, 2013. Disponível em: http://linkinghub.elsevier.com/retrieve/pii/S0928493112004183 . Acesso em: 27 nov. 2013.
24. CHEN, J. C.; LIN, Z. H.; MA, X. X. Evidence of the production of silver nanoparticles via pretreatment of *Phoma* sp.3.2883 with silver nitrate. **Letters in Applied Microbiology**, v. 37, n. 2, p. 105–108, 2003.. Disponível em: http://doi.wiley.com/10.1046/j.1472-765X.2003.01348.x . Acesso em: 28 nov. 2013.

25. CHEN, X.; SCHLUESENER, H.J. Nanosilver: A nanoproduct in medical application. **Toxicology Letters**, v. 176, n. 1, p. 1–12, 2008. Disponível em: http://linkinghub.elsevier.com/retrieve/pii/S0378427407009769 . Acesso em: 29 out. 2013.
26. CHEN, X; YAN, J-K; WU, J-Y. Characterization and antibacterial activity of silver nanoparticles prepared with a fungal exopolysaccharide in water. **Food Hydrocolloids**, v. 53, n. 1, p. 69-74, 2016. Disponível em: http://linkinghub.elsevier.com/retrieve/pii/S0268005X14004743 . Acesso em: 1 jul. 2016.
27. CUNHA, F. A. *et al*. Silver nanoparticles-disk diffusion test against *Escherichia coli* isolates. **Revista do Instituto de Medicina Tropical de São Paulo**, v. 58, n. 1, p. 2–4, 2016. Disponível em: http://www.imt.usp.br/wp-content/uploads/revista/vol58/Trab73 .pdf Acesso em: 2 ago. 2016.
28. DAR, M. A.; INGLE, A.; RAI, M. Enhanced antimicrobial activity of silver nanoparticles synthesized by *Cryphonectria* sp. evaluated singly and in combination with antibiotics. **Nanomedicine: Nanotechnology, Biology and Medicine**, v. 9, n. 1, p. 105–110, 2013. Disponível em: http://linkinghub.elsevier.com/retrieve/pii/S1549963412001803 . Acesso em: 27 nov. 2014.
29. DERAEDT, C. *et al*. Sodium borohydride stabilizes very active gold nanoparticle catalysts. **Chem. Commun.**, v. 50, n. 91, p. 14194–14196, 2014. Disponível em: http://www.ncbi.nlm.nih.gov/pubmed/25283248 . Acesso em: 2 ago. 2016.
30. DEVI, L. S.; BAREH, D. A.; JOSHI, S. R. Studies on Biosynthesis of Antimicrobial Silver Nanoparticles Using Endophytic Fungi Isolated from the Ethno-medicinal Plant *Gloriosa superba* L. **Proceedings of the National Academy of Sciences, India Section B: Biological Sciences**, v. 84, n. 4, p. 1091–1099, 2014. Disponível em: http://link.springer.com/10.1007/s40011-013-0185-7 . Acesso em: 29 nov. 2015.
31. DEVI, L. S.; JOSHI, S. R. Antimicrobial and synergistic effects of silver nanoparticles synthesized using: Soil fungi of high altitudes of Eastern Himalaya. **Mycobiology**, v. 40, n. 1, p. 27–34, 2012. Disponível em: http://www.mycobiology.or.kr/DOIx.php?id=10.5941/MYCO.2012.40.1.027 Acesso em: 29 out. 2013.
32. DEVI, L. S.; JOSHI, S. R. Ultrastructures of silver nanoparticles biosynthesized using endophytic fungi. **Journal of Microscopy and Ultrastructure**, v. 3, n. 1, p. 29–37,

2015. Disponível em: http://www.sciencedirect.com/science/article/pii/S2213879X14000777 . Acesso em: 2 jul. 2016.

33. DHAKSHINAMOORTHY, A; GARCIA, H. Catalysis by metal nanoparticles embedded on metal–organic frameworks. **Chemical Society Reviews**, v. 41, n. 15, p. 5262, 2012. Disponível em: http://xlink.rsc.org/?DOI=c2cs35047e . Acesso em: 2 jul. 2016.
34. DU, L. *et al*. Synthesis of small silver nanoparticles under light radiation by fungus *Penicillium oxalicum* and its application for the catalytic reduction of methylene blue. **Materials Chemistry and Physics**, v. 160, p. 40–47, 2015. Disponível em: http://linkinghub.elsevier.com/retrieve/pii/S0254058415300109 . Acesso em: 29 out. 2013.
35. DURÁN, N. *et al*. Mechanistic aspects of biosynthesis of silver nanoparticles by several *Fusarium oxysporum* strains. **Journal of nanobiotechnology**, v. 3, p. 8, 2005. Disponível em: http://www.pubmedcentral.nih.gov/articlerender.fcgi?artid=1180851&tool=pmcentrez&rendertype=abstract . Acesso em: 21 nov. 2014.
36. DYKMAN, L; KHLEBTSOV, N. Gold nanoparticles in biomedical applications: recent advances and perspectives. **Chem. Soc. Rev.**, v. 41, n. 6, p. 2256–2282, 2012. Disponível em: http://www.ncbi.nlm.nih.gov/pubmed/22130549 . Acesso em: 29 out. 2013.
37. EL-RAFIE, M.H. *et al*. Antimicrobial effect of silver nanoparticles produced by fungal process on cotton fabrics. **Carbohydrate Polymers**, v. 80, n. 3, p. 779–782, 2010. Disponível em: http://www.sciencedirect.com/science/article/pii/S0144861709007334 . Acesso em: 29 set. 2013.
38. EL-SAYED, I. H.; HUANG, X.; EL-SAYED, M. A. Surface Plasmon Resonance Scattering and Absorption of anti-EGFR Antibody Conjugated Gold Nanoparticles in Cancer Diagnostics: Applications in Oral Cancer. **Nano Letters**, v. 5, n. 5, p. 829–834, 2005. Disponível em: http://pubs.acs.org/doi/abs/10.1021/nl050074e . Acesso em: 3 ago. 2016.
39. EL-SONBATY, S. M. Fungus-mediated synthesis of silver nanoparticles and evaluation of antitumor activity. **Cancer Nanotechnology**, v. 4, n. 4-5, p. 73–79,

2013. Disponível em: http://link.springer.com/10.1007/s12645-013-0038-3 . Acesso em: 29 out. 2013.

40. FILIPPO, E. *et al*. Green synthesis of silver nanoparticles with sucrose and maltose: Morphological and structural characterization. **Journal of Non-Crystalline Solids**, v. 356, n. 6-8, p. 344–350, 2010. Disponível em: http://linkinghub.elsevier.com/retrieve/pii/S0022309309007273 . Acesso em: 3 ago. 2016.
41. GADE, A. K. *et al*. Exploitation of *Aspergillus niger* for Synthesis of Silver Nanoparticles. **Journal of Biobased Materials and Bioenergy**, v. 2, n. 3, p. 243–247, 2008. Disponível em: http://openurl.ingenta.com/content/xref?genre=article&issn=1556-6560&volume=2&issue=3&spage=243 . Acesso em: 29 nov. 2014.
42. GADE, A. K. *et al*. Green synthesis of silver nanoparticles by *Phoma glomerata*. **Micron (Oxford, England : 1993)**, v. 59, p. 52–9, 2014. Disponível em: http://www.ncbi.nlm.nih.gov/pubmed/24530365 . Acesso em: 29 nov. 2014.
43. GAJBHIYE, M. *et al*. Fungus-mediated synthesis of silver nanoparticles and their activity against pathogenic fungi in combination with fluconazole. **Nanomedicine : nanotechnology, biology, and medicine**, v. 5, n. 4, p. 382–6, 2009. Disponível em: http://www.ncbi.nlm.nih.gov/pubmed/19616127 . Acesso em: 28 nov. 2014.
44. GANACHARI, S. V. et al. Extracellular Biosynthesis of Silver Nanoparticles Using Fungi *Penicillium diversum* and Their Antimicrobial Activity Studies. **BioNanoScience**, v. 2, n. 4, p. 316–321, 2012. Disponível em: http://link.springer.com/10.1007/s12668-012-0046-5 . Acesso em: 29 out. 2013.
45. HAU, S. K. *et al*. Air-stable inverted flexible polymer solar cells using zinc oxide nanoparticles as an electron selective layer. **Applied Physics Letters**, v. 92, n. 25, p. 253301, 2008. Disponível em: http://scitation.aip.org/content/aip/journal/apl/92/25/10.1063/1.2945281 . Acesso; 1 ago. 2016.
46. HULKOTI, N. I.; TARANATH, T.C. Biosynthesis of nanoparticles using microbes—A review. **Colloids and Surfaces B: Biointerfaces**, v. 121, p. 474–483, 2014. Disponível em: http://dx.doi.org/10.1016/j.colsurfb.2014.05.027 . Acesso em: 29 jult. 2013.
47. INGLE, A. *et al*. *Fusarium solani:* a novel biological agent for the extracellular synthesis of silver nanoparticles. **Journal of Nanoparticle Research**, v. 11, n. 8,

p. 2079–2085, 2008. Disponível em: http://link.springer.com/10.1007/s11051-008-9573-y . Acesso em: 21 nov. 2014.

48. JAIN, N. *et al*. Extracellular biosynthesis and characterization of silver nanoparticles using *Aspergillus flavus* NJP08: a mechanism perspective. **Nanoscale**, v. 3, n. 2, p. 635–41, 2011. Disponível em: http://www.ncbi.nlm.nih.gov/pubmed/21088776 . Acesso em: 28 nov. 2014.
49. JIA, H. *et al*. Platinum nanoparticles decorated dendrite-like gold nanostructure on glassy carbon electrodes for enhancing electrocatalysis performance to glucose oxidation. **Applied Surface Science**, v. 384, p. 58–64, 2016. Disponível em: http://linkinghub.elsevier.com/retrieve/pii/S0169433216310170 . Acesso em: 1 ago. 2016.
50. JIANG, Z.; LIU, C.; SUN, L. Catalytic Properties of Silver Nanoparticles Supported on Silica Spheres. **The Journal of Physical Chemistry B**, v. 109, n. 5, p. 1730–1735, 2005. Disponível em: http://pubs.acs.org/doi/abs/10.1021/jp046032g . Acesso em: 3 ago. 2016.
51. JUNEJO, Y.; GÜNER, A.; BAYKAL, A. Synthesis and characterization of amoxicillin derived silver nanoparticles: Its catalytic effect on degradation of some pharmaceutical antibiotics. **Applied Surface Science**, v. 317, p. 914–922, 2014. Disponível em: http://www.sciencedirect.com/science/article/pii/S0169433214019114 . Acesso em: 7 fev. 2014.
52. KIRTHI, A. V. *et al*. Novel approach to synthesis silver nanoparticles using plant pathogenic fungi, *Puccinia graminis*. **Materials Letters**, v. 81, p. 69–72, 2012. Disponível em: http://linkinghub.elsevier.com/retrieve/pii/S0167577X12005939 Acesso em: 29 out. 2013.
53. KUMAR R. R.; POORNIMA P. K..; THAMARAISELVI, K. Mycogenic synthesis of silver nanoparticles by the Japanese environmental isolate *Aspergillus tamarii*. **Journal of Nanoparticle Research**, v. 14, n. 5, p. 860, 2012. Disponível em: http://link.springer.com/10.1007/s11051-012-0860-2 . Acesso em: 29 dez. 2013.
54. LI, G. *et al*. Fungus-mediated green synthesis of silver nanoparticles using *Aspergillus terreus*. **International journal of molecular sciences**, v. 13, n. 1, p. 466–76, 2012. Disponível em: http://www.pubmedcentral.nih.gov/articlerender.fcgi?artid=3269698&tool=pmcentrez&rendertype=abstract . Acesso em: 19 nov. 2014.

55. LI, Q. *et al*. Antimicrobial nanomaterials for water disinfection and microbial control: Potential applications and implications. **Water Research**, v. 42, n. 18, p. 4591–4602, 2008. Disponível em: http://dx.doi.org/10.1016/j.watres.2008.08.015 . Acesso em: 6 out. 2013.
56. LINIC, S.; CHRISTOPHER, P.; INGRAM, D.B. Plasmonic-metal nanostructures for efficient conversion of solar to chemical energy. **Nature Materials**, v. 10, n. 12, p. 911–921, 2011. Disponível em: http://dx.doi.org/10.1038/nmat3151 . Acesso em: 29 out. 2015.
57. MAFUNÉ, F. *et al*. Formation and Size Control of Silver Nanoparticles by Laser Ablation in Aqueous Solution. **The Journal of Physical Chemistry B**, v. 104, n. 39, p. 9111–9117, 2000. Disponível em: http://pubs.acs.org/doi/abs/10.1021/jp001336y. Acesso em: 2 ago. 2016.
58. MALISZEWSKA, I.; SZEWCZYK, K.; WASZAK, K. Biological synthesis of silver nanoparticles. **Journal of Physics: Conference Series**, v. 146, p. 012025, 2009. Disponível em: http://stacks.iop.org/1742-6596/146/i=1/a=012025?key=crossref.ee213ba1ea719ac1e538f613719a6488 .
59. MALLMANN, E. J. J. *et al*. Antifungal activity of silver nanoparticles obtained by green synthesis. **Revista do Instituto de Medicina Tropical de São Paulo**, v. 57, n. 2, p. 165–167, 2015. Disponível em: http://www.scielo.br/scielo.php?script=sci_arttext&pid=S0036-46652015000200165&lng=en&nrm=iso&tlng=en . Acesso em: 2 ago. 2016
60. MASHWANI, Z. *et al*. Applications of plant terpenoids in the synthesis of colloidal silver nanoparticles. **Advances in Colloid and Interface Science**, v. 234, p. 132–141, 2016. Disponível em: http://linkinghub.elsevier.com/retrieve/pii/S0001868615300397 . Acesso em: 2 ago. 2016.
61. MUKHERJEE, P. *et al*. Green synthesis of highly stabilized nanocrystalline silver particles by a non-pathogenic and agriculturally important fungus *T. asperellum.* **Nanotechnology**, v. 19, n. 7, p. 075103, 2008. Disponível em: http://www.ncbi.nlm.nih.gov/pubmed/21817628 . Acesso em: 29 nov. 2014.
62. NAQVI, S. Z. *et al*. Combined efficacy of biologically synthesized silver nanoparticles and different antibiotics against multidrug-resistant bacteria. **International Journal of Nanomedicine**, v. 8, p. 3187–3195, 2013. Disponível em: http://www.dovepress.com/combined-efficacy-of-biologically-synthesized-silver-nanoparticles-and-peer-reviewed-article-IJN . Acesso em: 30 ago. 2015.

63. NARAYANAN, K. B.; PARK, H.H.; SAKTHIVEL, N. Extracellular synthesis of mycogenic silver nanoparticles by *Cylindrocladium floridanum* and its homogeneous catalytic degradation of 4-nitrophenol. **Spectrochimica acta. Part A, Molecular and biomolecular spectroscopy**, v. 116, p. 485–90, 2013. Disponível em: http://www.ncbi.nlm.nih.gov/pubmed/23973598 . Acesso em: 29 nov. 2014.
64. PANÁČEK, A. *et al*. Antifungal activity of silver nanoparticles against Candida spp. **Biomaterials**, v. 30, n. 31, p. 6333–6340, 2009. Disponível em: http://linkinghub.elsevier.com/retrieve/pii/S0142961209008023 . Acesso em: 3 ago. 2016.
65. PELGRIFT, R. Y.; FRIEDMAN, A.J. Nanotechnology as a therapeutic tool to combat microbial resistance. **Advanced Drug Delivery Reviews**, v. 65, n. 13-14, p. 1803–1815, 2013. Disponível em: http://dx.doi.org/10.1016/j.addr.2013.07.011 . Acesso em: 29 nov. 2014.
66. PEREIRA, L. *et al*. Synthesis, characterization and antifungal activity of chemically and fungal-produced silver nanoparticles against *Trichophyton rubrum*. **Journal of Applied Microbiology**, v. 117, n. 6, p. 1601–1613, 2014. Disponível em: http://doi.wiley.com/10.1111/jam.12652 . Acesso em: 1 ago. 2015.
67. PETTEGREW, C. *et al*. Silver Nanoparticle Synthesis Using Monosaccharides and Their Growth Inhibitory Activity against Gram-Negative and Positive Bacteria. **ISRN Nanotechnology**, v. 2014, p. 1–8, 2014. Disponível em: http://www.hindawi.com/journals/isrn.nanotechnology/2014/480284/ . Acesso em: 3 ago. 2016.
68. PHILIP, D. Honey mediated green synthesis of silver nanoparticles. **Spectrochimica Acta Part A: Molecular and Biomolecular Spectroscopy**, v. 75, n. 3, p. 1078–1081, 2010. Disponível em: http://linkinghub.elsevier.com/retrieve/pii/S1386142509007057 . Acesso em: 3 ago. 2016.
69. QIAN, Y. *et al*. Biosynthesis of silver nanoparticles by the endophytic fungus *Epicoccum nigrum* and their activity against pathogenic fungi. **Bioprocess and biosystems engineering**, v. 36, n. 11, p. 1613–9, 2013. Disponível em: http://www.ncbi.nlm.nih.gov/pubmed/23463299 . Acesso em: 27 nov. 2014.
70. QU, X.; ALVAREZ, P. J. J.; LI, Q. Applications of nanotechnology in water and wastewater treatment. **Water Research**, v. 47, n. 12, p. 3931–3946, 2013. Disponível em: http://dx.doi.org/10.1016/j.watres.2012.09.058 . Acesso em: 12 out 2013.

71. RAHEMAN, F. *et al*. Novel Antimicrobial Agent Synthesized from an Endophytic Fungus *Pestalotia* sp . Isolated from Leaves of *Syzygium cumini* (L). **Nano Biomed Eng**, v. 3, p. 174–178, 2011. Disponível em : https://www.researchgate.net/publication/216532614 Acesso em: 12 set 2013.
72. RAMAN, J. *et al*. Mycosynthesis and characterization of silver nanoparticles from *Pleurotus djamor* var. *roseus* and their in vitro cytotoxicity effect on PC3 cells. **Process Biochemistry**, v. 50, n. 1, p. 140–147, 2015. Disponível em: http://linkinghub.elsevier.com/retrieve/pii/S1359511314005480 . Acesso em: 12 abr 2014.
73. RUPARELIA, J. P. *et al*. Strain specificity in antimicrobial activity of silver and copper nanoparticles. **Acta Biomaterialia**, v. 4, n. 3, p. 707–716, 2008. Disponível em: http://linkinghub.elsevier.com/retrieve/pii/S174270610700195X . Acesso em: 1 ago. 2016.
74. SALUNKHE, R. B. *et al*. Studies on silver accumulation and nanoparticle synthesis By *Cochliobolus lunatus*. **Applied biochemistry and biotechnology**, v. 165, n. 1, p. 221–34, 2011. Disponível em: http://www.ncbi.nlm.nih.gov/pubmed/21505806 . Acesso em: 27 nov. 2014.
75. SANGHI, R.; VERMA, P. Biomimetic synthesis and characterisation of protein capped silver nanoparticles. **Bioresource technology**, v. 100, n. 1, p. 501–4, 2009. Disponível em: http://www.ncbi.nlm.nih.gov/pubmed/18625550 . Acesso em: 29 nov. 2014.
76. SAPSFORD, K. E. *et al*. Analyzing Nanomaterial Bioconjugates: A Review of Current and Emerging Purification and Characterization Techniques. **Analytical Chemistry**, v. 83, n. 12, p. 4453–4488, 2011. Disponível em: http://pubs.acs.org/doi/abs/10.1021/ac200853a . Acesso em: 7 fev. 2014.
77. SARAVANAN, M; NANDA, A. Extracellular synthesis of silver bionanoparticles from *Aspergillus clavatus* and its antimicrobial activity against MRSA and MRSE. **Colloids and surfaces. B, Biointerfaces**, v. 77, n. 2, p. 214–8, 2010. Disponível em: http://www.ncbi.nlm.nih.gov/pubmed/20189360 . Acesso em: 27 nov. 2014.
78. SARINA, S; WACLAWIK, E. R.; ZHU, H. Photocatalysis on supported gold and silver nanoparticles under ultraviolet and visible light irradiation. **Green Chemistry**, v. 15, n. 7, p. 1814, 2013. Disponível em: http://xlink.rsc.org/?DOI=c3gc40450a . Acesso em: 11 ago. 2016.

79. SHALIGRAM, N. S. *et al*. Biosynthesis of silver nanoparticles using aqueous extract from the compactin producing fungal strain. **Process Biochemistry**, v. 44, n. 8, p. 939–943, 2009. Disponível em: http://linkinghub.elsevier.com/retrieve/pii/S1359511309001305 . Acesso em: 28 nov. 2014.

80. SHARMA, V. K.; YNGARD, R.A.; LIN, Y. Silver nanoparticles: Green synthesis and their antimicrobial activities. **Advances in Colloid and Interface Science**, v. 145, n. 1-2, p. 83–96, 2009. http://www.ncbi.nlm.nih.gov/pubmed/18945421 Acesso em: 1 nov 2013.

81. SONI, N.; PRAKASH, S. Fungal-mediated nano silver: an effective adulticide against mosquito. **Parasitology Research**, v. 111, n. 5, p. 2091–2098, 2012b. Disponível em: http://link.springer.com/10.1007/s00436-012-3056-x . Acesso em: 28 nov. 2014.

82. SONI, N.; PRAKASH, S. Microbial synthesis of spherical nanosilver and nanogold for mosquito control. **Annals of Microbiology**, v. 64, n. 3, p. 1099–1111, 2014. Disponível em: http://link.springer.com/10.1007/s13213-013-0749-z . Acesso em: 1 nov 2013.

83. SUNITHA, A. *et al*. Evaluation of Antimicrobial Activity of Biosynthesized Iron and Silver Nanoparticles Using the Fungi *Fusarium* and *Actinomycets* sp. on Human Pathogen. **Nano Biomed Eng**, v. 5, n. Iii, p. 39–45, 2013. Disponível em: http://nanobe.org/Data/View/219. Acesso em 1 jul 2016.

84. THOMANN, I. *et al*. Plasmon Enhanced Solar-to-Fuel Energy Conversion. **Nano Letters**, v. 11, n. 8, p. 3440–3446, 2011. Disponível em: http://pubs.acs.org/doi/abs/10.1021/nl201908s . Acesso em 12 fev 2016.

85. THUC, D. T. *et al*. Green synthesis of colloidal silver nanoparticles through electrochemical method and their antibacterial activity. **Materials Letters**, v. 181, p. 173–177, 2016. Disponível em: http://linkinghub.elsevier.com/retrieve/pii/S0167577X16309648 . Acesso em: 2 ago. 2016.

86. VAHABI, K.; MANSOORI, G. A; KARIMI, S. Biosynthesis of Silver Nanoparticles by Fungus *Trichoderma reesei* (A Route for Large-Scale Production of AgNPs). **Insciences Journal**, v. 1, n. 1, p. 65–79, 2011. Disponível em: http://journal.insciences.org/1664-171x-1-1-65/ . Acesso em: 29 nov. 2014.

87. VERMA, V. C.; KHARWAR, R. N.; GANGE, A. C. Biosynthesis of antimicrobial silver nanoparticles by the endophytic fungus *Aspergillus clavatus*. **Nanomedicine**

(London, England), v. 5, n. 1, p. 33–40, 2010. Disponível em: http://www.ncbi.nlm.nih.gov/pubmed/20025462 . Acesso em: 29 nov. 2014.

88. VIGNESHWARAN, N. *et al*. A novel one-pot "green" synthesis of stable silver nanoparticles using soluble starch. **Carbohydrate Research**, v. 341, n. 12, p. 2012–2018, 2006. Disponível em: http://linkinghub.elsevier.com/retrieve/pii/S0008621506002187 . Acesso em: 3 ago. 2016.
89. VIGNESHWARAN, N. *et al*. Biological synthesis of silver nanoparticles using the fungus *Aspergillus flavus*. **Materials Letters**, v. 61, n. 6, p. 1413–1418, 2007. Disponível em: http://www.sciencedirect.com/science/article/pii/S0167577X06008512 . Acesso em: 29 nov. 2014.
90. VIGNESHWARAN, N. *et al*. Biomimetics of silver nanoparticles by white rot fungus, *Phaenerochaete chrysosporium*. **Colloids and surfaces. B, Biointerfaces**, v. 53, n. 1, p. 55–9, 2006. Disponível em: http://www.ncbi.nlm.nih.gov/pubmed/16962745 . Acesso em: 22 nov. 2014.
91. WANG, H. *et al*. Preparation of silver nanoparticles by chemical reduction method. **Colloids and Surfaces A: Physicochemical and Engineering Aspects**, v. 256, n. 2-3, p. 111–115, 2005. Disponível em: http://linkinghub.elsevier.com/retrieve/pii/S0927775705000142 . Acesso em: 3 ago. 2016.
92. WANG, L. *et al*. Antibacterial activities of the novel silver nanoparticles biosynthesized using Cordyceps militaris extract. **Current Applied Physics**, v. 16, n. 9, p. 969–973, 2016. Disponível em: http://dx.doi.org/10.1016/j.cap.2016.05.025 . Acesso em: 3 fev. 2014.
93. WILLETS, K. A.; VAN DUYNE, R. P. Localized Surface Plasmon Resonance Spectroscopy and Sensing. **Annual Review of Physical Chemistry**, v. 58, n. 1, p. 267–297, 2007. Disponível em: http://www.annualreviews.org/doi/abs/10.1146/annurev.physchem.58.032806.104607 . Acesso em: 1 ago. 2016.
94. XUE, B. *et al*. Biosynthesis of silver nanoparticles by the fungus *Arthroderma fulvum* and its antifungal activity against genera of *Candida*, *Aspergillus* and *Fusarium*. **International Journal of Nanomedicine**, p. 1899, 2016. Disponível em: http://dx.doi.org/10.2147/IJN.S98339 . Acesso em: 7 fev. 2014.

95. ZHANG, Q. *et al*. A Systematic Study of the Synthesis of Silver Nanoplates: Is Citrate a “Magic” Reagent? **Journal of the American Chemical Society**, v. 133, n. 46, p. 18931–18939, 2011. Disponível em: http://www.ncbi.nlm.nih.gov/pubmed/21999679 . Acesso em: 2 ago. 2016.

96. ZHANG, S; TANG, Y; VLAHOVIC, B. A Review on Preparation and Applications of Silver-Containing Nanofibers. **Nanoscale Research Letters**, v. 11, n. 1, p. 80, 2016. Disponível em: http://www.scopus.com/inward/record.url?eid=2-s2.0-84957935901&partnerID=tZOtx3y1 . Acesso em: 11 ago. 2016.

CHAPTER TWO

Activity of silver nanoparticles associated with ciprofloxacin against *Escherichia coli*

ABSTRACT

Nanotechnology can be a valuable ally in the treatment of infections. Silver nanoparticles (AgNPs) are structures that have antimicrobial activity. The objective of this study was to produce AgNPs by green methods, characterize these structures, and assess their antimicrobial activity against *Escherichia coli* associated with the antibiotic ciprofloxacin. AgNPs were characterized by spectroscopic and microscopic techniques. Antimicrobial activity was evaluated by the disk diffusion method against 10 strains of *E. coli*. The synthesized AgNPs showed a spherical shape and a size of 85.07 ± 12.86 nm (mean ± SD). AgNPs increased activity of ciprofloxacin by 40% and may represent a new therapeutic option for the treatment of bacterial infections.

Keywords: Silver nanoparticles; Antimicrobial activity; *Escherichia coli.*

INTRODUCTION

Nanotechnology involves the study of bodies that have dimensions of up to 100 nm in any one direction and possess properties that differ from bulk material (CHIU, RUAN, HUANG, 2013). This peculiarity opens a new area of knowledge that can open a technological frontier, with the possibility of developing new compounds that help improve people's lives (CHERNOUSOVA, EPPLE, 2013; CHIU, RUAN, HUANG, 2013).

There is an immense perspective of the use of nanoparticles in the diagnosis and treatment of human and animal diseases (DOANE, BURDA 2012). The main products available are those for personal hygiene, such as toothpaste, shaving creams, and deodorants. These products mainly contain silver nanoparticles (AgNPs), due to their known antiseptic action (CHERNOUSOVA, EPPLE, 2013). AgNPs have various applications, including antiseptic, antibacterial, and antifungal. Silver is a cheaper metal than gold, which makes it attractive for research. Moreover, silver in the nanoparticle state has peculiar optical properties, allowing its use in technological products (ARVIZO et al., 2012; HERVÉS et al., 2012). The use of medical catheters covered with a nanometer-thin layer of AgNPs can prevent the colonization of micro-organisms and thus decrease the length of hospital stay of patients, because it prevents infections (JHA et al., 2014).

The antibacterial activity of AgNPs is well known (KHARISSOVA et al., 2013; RAI et al., 2012). These particles act by causing damage to membranes and to DNA, which

prevents the reproduction of the microorganism and leads to death (RIZZELLO, POMPA, 2014). In addition to its intrinsic bactericidal property, the microorganism-killing power of AgNPs can be increased when associated with antibiotics (GAJBHIYE et al., 2009). This mechanism may be useful in the treatment of multidrug-resistant infections, and may represent an important therapeutic alternative (FAYAZ et al., 2010). Ciprofloxacin is a very useful antibiotic that acts by inhibiting bacterial DNA synthesis, resulting in the death of the microorganism (CASTRO et al., 2013). (FIGURE S1 Supporting Information Chapter 2).

The objective of this study was to synthesize, characterize and evaluate the activity of AgNPs produced by green synthesis and associated with the antibiotic ciprofloxacin against strains of *Escherichia coli.*

MATERIALS AND METHODS

Synthesis of AgNPs

AgNP synthesis was performed using glucose as a reducing agent and sodium dodecyl sulfate (SDS) as a stabilizing agent. Briefly, 1.00 g glucose and 0.5 g of SDS were added to 500 mL of a solution of $AgNO_3$ (5 mM). The solution was continuously stirred and the temperature was maintained at 50° C to favor the reaction. Then 1.0 mL 0.2 M NaOH was added to mixture. The reaction was maintained under these conditions for 30 min, after which time stirring and heating were suspended (DARROUDI et al., 2011; MALLMANN et al., 2015).

Characterization of the nanoparticles

The AgNPs were purified by ultracentrifugation at 10,000 rpm for 20 min, and characterization was carried out using spectrophotometric reading of 300 to 700 nm (UV-Vis). The size was determined by dynamic light scattering (DLS), and by full width at half maximum (FWHM) measure of UV-Vis of AgNPs, the shape was determined by scanning electron microscopy (SEM) and atomic force microscopy (AFM) (AGNIHOTRI et al., 2014; LIN et al., 2014). The final concentration of Ag in the AgNP stock suspension was determined through inductively coupled plasma spectrometry (ICP).

Microbiological tests

This study used 10 strains of *Escherichia coli*; the bacteria belong to the collection maintained at the Microbiology Laboratory of the Department of Clinical Analysis, School of Pharmacy, Federal University of Ceará (see FIGURE S2 Supporting Information Chapter 2). The tests were performed by the disk diffusion (DD) method on Muller-Hinton agar. In this experiment we used three types of discs: (1) paper disc (10 mm) saturated with 10 µL (equivalent to 15 µg) of AgNPs; (2) ciprofloxacin discs with (Cipro) 5 µg (Cecon®); and (3) ciprofloxacin disks saturated with 10 µL (equivalent to 15 µg) of AgNPs. The *E. coli* were suspended in saline solution and plated in the culture medium, then the discs were placed. The plates were incubated at 35°C for 24 hours, after this time the zones of inhibition were measured (MALLMANN *et al*., 2015).

The synergism was evaluated by the formula $\{(C^2 - B^2) / B^2\}$ x100, where, B = the inhibition zones of the ciprofloxacin alone and C = ciprofloxacin + AgNP. This formula allows us find the amount of increase of the inhibition zone around the bacteria caused by the antibiotic in association with AgNPs (FAYAZ et al., 2010).

Statistical analysis was performed using the Student's *t*-test to evaluate the averages of inhibition zones of Cipro and Cipro associated with AgNPs. It was considered significant at $p < 0.05$.

RESULTS AND DISCUSSION

Processes that use sugars in obtaining AgNPs are called green synthesis, because of the absence of toxic compounds and no formation of toxic waste. Furthermore, sugars are cheap and affordable (KHARISSOVA et al., 2013). In our study, we used glucose for synthesis and SDS for stabilization (see FIGURE S3 Supporting Information Chapter 2). Nanoparticles were formed with an average size of 85.07 ± 12.86 nm (mean ± SD) (FIGURE 1) and about 100.0 nm when measured by the FWHM (see FIGURE S4 Supporting Information Chapter 2). UV–Vis spectra confirmed efficient synthesis of AgNPs, these particles absorbed energy at 420 nm, as can be seen in FIGURE 2; AgNPs exhibited a spherical shape, as can be seen in FIGURE 3 and FIGURE 4. The energy dispersive X-ray spectroscopy (EDX) of AgNPs shows a composition (see FIGURE S5 Supporting Information Chapter 2). AgNP synthesis using glucose is a recurring theme in the literature (DARROUDI et al., 2011; MALLMANN et al., 2015). The particles are spherical and stable,

and SDS enhances the antimicrobial activity (KORA et al., 2009; LIN et al., 2014; SHARMA et al., 2009)

FIGURE 1- Dynamic light scattering (DLS) of AgNPs.

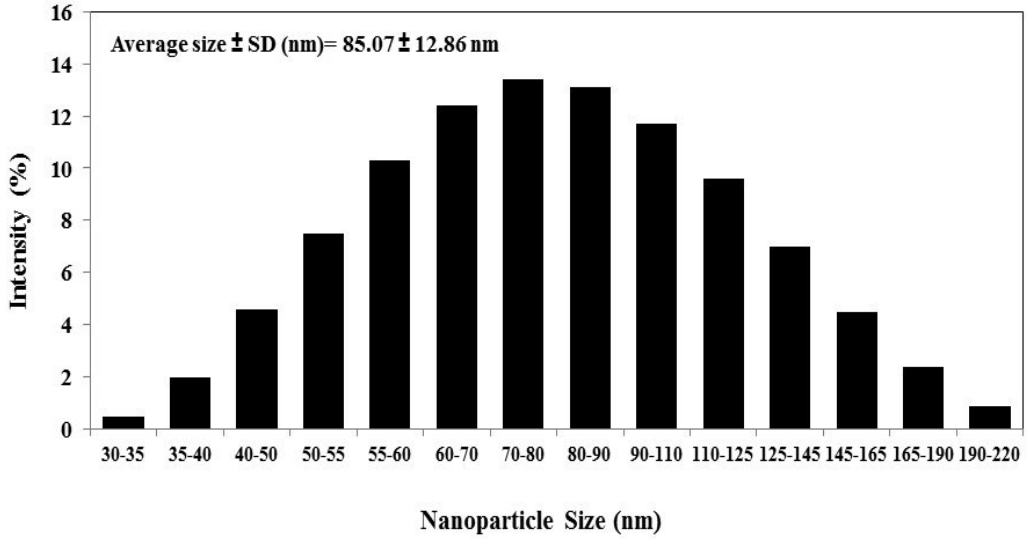

Source: Author

FIGURE 2- UV-vis spectrum of AgNPs. Inset- AgNPs suspension

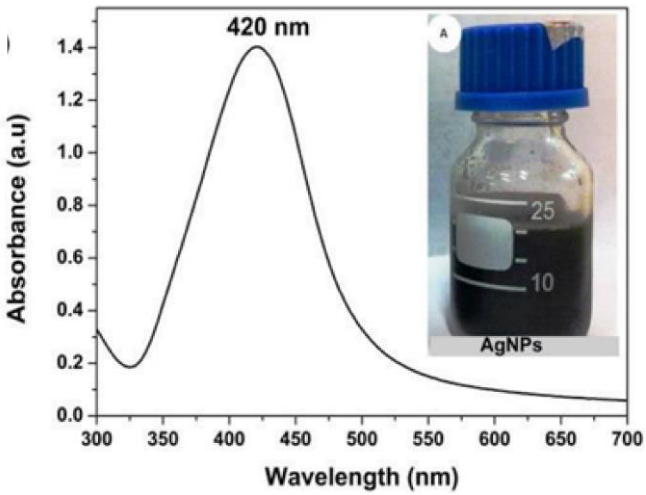

Source: Author

FIGURE 3- Scanning electron microscopy (SEM) of AgNPs.

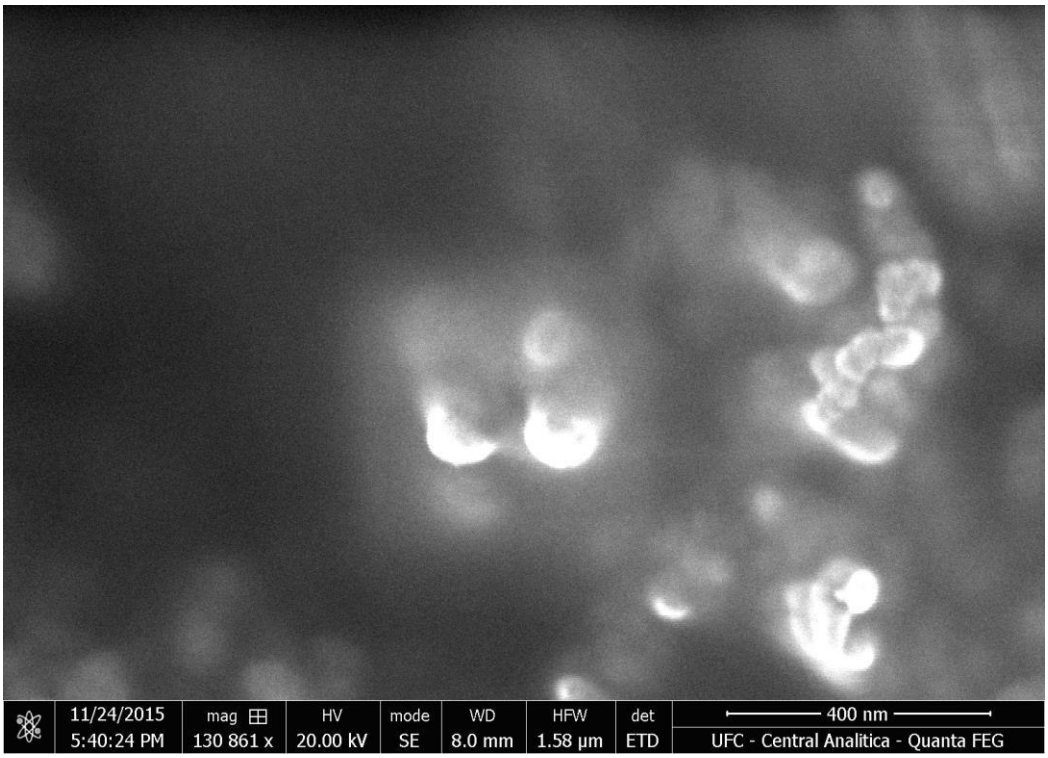

Source: Author

FIGURE 4- Atomic force microscopy (AFM) of AgNPs.

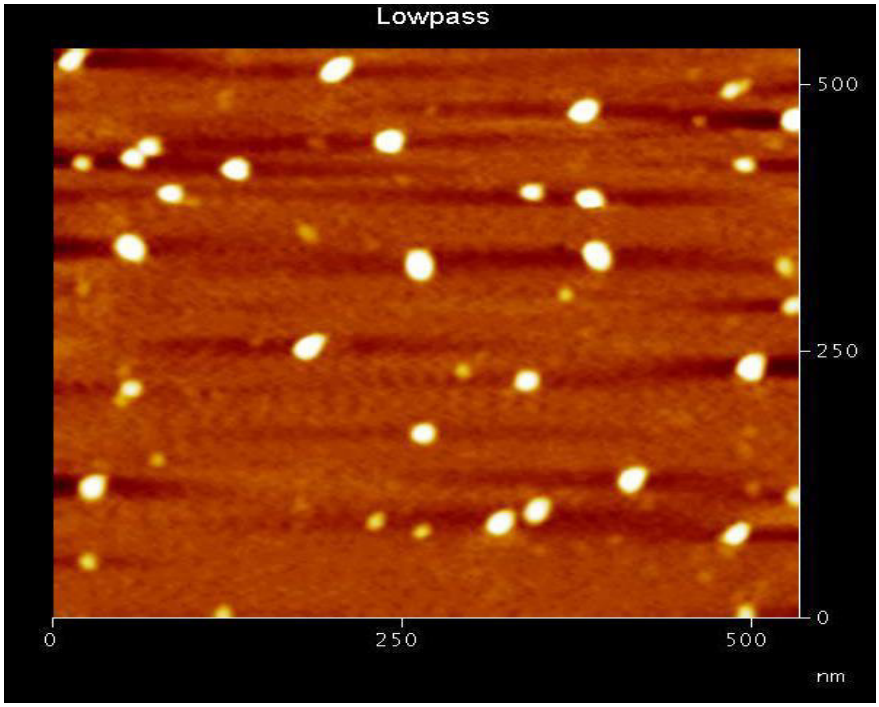

Source: Author

FIGURE 5- Comparison of activities: AgNPs, Cipro and Cipro + AgNPs.

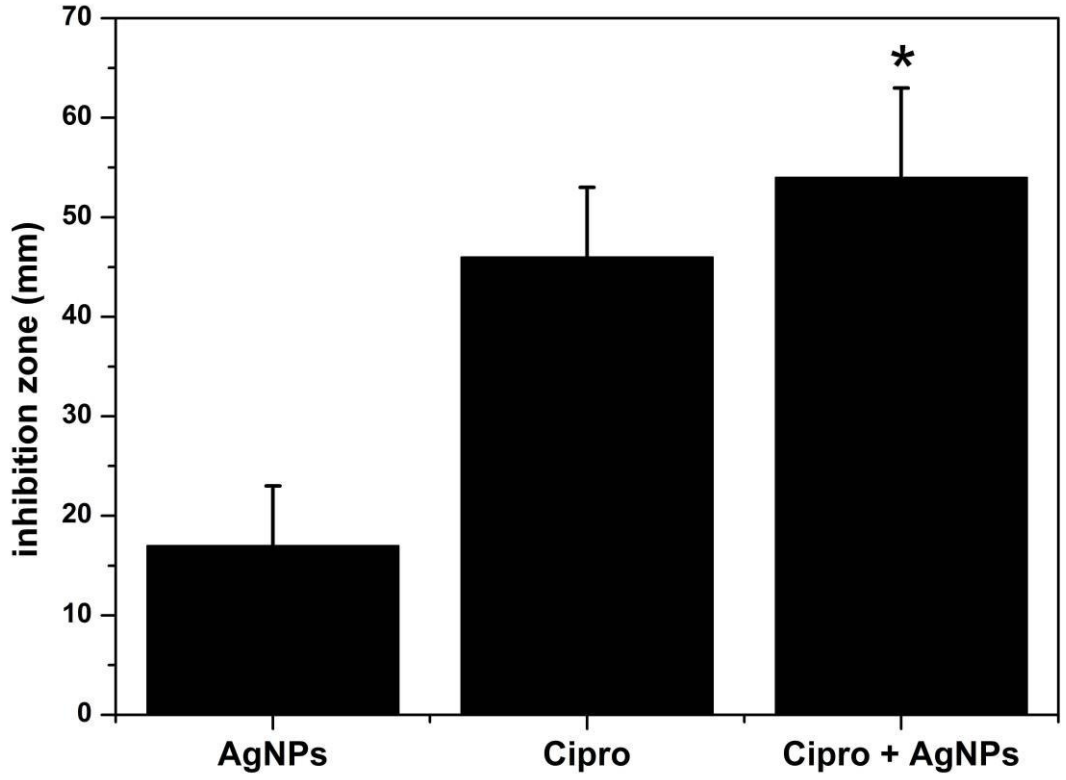

* Comparison of the inhibitory zones of cipro alone and cipro + AgNPs, $p= 0.03$.

Source: Author

Table 1- Antibacterial activity of AgNPs, cipro discs and cipro + AgNPs against *E.coli*

Bacteria *(n)*	Inhibition Zone (mean ± SD) mm			Increased fold area (%)
	A AgNPs	B cipro	C cipro + AgNPs	$(C^2 - B^2)/B^2)x100$
E. coli (10)	17.1 (±5.9)	45.9 (±7.4)	54.3(±8.6)	40%

Source: Author

AgNPs stand out for their antimicrobial activity (SHAHVERDI et al., 2007). The mechanism of action involves the inactivation of enzymes and DNA damage of microorganisms (JHA et al., 2014). In our study, we evaluated the effect of AgNPs alone and associated with the antibiotic ciprofloxacin (cipro). Ciprofloxacin alone produced a zone of

inhibition of 45.9 ± 7.4 mm; AgNPs alone showed a zone of inhibition of 17.1 ± 5.9 mm; and combination of cipro + AgNPs showed a zone of inhibition of 54.3 ± 8.6 mm, we can observe that the results were statistically significant with $p < 0.05$ (FIGURE 5). The association of cipro + AgNPs produced a 40% increase in the zone of inhibition when compared with the cipro alone (Table 1). The association AgNPs and antibiotics against bacteria and fungi have shown good results (FAYAZ et al., 2010; GAJBHIYE et al., 2009; SHAHVERDI et al., 2007). In FIGURE 6, we can observe the action of this association; the zone of inhibition on the disc containing cipro + AgNPs is much larger than the disc with cipro alone and AgNPs alone. The AgNPs bind proteins and DNA of the bacteria and ciprofloxacin damages DNA, and this combination enhances the effects on *E. coli* strains (CASTRO et al., 2013), (see FIGURE S6 Supporting Information Chapter 2).

FIGURE 6- Microbial activity of AgNPs alone and associated with Cipro.

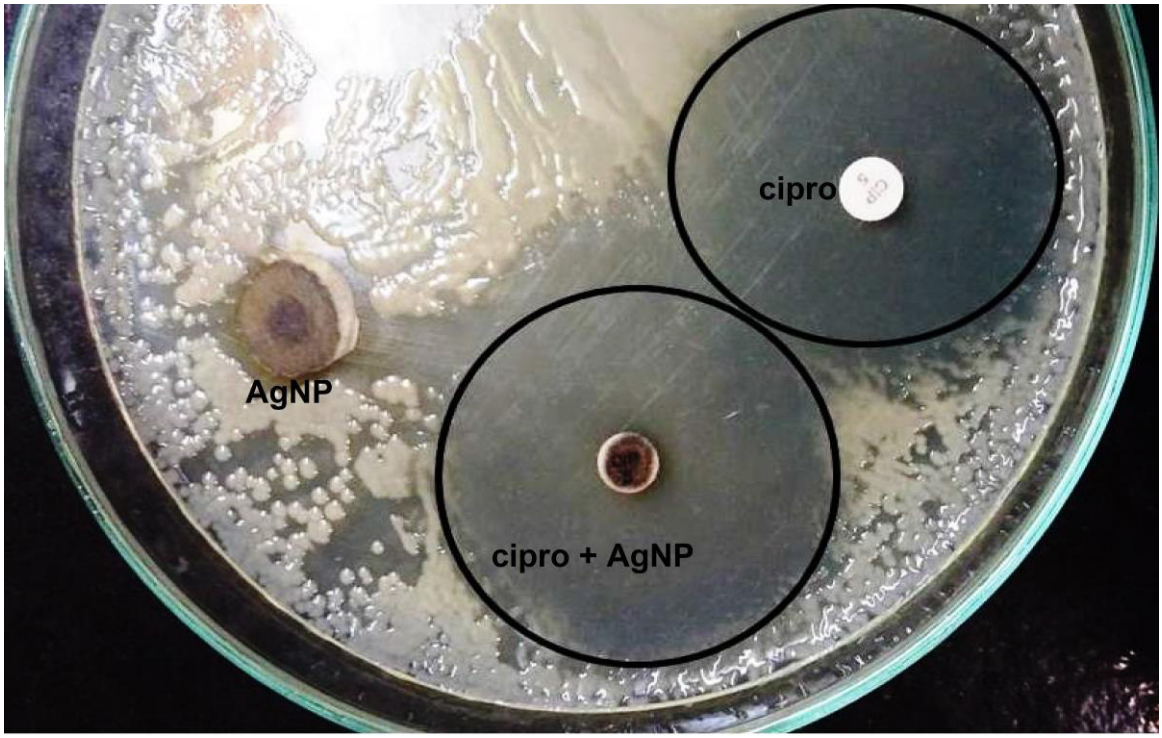

Source: Author

CONCLUSION

AgNPs were synthesized using glucose and SDS and were characterized through physical-chemical techniques: UV-Vis, DLS, SEM, and AFM; they showed a size of 85.07 ±

12.86 nm and a spherical shape. The AgNPs showed antimicrobial activity against *E. coli* and had increased activity of the antibiotic ciprofloxacin. AgNPs associated with antimicrobial agents can be a therapeutic option for the treatment of bacterial infections.

ACKNOWLEDGMENTS

The authors gratefully thank Central Analítica-UFC/CT-INFRA/MCTI-SISNANO/Pró-Equipamentos, UFC Department of Physics, CAPES, CNPq and Funcap, for the grant provided to support research on nanoparticles.

REFERENCES

1. AGNIHOTRI, S.; MUKHERJI, S.; MUKHERJI, S. Size-controlled silver nanoparticles synthesized over the range 5–100 nm using the same protocol and their antibacterial efficacy. **RSC Adv.**, v. 4, n. 8, p. 3974–3983, 2014. Disponível em: http://pubs.rsc.org/en/content/articlehtml/2014/ra/c3ra44507k . Acesso em: 7 fev. 2014.
2. ARVIZO, R. R. *et al*. Intrinsic therapeutic applications of noble metal nanoparticles: past, present and future. **Chem Soc Rev**, v. 41, n. 7, p. 2943–2970, 2012. Disponível em: http://www.ncbi.nlm.nih.gov/pubmed/22388295 Acesso 22 abr 2014.
3. CASTRO, W.; NAVARRO, M.; BIOT, C. Medicinal potential of ciprofloxacin and its derivatives. **Future Med Chem**.; 5: 81-96. 2013. Disponível em: http://www.future-science.com/doi/pdf/10.4155/fmc.12.181. Acesso 2 mai. 2015.
4. CHERNOUSOVA, S.; EPPLE, M. Silver as antibacterial agent: Ion, nanoparticle, and metal. **Angewandte Chemie - International Edition**, v. 52, n. 6, p. 1636–1653, 2013. . Disponível em: http://doi.wiley.com/10.1002/anie.201205923 . Acesso 12 abri. 2015.
5. CHIU, C-Y.; RUAN, L.; HUANG, Y. Biomolecular specificity controlled nanomaterial synthesis. **Chemical Society Reviews**, p. 2512–2527, 2013. Disponível em: http://xlink.rsc.org/?DOI=C2CS35347D . Acesso 12 jun. 2014.
6. DARROUDI, M. *et al*. Green synthesis and characterization of gelatin-based and sugar-reduced silver nanoparticles. **International Journal of Nanomedicine**, v. 6, n. 1, p. 569–574, 2011. Disponível em: http://www.dovepress.com/green-synthesis-and-characterization-of-gelatin-based-and-sugar-reduce-peer-reviewed-article-IJN . Acesso 23 set. 2014.

7. DOANE, T.L.; BURDA, C. The unique role of nanoparticles in nanomedicine: imaging, drug delivery and therapy. **Chemical Society reviews**, v. 41, n. 7, p. 2885–911, 2012. Disponível em: http://www.ncbi.nlm.nih.gov/pubmed/22286540 . Acesso em: 11 jul. 2014.
8. FAYAZ, A. M. *et al*. Biogenic synthesis of silver nanoparticles and their synergistic effect with antibiotics: a study against gram-positive and gram-negative bacteria. **Nanomedicine: Nanotechnology, Biology, and Medicine**, v. 6, n. 1, p. 103–109, 2010. Disponível em: http://dx.doi.org/10.1016/j.nano.2009.04.006 . Acesso em: 21 dez. 2013.
9. GAJBHIYE, M. *et al*. Fungus-mediated synthesis of silver nanoparticles and their activity against pathogenic fungi in combination with fluconazole. **Nanomedicine : nanotechnology, biology, and medicine**, v. 5, n. 4, p. 382–6, 2009. Disponível em: http://www.ncbi.nlm.nih.gov/pubmed/19616127 . Acesso em: 28 nov. 2014.
10. HERVÉS, P. *et al*. Catalysis by metallic nanoparticles in aqueous solution: model reactions. **Chemical Society Reviews**, v. 41, n. 17, p. 5577, 2012. . Disponível em: http://xlink.rsc.org/?DOI=c2cs35029g . Acesso em: 28 nov. 2014.
11. JHA, R.K. *et al*. An emerging interface between life science and nanotechnology: present status and prospects of reproductive healthcare aided by nano-biotechnology. **Nano reviews**, v. 5, n. 1, p. 1–19, 2014. Disponível em: http://www.pubmedcentral.nih.gov/articlerender.fcgi?artid=3943174&tool=pmcentrez&rendertype=abstract . Acesso em: 18 nov. 2015.
12. KHARISSOVA, O. V. *et al*. The greener synthesis of nanoparticles. **Trends in Biotechnology**, v. 31, n. 4, p. 240–248, 2013. Disponível em: http://linkinghub.elsevier.com/retrieve/pii/S0167779913000152 . Acesso em: 28 set. 2014.
13. KORA, A. J.; MANJUSHA, R.; ARUNACHALAM, J. Superior bactericidal activity of SDS capped silver nanoparticles: Synthesis and characterization. **Materials Science and Engineering C**, v. 29, n. 7, p. 2104–2109, 2009. Disponível em: http://dx.doi.org/10.1016/j.msec.2009.04.010 . Acesso em: 18 set. 2015.
14. LIN, P-C. *et al*. Techniques for physicochemical characterization of nanomaterials. **Biotechnology advances**, v. 32, n. 4, p. 711–26, 2014. Disponível em: http://www.pubmedcentral.nih.gov/articlerender.fcgi?artid=4024087&tool=pmcentrez&rendertype=abstract . Acesso em: 20 jul. 2014.

15. MALLMANN, E.J.J. et al. Antifungal activity of silver nanoparticles obtained by green synthesis. **Rev. Inst. Med. Trop. Sao Paulo**, v. 57, n. 15, p. 165–167, 2015. Disponível em: http://www.scielo.br/scielo.php?script=sci_arttext&pid=S0036-46652015000200165. Acesso em: 12 dez. 2015.
16. RAI, M.; YADAV, A.; GADE, A. Silver nanoparticles as a new generation of antimicrobials. **Biotechnology Advances**, v. 27, n. 1, p. 76–83, 2009. Disponível em: http://dx.doi.org/10.1016/j.biotechadv.2008.09.002 . Acesso em: 28 mar. 2015.
17. RIZZELLO, L.; POMPA, P.P. Nanosilver-based antibacterial drugs and devices: mechanisms, methodological drawbacks, and guidelines. **Chemical Society reviews**, v. 43, n. 5, p. 1501–18, 2014. Disponível em: http://www.ncbi.nlm.nih.gov/pubmed/24292075 . Acesso em: 18 out. 2014.
18. SHAHVERDI, A.R. *et al*. Synthesis and effect of silver nanoparticles on the antibacterial activity of different antibiotics against Staphylococcus aureus and *Escherichia coli*. **Nanomedicine: Nanotechnology, Biology, and Medicine**, v. 3, n. 2, p. 168–171, 2007. Disponível em: http://linkinghub.elsevier.com/retrieve/pii/S1549963407000469 . Acesso em: 3 nov. 2014.
19. SHARMA, V.K.; YNGARD, R. A.; LIN, Y. Silver nanoparticles: Green synthesis and their antimicrobial activities. **Advances in Colloid and Interface Science**, v. 145, n. 1-2, p. 83–96, 2009. Disponível em: http://dx.doi.org/10.1016/j.cis.2008.09.002v. Acesso em: 3 fev. 2014.

CHAPTER THREE

Improvement of antifungal activity of polyene antifungals against *Candida parapsilosis* through the synergistic effect with silver nanoparticles

ABSTRACT

Candidiasis is a fungal infection caused by yeasts of the genus *Candida* spp. Of the several pathogenic *Candida* species, we can highlight *C. parapsilosis* due to susceptibility profile. Amphotericin B and nystatin are polyene antifungal drugs most frequently used to combat this type of infection. Silver nanoparticles (AgNPs) also have antifungal properties and can also provide synergistic action when combined with classic antifungals. Therefore, the aim of this study was evaluate the synergistic action of AgNPs, amphotericin B and nystatin against *C. parapsilosis*. The synthesis of AgNPs were performed with glucose, and sodium dodecyl sulfate (SDS) was used as a stabilizer. The characterization of AgNPs was performed by UV-Visible spectroscopy, dynamic light scattering (DLS), scanning electron microscopy (SEM) and atomic force microscopy (AFM). The synergistic action was evaluated by the disk diffusion method. Synthesized AgNPs were shown to be quite uniform and stable. AgNPs, when combined with amphotericin B and nystatin, showed potent antifungal activity and increased the zone around the antifungal disk by 222.6 and 319.3%, respectively. These results contribute to a better understanding of the synergistic effect, that can be tested effectively for other drugs and offers another option for the treatment of fungal infections.

Keywords: C. *parapsilosis*; Silver nanoparticles; Polyene antifungals; Synergistic effect.

INTRODUCTION

Infections caused by yeasts of the genus *Candida* are highly relevant due to their high morbidity and mortality rates, which can be compared to septic shock. In Brazil, the incidence of these infections is 2 cases per 1,000 hospital admissions (COLOMBO et al., 2013; EGGIMANN et al., 2010). Infections caused by *Candida* spp. include about 80% of all fungal infections reported in hospitals; blood, urine and surgical wounds are the main body sites involved. *Candida parapsilosis* is yeast constantly isolated from candidemia. It exhibits mortality rates that are considered high. Its identification is no simple task, requiring biochemical, phenotypic and molecular methods (COLOMBO et al., 2013).

Of the drugs used to treat these diseases, we can highlight the polyene antibiotics, which are broad-spectrum antifungals such as nystatin and amphotericin B. The former is part of many topical preparations available on the market, and the latter is an intravenous drug, widely used in combating candidemia (DENNING AND HOPE, 2010).

The continuous use of these antifungals may promote the selection of resistant pathogenic fungi, not controlled by the previously effective fungicide, thereby jeopardizing its efficacy. Therefore, several strategies can be used to prevent or reduce fungal resistance, and one of the most common ones recently is to evaluate the synergism of antifungal drugs with other substances. For this purpose, the following can be used: essential oils (AMBER et al., 2010), formulations with other antibiotics (GAO et al., 2013; ZEIDLER et al., 2013), and drugs without antifungal indication (MENEZES et al., 2012), among others.

Silver nanoparticles (AgNPs) are structures with sizes up to 100 nm and exhibit different properties than those found in the source material. AgNPs are unstable and their synthesis involves many products, sometimes toxic, as the preparation methods can be chemical, biological or physical (LI et al., 2012; NATH, BANERJEE 2013). This kind of material has emerged as a promising and potent treatment against microorganisms due to its antibacterial, antiviral and antifungal effects, which are described in several studies (BINDHU et al.,. 2015; QUIAN et al., 2013).

In this way, the purpose of this study was evaluate the synergistic action between two types of polyene antifungals (nystatin and amphotericin B) (see FIGURE S1 and S2 Supporting Information Chapter 3) associated with AgNPs against strains of *C. parapsilosis* isolated from candidemia.

MATERIALS AND METHODS

Origin of the strains

Ten strains of *C. parapsilosis* isolated from candidemia of patients admitted to public hospitals in Fortaleza, Ceará, in Northeastern Brazil, were used in this study. These were identified by biochemical, phenotypic and molecular methods (VASCONCELOS et al., 2011).

Production of AgNPs

The AgNPs were synthesized using a solution of 5 mM silver nitrate (Dinâmica - São Paulo - Brazil), 1.0g glucose (Dinâmica - São Paulo - Brazil) as a reducing agent, and 0.5g sodium dodecyl sulfate (SDS) (Vetec - Rio de Janeiro - Brazil) as a stabilizer. Summarizing, the silver nitrate solution was heated to 50° C with subsequent addition of the

other reactants. The reaction system remained under constant stirring and was accelerated by adding of 1.0 ml NaOH 0.2 mol/L. After 30 min the solution became yellow, characteristic of the production of AgNPs (DARROUDI et al., 2011).

Characterization of the AgNPs

The AgNPs were characterized by the techniques of ultraviolet-visible spectroscopy (UV-Vis) in the range of 300-700nm on a Thermo Scientific GENESYS™ 10s spectrophotometer. The size and zeta potential were determined by the light scattering method using the Nanozetasizer (Malvern - United States). The morphology, distribution and size of the AgNPs were determined using Scanning Electron Microscopy (SEM) on a Quanta-450 (EIF) electron microscope with a field-emission gun (FEG), 100 mm stage and an X-ray detector (model 150, Oxford) for energy-dispersive X-ray spectroscopy (EDS), and atomic force microscopy (AFM) was performed on a Nanoscope III AFM (Digital Instruments) operating in tapping mode, using TESP7 silicon nitride tips (Veeco NanProbe). (FIGURE S3 Supporting Information Chapter 3).

Evaluation of the synergism of amphotericin B and nystatin with AgNPs

The synergism effect was evaluated by the disk diffusion method on Mueller-Hinton medium supplemented with 2% glucose and 0.5 µg/mL methylene blue. We used commercial discs containing amphotericin B 100µg (AB)- (Cecon®) and nystatin 100 IU (NY)- (Cecon®). Each disc was impregnated with 10 µL (equivalent to 15 µg) of AgNPs. The disks were labeled as Ag@AB (disk containing amphotericin B and AgNP); and Ag@NY (disk containing nystatin and AgNP). Four discs were placed in each plate with *C. parapsilosis* (BIRLA et al., 2009).

In this study, synergism was considered as an increase in the area around the antifungal discs impregnated with AgNPs. The following formula was used: $(B^2-A^2)/A^2$ and $(D^2-C^2)/C^2$, where A, B, C and D are the inhibition zones of the disc of amphotericin B (A), Ag@ANF (B), nystatin (C) and Ag@ NYS (D). Increases in area were considered as synergism; no change was seen as indifferent, and decrease was regarded as antagonism (BIRLA et al., 2009; MONTEIRO et al., 2013).

RESULTS AND DISCUSSION

FIGURE 1 shows the characterization of AgNPs used in this study. AgNPs absorb light at around 420 nm, where we observed a strong absorption in this region with a maximum at 415 nm (FIGURE 1 (b)). It can also observe the color difference between the solution of $AgNO_3$ and the strong yellowish coloration from the colloidal suspension of AgNPs, which occurs due to absorption of surface plasmon. The resonance of surface plasmon is absent both at atomic level and in clusters (MORTON et al., 2011).

FIGURE 1- Uv-Vis absorbance: (a) $AgNO_3$ and (b) AgNPs.

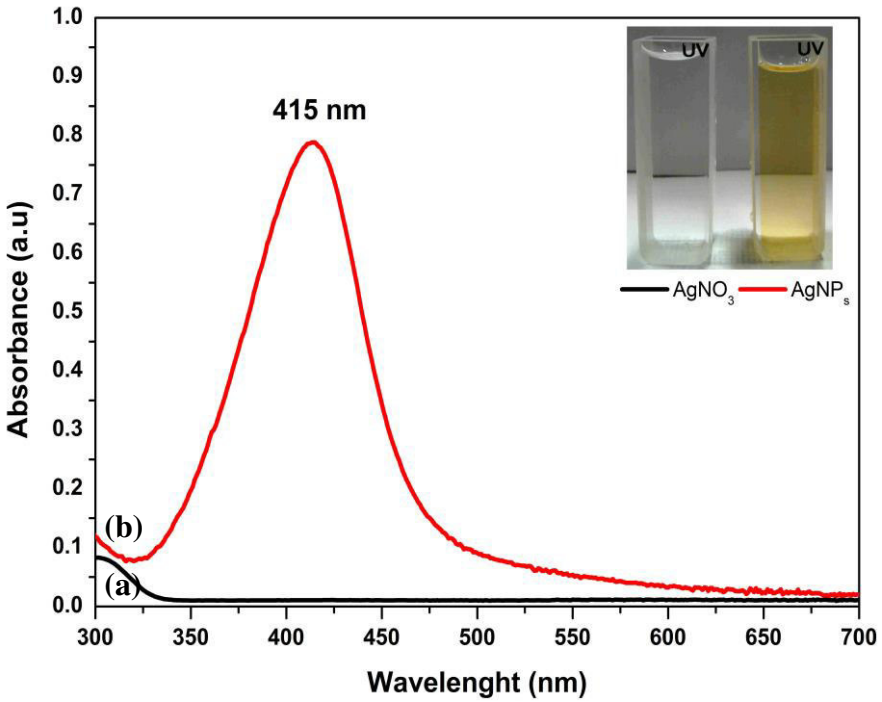

Source: Author

The average size found by the light scattering method (FIGURE 2) was 78.99 nm (± 38.11) on average (± standard deviation). The histogram generated by this technique shows nearly symmetrical monomodal particle size distribution. The zeta potential (ζ) was also measured in order to assess the stability of the colloidal suspension, where values over ± 30 mV characterized the nanoparticles as stable and difficult-to-coagulate. The sample of this study showed ζ= -39.7 mV (± 5.58). This value was higher than the one found by GHOSH et al., (2013), who by using citrate and borohydride produced AgNP with ζ= -23 mV. The AgNPs synthesized with glucose and stabilized with SDS, due to the structure of the SDS,

showed a rather negative zeta potential, which hinders the aggregation and subsequent precipitation thereof (NATH, BANERJEE, 2013; LIN et al., 2014).

FIGURE 2- DLS of AgNP-G.

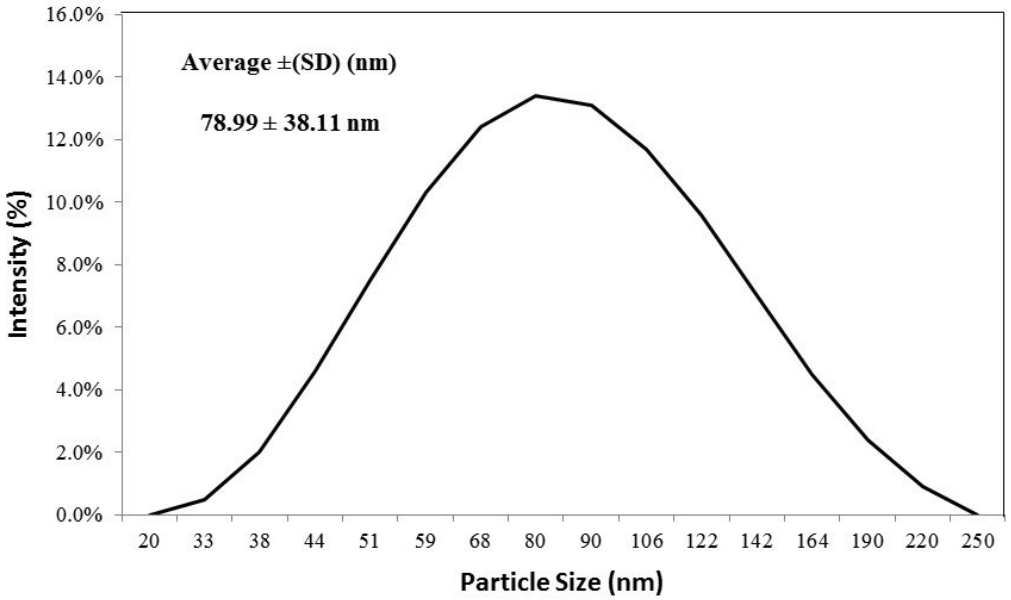

Source: Author

As can be seen in the SEM (FIGURE 3 (a)) and AFM (FIGURE 4 (a)) images, the nanoparticles are well distributed with no agglomerations. Our results are in agreement with other studies described in the literature (KHAN et al., 2013). FIGURES 3 and 4 also show the histograms of the sizes of AgNPs obtained by microscopy. An average size of 24.04 nm (± 17.93) (± standard deviation) was observed for SEM (FIGURE 3 (b)) and 18.17 nm (± 5.3) for AFM (FIGURE 4 (b)). When comparing the methods, we observed that light scattering provided a larger size. This value was found because the method includes the hydration layers, which substantially increases the size and the standard deviation. The values for the SEM also were somewhat high because we considered regions of clusters. SEM and AFM techniques are better suited in evaluating size, when compared to light scattering (LIN et al., 2014). In our study, all three methods showed agreement.

FIGURE 3- SEM of AgNP-G (a), histogram obtained from SEM images (b).

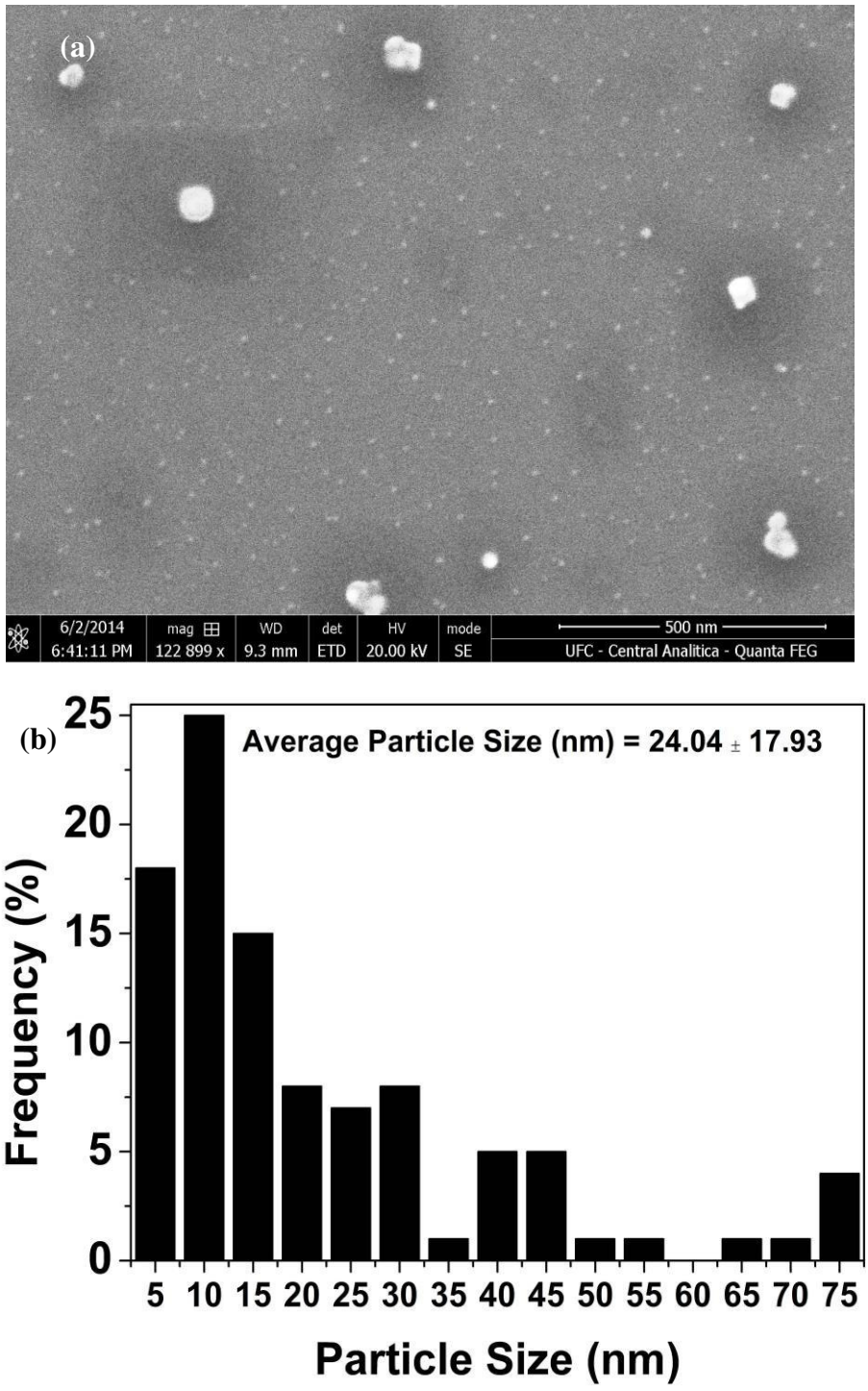

Source: Author

FIGURE 4- AFM of AgNP-G (a) and histogram obtained from AFM images (b).

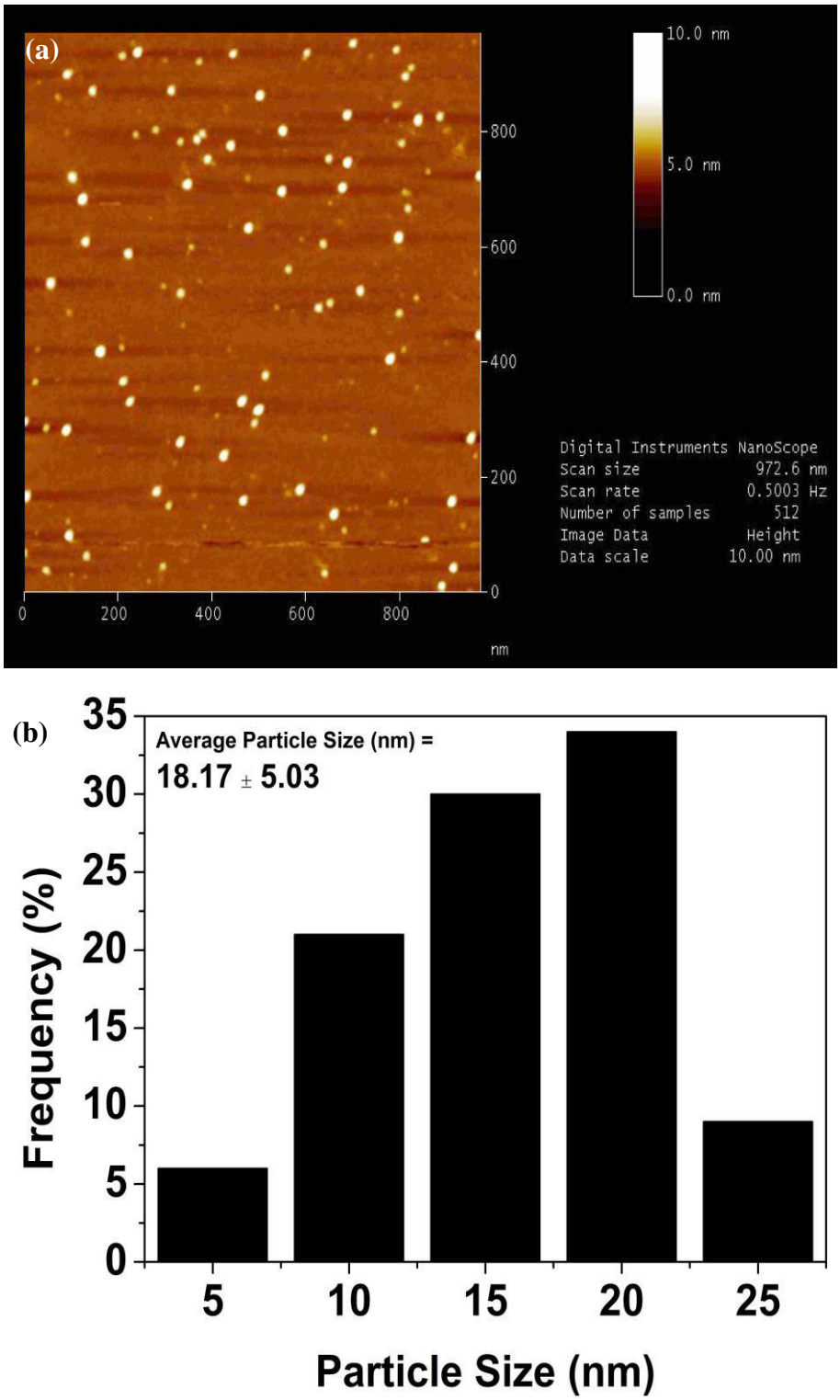

Source: Author

The identification of *C. parapsilosis* was carried out in a chromogenic medium. In such medium, this yeast exhibits a characteristic pink color, as shown in FIGURE 5 (a). The

identification was confirmed in micromorphology and molecular methods. FIGURE 5 (b) shows high synergistic activity with the combination of amphotericin B and nystatin with AgNPs. Therefore, the *C. parapsilosis* used in this study showed high sensitivity to polyene antifungals when combined with AgNPs.

FIGURE 5- (a) *C. parapsilosis* on chromogenic medium. (b) Effect of polyene antifungals alone and associated with AgNPs, 1- amphotericin B alone; 2-nystatin alone; 3-Ag@aAB; 4-Ag@NY. (c) Detail shows the effect of nystatin alone (1) and Ag@NY (2).

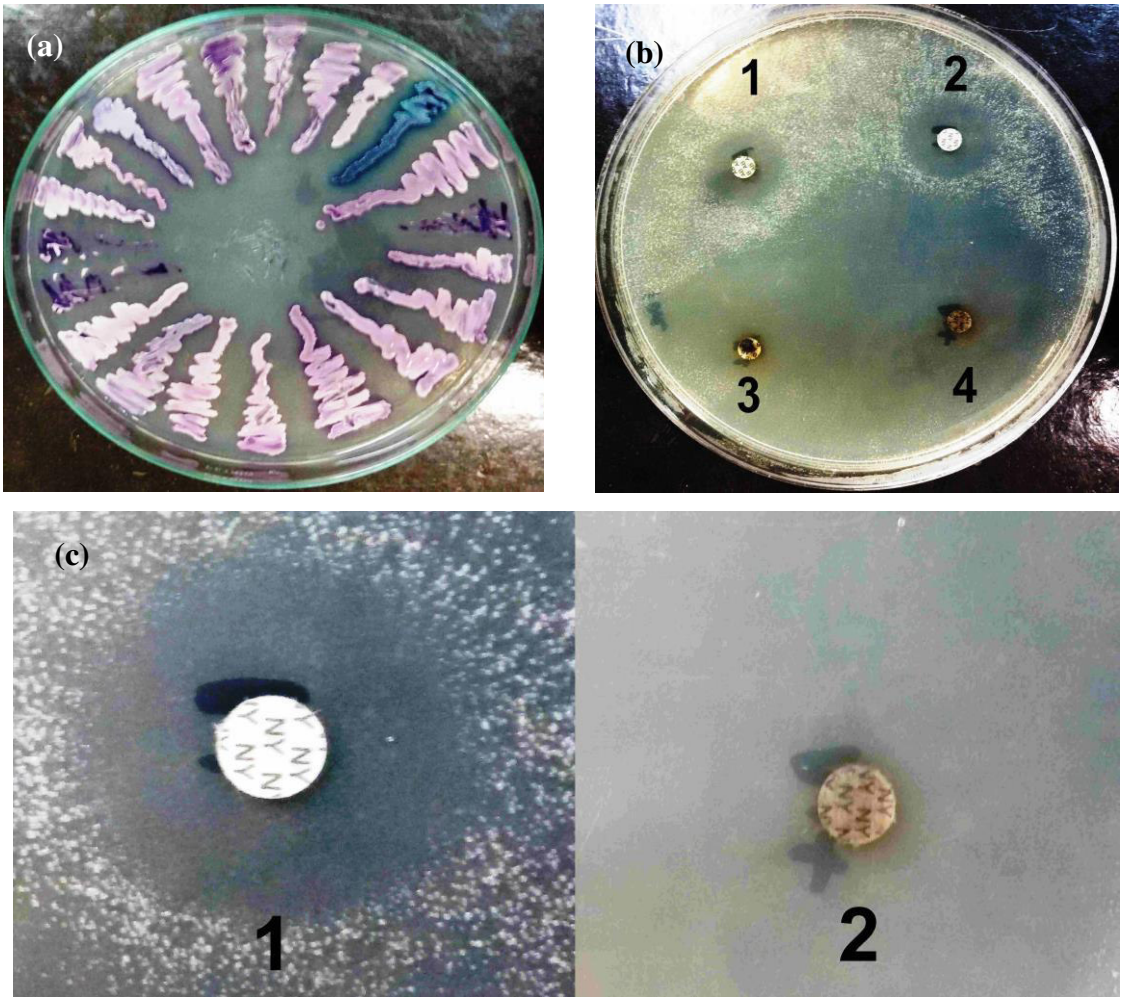

Source: Author

The disks impregnated with AgNPs showed an increased inhibition zone, which characterizes synergistic action. In FIGURE 5 (c), we can observe in detail the enlargement of the area around the nystatin disk (NY). This result can be observed numerically in Table 1 and, as can be seen in FIGURE 6, the combination of polyene antifungals and AgNPs were effective against *C. parapsilosis* and statistically significant.

Table 1- Antifungal activity of AB, NY discs alone and Ag@AB, Ag@NY against *C. parapsilosis*.

Yeasts(*n*)	Halo (mm)				Increased fold area (%)	
	A	B	C	D	$(B^2 - A^2)/A^2)$	$(D^2 - C^2)/C^2)$
	AB	Ag@AB	NY	Ag@NY	Ag@AB	Ag@NY
C. parapsilosis (10)	21.1	37.9	21.0	43.0	222.6	319.3

AB- amphotericin B; Ag@AB- amphotericin B +AgNP; NY- Nystatin, Ag@NY- Nystatin+AgNP. Mean surface area of the inhibition zone (mm^2) was calculated for each combination tested from the mean diameter. Increased fold area was calculated using $(B^2 - A^2)/A^2$ and $(D^2 - C^2)/C^2$ (x 100), where A and B and C are the inhibition zones for A, B, C and D, respectively.

Source: Author

The enlargement of the area around the disks of antifungals impregnated with AgNPs was 222.6% for Ag@AB and 319.3% for Ag@NY, when compared with discs containing only antifungal agents (Table 1). In a study analyzing the synergistic action of AgNPs and antimicrobials against a group of bacteria, using the same method used in this study, the increase in area was evident, which demonstrates the potential of these compounds (BIRLA et al., 2009).

GAJBHIYE et al., (2009), studying the antifungal activity of AgNP and fluconazole, observed a powerful synergistic effect, primarily against *C. albicans*. MONTEIRO et al., (2013), analyzing the effect of the combination of AgNPs and nystatin against biofilms of *C. albicans* and *C. glabrata*, observed a synergistic effect and highlighted the importance of this combination. Our results showed that the association of nystatin with AgNPs was extremely effective against *C. parapsilosis* (FIGURE 5(c)). In a study of AgNPs and the antifungals fluconazole and itraconazole against *C. albicans*, a strong synergistic effect was observed (SINGH et al., 2013). However, our results were more expressive, since the studies described above used few microbial strains, whereas 10 strains of *C. parapsilosis* were used in our study.

Polyene antifungals act by binding to the plasma membrane of *C. parapsilosis*, which leads to death (AMBER et al., 2010). AgNPs bind to important cell structures and cause significant cellular damage (RAI et al., 2009). The combination of both substances can have their effects potentiated, therefore showing a large zone of growth inhibition (FIGURE 6).

FIGURE 6- Effect of polyene antifungals alone and associated with AgNPs, AB-amphotericin B alone; NY-nystatin alone; 3-Ag@AB-Amphotericin B + AgNP; Ag@NY-Nystatin + AgNP.

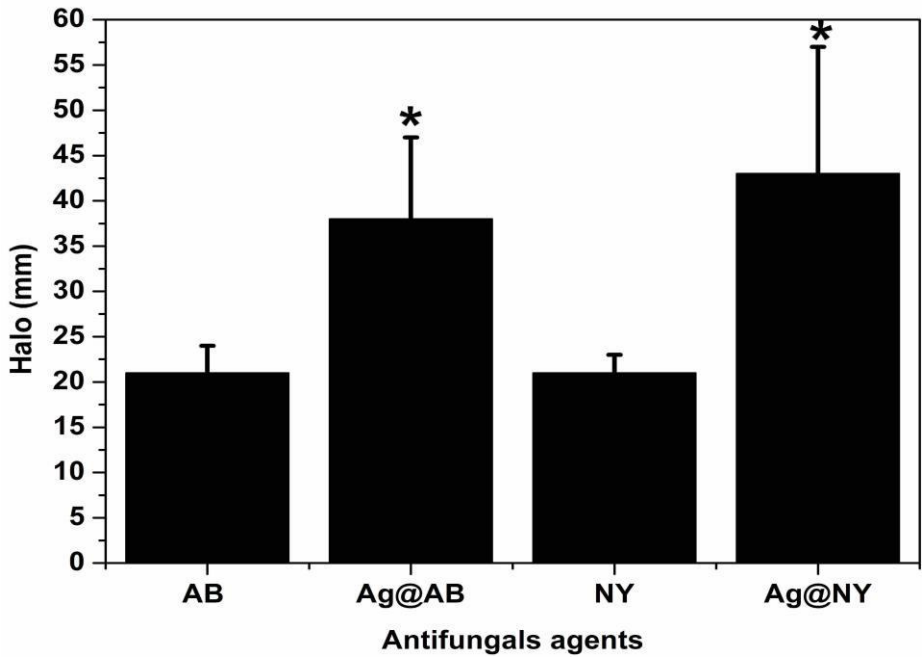

*Significantly different from antifungal discs $p<0.001$.

Source: Author

CONCLUSION

In summary, our results showed that this new technological product (polyene antifungals and AgNPs) can help fight fungal infections. Other studies with a larger number of strains and toxicity tests should be conducted to know the potential of this combination.

REFERENCES

1. AMBER, K. et al. Phytomedicine Anticandidal effect of *Ocimum sanctum* essential oil and its synergy with fluconazole and ketoconazole. **European Journal of Integrative Medicine**, v. 17, n. 12, p. 921–925, 2010. Disponível em: http://dx.doi.org/10.1016/j.phymed.2010.02.012 . Acesso em: 27 jul. 2016.
2. BINDHU, M. R.; UMADEVI, M. Antibacterial and catalytic activities of green synthesized silver nanoparticles **Spectrochimica Acta Part A : Molecular and Biomolecular Spectroscopy.** v. 135, p. 373–378, 2015. Disponível em: http://dx.doi.org/10.1016/j.saa.2014.07.045 . Acesso em: 17 mai. 2016.
3. BIRLA, S. S. et al. Fabrication of silver nanoparticles by *Phoma glomerata* and its combined effect against *Escherichia coli* , *Pseudomonas aeruginosa* and *Staphylococcus aureus*. **Letters in Applied Microbiology**, v. 48, n. 2, p. 173–179, 2009. Disponível em: http://doi.wiley.com/10.1111/j.1472-765X.2008.02510.x . Acesso em: 9 abr. 2014.
4. COLOMBO, A.L. et al. Original article Brazilian guidelines for the management of candidiasis – a joint meeting report of three medical societies : Sociedade Brasileira de Infectologia , Sociedade Paulista de Infectologia and Sociedade Brasileira de Medicina Tropical. **Brazilian Journal of Infectious Diseases**, v. 17, n. 3, p. 283–312, 2013. Disponível em: http://linkinghub.elsevier.com/retrieve/pii/S1413867013000998 . Acesso em: 12 nov. 2014.
5. DARROUDI, M. *et al*. Green synthesis and characterization of gelatin-based and sugar-reduced silver nanoparticles. **International Journal of Nanomedicine**, v. 6, n. 1, p. 569–574, 2011. http://www.dovepress.com/green-synthesis-and-characterization-of-gelatin-based-and-sugar-reduce-peer-reviewed-article-IJN . Acesso em: 2 jan. 2014.
6. DENNING, D. W.; HOPE, W. W. Therapy for fungal diseases : opportunities and priorities. **Trends in Microbiology**, v. 18, n. 5, p. 195–204, 2010. Disponível em: http://dx.doi.org/10.1016/j.tim.2010.02.004 . Acesso em: 15 out. 2015.
7. EGGIMANN P., PITTET D Candidemia y candidiasis generalizada. **EMC - Anestesia-Reanimación**, v.36, n.1, p.1–26. 2010. http://linkinghub.elsevier.com/retrieve/pii/S1280470310704394 . Acesso em: 23 ago. 2015.
8. GAO, Y. et al. Synergistic effect of doxycycline and fluconazole against Candida albicans biofilms and the impact of calcium channel blockers. **FEMS Yeast**

Research, v. 13, n. 5, p. 453–462, ago. 2013. Disponível em: http://femsyr.oxfordjournals.org/cgi/doi/10.1111/1567-1364.12048 . Acesso em: 27 jul. 2016.

9. GAJBHIYE, M. *et al*. Fungus-mediated synthesis of silver nanoparticles and their activity against pathogenic fungi in combination with fluconazole. **Nanomedicine : Nanotechnology, Biology, and Medicine**, v. 5, n. 4, p. 382–6, 2009. Disponível em: http://www.ncbi.nlm.nih.gov/pubmed/19616127 . Acesso em: 28 nov. 2014. Acesso em: 17 jul. 2014.
10. GHOSH I.N. et al. Synergistic action of cinnamaldehyde with silver nanoparticles against spore-forming bacteria: a case for judicious use of silver nanoparticles for antibacterial applications. **International Journal of Nanomedicine,** v8, n.1, p.4721–31, 2013. Disponível em: http://www.dovepress.com/synergistic-action-of-cinnamaldehyde-with-silver-nanoparticles-against-peer-reviewed-article-IJN . Acesso em: 18 dez. 2014.
11. KHAN, M. et al. Green synthesis of silver nanoparticles mediated by *Pulicaria glutinosa* extract. **International Journal of Nanomedicine**, v. 8, p. 1507–16,. 2013. Disponível em: http://www.pubmedcentral.nih.gov/articlerender.fcgi?artid=3633585&tool=pmcentrez&rendertype=abstract . Acesso em: 2 dez. 2014.
12. LI, G. et al. Fungus-mediated green synthesis of silver nanoparticles using *Aspergillus terreus*. **International journal of molecular sciences**, v. 13, n. 1, p. 466–76, jan. 2012. Disponível em: http://www.pubmedcentral.nih.gov/articlerender.fcgi?artid=3269698&tool=pmcentrez&rendertype=abstract . Acesso em: 19 nov. 2014.
13. LIN, P. et al. Techniques for physicochemical characterization of nanomaterials. **Biotechnology Advances**, v. 32, n. 4, p. 711–726, 2014. Disponível em: http://dx.doi.org/10.1016/j.biotechadv.2013.11.006 . Acesso em: 27 jul. 2015.
14. MENEZES, E. A. et al. *In vitro* synergism of simvastatin and fluconazole against *Candida* species. **Rev Inst Med Trop Sao Paulo.** v.54, n.1, p.197–199, 2012. Disponível em: http://www.ncbi.nlm.nih.gov/pubmed/22850990 .Acesso em: 14 jul. 2014.
15. MONTEIRO, D. R. et al. Antifungal activity of silver nanoparticles in combination with nystatin and chlorhexidine digluconate against *Candida albicans* and *Candida*

glabrata biofilms. **Mycoses**, v. 56, n. 6, p. 672–680, 2013. Disponível em: Disponível em: http://doi.wiley.com/10.1111/myc.12093 .Acesso em: 5 fev. 2014.

16. MORTON, S. M.; SILVERSTEIN, D. W.; JENSEN, L. Theoretical Studies of Plasmonics using Electronic Structure Methods. **Chemical Reviews**, v. 111, n. 6, p. 3962–3994, 8 jun. 2011. Disponível em: http://pubs.acs.org/doi/abs/10.1021/cr100265f . Acesso em: 31 jul. 2014.
17. NATH, D.; BANERJEE, P. Green nanotechnology - a new hope for medical biology. **Environmental Toxicology and Pharmacology**, v. 36, n. 3, p. 997–1014, nov. 2013. Disponível em: http://dx.doi.org/10.1016/j.etap.2013.09.002 . Acesso em: 22 mar. 2014.
18. QIAN, Y. et al. Biosynthesis of silver nanoparticles by the endophytic fungus *Epicoccum nigrum* and their activity against pathogenic fungi. **Bioprocess and Biosystems Engineering**, v. 36, n. 11, p. 1613–1619, 2013. Disponível em: http://link.springer.com/10.1007/s00449-013-0937-z . Acesso em: 7 set. 2015.
19. RAI, M.; YADAV, A.; GADE, A. Silver nanoparticles as a new generation of antimicrobials. **Biotechnology Advances**, v. 27, n. 1, p. 76–83, 2009. Disponível em: http://www.ncbi.nlm.nih.gov/pubmed/18854209 . Acesso em: 9 jul. 2014.
20. SINGH, M. et al. Metallic silver nanoparticle: A therapeutic agent in combination with antifungal drug against human fungal pathogen. **Bioprocess and Biosystems Engineering**, v. 36, n. 4, p. 407–415, 2013. Disponível em: http://link.springer.com/10.1007/s00449-012-0797-y . Acesso em: 19 dez. 2014
21. VASCONCELOS, A. A.; MENEZES, E. A.; CUNHA, F. A. Chromogenic Medium for Direct Susceptibility Testing of Candida spp. Isolated from Urine. **Mycopathologia**, v. 172, n. 2, p. 125–130, 2011. Disponível em: http://link.springer.com/10.1007/s11046-011-9407-9 . Acesso em: 27 jul. 2016.
22. ZEIDLER, U. et al. Synergy of the antibiotic colistin with echinocandin antifungals in Candida species. **Journal of Antimicrobial Chemotherapy**, v. 68, n. 6, p. 1285–1296, 1 jun. 2013. Disponível em: http://www.jac.oxfordjournals.org/cgi/doi/10.1093/jac/dks538 . Acesso em: 7 fev. 2016.

CHAPTER FOUR

Micofabrication of multifunctional silver nanoparticles by *Rhodotorula glutinis* and *Rhodotorula mucilaginosa*: antifungal, catalytic and cytotoxic activities

ABSTRACT

Silver nanoparticles (AgNPs) are structures with several technological applications and may be synthetized by chemical, physical and biological methods. Fungi have a wide enzymatic range and it is easy to handle. However, there are few reports of yeasts with biosynthetic ability to produce stable AgNPs. The purpose of this study was to isolate and identify soil yeasts (*Rhodotorula glutinis* and *Rhodotorula mucilaginosa*). After this step, the yeasts were used to obtain AgNPs, with a subsequent catalytic and antifungal activity evaluation. Silver Nanoparticles were characterized by UV–vis, DLS, FTIR, XPRD, EDX, SEM, TEM and AFM. The AgNPs produced by *R. glutinis* and *R. mucilaginosa* measured 15.45 nm ± 7.94 and 13.70 nm ± 8.21 (average ± SD), respectively, when analyzed by TEM. AgNPs showed high catalytic capacity in the degradation of 4-nitrophenol and methylene blue. AgNPs showed high antifungal activity against *C. parapsilosis* and increase the activity of fluconazole (42.2% for *R. glutinis* and 29.7% for *R. mucilaginosa*). The cytotoxicity of AgNPs was only observed at high concentrations. Finally, two yeasts with the ability to produce AgNPs were described, and these particles showed multifunctionality and can represent a technological alternative in many different areas with potential applications.

Keywords: Silver nanoparticles; *R. glutinis*; *R. mucilaginosa*; 4-nitrophenol.

INTRODUCTION

Nanotechnology is an expanding scientific field that studies nanostructures from the molecular structure, with a recent focus on metallic nanoparticles. The most extensively studied particles are silver, gold, copper, zinc, cadmium, among others (DURÁN et al., 2011). Nanoparticles are entities that possess from 1 to 100 nm in any of its dimensions (BIRLA et al., 2009; HULKOTI et al., 2014).

These structures have different chemical and physical properties compared to the bulk materials, and may be used in different technological fields. Applications vary and include catalysis (NARAYANAN et al., 2013; SUVITH et al., 2014; VIDHU, PHILIP, 2014a; VIDHU, PHILIP, 2014b), chemical sensors (CHEN, CHATTERJEE, 2013), drug release (SAPSFORD et al., 2013), cancer treatment and diagnostic (BERTRAND et al., 2014), and antibacterial agents (HAJIPOUR et al., 2012; PELGRIFT et al., 2013).

More specifically on silver nanoparticles (AgNPs), some points referring to their synthesis and stability are not fully understood yet (XIA et al., 2009). AgNPs synthesis can be done through chemical, physical and biological methods (IRAVANI et al., 2011; THAKKAR et al., 2010; XU et al., 2010). Chemical methods use toxic reagents such as hydrazine and ammonium that can cause damage to the environment and health of men and animals (GOLINSKA et al., 2014). Physical methods are time-consuming, require financial resources, demand trained personnel, and expensive machines that are difficult to operate effectively (PRABHU, POULOSE, 2012; XU et al., 2010). Biological methods use plants, micro-organisms, pigments and derived from cells to produce AgNPs. These methods are less polluting, because they do not use toxic reagents and generate biodegradable waste (ASMATHUNISHA, KATHIRESAN, 2013; NARAYANAN, SAKTHIVEL, 2010).

In the last years, interest in AgNPs synthetized by microorganisms, mainly bacteria and fungi has been raising considerably (HULKOTI et al., 2014; KALPANA, LEE, 2013). This interest is due to the fact that these organisms can furnish a synthesized route that is simple, cheap, sustainable and produce stable AgNPs, with determined sizes and form to be used with commercial intent (NARAYANAN, SAKTHIVEL, 2010; QUESTER et al., 2013).

Many studies describe AgNPs production by fungi. In general, the synthesis is simple, cheap, easy to be executed and with a good yield (BANU, RATHOD, RANGANATH, 2011; DAR, INGLE, RAI, 2013). The advantages of fungi when compared to bacteria are that they possess few nutritional demands, produce a large amount of biomass and can be easily handled. Furthermore, most species used in the AgNPs production are not pathogenic for humans and animals, which simplifies and cheapens the process (AHLUWALIA et al., 2014; DEVI, JOSHI, 2014).

Rhodotorula glutinis (Rg) and *Rhodotorula mucilaginosa* (Rm) are pigmented yeasts, important in the food industry, found in many parts of the world and can be isolated from different substrates, like soil, water, wood and decomposing fruits (AKSU, EREN, 2005; AKSU, EREN, 2007). They produce important pigments such as β-carotene, γ-carotene, torulene and lycopene (HERNANDEZ-ALMANZA et al., 2014). They also present big potential in the biodiesel industry, because they are able to convert the main subproduct of the biodiesel industry, glycerol, into carotenoids (CUTZU et al., 2013).

Among AgNPs functionalities, the catalytic activity deserves to be highlighted, mainly because effective and ecologically correct catalyzers for the degradation of pollutants are a necessity for present times. AgNPs from biological origin are being used as catalyzers, mainly in catalytic reduction of 4-nitrophenol (4-NP) and methylene blue (MB) (KUMARI,

PHILIP, 2013). 4-NP is a compound present in effluents from chemical industries that produce insecticide, medicines and inks. This compound presents high toxicity for animals by harming mitochondria. As it is soluble in water, 4-NP contaminates water and soil collections (EDISON, SETHURAMAN, 2013). MB is an organic sulfonated dye that may present acute toxicity (UDDIN et al., 2009). MB can be reduced by strong reducer agents like $NaBH_4$ in order to form organic molecules, however, the reaction is too slow (SUVITH, PHILIP, 2014), and this factor alone reveals the need of a catalyzer.

Other important functionality of AgNPs is the high antibacterial activity and its synergic action with antibiotics available in traditional medicine (DAR, INGLE, RAI, 2013). However, action against pathogenic yeast is still little known (GAJBHIYE et al., 2009). These particles could contribute to combat bacterial and fungal infections that are difficult to control (RAI et al., 2012).

In this way, the objectives of this work were to synthetize, purify, and characterize AgNPs obtained from *R. glutinis* (Rg) and *R. mucilaginosa* (Rm) isolated from soils in Ceará-Brazil. To the best of the authors' knowledge, this is the first report of extracellular synthesis of AgNPs by Rg e Rm yeasts. Additionally, these novel biogenic AgNPs were tested in order to evaluate antifungal activity against *C. parapsilosis* and for the catalytic reaction of 4-NP and MB degradation.

MATERIALS AND METHODS

Reagents

Silver nitrate (Dinâmica- São Paulo- Brazil- purity > 99%), malt extract (Himedia-India), yeast extract (Himedia-India), peptone (Himedia-India), glucose (Dinâmica- São Paulo- Brazil- purity> 99%), agar potato-glucose (Himedia-India), NaCl (Dinâmica- São Paulo- Brazil- purity > 99%), Mueller-Hinton medium agar (Himedia-India), 4-nitrophenol (4-NP) (Dinâmica- São Paulo- Brazil- purity > 99%), methylene blue (MB) (Dinâmica- São Paulo- Brazil- purity > 99%) and fluconazole (Sigma- United States) were purchased and used without purification and its fundamental properties were assured by the manufacturers.

Isolating and Identifying Yeasts

R. glutinis and R. mucilaginosa were isolated from the soil around the Pici Campus, Federal University of Ceará (Fortaleza-Ceará-Brazil); Latitude: 3°44′20.832″S, Longitude: 38°34′12.483″W; and 3°44′21.750″S, 38°34′12.350″W, respectively. 50.0 g of soil were collected and transported, in plastic bags placed in thermal boxes, to the Microbiology Laboratory of Yeasts of the Department of Clinical and Toxicological Analysis from the Federal University of Ceará. Samples were diluted in NaCl 0.9% and added to an aqueous medium containing MGYP (malt extract (0.3%), glucose (1%), yeast extract (0.3%), peptone (0.5%); antibiotics, pH 7) and incubated 25°C/72h. After growth, the samples were inoculated on potato glucose agar and maintained at 25°C/72h (see FIGURE S1 Supporting Information Chapter 4). Yeasts suggested to belong to the *Rhodotorulla* genus were seeded again on potato-glucose agar to obtain an isolated and pure strain. The identification of genus and species was carried out in the automated system VITEC®2 from BioMéreiux® S.A., YST card.

Biosynthesis of AgNPs

Two yeasts were selected, *R. glutinis* (Rg) e *R. mucilaginosa* (Rm), after isolation and identification. The yeasts grow in Erlenmeyer flasks of 500.0 mL containing 200.0 mL of MGYP at 25°C/72h. After growth, the fungal biomass was centrifuged at 4.000 rpm for 10 min and washed three times in order to remove wastes from the culture medium. Immediately after washing, the yeasts were weighted (5.0 g, humid weight) and put in an Erlenmeyer flask with 100.0 mL of autoclaved deionized water for 48h at 25°C without agitation. After this time, the suspensions containing yeasts were filtered with a 0.45 µm membrane. To 90.0 mL the filtrate was added 10.0 mL of 10 mM $AgNO_3$, final concentration 1 mM $AgNO_3$, and they were incubated at 25°C/168h. Aliquots were removed in 24-hour intervals and tests were conducted to assess AgNPs formation. The positive control contained only the yeast extract without $AgNO_3$ and the negative control contained only the solution of 1mM $AgNO_3$ (see FIGURE S2 Supporting Information Chapter 4).

Purification of AgNPs

After 168h of reactions the AgNPs were purified by centrifuging the suspension at 10,000 rpm for 20min. The solid waste was washed three times with deionized water then dried in a desiccator. The residue was used for the following characterization phases.

Characterization of AgNPs

The light absorption spectrum of Rg and Rm AgNPs were performed using a UV-Visible spectrophotometer (Thermo Scientific GENESYS ™ 10s), in the 300-700 nm wavelength range. The size of the AgNPs was assessed using dynamic light scattering (DLS). Measurements were made using a Zetasizer Nano ZS, (Malvern Instruments in United Kingdom) (see FIGURE S3 Supporting Information Chapter 4). The solid waste of dry AgNPs produced by Rg and Rm were mixed to KBr and the Fourier transform infrared spectroscopy (FT-IR) spectrum were registered in Perkin-Elmer FT-IR Spectrum, in the range of 4000-500 cm^{-1}, with a resolution of 4 cm^{-1}.

The X-ray diffraction (XRD) was carried out with the dried residue of AgNPs. The residue was placed on a glass support of 2.5 cm x 2.5 cm, and the spectrum was carried out using Cu-Kα radiation with 2θ from 30° to 70°. The results were analyzed by PAN analytical X-pert pro MRD (Amsterdam, Netherlands).

Scanning Electron Microscopy (SEM)

The morphology, distribution and size of the AgNPs were determined using Scanning Electron Microscopy (SEM) on a Quanta-450 (EIF) electron microscope with a field-emission gun (FEG), 100 mm stage and an X-ray detector (model 150, Oxford) for energy-dispersive X-ray spectroscopy (EDS).

Transmission Electron Microscopy (TEM)

Silver nanoparticles of Rg and Rm were analyzed by transmission electron microscopy (TEM) analysis. TEM samples were prepared by pouring a drop of the suspension of silver nanoparticles on carbon-coated copper grids and by allowing water to evaporate. The

shape and size of nanoparticles were determined from TEM micrographs. The software (Advanced Microscopy Techniques, Danvers, MA) for the digital TEM camera was calibrated for size measurements of the nanoparticles. TEM measurements were performed on a JEOL model 1200EX

Atomic Force Microscopy (AFM)

The Atomic Force Microscopy analyses were performed using a Multimode Nanoscope IIIa (Bruker, CA, USA), in Tapping Mode (or intermittent mode). In this scanning mode the AFM tip approaches the sample surface (but does not touch it) with beats of similar amplitude to the resonance amplitude of the AFM cantilever. In this way we avoid the action of lateral forces between the tip and delicate samples, preventing it to be dragged on the substrate surface or damaged in sample surface. We use a rectangular probe model TESPA7 (Veeco) with nominal spring constant of k = 20-80 N/m and resonance frequency of f = 291-326 kHz. The scan parameters for the nanoparticles images acquisition were 0.5 Hz of scan rate and 512 x 512 lines of resolution.

The ICP-OES measurements

Inductively coupled plasma optical emission spectroscopy (ICP-OES) was also carried out to determine the resulting Ag concentration in each AgNPs solutions. In preparation for ICP-OES, the samples were first digested in a solution of HNO_3 and HCl. A 20 μL of each sample was diluted to 1 mL with water and then heated to 80°C in a covered test tube. To this, 1 mL of HNO_3 was added, and the mixture was allowed to sit for 1 h at 80°C. HCl (2 mL) was then added to form aqua regia, and the mixture was allowed to sit for an additional hour. Following cooling, the solutions were dispersed into 10 mL of water in a volumetric flask.

Catalytic Activity of AgNPs

Catalytic Reduction of 4-NP

The catalytic activity of biogenic AgNPs with 4-NP was based on the protocol described by NARAYANAN, et al., 2013. Briefly, in a quartz cuvette it was added 2.77 mL

of ultra-pure water, 30 µL of 4-NP (0.01M) e 200 µL of $NaBH_4$ (0.1 M), all mixed immediately before the tests were performed. To this mixture, 25.0 µL (C_{AgNPs}= 50.0 µg/mL) of AgNPs produced by Rg and Rm were added. The reaction was probed by UV-Vis spectroscopy (250-500 nm) for a period of 30.0 minutes. Measurements were taken every 2.0 minutes. The reduction process was determined by the changes on the absorption at 400 nm over time. The progress of the reaction in the mixture without the presence of AgNPs was also monitored under the same conditions.

Catalytic reduction de MB

The evaluation of the catalytic activity of AgNPs from Rg and Rm was performed as described by SUVITH and PHILIP, 2014, with modifications. Briefly, four tubes were used; Tube 1: Methylene Blue (MB) (10.0 mL, $9.37x10^{-5}$ M) and water (3.0 mL); tube 2: MB and $NaBH_4$ (3.0 mL, $5.28x10^{-2}$ M); tube 3: MB, $NaBH_4$ and 25 µL ((C_{AgNPs}= 50.0 µg/mL) of AgNPs from Rg; tube 4: MB, $NaBH_4$, and 25 µL ((C_{AgNPs}= 50.0 µg/mL) of AgNPs from Rm. The tubes were shaken continuously during 1 min and left to rest for 30 min. The reaction was monitored by UV-Vis spectroscopy (250-500 nm) for a period of 30.0 minutes. Measurements were taken every 2.0 minutes.

Identification of Candida parapsilosis and Antifungal activity of AgNPs

A total of 35 strains of *Candida parapsilosis* isolated from blood samples were used in antifungal tests. The strains were plated on potato dextrose agar and incubated at 37°C for 24/48h. The presumptive identification and purity of the strains was performed in a chromogenic medium and incubated at 35°C for 24/48h (see FIGURES S4-S6 Supporting Information Chapter 4). PCR was used to confirm the identity of *C. parapsilosis*; we used the primers (SADH) (S1F, 5'-GTT GAT GCT GTT GGA TTG-3') and (S1R, 5'-CAA TGC CAA ATC TCC CAA-3'), and the PCR conditions were 95°C for 5 minutes followed by 40 cycles at 92°C for 1 minute, 45°C for 1 minute and 68°C for 1 minute. The extension was performed at 72°C for 7 minutes (VASCONCELOS, MENEZES, CUNHA, 2011).

The microdilution technique was used to determine minimal inhibitory concentrations (MICs), according to the M27-A3 protocol of the Clinical and Laboratory Standards Institute (CLSI) (see FIGURES S7 Supporting Information Chapter 4). (MENEZES et al., 2013; VASCONCELOS, MENEZES, CUNHA, 2011). The isolates were

cultured on potato dextrose agar at 35°C for 48 h. The inoculum was prepared by suspension of colonies in saline solution (0.85 %), and the number of cells was measured with a hemocytometer having been diluted to obtain 0.5×10^2 to 2.5×10^3 CFU/mL in each well. AgNPs were tested in the range 0.025 to 12.5 µg/mL, fluconazole was used as control and tested in the range 0.125 to 64 µg/mL. The samples were incubated at 35 °C for 48 h. MIC values were determined visually after 48 h incubation as the lowest concentration of drug that caused a significant diminution (90% inhibition) of growth relative to that of the growth control. These assays were performed in triplicate, and the quality control was performed with *Candida parapsilosis* ATCC 22019.

Antifungal activity of AgNPs associated with fluconazole (synergism)

The effect of synergism was evaluated by the disk diffusion method on Mueller-Hinton medium supplemented with 2% glucose and 0.5 µg/mL of methylene blue. Commercial discs containing fluconazole 25 µg were used (Cecon®). The discs were impregnated with 10 µL (equivalent to 0.5 µg AgNPs) de AgNPs produced by Rg and Rm, and then labeled as Ag@FluRg and Ag@FluRm (disk containing fluconazole and AgNPs from Rg and Rm, respectively). The discs were placed on each plate with *C. parapsilosis*. In this study, the synergistic effect was considered as an increase in the area around the disks impregnated with AgNPs compared to disks with fluconazole only. The evaluation of the synergistic effect was conducted under the following formulas: $(B^2-A^2) / A^2$ e $(C^2-A^2)/ A^2$, in which A, B e C are inhibition zones of (A) fluconazole disk, (B) Ag@FluRg and (C) Ag@fluRm (BIRLA, et al., 2009).

In vitro cytotoxicity of AgNPs produced by Rg and Rm

To determine the cytotoxic activity of the AgNPs on HK-2 (human kidney cells), 1×10^5 cells/mL in DMEM were grown in a 96-well plate at 37°C, 5% CO_2 for 24 hours, followed by treatment of cells with different concentrations (0.08 to 10 µg/mL) of AgNPs Rg and Rm for another 24 hours. To determine the cell viability, MTT at a concentration of 0.1µg/mL was added to the wells and incubated for 4 hours at 37°C, 5% CO_2 in dark. In metabolically active cells, MTT was reduced to an insoluble dark purple formazan. The formazan crystals were dissolved in dissolving buffer (11.0 g SDS in 50 mL of 0.02 M HCl and 50 mL isopropanol). The absorbance was read at 570 nm in ELISA reader (Biotek,

Germany), compared with the untreated cells and percentage of viable cells was calculated (RETTONDIN et al., 2016)

Statistical and Image Analysis

The size of AgNPs was realized using the Image J® free software (National Institutes of Health, USA, version 1.48v). The histograms were produced using OriginPro® 8 (OriginLab Corporation, Northampton, Massachusetts, USA). The inhibitions zones were expressed as arithmetic mean using SPSS software (SPSS Inc., Chicago, USA, version 16.0).

RESULTS AND DISCUSSION

Morphological and structural characterization

Yeasts are fungi that show similarities with bacteria, for they develop as isolated colonies and possess a wide enzymatic range, though they use for mediating the AgNPs synthesis is still very restrict (THAKKAR, MHATRE, PARIKH, 2010; MOHANPURIA, YADAV, 2008). *Yarrowia lipolytica,* a pigmented yeast, was successfully used in the production of AgNPs (APTE et al., 2013). *Saccharomyces boulardii*, another yeast that was used in the production of AgNPs (KALER, JAIN, BANERJEE, 2009). Our study used two pigmented yeasts of the *Rhodotorula* genus, *R. glutinis* (FIGURE 1(a)) and *R. mucilaginosa* (FIGURE 1 (b)), which proved very effective in the production of AgNPs.

FIGURES 1(c) and (d) show the AgNPs colloidal suspensions formed during the exposure process of each yeast filtrate to $AgNO_3$ 1mM solution. A characteristic AgNPs color can be observed, and this coloring is due to the excitation event on the nanoparticle surface, known as localized surface plasmon resonance (LSPR) (XIA et al., 2009). The colour intensity also depends upon size of AgNPs synthesized. The colour change during metallic nanoparticle synthesis is attributed to the collective oscillation of free conduction electrons induced by an interacting electromagnetic field (AHLUWALIA et al., 2014).

The submicroscopic particles and the NPs, in their aqueous dispersions, can be detected simply by a laser pointer. The incident light is scattered on the particles and this way passes through the dispersion, which can be observed (under the angle of 90°) as the Tyndall effect. We can observe this effect in FIGURE S8 Supporting Information Chapter 4.

The AgNPs descripted in this study absorb around at 400 nm (FIGURES 2(a) and (b)), and this absorption depends on the size, shape, and many other factors such as the dielectric constant of the medium in which they are suspended (BALAJI et al., 2009).

FIGURE 1- *R. glutinis* (a), *R. mucilaginosa* (b), AgNPs by *R. glutinis* (c), AgNPs by *R. mucilaginosa* (d).

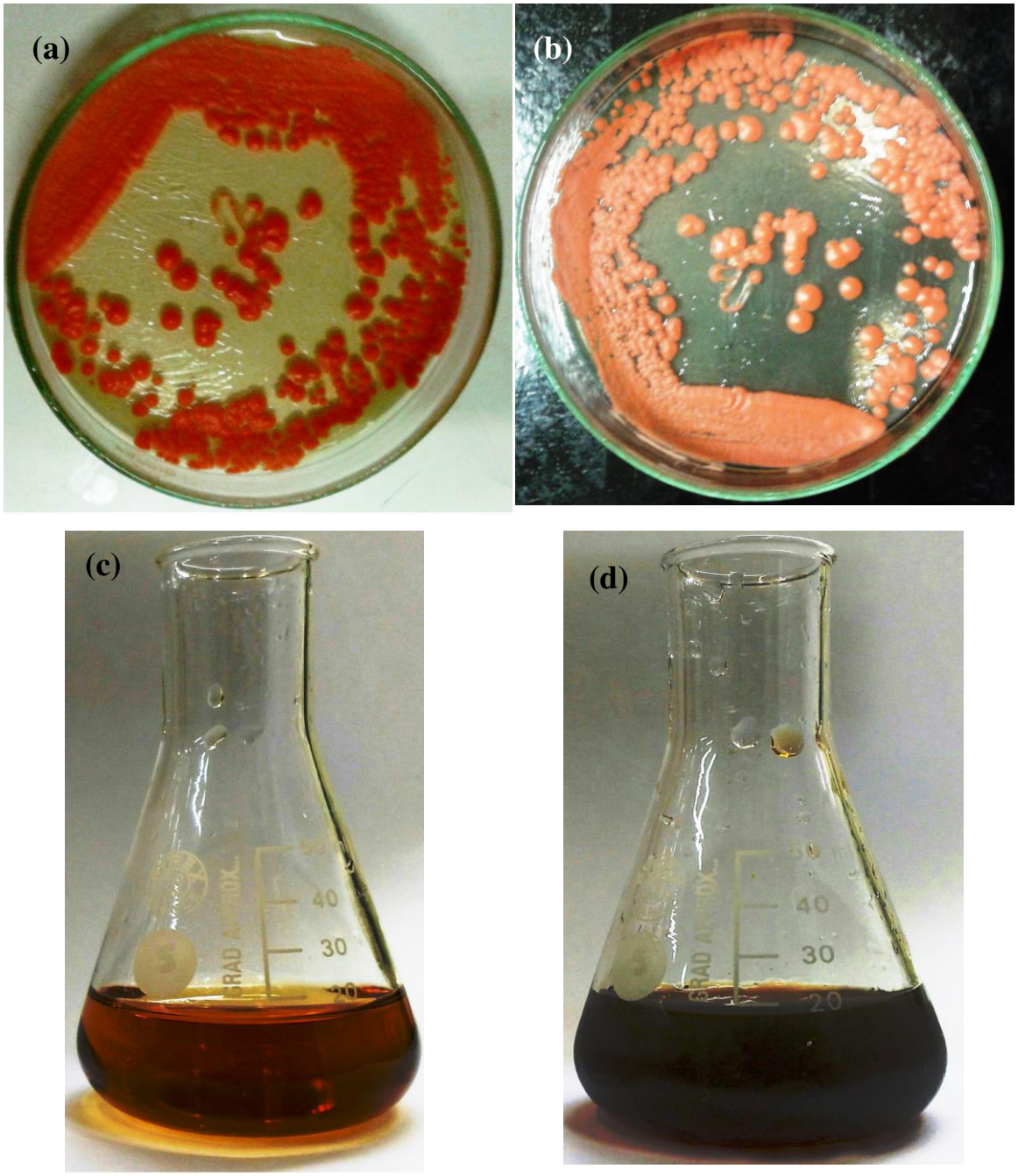

Source: Author

FIGURE 2- UV–Vis of AgNPs: *R. glutinis* (a); *R. mucilaginosa* (b).

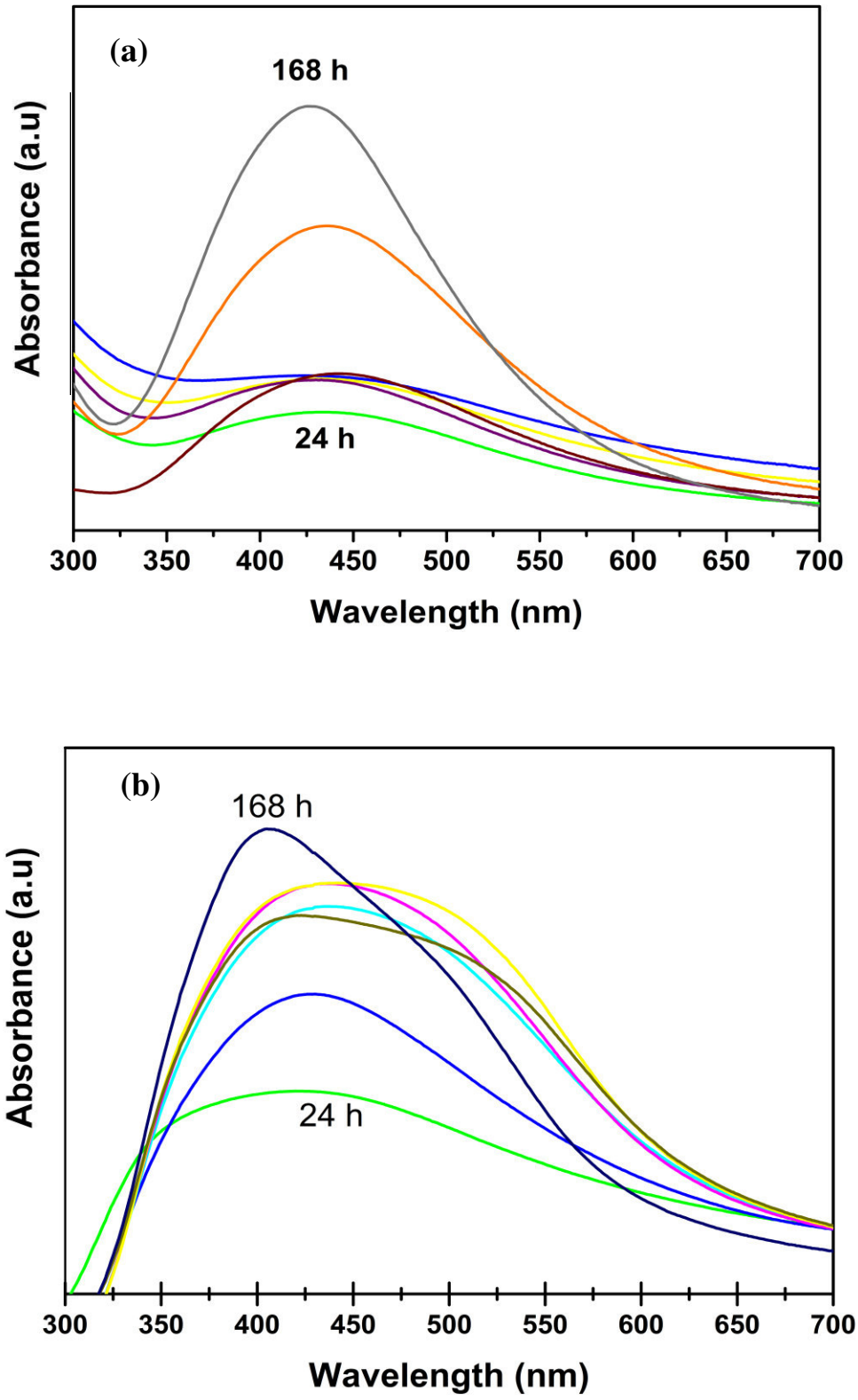

Source: Author

In the details of FIGURES 2(a) and (b), we can observe the absorbance evolution over the days, with a rising in the intensity with time, associated with the concentration of AgNPs in reactional medium. Therefore, the two yeasts *R. glutinis* and *R. mucilaginosa* were able to produce AgNPs.

The yeasts described in this study (Rg and Rm) were able to produce AgNPs after 24 hours of exposure to the 1mM $AgNO_3$ solution. However, other fungi such as *Fusarium solani* was able to produce AgNPs in only 2h of exposure (INGLE et al., 2009). In other examples such as *Pestalotia* sp. (RAHEMAN et al., 2011) and *Guignardia mangiferae* (BALAKUMARAN, RAMACHANDRAN, KALAICHELVAN, 2015), they were able to produce AgNPs after 2h and 12h of exposure, respectively. However, many studied fungi, including *Rhodotorulla* described in this study, produce AgNPs in a minimum period of 24h (AMERASAN et al., 2016, GOSWAMI, SARKAR, GHOSH, 2013, JEBALI, RAMEZANI, KAZEMI, 2011). This time difference in the production of AgNPs depends on the constituents of the fungal extract. The components present in this extract define the reduction and stabilization of the AgNPs (YADAV et al., 2015).

AgNPs formed by fungi obviously depend on the species involved. They can vary in size, shape, capping proteins, and these changes directly interfere on the maximum UV-Vis absorption band (MADDEN et al., 2015). The fungus *Cladosporium cladosporioides* (BALAJI et al., 2009), produced AgNPs with a maximum absorption at 415 nm, while *Mucor circinelloides* (SATHISHKUMAR et al., 2015), and *Cylindrocladium floridanum* (NARAYANAN, PARK, SAKTHIVEL, 2013), were at 440 and 436 nm, respectively. As it can be observed, the maximum absorption depends on the species studied, since it involves substances produced by each fungal species.

FIGURE 3 presents the DLS measurements of AgNPs produced by Rg (FIG. 3 (a)) and Rm (FIG. 3. (b)), respectively. Rg produced AgNPs with size 108.9 ± 65.7 nm (Average ± SD), while Rm was 119.0 ± 59.4 nm (Average ± SD). The AgNP produced by both yeasts exhibited polydispersity index (PDI) below 0.250, which characterize monodisperse particles (DU et al., 2015). JAIN et al., 2011 when studying AgNPs produced by *Aspergillus flavus* observed that 80% of the particles had sizes of 17 ± 5.9 nm. CHAN, DON., 2013, by studying various fungi with the ability to produce AgNPs, observed that the studied species produced particles with PDI below 0.25. Our results are consistent with those found in the literature for AgNPs produced by fungi.

FIGURE 3- DLS and zeta potential of AgNPs by *R. glutinis* (a) and *R. mucilaginosa* (b).

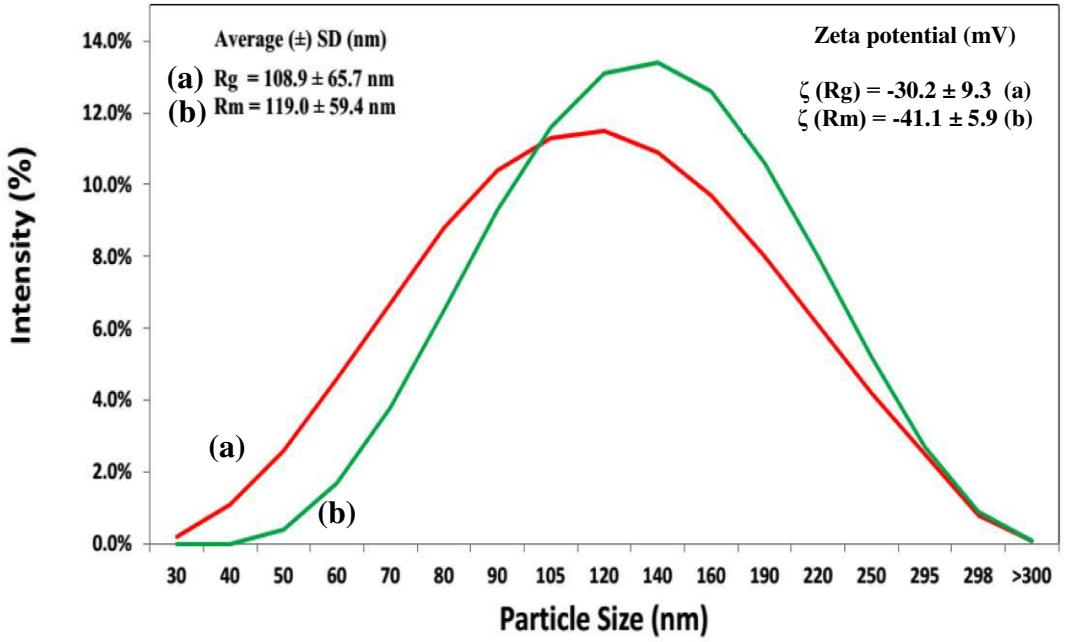

Source: Author

In the colloidal suspensions produced by AgNPs, the values of zeta potential (ζ) were -30.2 ± 9.3 and -41.1 ± 5.9 mV for Rg and Rm (FIG. 3), respectively. Values of ζ bigger than ±30 mV provide stability to the solutions and avoid flocculation and precipitation of AgNPs (LIN et al., 2014).

RODRIGUES et al., 2013, when studying isolated fungi from the Brazilian seacoast with the ability to produce AgNPs found positive and negative ζ potential, higher than 10 mV in magnitude (±10). *Agaricus bisporus* was able to produce AgNPs with ζ of −7.23 mV (EL-SONBATY, 2013).

AHLUWALIA et al., 2014, when working with fungus *T. harzianum* found a ζ of −17.19 mV. DU et al., 2015, when studying the fungus *Penicillium oxalicum*, evaluated the ζ in different pHs and observed a variation from -4.18 mV to -20.6 mV. Therefore, the size of the particle and ζ are important properties that may influence in the biological activity of the nanoparticles, and these properties are key factors on the interaction with surfaces (EL-SONBATY, 2013). Our results were superior to various found in the literature, which shows the stability of AgNPs produced by Rg and Rm. The AgNPs produced by Rm and Rg are stable after 15 months after the synthesis (see FIGURE S9 Supporting Information Chapter 4).

AgNPs synthesis in fungal extract occurs due to enzymes present in the extract (AHMAD et al., 2003). Colloidal stabilization occurs when proteins adsorbed on the surface of AgNPs avoid approximation and subsequent flocculation and precipitation. Therefore, with the objective of characterizing the biological molecules bound to the surface of the AgNPs, the samples were analyzed by FTIR. In FIGURE 4(a) and (b) and Table 1, the spectra of AgNPs from the yeasts studied in this work are shown and compared with another works (AMERASAN, et al., 2015; BARTH 2007; GOSWAMI, SARKAR, GHOSH, 2013; NARAYANAN, PARK, SAKTHIVEL, 2013; SALUNKHE et al., 2011; VIGNESHWARAN et al., 2007). The band exhibited in 3395 and 3422 cm^{-1} are due to the stretching of the hydroxyl groups (–OH), that may have four origins: residual water from drying, polysaccharides produced by the yeasts to stabilize the AgNPs, protein wastes present in the AgNPs capping, and may be due to stretching of secondary amines (-N-H) (AMERASAN, et al., 2015; CHAN, DON, 2013; CHEN, YAN, WU, 2016; NARAYANAN, PARK, SAKTHIVEL, 2013). The strong band at 1370 cm^{-1} is characteristic of N-O stretching of nitro groups (AJITHA, REDDY, REDDY, 2014).

FIGURE 4- The FTIR spectrum of AgNPs produced by *R. glutinis* (a) and *R. mucilaginosa* (b).

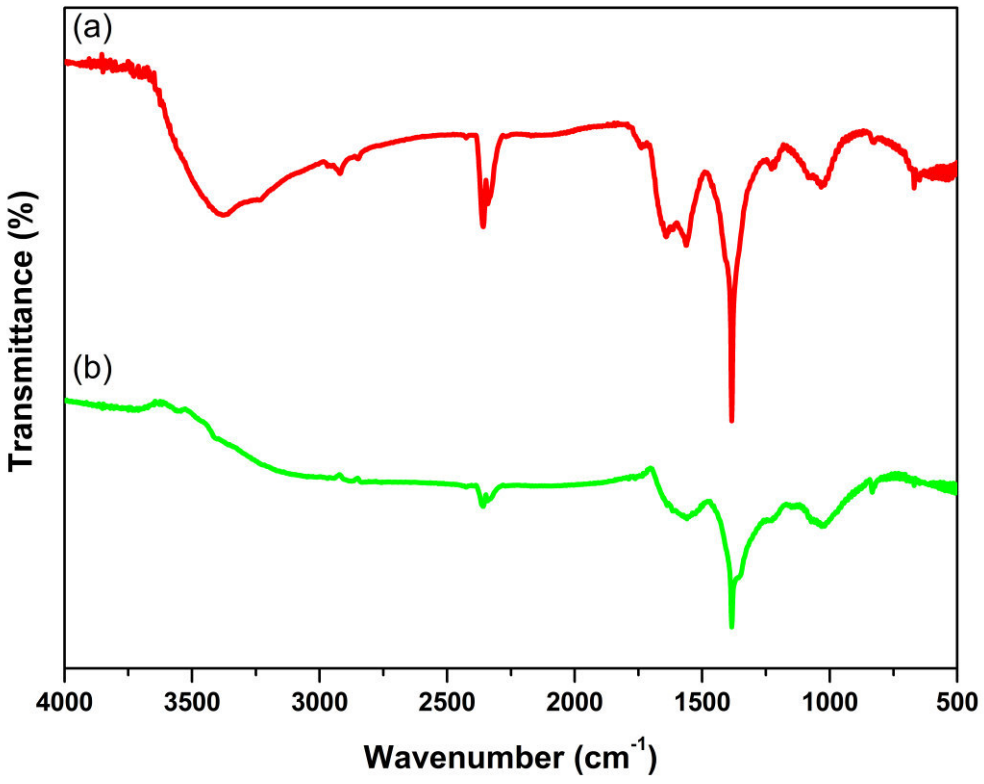

Source: Author

Table 1- FTIR of AgNPs produced by *R. glutinis* and *R. mucilaginosa.*

Major Peaks	Wavenumber (cm^{-1})		Assignment	Reference
	R. glutinis	*R. mucilaginosa*		
1	3395	3422	Hydroxyl (-OH)	NARAYANAN et al., 2013
2	2359	2359	Aliphathic C-H	GOSWAMI et al., 2013
3	2332	2319	Aliphathic C-H	SALUNKHE et al., 2011
4	1658	1644	Amide I (-C–N)	AMERASAN et al. 2015
5	1557	1550	Amide II (-C–N)	BARTH 2007
6	1370	1370	Nitro (-NO)	AJITHA, et al., 2014
7	1384	1386	Aromatic amines	SALUNKHE et al., 2011
8	1016	1016	Aliphatic amines	VIGNESHWARAN et al., 2007

Source: Author

The profile of XRPD from the samples is shown in FIGURE 5(a) and (b). The diffraction peaks are 38.2°, 44.3° and 64.6°, corresponding to the indexed plans (111), (200) and (220), respectively. They are characteristic of a face-centered-cubic (fcc) system, corresponding to metallic silver phase, JCPDS file No. 04-0783. The other peaks are related to protein impurities produced by yeasts (VERMA, KHARWAR, GANGE, 2010). The XRD patterns indicate that the AgNPs are formed in the metallic phase, although AgNPs-Rg are less crystalline than AgNPs-Rm. The same aspect has been confirmed by several studies with AgNPs produced by fungi (NARAYANAN, PARK, SAKTHIVEL, 2013; NAQVI et al., 2013; SHALIGRAM et al., 2009).

FIGURE 5- XRPD of AgNPs *R. glutinis* (a) and *R. mucilaginosa* (b). (*) impurities.

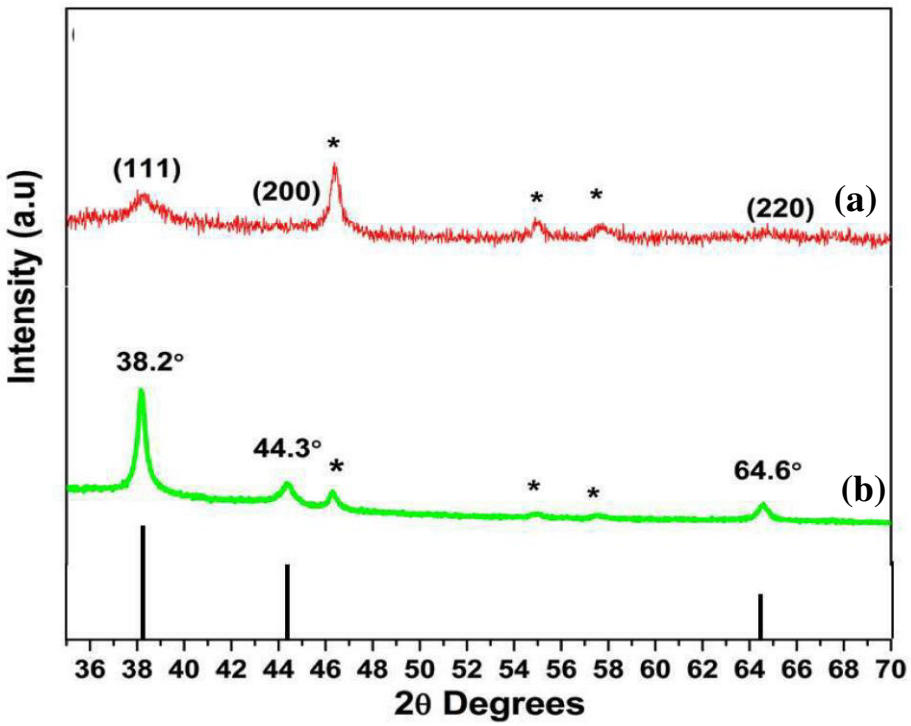

Source: Author

FIGURES 6a and 7a show images produced by the AgNPs Rg and Rm, obtained by SEM. The images show spherical and irregular shaped AgNPs with different sizes. The energy-dispersive X-ray (EDX) was used to determine the elemental composition of material (FIGURES 6b and 7b), where we can observe the absorption of silver that is 3 keV (KALIMUTHU et al., 2008). The histograms were constructed with 100 AgNPs count and showed that they possessed different sizes AgNPs-Rg (31.6 nm ± 18.4 (average ± SD)) e AgNPs-Rm (66.4 nm ± 24.5 (average ± SD)) (FIGURES 6c and 7c),. The images by SEM of AgNPs show which are highly dispersed and small size, mainly AgNP-Rg. The size is characteristic of fungal species involved. The SEM technique has already been used in other studies to characterize fungal AgNPs (AMERASAN et al., 2016; APTE et al., 2013; BANU, RATHOD, RANGANATH, 2011).

FIGURE 6- SEM (a), EDX (b) and histogram (c) of AgNPs produced by *R. glutinis*.

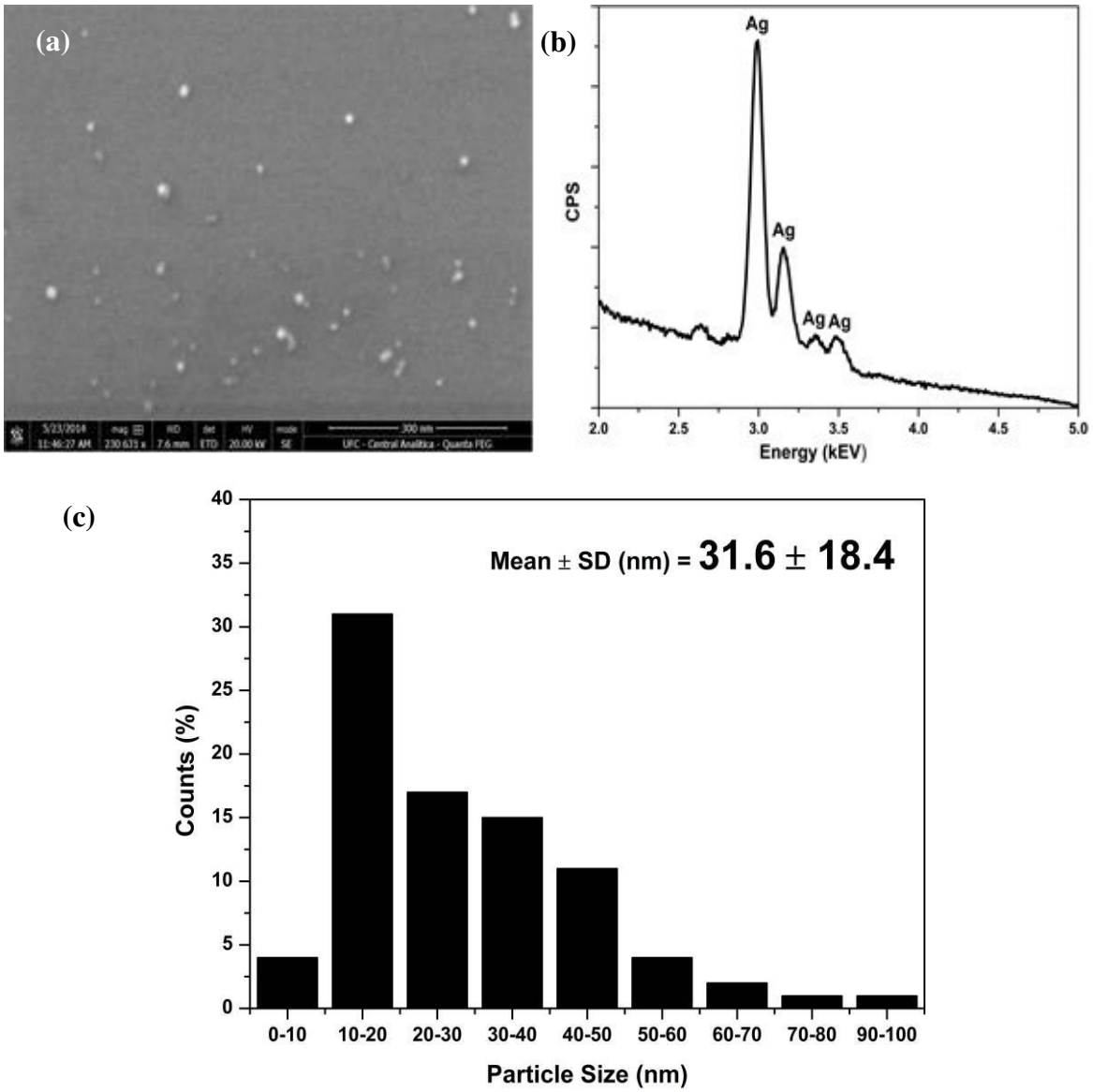

Source: Author

FIGURE 7- SEM (a), EDX (b) and histogram (c) of AgNPs produced by *R. mucilaginosa*.

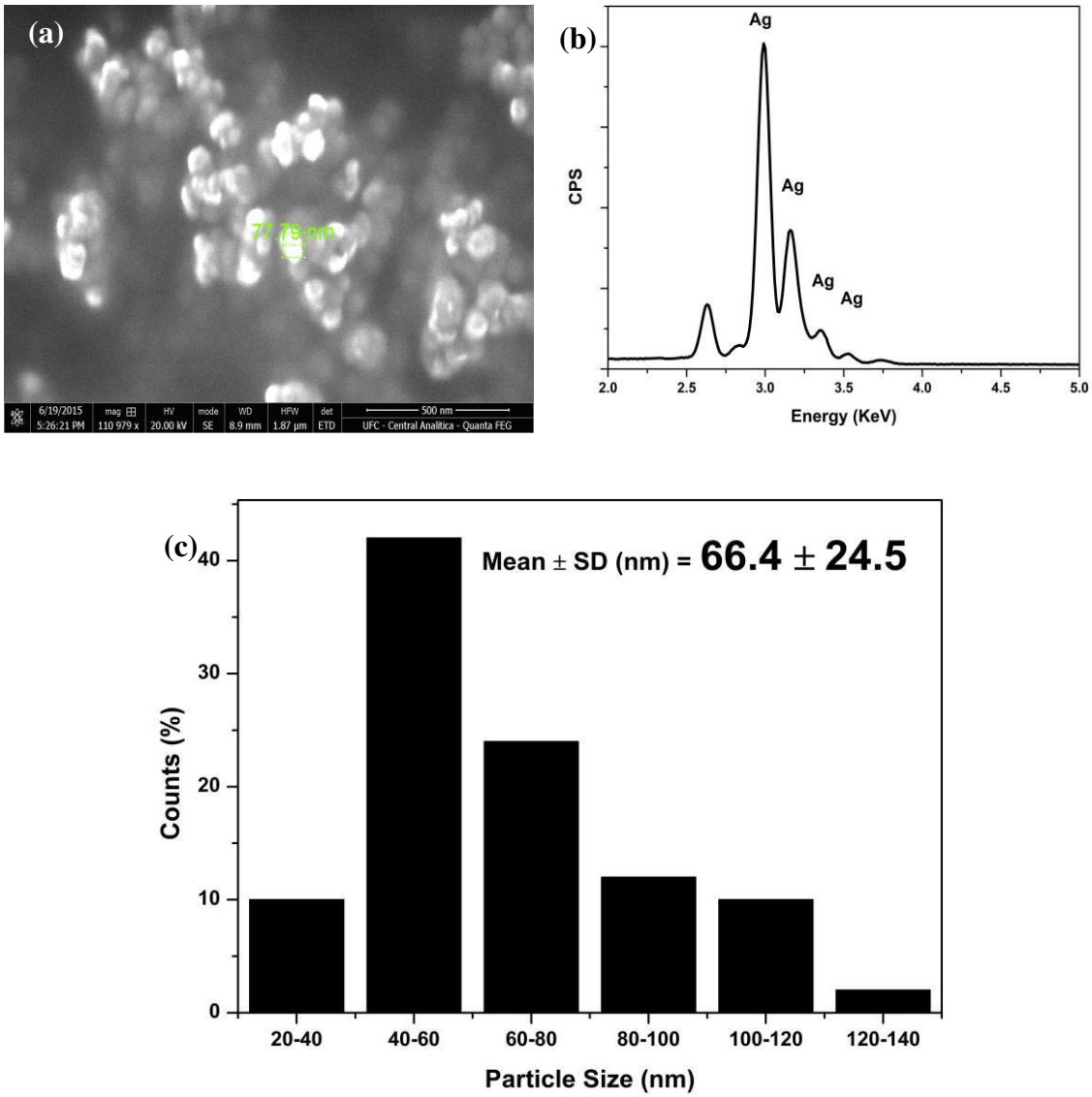

Source: Author

FIGURES 8 and 9 show the images of AgNPs obtained by TEM. The purpose of this measure was to determine the size and shape of the particles. In FIGURE 8a and b we observe that the AgNPs produced by Rg are immersed in a reticular structure that is the proteic material from the capping (AHMAD et al., 2003). In FIGURE 8c the histogram of the AgNPs produced by Rg is shown, where AgNPs have the size 15.45 nm ± 7.94 (average ± SD). In FIGURE 9(a) we can observe just one AgNP crystallite produced by Rm and in FIGURE 9(b) it was possible to calculate the distance between the crystalline planes (111), which was 0.25 nm, value consistent with that found by GOSWAMI et al., 2013 and SANYASI et al., 2016. In FIGURE 9(c), we can observe the histogram of AgNPs sizing from

13.70 nm ± 8.21 (average ± SD). It was observed that AgNPs produced by Rm are smaller than those by Rg. ANTHONY et al., 2014, when evaluating the AgNPs produced by mushrooms observed particles with the size 10 ± 5 nm.

The size of the AgNPs varies according to the fungal species involved in their synthesis. VERMA et al., 2010 found AgNPs with sizes of 10 to 25 nm, with spherical morphology, when they studied the fungus *Aspergillus clavatus*. The fungus *Pestalotia* sp. was used for the production of AgNPs and a size of 12.40 nm was found (RAHEMAN et al., 2011). Thus, one can be observed that AgNPs produced by Rm and Rg have a size range within those found by other studies.

The images acquired by TEM show that the AgNPs produced by both yeasts presented spherical form and are well distributed with no signs of agglomeration. In a study using the fungus *Agaricus bisporus* (EL-SONBATY et al., 2013), spherical particles with sizes varying from 8 to 20 nm were also found. The TEM images in our work show AgNPs spaced from each other and in contact with the protein material. This material is the capping agent produced by the fungi, as described previously (ALANI, MOO-YOUNG, ANDERSON, 2012). More images can be seen in FIGURES S10 and S11 Supporting Information Chapter 4.

FIGURE 8- TEM (a, b) and histogram (c) of AgNPs produced by *R. glutinis*.

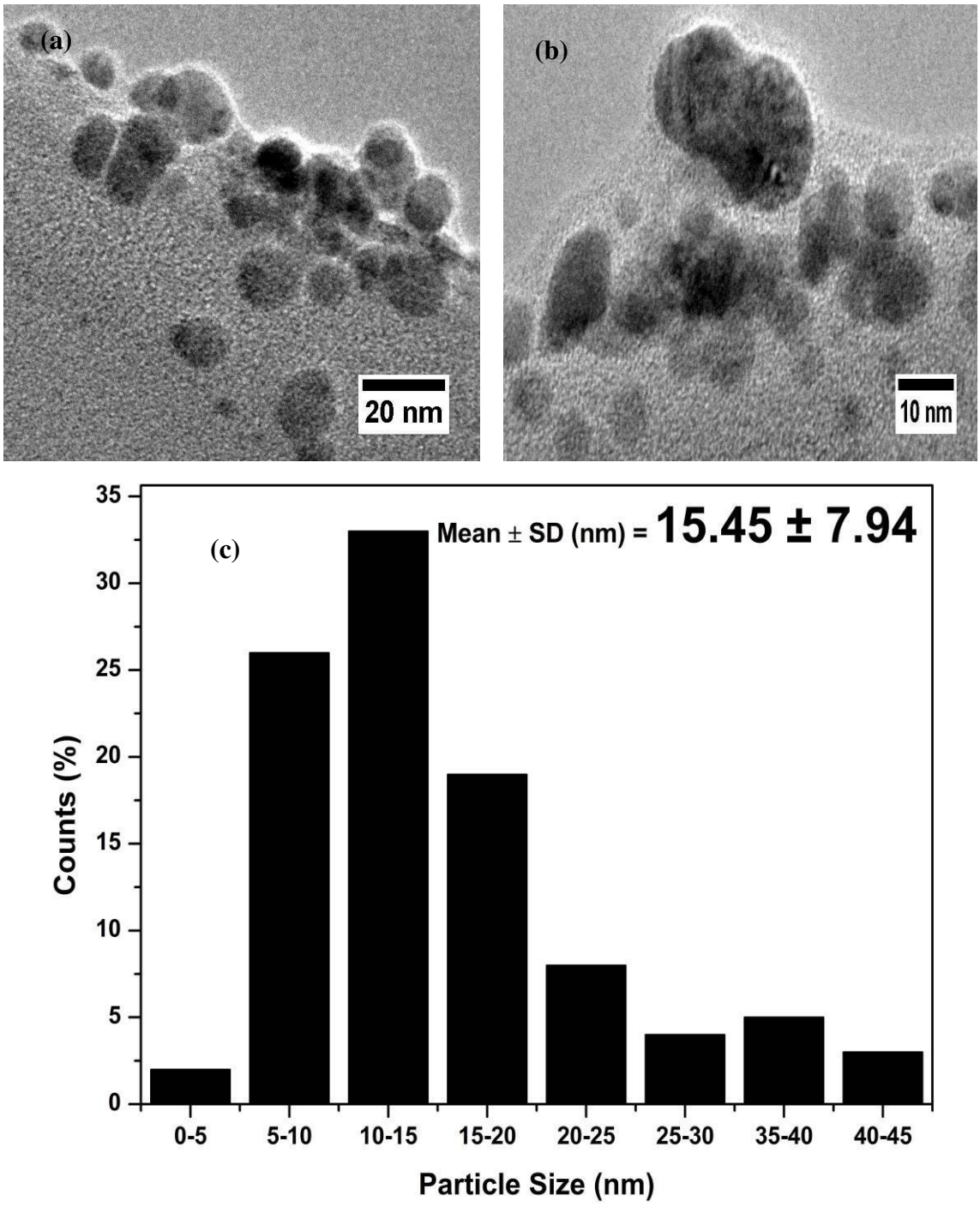

Source: Author

FIGURE 9- TEM and histogram of AgNPs produced by *R. mucilaginosa* (a, b, c).

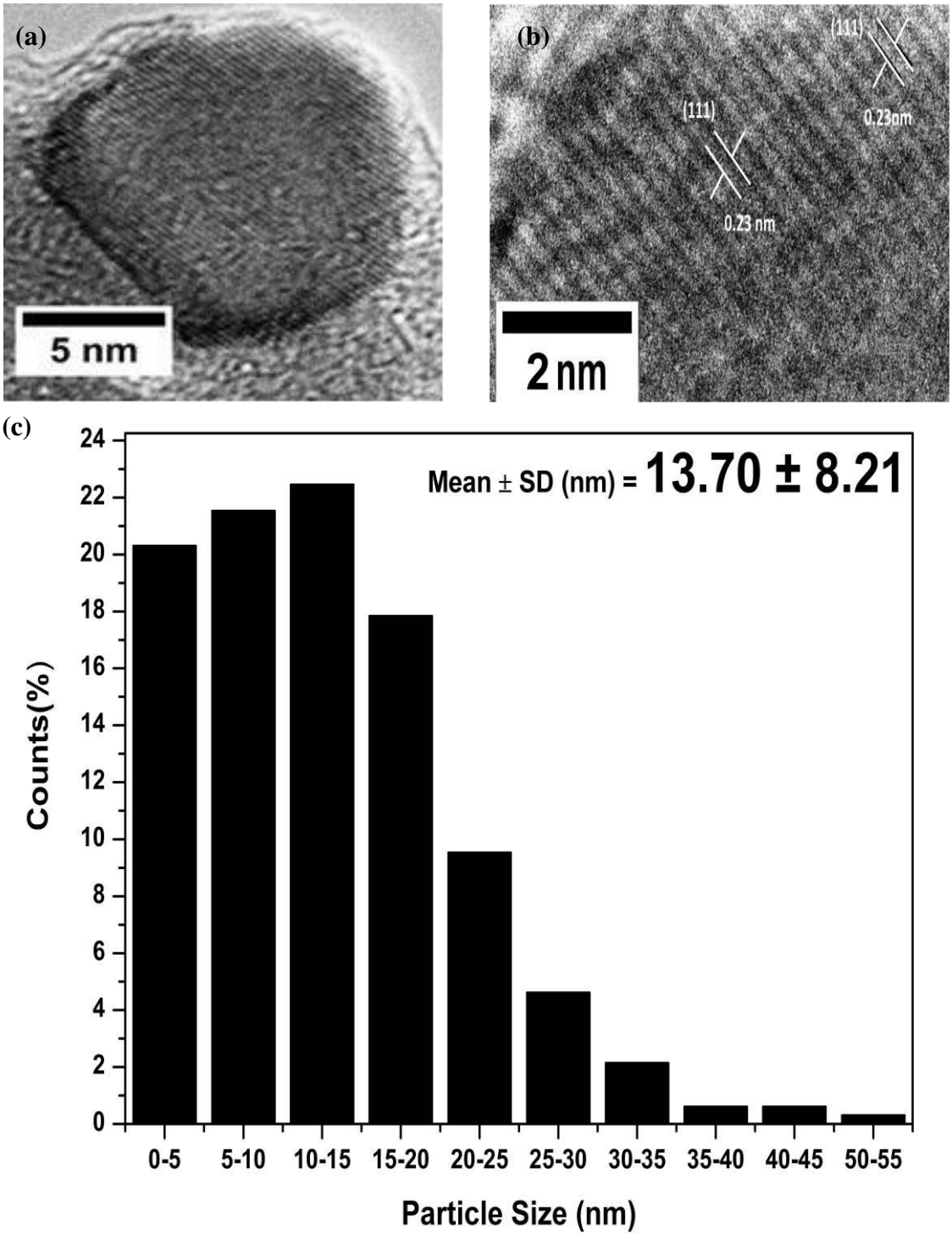

Source: Author

In FIGURES 10 and 11, AFM images obtained from the AgNPs produced by the yeasts described in this study are shown. Once again, the results showed AgNPs with spherical morphology with uniform distribution with no signs of agglomeration. In FIGURES

10a, b and 11a, b, the details of the AgNPs are shown and we can observe the highlighted proteic material used in its stabilization. In FIGURES 10c and 11c the histograms of the AgNPs produced by Rg and Rm are shown, where AgNPs have the size 35.56 nm ± 21.43 (average ± SD) and 18.46 nm ± 7.31 (average ± SD), respectively. More images can be seen in FIGURES S12 and S13 Supporting Information Chapter 4.

FIGURE 10- AFM and histogram of AgNPs produced by *R. glutinis* (a, b, c).

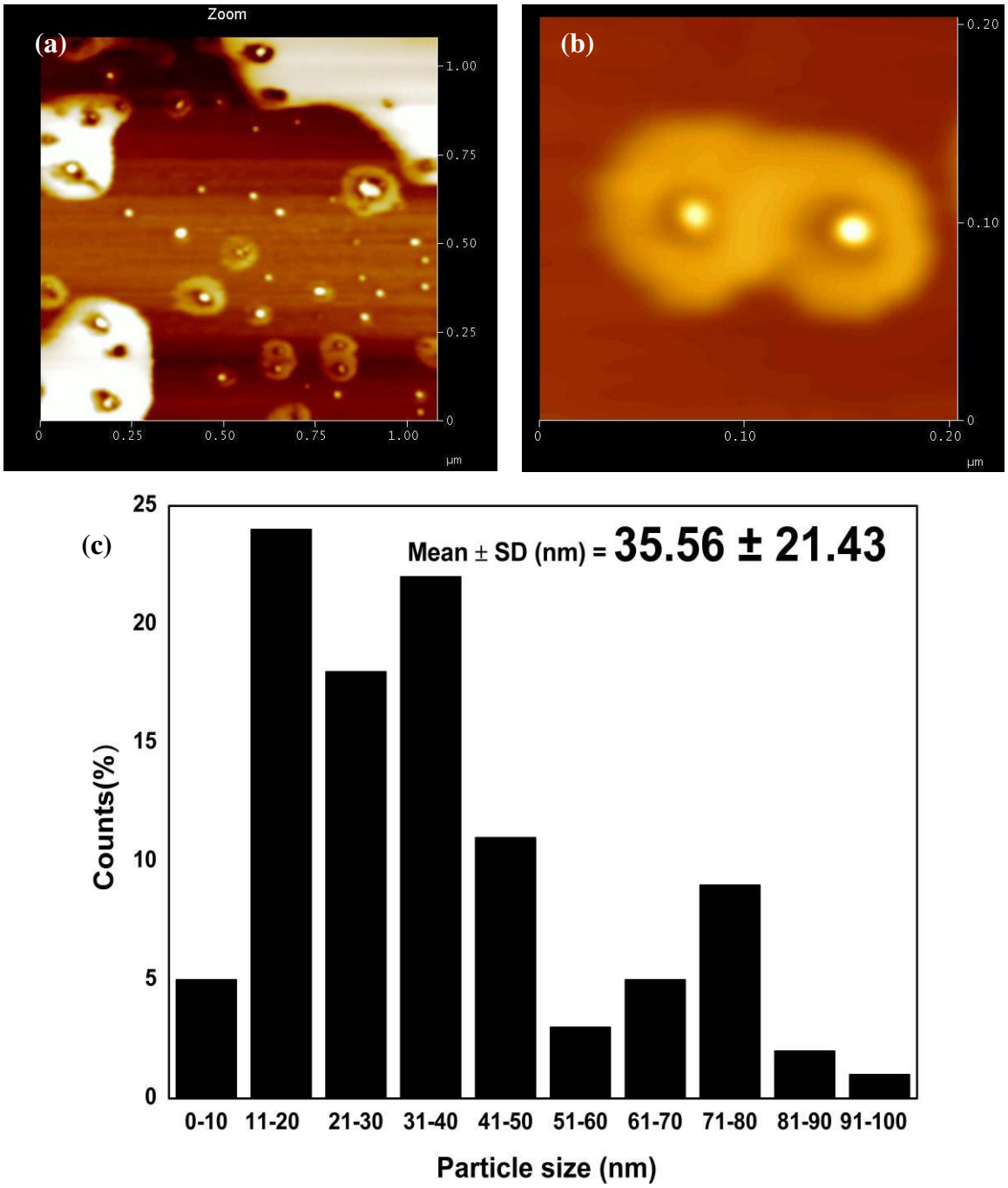

Source: Author

FIGURE 11- AFM and histogram of AgNPs produced by *R. mucilaginosa* (a, b, c).

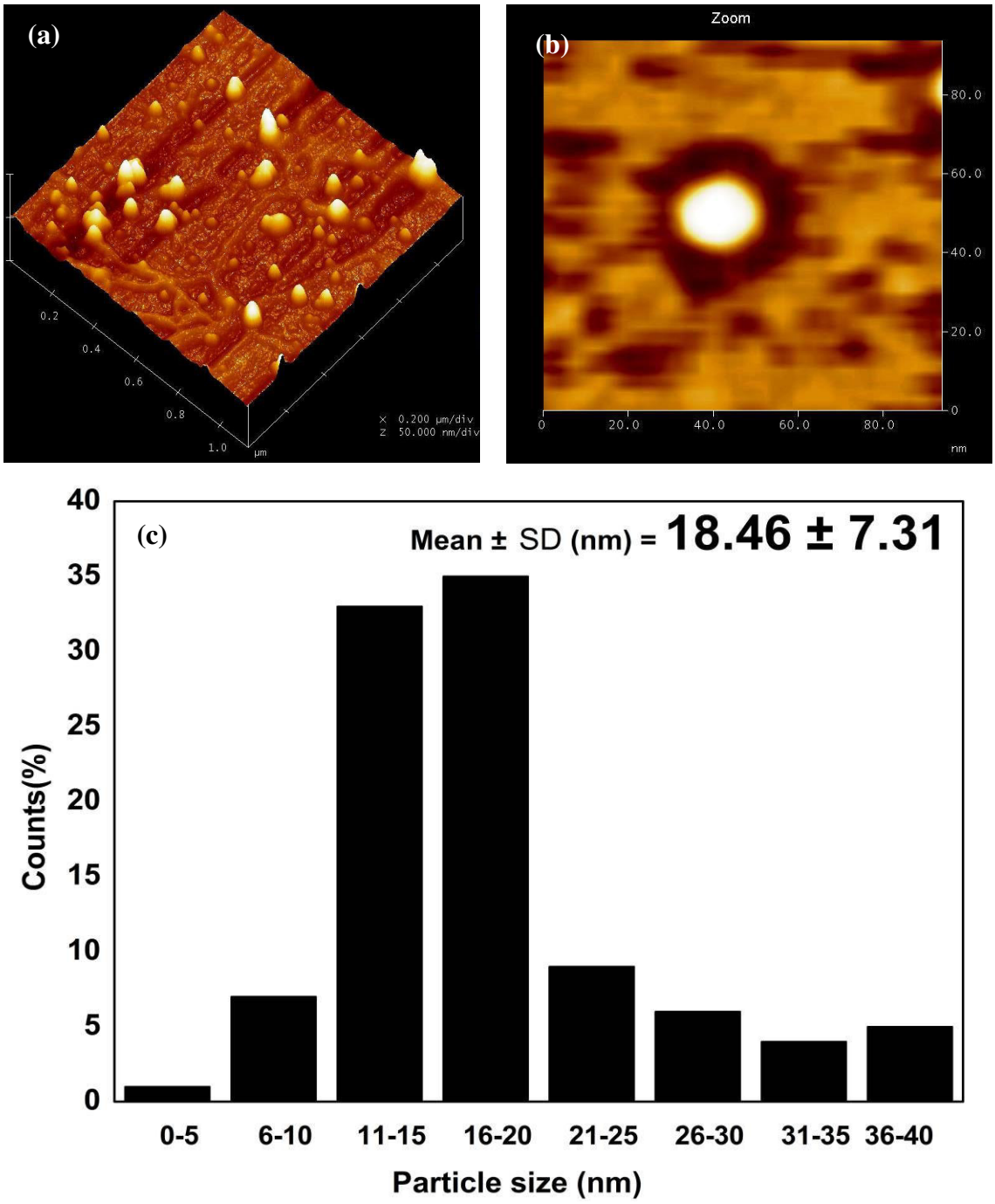

Source: Author

A summary of the sizes found by the four techniques (DLS, SEM, TEM and AFM) described in this study is shown in Table 2. The differences observed are caused by the fact that nanoparticles in suspension present diffuse layers on their surfaces with varied amount of proteins, ions, and water molecules which induce light scattering during the DLS measurement (not only the AgNPs scatter light). That would explain the higher size of the AgNPs determined by DLS technique when compared to other techniques (CHEN, YAN,

WU, 2015). In our study we can observe in FIGURES 10 b and 11b, that the center of the AgNP is occupied by a metallic material (Ag), shown by XRD and TEM, surrounded by proteic material that stabilizes it, shown by AFM.

Table 2- Size comparison of AgNps by different techniques.

Yeasts	**Size Mean (nm)**			
	DLS	**SEM**	**TEM**	**AFM**
R. glutinis	108.1	31.6	15.45	35.56
R. mucilaginosa	119.0	66.4	13.70	18.46

Source: Author

Based on all the techniques realized in the characterization of AgNPs (UV-Vis, DLS, FTIR, XRD, EDX, SEM, AFM, TEM) build a theoretical model of AgNPs and compare it with a real image produced by AFM (FIGURE 12). In our model we have a core with metallic silver stabilized with proteins, this model has been described in another fungus *Aspergillus flavus* NJP08 (JAIN et al., 2011).

FIGURE 12- AFM (a) and cartoon (b) of AgNPs.

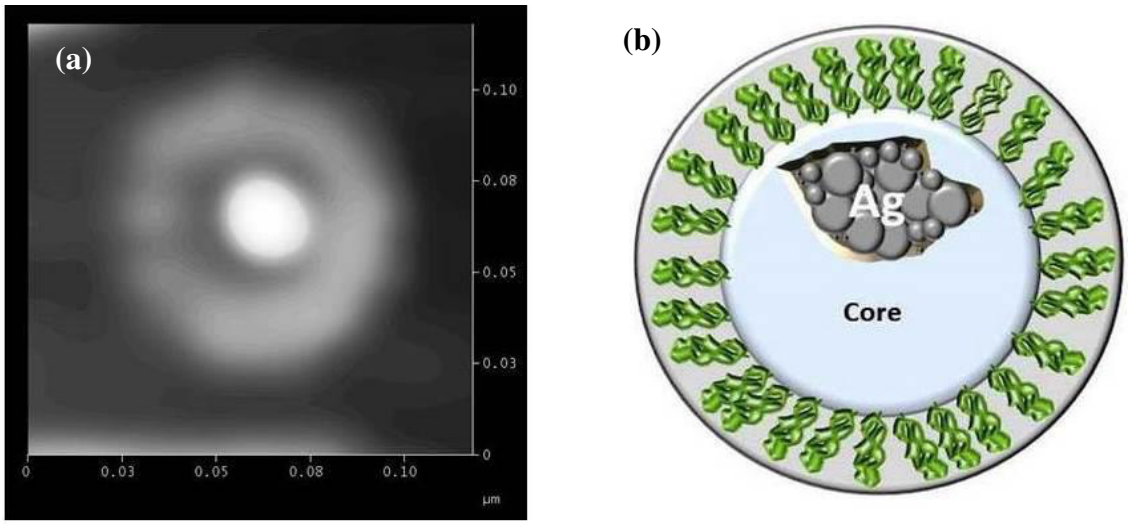

Source: Author

The role of proteins as capping agent of AgNPs is still controversial, however, have been found very on the subject. Depending on AgNPs and the reaction medium in which it is inserted up to 500 types of proteins may participate in the interactions and stabilization of AgNPs (DURÁN et al., 2015). Moreover, physicochemical properties of NPs determine the type of corona formed (PEARSON, JUETTNER, HONG, 2014).

Catalytic activities

The contemporary society uses a variety of chemical products such as drugs, pesticides, inks, dyes, among others. The production of these molecules generate tons of waste annually, some which are highly toxic and cannot be discarded without previous treatment due to the damage for human and animal health, and for the environment. Among these wastes, we can highlight the importance of methylene blue (MB) and 4- nitrofenol (4-NP) (VIDHU, PHILIP, 2014a; VIDHU, PHILIP, 2014b).

In FIGURES 13a and 14a, it can be observed the assays on the kinetic reaction of degradation of the 4-NP by AgNPs produced by Rg and Rm, respectively, in the presence of $NaBH_4$. Catalytic reduction was observed during 30 minutes and the kinetic of both reactions is of pseudo-first order (Figs. 13(b) and 14(b)), which converges with the results described in the literature for the degradation of 4-NP (NARAYANAN, PARK, SAKTHIVEL, 2013; JIANG et al., 2011; PRADHAN, PAL, PAL, 2002). Such reactions comprise a heterogeneous catalysis process that was adjusted to a Langmuir–Hinshelwood model (Figs.13(c) and 14(c)), which is characterized by a long induction period, as it can be seen in Figs. 13(b) and 14(b) (GAJBHIYE et al., 2009; HERVÉS et al., 2012).

The use of fungi-produced AgNPs for the degradation of 4-NP is not very common. NARAYANAN, PARK, SAKTHIVEL, 2013, used *Cylindrocladium floridanum* in the degradation of 4-NP, however the reaction occurred in 60 min and with a $R^2 = 0.9752$. In our study, the reaction occurred in 30 min and the correlation coefficients were $R^2 = 0.9899$ and $R^2 = 0.9823$, for Rg and Rm, respectively. Table 3 shows the kinetic parameters for the 4-NP degradation. The performance of Rg and Rm was better than *C. floridanum* when considering the kinetic constants (k). In our tests, it was observed a $k = 2.04 \times 10^{-3}$ and 1.70×10^{-3} s^{-1} for AgNPs of Rg and Rm, respectively (Table 3). Big variations for the degradation constants occurred because of the type of AgNPs used: some of them are from biological origin and others are from chemical origin (DESHMUKH et al., 2013; GANGULA et al., 2011; GAVADE et al., 2015).

FIGURE 13- Catalytic reduction of 4-NP by AgNPs produced by *R. glutinis* (a, b). Inset shows the mechanism that follows the Langmuir-Hinshelwood model of heterogeneous catalysis (c).

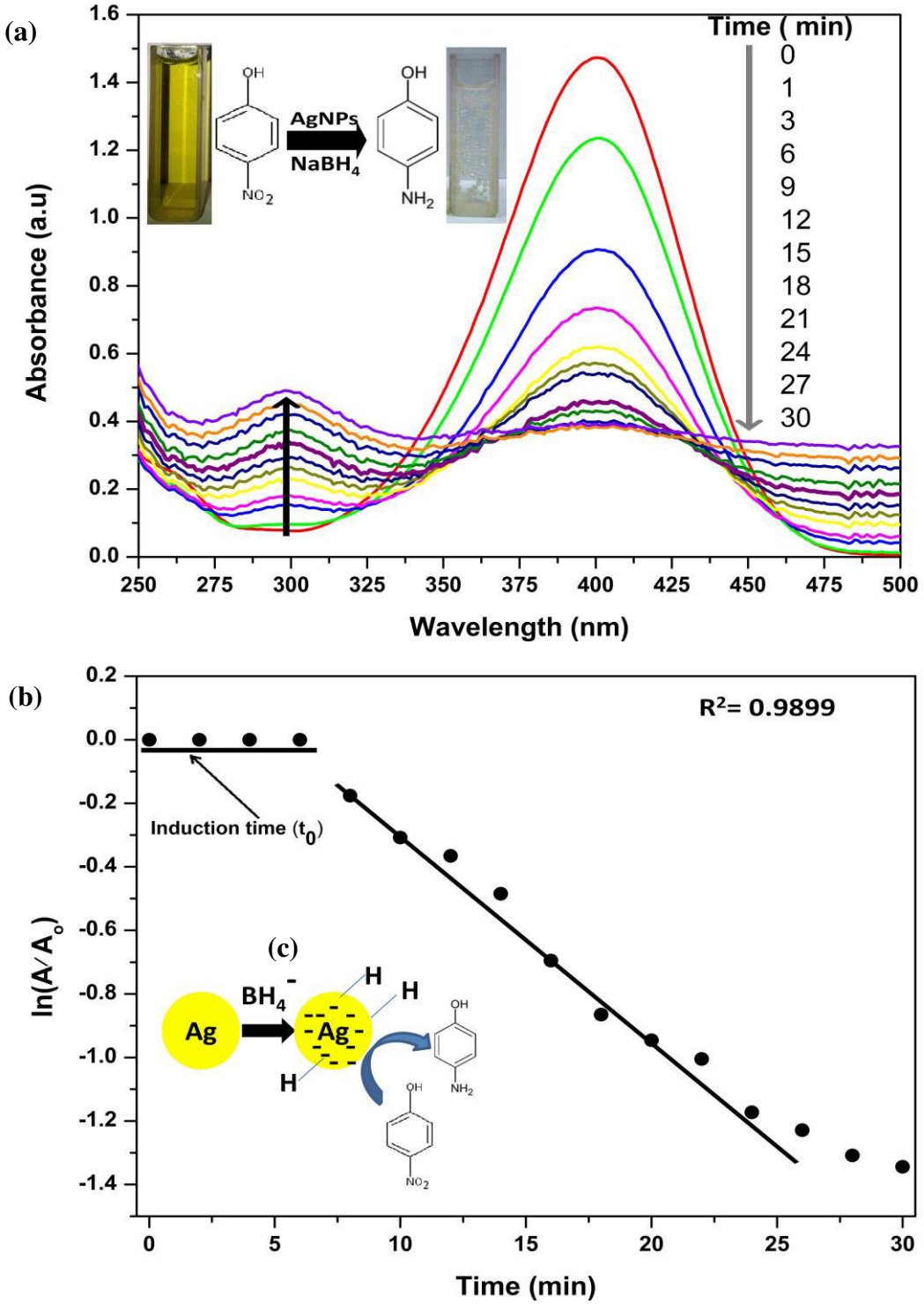

Source: Author

FIGURE 14- Catalytic reduction of 4-NP by AgNPs produced by *R. mucilaginosa* (a, b). Inset shows the mechanism that follows the Langmuir-Hinshelwood model of heterogeneous catalysis (c).

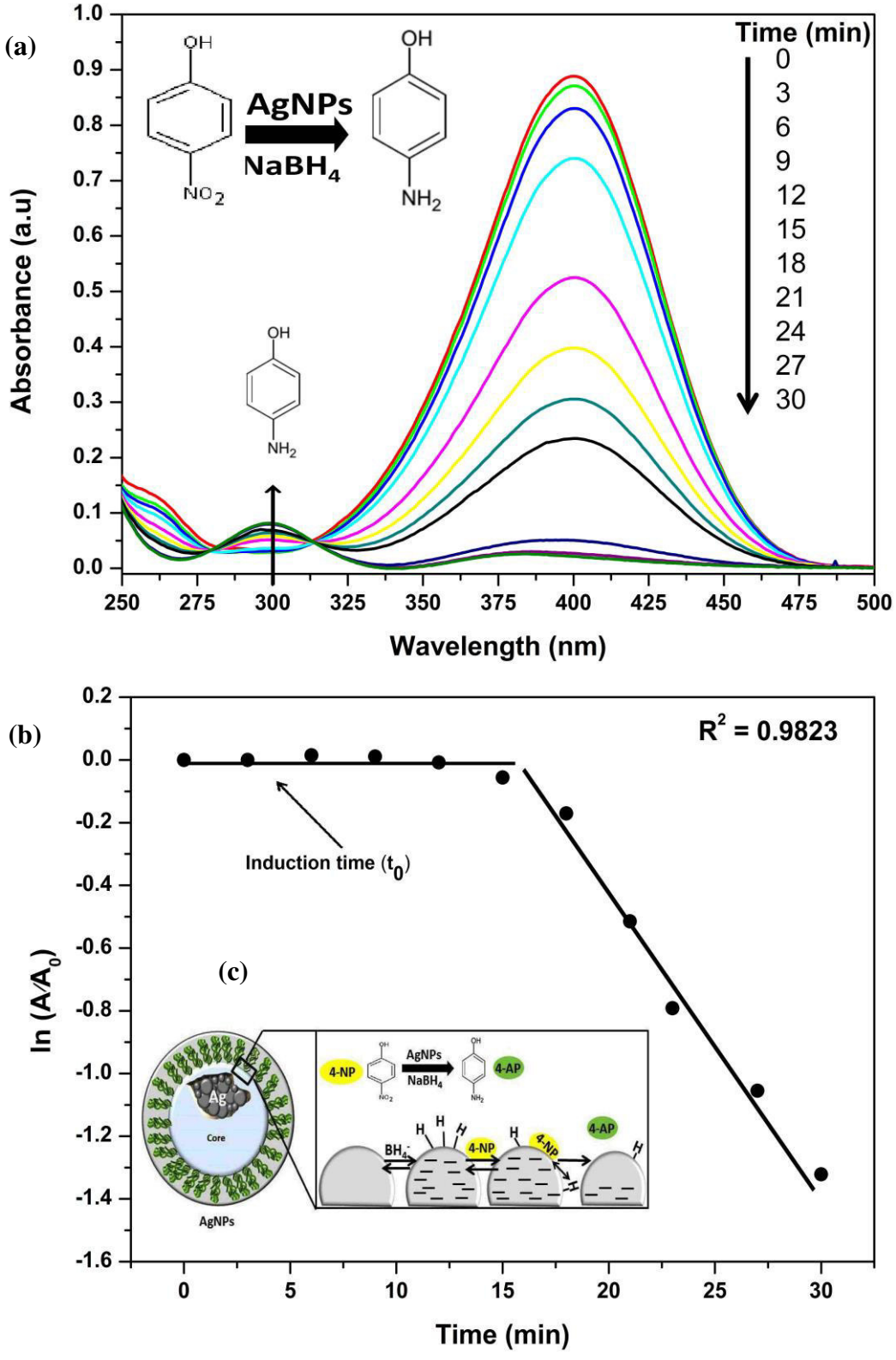

Source: Author

FIGURE 15- Catalytic reduction of MB using AgNPs produced by *R. glutinis* (a,b).

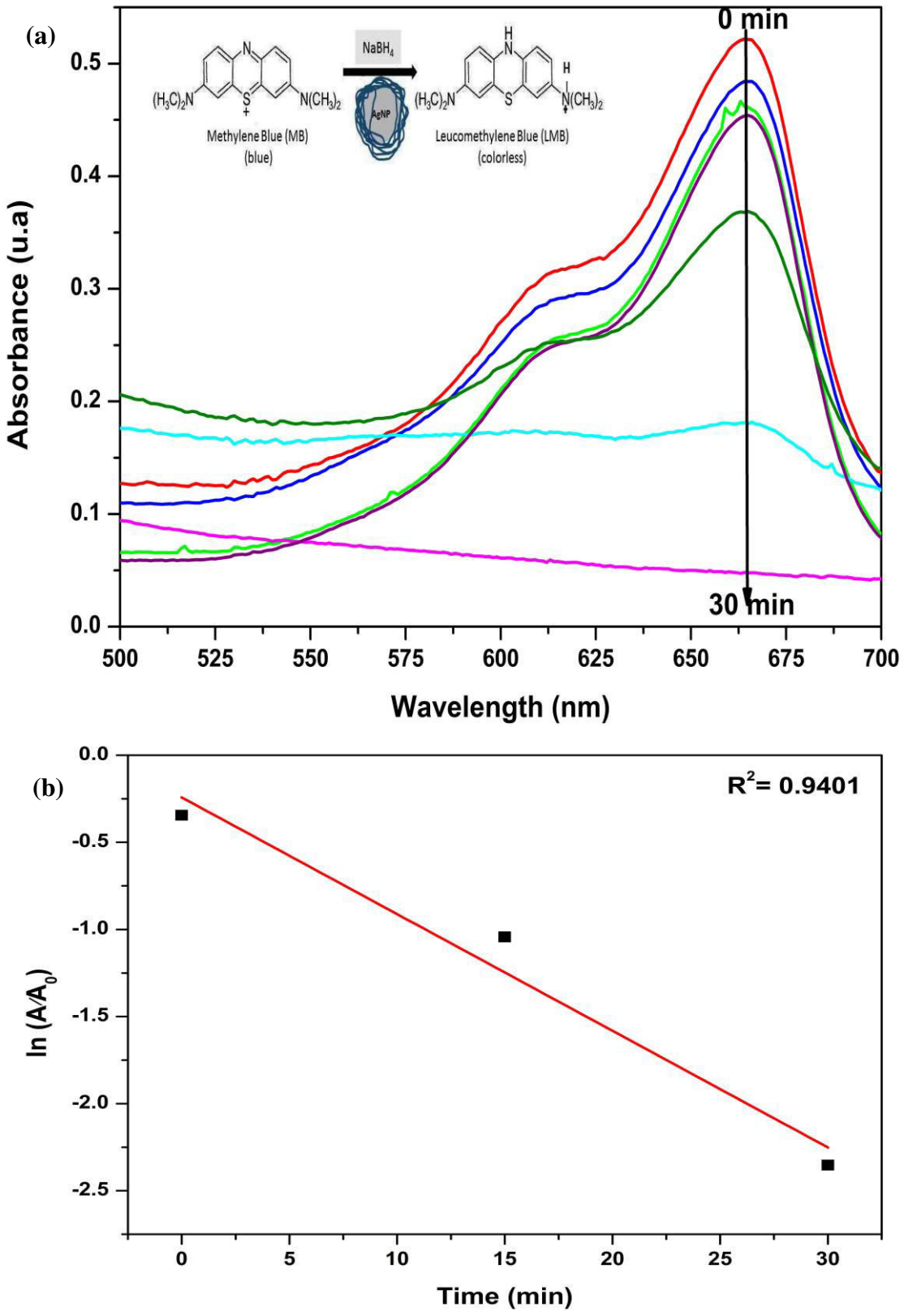

Source: Author

FIGURE 16- Catalytic reduction of MB using AgNPs produced by *R. mucilaginosa* (a,b).

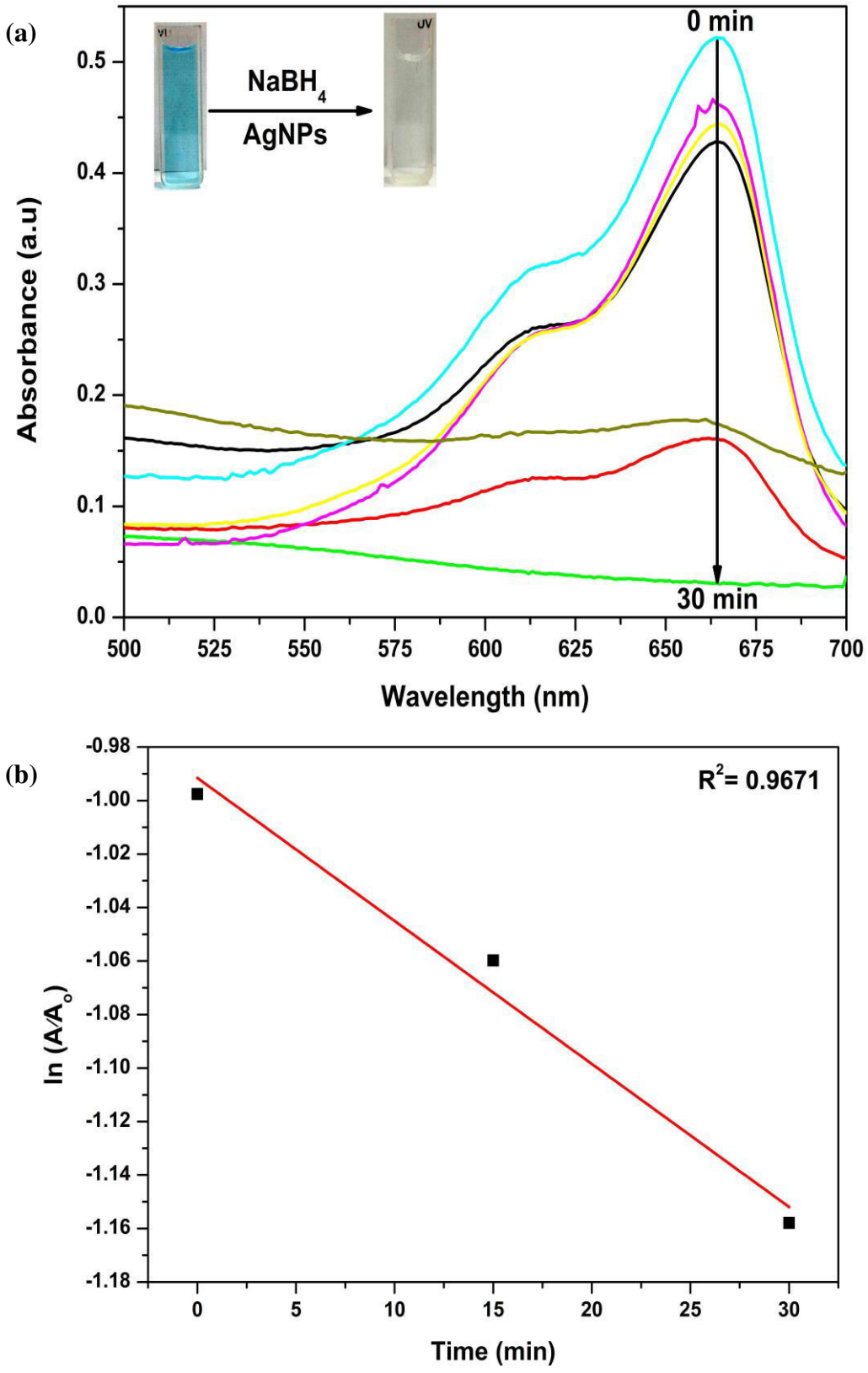

Source: Author

These variations can also be attributed to size difference of the AgNP, smaller particles tend to resist better to the oxidative process, remaining active for longer periods (GANGULA et al., 2011). The longer induction period for AgNPs derived from Rm is due to the nature and composition of the proteins present on the surface of the AgNPs, that may hamper the initial adhesion of molecules of 4-NP and of BH_4^-, which delays the beginning of the reaction (HERVÉS et al., 2012). (FIGURE S14 in Supporting Information Chapter 4).

Other important dye is the methylene blue (MB). Due to adverse effects on the environment, the removal of MB from residual waters is an important issue and a key challenge to researchers. Thus, the use of nanoparticles in order to degrade MB is of great importance (TAHIR et al., 2015; UDDIN et al., 2009). The AgNPs studied here were used in the reduction of MB, as shown in FIGURES 15a and 16a.

The effect of biogenic AgNPs on MB is well documented, however this is the first time that AgNPs produced by Rg and Rm yeasts are used (VANAJA et al., 2014). In our tests, it was observed a k= 1.10 x 10^{-3} and 0.90 x 10^{-3} s^{-1} for AgNPs of Rg and Rm (Table 3), respectively. In a study performed by KUMARI and PHILIP, 2013, AgNPs produced with coconut oil were used and they presented catalytic activity in the reduction of MB, with k= 3.86 x 10^{-3} s^{-1} and 1.95 x 10^{-3} s^{-1}.

The AgNPs produced in this study reduced the MB in 30 min, as can be seen in FIGURES 15(a) and 16(a). The kinetics of the catalytic reaction was of pseudo-first order, since we observed a linear reaction between ln (A/A_0) as a function of time (FIGURES 15(b) and 16(b)). Some authors differ on the order of degradation reaction of MB. Some of them affirm that the reaction is of pseudo-first order and others affirm that the reaction is of second order (VIDHU, PHILIP, 2014a; VIDHU, PHILIP, 2014b). Our study found that the reactions described for the AgNPs produced by yeasts were better adjusted for pseudo-first order. SUVITH and PHILIP, 2014, also concluded in their work that pseudo-first order is the kinetics observed in AgNPs of biogenic origin in the degradation of MB.

Table 3- Kinetic Parameters for catalytic reduction of 4-NP and MB using AgNPs produced by *R. glutinis* e *R. mucilaginosa*.

4-nitrophenol (4-NP)		**Methylene blue (MB)**	
k_{app} ($x10^{-3}$) s^{-1}	**Reference**	**k ($x10^{-3}$) s^{-1}**	**Reference**
1.10	NARAYANAN et al.,	2.78	KUMAR et al., 2014
	2013$^{\Psi}$.	1.95	KUMARI E PHILIP,
2.30	PRADHAN et al., 2002.		2013
4.06	GANGULA et al., 2011.	3.86	KUMARI E PHILIP,
2.15	JIANG et al., 2011.		2013
4.19-9.18	GU et al., 2014.	2.50	SUVITH E PHILIP, 2014
5.0-19.50	DESMUNK et al., 2013.	3.74	SUVITH E PHILIP, 2014
3.89	JANANI et al., 2014.	2.50	RAJAN et al., 2015
4.05	AI et al., 2013.	5.69	RAJAN et al., 2015
1.26	ZHENG et al., 2015	28.00	VIDHU E PHILIP, 2014a
3.67	GAVADE et al., 2015	7.36	VIDHU E PHILIP, 2014a
1.34-2.33	JOSEPH et al., 2015	17.0	VIDHU E PHILIP, 2014b
5.42	ZHAO et al., 2015	11.9	VIDHU E PHILIP, 2014b
2.04	This work	8.12	VIDHU E PHILIP, 2014b
1.70	This work	**1.10**	This work
		0.90	This work

Source: Author. $^{\Psi}$ -fungi

Antifungal Activity

AgNPs may have multiple applications and one of the most discussed is the antimicrobial, mainly against bacteria (KIM etal., 2007; RAI et al., 2014; SHARMA, YNGARD, LIN, 2009). However, activity against *Candida parapsilosis* an emergent yeast is still little discussed (PANACEK et al., 2009). In our study, *C. parapsilosis* were extremely susceptible to AgNps produced by Rg and Rm. The $MIC_{90\%}$ of Rg ranges of 0.40-0.025 µg⁄mL and $MIC_{90\%}$ of Rm ranges of 0.80-0.025 µg⁄mL (Table 4). All strains were susceptible to fluconazole with $MIC_{90\%}$ ranges of 2-8 µg⁄mL. In previous studies evaluating the MIC AgNPs against *C. parapsilosis* was observed MIC 0.8µg⁄mL (PANACEK et al., 2009), much higher than those found in our study. However, in the study cited was only one tested strains of *C. parapsilosis*, and our study were evaluated 35 strains, AgNPs tested in our work has a protein corona, which can help in antifungal function, and AgNPs described by PANACEK et al., 2009, they were synthetic with SDS capping, tween 80 and PVP. Our work is the first to describe the fungal effect on such a large number of strains of a single species. In another work with synthetic AgNPs, evaluated three strains: 1 *C. glabrata*, 1 *C. tropicalis* e 1 *C.*

albicans, was found $MIC_{90\%}$ range 30-60 µg/mL,(KHATOON et al., 2015). The differences found in antifungal action AgNPs Rg and Rm may be due to protein corona somehow modulates the biological responses of silver nanoparticles (DÚRAN et al., 2015).

C. albicans fluconazole resistance shows MIC of 0.25-2 µg/mL for AgNPs. AgNPs are useful even in strains that do not respond to conventional treatment (ALIMEHR et al., 2015). These findings coincide with those described in our work because they show that biological or synthetic AgNPs have excellent activity against *Candida* spp. (VAZQUEZ-MUÑOZ, AVALOS-BORJA, CASTRO-LONGORIA, 2014; WADY et al., 2014).

AgNPs produced by yeasts (Rg and Rm) were tested in regard to the antifungal activity by conjugating it with fluconazole against *C. parapsilosis*, as we can observe in FIGURE 17. The AgNPs resulting from Rg and Rm increased the action of fluconazole in 42.2 and 29.7%, respectively, and may represent an alternative in the treatment of fungal infections that are resistant to the usual antifungal (Table 5) (YEHIA, AL-SHEIKH, 2014).

GAJBHIYE et al., 2009, assessed biogenic AgNPs associated to fluconazole and observed an elevation of the activity in all tested fungal species. However, *C. parapsilosis* was not tested, which is considered important yeast specie in systematic fungal infections (ZICCARDI et al., 2015).

Table 4- *In vitro* susceptibilities of 35 *C. parapsilosis* bloodstream isolates.

Species (n^0. isolates tested)	AgNP	No. of isolates with minimal inhibitory concentration (µg/mL) of									
		0.025	0.05	0.10	0.20	0.40	0.80	1.56	3.12	6.25	12.5
C. parapsilosis (35)	Rg	(11)	(16)	(7)		(1)					
	Rm	(11)	(23)				(1)				

Rg – *R. glutinis*; Rm- *R. mucilaginosa*

Source: Author

The effect of AgNPs on *Candida* spp. species is currently being discussed. They possibly can interfere with the cellular division process and cause damage to the plasmatic membrane and induce apoptotic through the increase of hydroxyl radicals, leading to death, along with fluconazole, which acts on the synthesis of membrane components (HWANG et al., 2012; KIM et al., 2009). This action was increased by a synergic effect described in our study.

Table 5- Antifungal activity of fluconazole alone (25 µg), AgNPsRg (0.5 µg) and AgNPsRm (0.5 µg) plus fluconazole.

Yeasts(*n*)	Zone of Inhibition (mm) (Mean±SD)			Increased fold area (x100)	
	A Flu	B Ag@Flu Rg	C Ag@Flu Rm	$((B^2-A^2)/A^2)$	$((C^2-A^2)/A^2)$
C. parapsilosis (13)	28.8(±9.9)	34.3(±8.9)	32.8(±8.0)	42.2	29.7

Flu-fluconazole; Ag@Flu Rg - Silver nanoparticle produced by *R. glutinis* plus fluconazole; Ag@Flu Rm - Silver nanoparticle produced by *R. mucilaginosa* plus fluconazole. Increased fold area was calculated using $(B^2 - A^2)/A^2$ and $(C^2 - A^2)/A^2$ (x 100), where A and B and C are the inhibition zones for A, B and C, respectively.

Source: Author

Cytotoxicity Effects

In FIGURE 18a, we can observer that the cellular viability only begins to significantly decline in the concentration 5.0 µg/mL on to AgNP produced by Rg. In FIGURE 17b, we observed a lower toxicity AgNPs produced by Rm, because for this nanoparticle toxicity was detected at concentrations 10.0 µg/mL. The concentrations tested in which were observed cytotoxic effects were far above those who killed the *Candida* strains. This demonstrates the feasibility of biological AgNPs produced by yeast, since the toxicity is only at high levels.

Metallic nanoparticles show toxicity to the cells of the renal glomerular system because generate toxic oxygen radicals (ROS) (PUJALTÉ et al., 2011). In our study the toxicity of the same cells was observed at high concentrations, above 10 µg/mL. In a study conducted with keratinocytes and fibroblasts was observed that AgNPs were less toxic than the Ag^+ ion and the non-toxic concentration of AgNP ranged 0.25–25 µg/mL (GALANDAKOVA et al., 2016). These results are within the ranges found in our result for AgNPs Rg concentration non-toxic 0.08–2.5 µg/mL and the AgNPs Rm 0.25–5.0 µg/mL.

FIGURE 17- Anticandidal effect of fluconazole plus AgNPs produced by *R. glutinis* (Ag@Flu Rg) and *R. mucilaginosa* (Ag@Flu Rm).

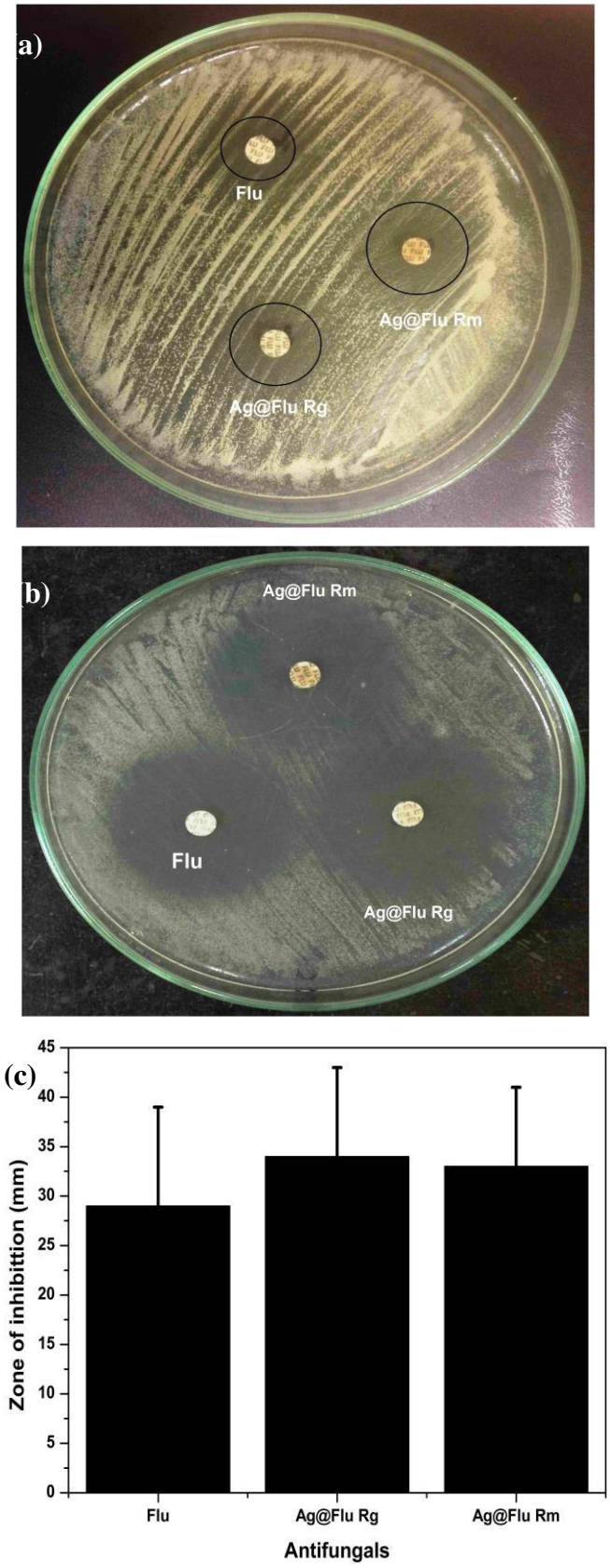

Source: Author

FIGURE 18- Cytotoxic effect of AgNPs produced by *R. glutinis* (a) and *R. mucilaginosa* (b).* $p < 0.05$

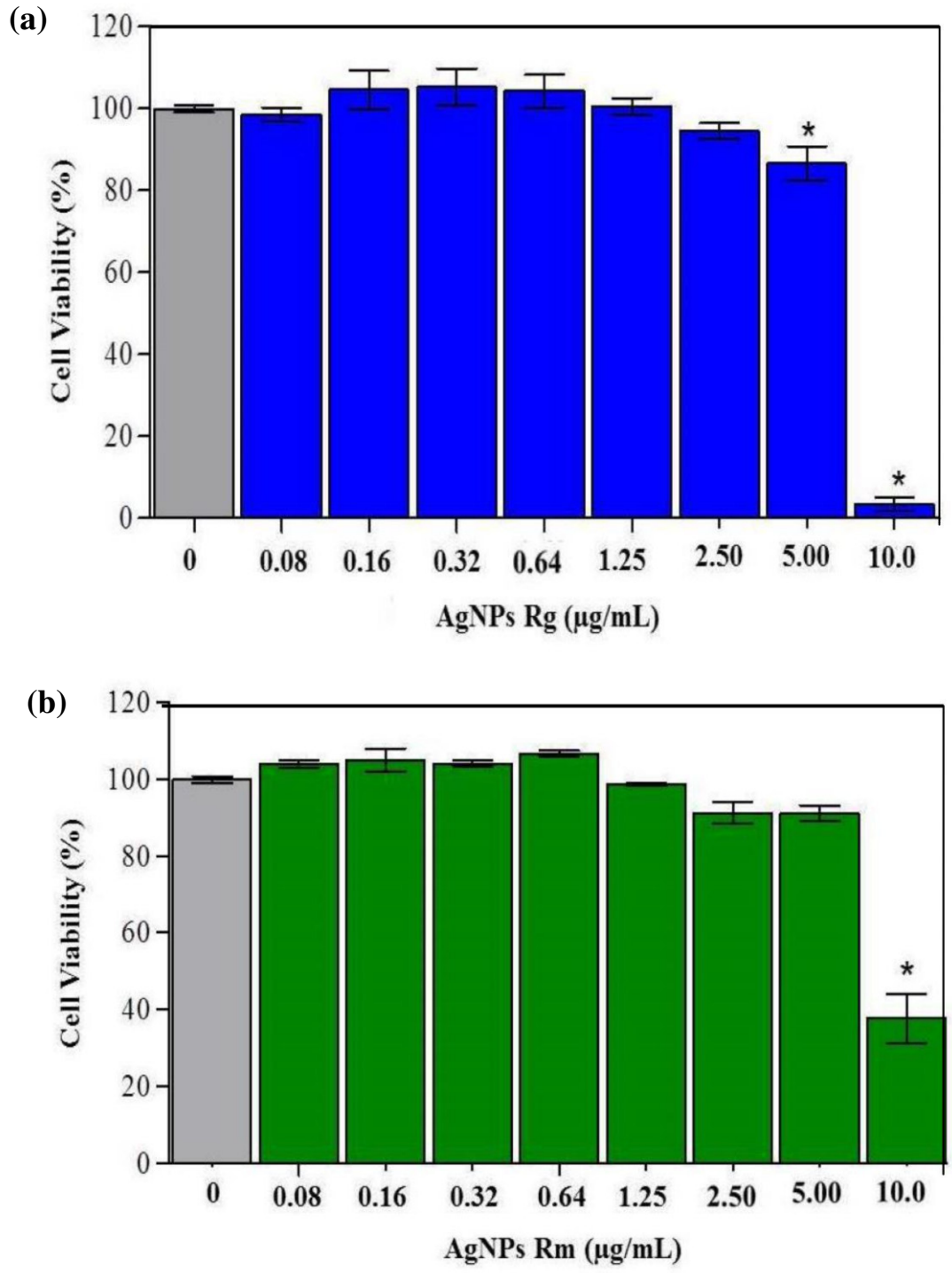

Source: Author

CONCLUSION

In conclusion, we describe in this work two new yeasts, isolated from Brazilian soil, able for the synthesis of AgNPs. These particles were characterized by techniques that allowed to determine the morphology, size, proteic capping agents and zeta potential. It was also the first time that AgNPs of fungal origin were able to catalytically reduce two important pollutants (4-NP and MB). Additionally, we showed that AgNPs possess antifungal activity alone and when associated with fluconazole against *C. parapsilosi*s and may represent an option for treating fungal infections.

REFERENCES

1. AHLUWALIA, V. *et al*. Green synthesis of silver nanoparticles by *Trichoderma harzianum* and their bio-efficacy evaluation against *Staphylococcus aureus* and *Klebsiella pneumoniae*. **Industrial Crops and Products**, v. 55, p. 202–206, 2014. Disponível em: http://linkinghub.elsevier.com/retrieve/pii/S0926669014000338 Acesso em: 2 jul. 2016.
2. AHMAD, A. *et al*. Extracellular biosynthesis of silver nanoparticles using the fungus Fusarium oxysporum. **Colloids and Surfaces B: Biointerfaces**, v. 28, n. 4, p. 313–318, 2003. Disponível em: http://linkinghub.elsevier.com/retrieve/pii/S0927776502001741 . Acesso em: 21 set. 2013.
3. AI, L.; JIANG, J. Catalytic reduction of 4-nitrophenol by silver nanoparticles stabilized on environmentally benign macroscopic biopolymer hydrogel. **Bioresource Technology**, v. 132, p. 374–377, 2013. Disponível em: http://linkinghub.elsevier.com/retrieve/pii/S0960852412016707 . Acesso em: 14 nov. 2014.
4. AJITHA, B.; REDDY, Y A. K.; REDDY, P S. Biosynthesis of silver nanoparticles using *Plectranthus amboinicus* leaf extract and its antimicrobial activity. **Spectrochimica Acta Part A: Molecular and Biomolecular Spectroscopy**, v. 128, p. 257–262, 2014. Disponível em: http://linkinghub.elsevier.com/retrieve/pii/S1386142514002923 . Acesso em: 9 ago. 2016.
5. AKSU, Z.; EREN, A. T. Carotenoids production by the yeast Rhodotorula mucilaginosa: Use of agricultural wastes as a carbon source. **Process Biochemistry**, v. 40, n. 9, p. 2985–2991, 2005. Disponível em: http://linkinghub.elsevier.com/retrieve/pii/S1359511305001157. Acesso em: 4 abr. 2015.
6. AKSU, Z.; EREN, A. T. Production of carotenoids by the isolated yeast of Rhodotorula glutinis. **Biochemical Engineering Journal**, v. 35, n. 2, p. 107–113, 2007. Disponível em: http://linkinghub.elsevier.com/retrieve/pii/S1369703X07000083. Acesso em: 4 abr. 2015.
7. ALANI, F.; MOO-YOUNG, M.; ANDERSON, W. Biosynthesis of silver nanoparticles by a new strain of *Streptomyces* sp. compared with *Aspergillus fumigatus*. **World**

Journal of Microbiology and Biotechnology, v. 28, n. 3, p. 1081–1086, 2012. Disponível em: http://link.springer.com/10.1007/s11274-011-0906-0 . Acesso em: 1 jul. 2016.

8. ALIMEHR, S. *et al*. Comparison of Difference Between Fluconazole and Silver Nanoparticles in Antimicrobial Effect on Fluconazole-Resistant Candida Albicans Strains. **Archives of Pediatric Infectious Diseases**, v. 3, n. 2, p. 0–3, 2015. Disponível em: http://www.pedinfect.com/?page=article&article_id=21481 . Acesso em: 5 ago. 2016.
9. AMERASAN, D. *et al*. Myco-synthesis of silver nanoparticles using *Metarhizium anisopliae* against the rural malaria vector *Anopheles culicifacies* Giles (Diptera: Culicidae). **Journal of Pest Science**, 2016. Disponível em: http://link.springer.com/10.1007/s10340-015-0675-x . Acesso em: 1 jul. 2016.
10. ANTHONY, K. J. P. *et al*. Synthesis of silver nanoparticles using pine mushroom extract: A potential antimicrobial agent against *E. coli* and *B. subtilis*. **Journal of Industrial and Engineering Chemistry**, v. 20, n. 4, p. 2325–2331, 2014. Disponível em: http://linkinghub.elsevier.com/retrieve/pii/S1226086X13004887 Acesso em: 1 abr. 2016.
11. APTE, M. *et al*. Psychrotrophic yeast *Yarrowia lipolytica* NCYC 789 mediates the synthesis of antimicrobial silver nanoparticles via cell-associated melanin. **AMB Express**, v. 3, n. 1, p. 32, 2013. Disponível em: http://www.pubmedcentral.nih.gov/articlerender.fcgi?artid=3702394&tool=pmcentrez&rendertype=abstract . Acesso em: 1 dez. 2014.
12. ASMATHUNISHA, N; KATHIRESAN, K. A review on biosynthesis of nanoparticles by marine organisms. **Colloids and surfaces. B, Biointerfaces**, v. 103, p. 283–7, 2013. Disponível em: http://www.ncbi.nlm.nih.gov/pubmed/23202242. Acesso em: 4 nov. 2014.
13. BALAJI, D. S. *et al*. Extracellular biosynthesis of functionalized silver nanoparticles by strains of *Cladosporium cladosporioides* fungus. **Colloids and surfaces. B, Biointerfaces**, v. 68, n. 1, p. 88–92, 2009. Disponível em: http://www.ncbi.nlm.nih.gov/pubmed/18995994 . Acesso em: 29 nov. 2014.
14. BALAKUMARAN, M.D.; RAMACHANDRAN, R.; KALAICHELVAN, P.T. Exploitation of endophytic fungus, *Guignardia mangiferae* for extracellular synthesis of silver nanoparticles and their in vitro biological activities. **Microbiological Research**, v. 178, p. 9–17, 2015. Disponível em:

http://linkinghub.elsevier.com/retrieve/pii/S0944501315001068 . Acesso em: 5 jan. 2016

15. BANU, A.; RATHOD, V.; RANGANATH, E. Silver nanoparticle production by *Rhizopus stolonifer* and its antibacterial activity against extended spectrum β-lactamase producing (ESBL) strains of *Enterobacteriaceae*. **Materials Research Bulletin**, v. 46, n. 9, p. 1417–1423, 2011. Disponível em: http://linkinghub.elsevier.com/retrieve/pii/S0025540811002108. Acesso em: 1 abr. 2016.
16. BARTH, A. Infrared spectroscopy of proteins. **Biochimica et Biophysica Acta (BBA) - Bioenergetics**, v. 1767, n. 9, p. 1073–1101, 2007. Disponível em: http://linkinghub.elsevier.com/retrieve/pii/S0005272807001375 . Acesso em: 30 nov. 2015.
17. BERTRAND, N. *et al*. Cancer nanotechnology: The impact of passive and active targeting in the era of modern cancer biology. **Advanced Drug Delivery Reviews**, v. 66, p. 2–25, 2014. Disponível em: http://dx.doi.org/10.1016/j.addr.2013.11.009. Acesso em: 01 set. 2014.
18. BIRLA, S. S. *et al*. Fabrication of silver nanoparticles by *Phoma glomerata* and its combined effect against *Escherichia coli*, *Pseudomonas aeruginosa* and *Staphylococcus aureus*. **Letters in applied microbiology**, v. 48, n. 2, p. 173–9, 2009. Disponível em: http://www.ncbi.nlm.nih.gov/pubmed/19141039 . Acesso em: 28 nov. 2014.
19. BIRLA, S. S. *et al*. Rapid synthesis of silver nanoparticles from *Fusarium oxysporum* by optimizing physicocultural conditions. **The Scientific World Journal**, v. 2013, p. 796018, 2013. Disponível em: http://www.pubmedcentral.nih.gov/articlerender.fcgi?artid=3810422&tool=pmcentrez&rendertype=abstract . Acesso em: 17 jun. 2015
20. CHAN, Y. S; DON M. M. Biosynthesis and structural characterization of Ag nanoparticles from white rot fungi. **Materials Science and Engineering: C**, v. 33, n. 1, p. 282–288, 2013. Disponível em: http://linkinghub.elsevier.com/retrieve/pii/S0928493112004183 . Acesso em: 27 nov. 2013.
21. CHEN, A; CHATTERJEE, S. Nanomaterials based electrochemical sensors for biomedical applications. **Chemical Society reviews**, v. 42, n. 12, p. 5425–38, 2013. Disponível em: http://www.ncbi.nlm.nih.gov/pubmed/23508125 . Acesso em: 22 out. 2014.

22. CHEN, X; YAN, J-K; WU, J-Y. Characterization and antibacterial activity of silver nanoparticles prepared with a fungal exopolysaccharide in water. **Food Hydrocolloids**, v. 53, n. 1, p. 69-74, 2016. Disponível em: http://linkinghub.elsevier.com/retrieve/pii/S0268005X14004743 . Acesso em: 1 jul. 2016.
23. CUTZU, R. *et al*. From crude glycerol to carotenoids by using a *Rhodotorula glutinis* mutant. **World Journal of Microbiology and Biotechnology**, v. 29, n. 6, p. 1009–1017, 2013. Disponível em: http://link.springer.com/10.1007/s11274-013-1264-x . Acesso em: 1 jun. 2016.
24. DAR, M. A.; INGLE, A.; RAI, M. Enhanced antimicrobial activity of silver nanoparticles synthesized by *Cryphonectria* sp. evaluated singly and in combination with antibiotics. **Nanomedicine: Nanotechnology, Biology and Medicine**, v. 9, n. 1, p. 105–110, 2013. Disponível em: http://linkinghub.elsevier.com/retrieve/pii/S1549963412001803 . Acesso em: 27 nov. 2014.
25. DESHMUKH, S.P. *et al*. Titania–supported silver nanoparticles: An efficient and reusable catalyst for reduction of 4-nitrophenol. **Applied Surface Science**, v. 273, p. 676–683, 2013. Disponível em: http://dx.doi.org/10.1016/j.apsusc.2013.02.110v. Acesso em: 27 nov. 2014.
26. DEVI, L. S.; BAREH, D. A.; JOSHI, S. R. Studies on Biosynthesis of Antimicrobial Silver Nanoparticles Using Endophytic Fungi Isolated from the Ethno-medicinal Plant *Gloriosa superba* L. **Proceedings of the National Academy of Sciences, India Section B: Biological Sciences**, v. 84, n. 4, p. 1091–1099, 2014. Disponível em: http://link.springer.com/10.1007/s40011-013-0185-7 . Acesso em: 29 nov. 2015.
27. DU, L. *et al*. Synthesis of small silver nanoparticles under light radiation by fungus *Penicillium oxalicum* and its application for the catalytic reduction of methylene blue. **Materials Chemistry and Physics**, v. 160, p. 40–47, 2015. Disponível em: http://linkinghub.elsevier.com/retrieve/pii/S0254058415300109 . Acesso em: 29 out. 2013.
28. DURÁN, N. *et al*. Mechanistic aspects in the biogenic synthesis of extracellular metal nanoparticles by peptides, bacteria, fungi, and plants. **Applied microbiology and biotechnology**, v. 90, n. 5, p. 1609–24, 2011. Disponível em: http://www.ncbi.nlm.nih.gov/pubmed/21484205 . Acesso em: 27 nov. 2014.

29. DURÁN, N. *et al*. Silver nanoparticle protein corona and toxicity: a mini-review. **Journal of Nanobiotechnology**, v. 13, n. 1, p. 55, 2015. Disponível em: <http://www.jnanobiotechnology.com/content/13/1/55>. Acesso em: 5 ago. 2016.
30. EDISON, T. J. I; SETHURAMAN, M. G. Biogenic robust synthesis of silver nanoparticles using *Punica granatum* peel and its application as a green catalyst for the reduction of an anthropogenic pollutant 4-nitrophenol. **Spectrochimica Acta - Part A: Molecular and Biomolecular Spectroscopy**, v. 104, p. 262–264, 2013. Disponível em: http://dx.doi.org/10.1016/j.saa.2012.11.084 . Acesso em: 30 nov. 2015.
31. EL-SONBATY, S. M. Fungus-mediated synthesis of silver nanoparticles and evaluation of antitumor activity. **Cancer Nanotechnology**, v. 4, n. 4-5, p. 73–79, 2013. Disponível em: http://link.springer.com/10.1007/s12645-013-0038-3 . Acesso em: 29 out. 2013.
32. GAJBHIYE, M. *et al*. Fungus-mediated synthesis of silver nanoparticles and their activity against pathogenic fungi in combination with fluconazole. **Nanomedicine : nanotechnology, biology, and medicine**, v. 5, n. 4, p. 382–6, 2009. Disponível em: http://www.ncbi.nlm.nih.gov/pubmed/19616127 . Acesso em: 28 nov. 2014.
33. GALANDAKOVA, A. *et al*. Effects of silver nanoparticles on human dermal fibroblasts and epidermal keratinocytes. **Human & Experimental Toxicology**, v. 35, n. 9, p. 946–957, 2016. Disponível em: http://www.ncbi.nlm.nih.gov/pubmed/26500221\nhttp://het.sagepub.com/content/early/2015/10/22/0960327115611969.full.pdf . Acesso em: 5 ago. 2016.
34. GANGULA, A.*et al*. Catalytic Reduction of 4-Nitrophenol using Biogenic Gold and Silver Nanoparticles Derived from *Breynia rhamnoides*. **Langmuir**, v. 27, n. 24, p. 15268–15274, 2011. Disponível em: http://pubs.acs.org/doi/abs/10.1021/la2034559 . Acesso em: 30 out. 2013.
35. GAVADE, N.L. *et al*. Biogenic synthesis of multi-applicative silver nanoparticles by using Ziziphus Jujuba leaf extract. **Spectrochimica Acta Part A: Molecular and Biomolecular Spectroscopy**, v. 136, p. 953–960, 2015. Disponível em: http://linkinghub.elsevier.com/retrieve/pii/S1386142514014760 . Acesso em: 12 jul. 2016.
36. GOLINSKA, P. *et al*. Biogenic synthesis of metal nanoparticles from actinomycetes: biomedical applications and cytotoxicity. **Applied Microbiology and Biotechnology**, v. 98, n. 19, p. 8083–8097, 2014. Disponível em: http://link.springer.com/10.1007/s00253-014-5953-7. Acesso em: 20 mai. 2013.

37. GOSWAMI, A. M.; SARKAR, T. S.; GHOSH, S. An Ecofriendly synthesis of silver nano-bioconjugates by *Penicillium citrinum* (MTCC9999) and its antimicrobial effect. **AMB Express**, v. 3, n. 1, p. 16, 2013. Disponível em: http://www.pubmedcentral.nih.gov/articlerender.fcgi?artid=3610205&tool=pmcentrez&rendertype=abstract . Acesso em: 28 nov. 2014.
38. GU, S. *et al*. Kinetic analysis of the reduction of 4-nitrophenol catalyzed by Au/Pd nanoalloys immobilized in spherical polyelectrolyte brushes. **Phys. Chem. Chem. Phys.**, p. 22–24, 2015. Disponível em: http://xlink.rsc.org/?DOI=C5CP00519A . Acesso em: 13 mai. 2016.
39. HAJIPOUR, M. J. *et al*. Antibacterial properties of nanoparticles. **Trends in Biotechnology**, v. 30, n. 10, p. 499–511, 2012. Disponível em: http://linkinghub.elsevier.com/retrieve/pii/S0167779912000959. Acesso em: 19 fev. 2015.
40. HERNANDEZ-ALMANZA, A. *et al*. *Rhodotorula glutinis* as source of pigments and metabolites for food industry. **Food Bioscience**, v. 5, p. 64–72, 2014. Disponível em: http://linkinghub.elsevier.com/retrieve/pii/S2212429213000849 . Acesso em: 20 fev. 2015.
41. HERVÉS, P. *et al*. Catalysis by metallic nanoparticles in aqueous solution: model reactions. **Chemical Society Reviews**, v. 41, n. 17, p. 5577, 2012. Disponível em: http://xlink.rsc.org/?DOI=c2cs35029g . Acesso em: 21 fev. 2014.
42. HULKOTI, N. I.; TARANATH, T.C. Biosynthesis of nanoparticles using microbes—A review. **Colloids and Surfaces B: Biointerfaces**, v. 121, p. 474–483, 2014. Disponível em: http://dx.doi.org/10.1016/j.colsurfb.2014.05.027 . Acesso em: 29 jul. 2013.
43. HWANG, I. *et al*. Silver nanoparticles induce apoptotic cell death in *Candida albicans* through the increase of hydroxyl radicals. **FEBS Journal**, v. 279, n. 7, p. 1327–1338, 2012. Disponível em: http://doi.wiley.com/10.1111/j.1742-4658.2012.08527.x . Acesso em: 05 ago. 2016.
44. INGLE, A. *et al*. *Fusarium solani:* a novel biological agent for the extracellular synthesis of silver nanoparticles. **Journal of Nanoparticle Research**, v. 11, n. 8, p. 2079–2085, 2009. Disponível em: http://link.springer.com/10.1007/s11051-008-9573-y . Acesso em: 21 nov. 2014.
45. IRAVANI, S. Green synthesis of metal nanoparticles using plants. **Green Chemistry**, v. 13, n. 10, p. 2638, 2011. Disponível em: http://xlink.rsc.org/?DOI=c1gc15386b . Acesso em: 22 jan. 2014.

46. JAIN, N. *et al*. Extracellular biosynthesis and characterization of silver nanoparticles using *Aspergillus flavus* NJP08: a mechanism perspective. **Nanoscale**, v. 3, n. 2, p. 635–41, 2011. Disponível em: http://www.ncbi.nlm.nih.gov/pubmed/21088776 . Acesso em: 28 nov. 2014.
47. JANANI, S.; STEVENSON, P.; VEERAPPAN, A. Activity of catalytic silver nanoparticles modulated by capping agent hydrophobicity. **Colloids and Surfaces B: Biointerfaces**, v. 117, p. 528–533, 2014. Disponível em: http://linkinghub.elsevier.com/retrieve/pii/S0927776514001283 . Acesso em: 12 jul. 2016.
48. JEBALI, A.; RAMEZANI, F.; KAZEMI, B. Biosynthesis of Silver Nanoparticles by *Geotricum* sp. **Journal of Cluster Science**, v. 22, n. 2, p. 225–232, 2011. Disponível em: http://link.springer.com/10.1007/s10876-011-0375-5 . Acesso em: 21 fev. 2013.
49. JIANG, D. *et al*. Facile route to silver submicron-sized particles and their catalytic activity towards 4-nitrophenol reduction. **Journal of Alloys and Compounds**, v. 509, n. 5, p. 1975–1979, 2011. Disponível em: http://linkinghub.elsevier.com/retrieve/pii/S0925838810026368 . Acesso em: 21 fev. 2013.
50. JOSEPH, S; MATHEW, B. Microwave assisted facile green synthesis of silver and gold nanocatalysts using the leaf extract of *Aerva lanata*. **Spectrochimica Acta Part A: Molecular and Biomolecular Spectroscopy**, v. 136, p. 1371–1379, 2015. Disponível em: http://linkinghub.elsevier.com/retrieve/pii/S1386142514015200 . Acesso em: 12 jul. 2016.
51. KALER, A.; JAIN, S.; BANERJEE, U. C. Green and rapid synthesis of anticancerous silver nanoparticles by Saccharomyces boulardii and insight into mechanism of nanoparticle synthesis. **BioMed research international**, v. 2013, p. 872940, 2013. Disponível em: http://www.pubmedcentral.nih.gov/articlerender.fcgi?artid=3835627&tool=pmcentrez&rendertype=abstract . Acesso em: 18 dez. 2015.
52. KALIMUTHU, K. et al. Biosynthesis of silver nanocrystals by Bacillus licheniformis. Colloids and Surfaces B: Biointerfaces, v. 65, n. 1, p. 150–153, 2008. Disponível em: http://linkinghub.elsevier.com/retrieve/pii/S0927776508000945 . Acesso em: 9 ago. 2016.
53. KALPANA, D.; LEE, Y. S. Synthesis and characterization of bactericidal silver nanoparticles using cultural filtrate of simulated microgravity grown *Klebsiella*

pneumoniae. **Enzyme and microbial technology**, v. 52, n. 3, p. 151–6, 2013. Disponível em: http://www.ncbi.nlm.nih.gov/pubmed/23410925 . Acesso em: 3 nov. 2014.

54. KHATOON, N. *et al*. Biosynthesis, Characterization, and Antifungal Activity of the Silver Nanoparticles Against Pathogenic Candida species. **BioNanoScience**, v. 5, n. 2, p. 65–74, 2015. Disponível em: http://link.springer.com/10.1007/s12668-015-0163-z . Acesso em: 5 ago. 2016.
55. KIM, J. S. *et al*. Antimicrobial effects of silver nanoparticles. **Nanomedicine: Nanotechnology, Biology and Medicine**, v. 3, n. 1, p. 95–101, 2007. Disponível em: http://linkinghub.elsevier.com/retrieve/pii/S1549963406003467 . Acesso em: 31 jul. 2014.
56. KIM, K-J. *et al*. Antifungal activity and mode of action of silver nano-particles on *Candida albicans*. **BioMetals**, v. 22, n. 2, p. 235–242, 2009. Disponível em: http://www.ncbi.nlm.nih.gov/pubmed/18769871 . Acesso em: 13 dez. 2014.
57. KUMARI, M. M.; PHILIP, D. Facile one-pot synthesis of gold and silver nanocatalysts using edible coconut oil. **Spectrochimica Acta Part A: Molecular and Biomolecular Spectroscopy**, v. 111, p. 154–160, 2013. Disponível em: http://dx.doi.org/10.1016/j.saa.2013.03.076 . Acesso em: 29 jan. 2015.
58. LIN, P-C *et al*. Techniques for physicochemical characterization of nanomaterials. **Biotechnology Advances**, v. 32, n. 4, p. 711–726, 2014. Disponível em: http://linkinghub.elsevier.com/retrieve/pii/S0734975013002115. Acesso em: 20 ago. 2014.
59. MADDEN, O. *et al*. Mycofabrication of common plasmonic colloids, theoretical considerations, mechanism and potential applications. **Advances in Colloid and Interface Science**, 2015. Disponível em: http://linkinghub.elsevier.com/retrieve/pii/S0001868615001438 . Acesso em: 27 nov. 2014.
60. MENEZES, E. A. et al. Correlation between microdilution, Etest, and disk diffusion methods for antifungal susceptibility testing of fluconazole against *Candida* sp. blood isolates. **Revista da Sociedade Brasileira de Medicina Tropical**, v. 46, n. 1, p. 106–107, 2013. Disponível em: http://www.scielo.br/scielo.php?script=sci_arttext&pid=S0037-86822013000100106&lng=en&nrm=iso&tlng=en . Acesso em: 1 ago. 2014.

61. MOHANPURIA, P.; RANA, N. K.; YADAV, S. K.. Biosynthesis of nanoparticles: technological concepts and future applications. **Journal of Nanoparticle Research**, v. 10, n. 3, p. 507–517, 2008. Disponível em: http://link.springer.com/10.1007/s11051-007-9275-x . Acesso em: 10 set. 2013.
62. NAQVI, S. Z. *et al*. Combined efficacy of biologically synthesized silver nanoparticles and different antibiotics against multidrug-resistant bacteria. **International Journal of Nanomedicine**, v. 8, p. 3187–3195, 2013. Disponível em: http://www.dovepress.com/combined-efficacy-of-biologically-synthesized-silver-nanoparticles-and-peer-reviewed-article-IJN . Acesso em: 30 ago. 2015.
63. NARAYANAN, K. B.; PARK, H.H.; SAKTHIVEL, N. Extracellular synthesis of mycogenic silver nanoparticles by *Cylindrocladium floridanum* and its homogeneous catalytic degradation of 4-nitrophenol. **Spectrochimica acta. Part A, Molecular and biomolecular spectroscopy**, v. 116, p. 485–90, 2013. Disponível em: http://www.ncbi.nlm.nih.gov/pubmed/23973598 . Acesso em: 29 nov. 2014.
64. NARAYANAN, K. B.; SAKTHIVEL, N. Biological synthesis of metal nanoparticles by microbes. **Advances in colloid and interface science**, v. 156, n. 1-2, p. 1–13, 2010. Disponível em: http://www.ncbi.nlm.nih.gov/pubmed/20181326. Acesso em: 18 jul. 2014.
65. PANÁČEK, Aleš *et al*. Antifungal activity of silver nanoparticles against *Candida* spp. **Biomaterials**, v. 30, n. 31, p. 6333–6340, 2009. Disponível em: http://linkinghub.elsevier.com/retrieve/pii/S0142961209008023 . Acesso em: 9 set. 2013.
66. PEARSON, R. M; JUETTNER, V. V; HONG, S. Biomolecular corona on nanoparticles: a survey of recent literature and its implications in targeted drug delivery. **Frontiers in Chemistry**, v. 2, n. November, p. 108, 2014. Disponível em: http://journal.frontiersin.org/article/10.3389/fchem.2014.00108/abstract . Acesso em: 10 ago. 2016.
67. PELGRIFT, R. Y.; FRIEDMAN, A.J. Nanotechnology as a therapeutic tool to combat microbial resistance. **Advanced Drug Delivery Reviews**, v. 65, n. 13-14, p. 1803–1815, 2013. Disponível em: http://dx.doi.org/10.1016/j.addr.2013.07.011 . Acesso em: 29 nov. 2014.
68. PRABHU, S.; POULOSE, E. K. Silver nanoparticles: mechanism of antimicrobial action, synthesis, medical applications, and toxicity effects. **International Nano**

Letters, v. 2, n. 1, p. 32, 2012. Disponível em: http://link.springer.com/article/10.1186/2228-5326-2-32. Acesso em: 30 jun. 2013.

69. PRADHAN, N.; PAL, A; PAL, T. Silver nanoparticle catalyzed reduction of aromatic nitro compounds. **Colloids and Surfaces A: Physicochemical and Engineering Aspects**, v. 196, n. 2-3, p. 247–257, 2002. Disponível em: http://www.sciencedirect.com/science/article/pii/S0927775701010408. Acesso em: 12 out. 2014.
70. PUJALTÉ, I. *et al*. Cytotoxicity and oxidative stress induced by different metallic nanoparticles on human kidney cells. **Particle and Fibre Toxicology**, v. 8, n. 1, p. 10, 2011. Disponível em: http://www.particleandfibretoxicology.com/content/8/1/10 . Acesso em: 5 ago. 2016.
71. QUESTER, K.; AVALOS-BORJA, M.; CASTRO-LONGORIA, E. Biosynthesis and microscopic study of metallic nanoparticles. **Micron (Oxford, England : 1993)**, v. 54-55, p. 1–27, 2013. Disponível em: http://www.ncbi.nlm.nih.gov/pubmed/23928107. Acesso em: 12 out. 2014.
72. RAHEMAN, F. *et al*. Novel Antimicrobial Agent Synthesized from an Endophytic Fungus *Pestalotia* sp . Isolated from Leaves of *Syzygium cumini* (L). **Nano Biomed Eng**, v. 3, p. 174–178, 2011. Disponível em : https://www.researchgate.net/publication/216532614 Acesso em: 12 set 2013.
73. RAI, M. K. *et al*. Broad-spectrum bioactivities of silver nanoparticles: the emerging trends and future prospects. **Applied Microbiology and Biotechnology**, v. 98, n. 5, p. 1951–1961, 2014. Disponível em: http://link.springer.com/10.1007/s00253-013-5473-x . Acesso em: 12 abr. 2015.
74. RETTONDIN, A.R. *et al*. Gold(III) complexes with ONS-Tridentate thiosemicarbazones: Toward selective trypanocidal drugs. **European Journal of Medicinal Chemistry**, v. 120, p. 217–226, 2016. Disponível em: http://linkinghub.elsevier.com/retrieve/pii/S0223523416303695 . Acesso em: 12 abr. 2016.
75. RODRIGUES, A. G. *et al*. Biogenic antimicrobial silver nanoparticles produced by fungi. **Applied Microbiology and Biotechnology**, v. 97, n. 2, p. 775–782, 2013. Disponível em: <http://link.springer.com/10.1007/s00253-012-4209-7>. Acesso em: 13 abr. 2015.
76. SALUNKHE, R. B. *et al*. Studies on silver accumulation and nanoparticle synthesis By *Cochliobolus lunatus*. **Applied biochemistry and biotechnology**, v. 165, n. 1, p. 221–

34, 2011. Disponível em: http://www.ncbi.nlm.nih.gov/pubmed/21505806 . Acesso em: 27 nov. 2014.

77. SANYASI, S. *et al*. Polysaccharide-capped silver Nanoparticles inhibit biofilm formation and eliminate multi-drug-resistant bacteria by disrupting bacterial cytoskeleton with reduced cytotoxicity towards mammalian cells. **Scientific Reports**, v. 6, , p. 24929-24914, 2016. Disponível em: http://dx.doi.org/10.1038/srep24929 . Acesso em: 10 ago. 2016.
78. SAPSFORD, K. E. *et al*. Functionalizing Nanoparticles with Biological Molecules: Developing Chemistries that Facilitate Nanotechnology. **Chemical Reviews**, v. 113, n. 3, p. 1904–2074, 2013. Disponível em: http://pubs.acs.org/doi/abs/10.1021/cr300143v . Acesso em: 29 dez. 2014.
79. SATHISHKUMAR, Y. *et al*. Shape-controlled extracellular synthesis of silver nanocubes by *Mucor circinelloides*. **Materials Letters**, v. 159, p. 481–483, 2015. Disponível em: http://linkinghub.elsevier.com/retrieve/pii/S0167577X15301774 . Acesso em: 11 ago. 2014.
80. SHALIGRAM, N. S. *et al*. Biosynthesis of silver nanoparticles using aqueous extract from the compactin producing fungal strain. **Process Biochemistry**, v. 44, n. 8, p. 939–943, 2009. Disponível em: http://linkinghub.elsevier.com/retrieve/pii/S1359511309001305 . Acesso em: 14 abr. 2015.
81. SHARMA, V. K.; YNGARD, R.A.; LIN, Y. Silver nanoparticles: Green synthesis and their antimicrobial activities. **Advances in Colloid and Interface Science**, v. 145, n. 1-2, p. 83–96, 2009. http://www.ncbi.nlm.nih.gov/pubmed/18945421 Acesso em: 1 nov 2013.
82. SUVITH, V. S.; PHILIP, D. Catalytic degradation of methylene blue using biosynthesized gold and silver nanoparticles. **Spectrochimica Acta - Part A: Molecular and Biomolecular Spectroscopy**, v. 118, p. 526–532, 2014. Disponível em: http://dx.doi.org/10.1016/j.micron.2013.10.006. Acesso em: 1 nov 2013.
83. TAHIR, Kamran *et al*. An efficient photo catalytic activity of green synthesized silver nanoparticles using *Salvadora persica* stem extract. **Separation and Purification Technology**, v. 150, p. 316–324, 2015. Disponível em: http://dx.doi.org/10.1016/j.seppur.2015.07.012 . Acesso em 2 jul 2016.
84. THAKKAR, K. N.; MHATRE, S. S.; PARIKH, R.Y. Biological synthesis of metallic nanoparticles. **Nanomedicine : nanotechnology, biology, and medicine**, v. 6, n. 2,

p. 257–62, 2010. Disponível em: http://www.ncbi.nlm.nih.gov/pubmed/19616126 . Acesso em: 12 out. 2014.

85. UDDIN, M. T. *et al*. Adsorptive removal of methylene blue by tea waste. **Journal of Hazardous Materials**, v. 164, n. 1, p. 53–60, 2009. Disponível em: http://linkinghub.elsevier.com/retrieve/pii/S0304389408011679. Acesso em 15 mar. 2016.
86. VANAJA, M *et al*. Degradation of Methylene Blue Using Biologically Synthesized Silver Nanoparticles. **Bioinorganic Chemistry and Applications**, v. 2014, p. 1–8, 2014. Disponível em: http://www.hindawi.com/journals/bca/2014/742346/ . Acesso em: 3 mar. 2015.
87. VASCONCELOS, A. A; MENEZES, E. A.; CUNHA, F. A. Chromogenic Medium for Direct Susceptibility Testing of *Candida* spp. Isolated from Urine. **Mycopathologia**, v. 172, n. 2, p. 125–130, 2011. Disponível em: http://link.springer.com/10.1007/s11046-011-9407-9 . Acesso em: 2 out. 2013.
88. VAZQUEZ-MUÑOZ, R.; AVALOS-BORJA, M.; CASTRO-LONGORIA, E. Ultrastructural Analysis of *Candida albicans* When Exposed to Silver Nanoparticles. **PLoS ONE**, v. 9, n. 10, p. e108876, 2014. Disponível em: http://dx.plos.org/10.1371/journal.pone.0108876 . Acesso em: 5 ago. 2016.
89. VERMA, V. C.; KHARWAR, R. N.; GANGE, A. C. Biosynthesis of antimicrobial silver nanoparticles by the endophytic fungus *Aspergillus clavatus*. **Nanomedicine (London, England)**, v. 5, n. 1, p. 33–40, 2010. Disponível em: http://www.ncbi.nlm.nih.gov/pubmed/20025462 . Acesso em: 29 nov. 2014.
90. VIDHU, V. K.; PHILIP, D Catalytic degradation of organic dyes using biosynthesized silver nanoparticles. **Micron (Oxford, England : 1993)**, v. 56, p. 54–62, 2014b. Disponível em: http://www.ncbi.nlm.nih.gov/pubmed/24210247 . Acesso em: 18 nov. 2014.
91. VIDHU, V. K.; PHILIP, D. Spectroscopic, microscopic and catalytic properties of silver nanoparticles synthesized using *Saraca indica* flower. **Spectrochimica acta. Part A, Molecular and biomolecular spectroscopy**, v. 117, p. 102–8, 2014a. Disponível em: http://www.ncbi.nlm.nih.gov/pubmed/23988525 . Acesso em: 2 dez. 2014.
92. VIGNESHWARAN, N. *et al*. Biological synthesis of silver nanoparticles using the fungus *Aspergillus flavus*. **Materials Letters**, v. 61, n. 6, p. 1413–1418, 2007. Disponível em: http://www.sciencedirect.com/science/article/pii/S0167577X06008512 . Acesso em: 29 nov. 2014.

93. WADY, A. F. *et al*. Effect of a Silver Nanoparticles Solution on Staphylococcus aureus and Candida spp. **Journal of Nanomaterials**, v. 2014, p. 1–7, 2014. Disponível em: http://www.hindawi.com/journals/jnm/2014/545279/ . Acesso em: 5 ago. 2016.

94. XIA, Y. *et al*. Shape-controlled synthesis of metal nanocrystals: simple chemistry meets complex physics? **Angewandte Chemie (International ed. in English)**, v. 48, n. 1, p. 60–103, 2009. Disponível em: http://www.pubmedcentral.nih.gov/articlerender.fcgi?artid=2791829&tool=pmcentrez&rendertype=abstract . Acesso em: 10 jul. 2014.

95. XU, H.; SUSLICK, K. S. Sonochemical synthesis of highly fluorescent Ag nanoclusters. **ACS Nano**, v. 4, n. 6, p. 3209–3214, 2010. Disponível em: http://pubs.acs.org/doi/abs/10.1021/nn100987k . Acesso em: 11 jun. 2014.

96. YADAV, A. *et al*. Fungi as an efficient mycosystem for the synthesis of metal nanoparticles: progress and key aspects of research. **Biotechnology Letters**, v. 37, n. 11, p. 2099–2120, 2015. Disponível em: http://dx.doi.org/10.1007/s10529-015-1901-6 . Acesso em: 3 fev. 2014.

97. YEHIA, R. S.; AL-SHEIKH, H.. Biosynthesis and characterization of silver nanoparticles produced by *Pleurotus ostreatus* and their anticandidal and anticancer activities. **World Journal of Microbiology and Biotechnology**, v. 30, n. 11, p. 2797–2803, 2014. Disponível em: http://link.springer.com/10.1007/s11274-014-1703-3 . Acesso em: 7 fev. 2015.

98. ZHAO, X. H. *et al*. Alginate fibers embedded with silver nanoparticles as efficient catalysts for reduction of 4-nitrophenol. **RSC Adv.**, v. 5, n. 61, p. 49534–49540, 2015. Disponível em: http://www.scopus.com/inward/record.url?eid=2-s2.0-84930941544&partnerID=tZOtx3y1 Acesso em: 6 fev. 2016.

99. ZHENG, Z. *et al*. In situ synthesis of silver nanoparticles dispersed or wrapped by a *Cordyceps sinensis* exopolysaccharide in water and their catalytic activity. **RSC Adv.**, v. 5, n. 85, p. 69790–69799, 2015. Disponível em: http://pubs.rsc.org/en/content/articlehtml/2015/ra/c5ra09452f . Acesso em: 6 fev. 2016.

100. ZICCARDI, M. *et al*. *Candida parapsilosis* (sensu lato) isolated from hospitals located in the Southeast of Brazil: Species distribution, antifungal susceptibility and virulence attributes. **International Journal of Medical Microbiology**, v. 305, n. 8, p. 848–859, 2015. Disponível em: http://linkinghub.elsevier.com/retrieve/pii/S1438422115300023 . Acesso em: 13 jul. 2016.

CHAPTER FIVE

Ceftazidime and 4-nitrophenol inactivation using alginate's sphere inlaid with mycogenic silver nanoparticles

ABSTRACT

Silver nanoparticles (AgNPs) produced by fungi are classified as green chemistry, because it do not use toxic reagents in their production not generate waste that harm the environment and the health of humans and animals. The placement of these particles in polymeric matrices such as alginate, chitosan and agarose, produces structures with new technological applications. The aim of this work was to produce alginate spheres impregnated with AgNPs of fungal origin, characterize these spheres trough UV-Vis, FTIR, XRD, SEM and AFM and evaluate its catalytic activity in reducing pollutant 4-nitrophenol (4-NP) and antibiotic ceftazidime (Ceft). The size produced spheres Ag@AlgRg and Ag@Alg Rm were measured 2.49 mm and 2.78 mm, respectively. The plasmon band was detected at around 400 nm. The exploring of the spheres surface showed a roughness structure and the AgNPs distributed throughout the sphere. The catalytic activity of the spheres was detected and about 95% of the pollutant 4-nitrophenol (4-NP) has been removed at 30 min. The spheres were also able to degrade the antibiotic ceftazidime (Ceft). The degraded drug did not show activity against *Klebsiella pneumoniae* and *Escherichia coli*, bacteria that cause important diseases in humans and animals. This multi-focal catalytic activity can be valuable, since these components (4-NP and Ceft) contaminate sewage and may contaminate water collections.

Keywords: Ceftazidime; 4-nitrophenol; Silver nanoparticles; Alginate's spheres.

INTRODUCTION

Modern society faces a large amount of pollutants generated by the processing industries, one of the leading 4- nitrophenol (YIN et al., 2016). The forms of disposal of this pollutant vary and may offer a risk to the health of men and animals and the environmental balance. New catalytic routes of these pollutants are needed to ensure the growth of the industry and keep the environment safe. The nanocatalysts of noble metals are the most promising candidates for various applications in these new catalytic routes (AI, YUE, JIANG, 2012) .

Disposal of drugs is another problem that profoundly impacts the environment (VERLICCHI, ZAMBELLO, 2015). An aside is the disposal of Pharmaceutical and Personal

Care Products (PPCPs), including many antibiotics beta-lactams such as ceftazidime (Ceft) (HU, YU, SUN, 2016). Every day, tons of these PPCPs are thrown into sewers without any treatment (FENG et al., 2016). The most immediate result of this is the selection of resistant strains of bacteria. The microflora present in sewage is amended in a such way that favors the prevalence of bacteria that express high levels of resistance, some bacteria found in sewage, are resistant to about 10 antimicrobials (BAQUERO, MARTÍNEZ, CANTÓN, 2008). The effect of this in long-term may be the end of the golden age of antibacterials (VIENS, LITTMANN, 2015).

Alginate is a naturally occurring polysaccharide consisting of β-D- mannuronic acid and α-L-guluronic acid with 1-4 bonds, with a large and varied sequence (AI et al., 2012; BABU et al., 2010). One of the most interesting properties of alginate is the ability to form a three-dimensional network when comes into contact with ions, especially divalent ions (Ca^{2+}, Sr^{2+}, Ba^{2+}).

The development of polymers containing metal nanoparticles is an issue that has attracted attention of several research groups and the reasons are varied, polymers containing these particles can show catalytic, optical and antimicrobial activities, and also release drugs (AI et al., 2013; BOGUN et al., 2013; BOZANIC et al., 2011; CHEN et al., 2014).

Silver nanoparticles (AgNPs) produced by fungi is a current topic, because it is a green method that minimizes risks to the environment and some of these AgNPs exhibit catalytic activity on major pollutants such as methylene blue and 4-nitrophenol (DU et al., 2015; NARAYANAN, PARK, SAKTHIVEL, 2013).

The aim of this study was to produce alginate spheres functionalized with AgNPs produced by fungi *Rhodotorula glutinis* (Rg) and *Rhodotorula mucilaginosa* (Rm) and evaluate its catalytic activity in the degradation of 4-nitrophenol (4-NP) and inactivation of the antibiotic ceftazidime (Ceft).

MATERIALS AND METHODS

Materials

Sodium borohydride ($NaBH_4$), (Dinâmica- São Paulo-Brasil), sodium alginate (Sigma-USA), calcium chloride ($CaCl_2$) (ProQuimios- Rio de Janeiro- Brasil), 4-nitrophenol (Dinâmica- São Paulo-Brasil), and ceftazidime (Cellofarm-Rio de Janeiro-Brasil) were used without further purification.

Source of AgNPs

The AgNPs suspensions used this were produced and characterized in Chapter 4.

Preparation of spheres Ag@Alg Rg/Rm

A schematic diagram of the production of the Ag@Alg spheres is shown in FIGURE S1 Supporting Information Chapter 5. Initially, 1.0 g of sodium alginate powder was dissolved in 100.0 mL of AgNPs solution (50 ug/mL) produced by *R. glutinis* and *R. mucilaginosa,* separately. The solutions were maintained under stirring for 30 min at 50 °C. After this time, the solution was aspirated with a volumetric pipette and dropped into a calcium chloride solution (0.2 M) to occur the process of formation of the spheres. Then they were removed from the solution and washed three times with deionized water in order to remove the excess ions and AgNPs not strongly adhered to the spheres. The spheres were labeled with Ag@AlgRg to those produced using AgNPs by *R. glutinis* and Ag@AlgRm produced using AgNPs by *R. mucilaginosa.*

Characterization of spheres Ag@Alg Rg/Rm

Ultraviolet−visible (UV-vis) spectra, Fourier transform infrared spectroscopy (FTIR), X-ray diffraction (XRD), scanning electron microscopy (SEM), energy dispersive X-ray spectrometry (EDX), and atomic force microscopy (AFM) analyses were used to characterize spheres structure, composition, size, and morphology.

Reduction's 4-NP by Ag@Alg Rg and Ag@Alg Rm

To carry out the catalytic reduction of 4-NP, an aqueous solution of $NaBH_4$ (2.5 mL, 0.05M), prepared immediately before use, it was mixed with the aqueous solution of 4-NP (25 uL, 10 mM) in a quartz cuvette, to this mixture were add 8 spheres of Ag@Agl Rg/Rm (see FIGURE S2 in Supporting Information Chapter 5). The absorbance of the mixture was measured 250-550 nm (AI, JIANG, 2013).

Characterization of Ceftazidime

Ceftazidime is a semisynthetic, broad-spectrum, beta-lactam antibiotic. Ceftazidime is a white to cream-colored crystalline powder. The structure of ceftazidime can be seen in FIGURE S3 Supporting Information Chapter 5. A solution of 1.0 mM ceftazidime (work solution) was prepared. Ceftazidime was characterized by UV-Vis and FTIR using KBr in the

region 500-4000 cm^{-1} of 2 cm^{-1} interval (see in FIGURE S4 and S5 Supporting Information Chapter 5).

Ceftazidime's degradation by Ag@Alg Rg and Ag@Alg Rm

In a quartz cuvette were placed 0.2 mL Ceft (0.12 mM), with 2.70 mL of Milli-Q water and 0.1 mL of $NaBH_4$ (0.1M). To these cuvettes were added 8 spheres Ag@Alg Rg and Ag@Alg Rm, separately. Samples were analyzed for 30 min in a spectrophotometer UV-Vis, range of 200-350 nm, as control was used a quartz cuvette with 0.2 mL Ceft (0.12 mM), with 2.70 mL of Milli-Q water and 0.1 mL of $NaBH_4$ (0.1M) and 8 alginate spheres without AgNPs (JUNEJO, GÜNERC, BAYKAL, 2014). Proceed samples were used in the next step.

Antimicrobial efficacy of ceftazidime degraded

Klebsiella pneumoniae ATCC 13883 and *Escherichia coli* ATCC 25922 were used to evaluate the efficacy of ceftazidime degraded. On a Muller-Hinton agar plate were seeded both strains, and were performed 3 well. The well 1 was placed 100 µL of solution 0.12 mM Ceft treated with the alginate spheres without AgNPs; well 2 was placed 100 µL of 0.12 mM solution Ceft treated with Ag@Alg Rg spheres; and well 3 was added 100 µL of the solution 0.12 mM Ceft treated with Ag@Alg Rm spheres. The plates were incubated at 35°C/24 h, after this time the zones of inhibition of Ceft were mensured.

RESULTS AND DISCUSSION

The synthesis of alginate spheres containing AgNPs (Ag@Alg) has aroused interest due its ease of preparation, low cost and catalytic properties (WANG et al., 2016). In our study spheres were synthesized with AgNPs solutions of fungal origin. This production method is a green method, because it uses nontoxic reactants and the amount of waste generated is minimal. As we can see in FIGURE 1, the Ag@AlgRg/Rm showed the characteristic brown color of AgNPs, we can see that the Alginate spheres without AgNPs are white. We can see that the Ag@AlgRm are darker than the Ag@AlgRg, this is due to the color of the original colloidal suspensions. The color can vary according to the used solution (PAL et al., 2015).

In several works describing the production of these spheres AgNPs are generated within the reticulated structure of the alginate "*in situ*", typically by light irradiation or microwave (AI, JIANG, 2013; PAL et al., 2015; WANG et al., 2016). In our study, the method was innovative and consisted of the use of colloidal suspensions with AgNPs previously produced by the fungi *R. glutinis* and *R. mucilaginosa*. This new technique ensures that all the spheres have the same amount and distribution of AgNPs, once they are formed within the colloidal suspension. We have no record of studies in the literature have used this methodology.

We noted that all areas have similar coloring and at 50 spheres counting it was found that they had, when wet, the diameters of 2.78 ± 0.52 mm (mean ± SD) for Ag@Alg Rg and 2.49 ± 0.45 mm (mean ± SD) for Ag@AlgRm (see FIGURE S6 in Supporting Information Chapter 5). The size of the sphere depends on several factors such as the concentration of alginate, the concentration of divalent ions and dripper (PANKONGADISAK et al., 2014). In our study we used the alginate 1% and dripping was accomplished with a volumetric pipette of large diameter which gave large spheres, but it is possible to produce spheres of various sizes. In a study using electrospray followed by lyophilization it was possible to obtain spheres of size 0.307 mm ± 0.23(mean ± SD) (PANKONGADISAK et al., 2014), approximately 10 times smaller than those obtained in our work. In a process using $NaBH_4$ as a reducing agent for silver ions and an electronic injecting system of alginate, spheres were obtained 2.4 mm ± 0.4 mm (LIN et al., 2013), similar diameters to those found in this work.

FIGURE 1- Ag@Alg Rm - sphere with AgNPs produced by *R. mucilaginosa;* Ag@Alg Rg- sphere with AgNPs produced by *R. glutinis* and alginate's spheres.

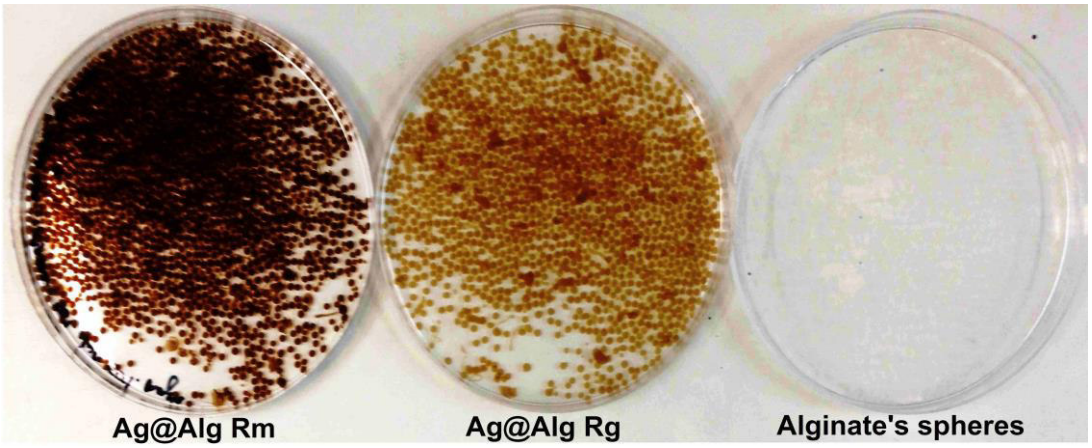

Source: Author

The spheres were analyzed by UV-Vis spectroscopy and had shown plasmon band which is characteristic of AgNPs (FIGURE 2). Both spheres showed absorption at around 400 nm. Gels containing AgNPs immersed in alginate described in other studies show the same band plasmon identified in our work (VIMALA et al., 2010; ZHAO et al., 2014). The plasmon band shows that the process did not change the AgNPs and they are available in spheres.

FIGURE 2- UV-VIS of Ag@AlgRg (a) and Ag@AlgRm (b).

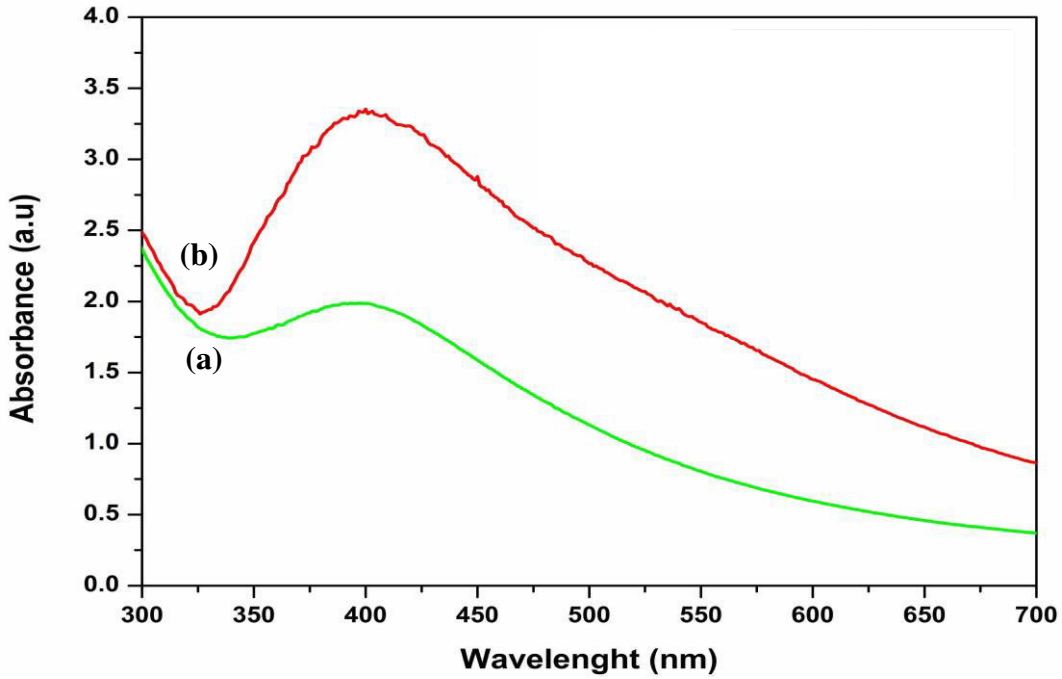

Source: Author

FIGURE 3 shows the FTIR of samples of alginate spheres without and with association with mycogenic AgNPs. Bands 3439, 3445 and 3432 cm^{-1} are due to stretching of the grouping -OH (ZAHRAN et al., 2014). The intense bands in 1632, 1639 and 1633 cm^{-1} are due to asymmetric stretching of the carboxylate ions -COO (SHARMA et al., 2012;. ZHAO et al., 2014). Bands in 1440, 1427 and 1420 cm^{-1} are attributed to deformations wagging of the groups -C-H or due to the symmetric stretching of the carboxylate ions (SHARMA et al., 2012; ZAHRAN et al., 2014.). The deformations around 1000 cm^{-1} correspond to stretches of groups -O-O-C present in glycosidic groups of alginate (CHINKAP, MYUNGHEE, NUE, 2004). Our findings were similar to those described by ZHAO et al., 2014, however, the AgNPs in our study were already formed when alginate beads were added, it would explain the similarity found in FTIR. In the other described

studies the AgNPs are formed within the alginate fabric, which acts as a reducing and capping agent (SHARMA et al., 2012; ZAHRAN et al., 2014; ZHAO et al., 2014).

FIGURE 3- FTIR: alginate's spheres (a); Ag@AlgRg (b) and Ag@AlgRm (c).

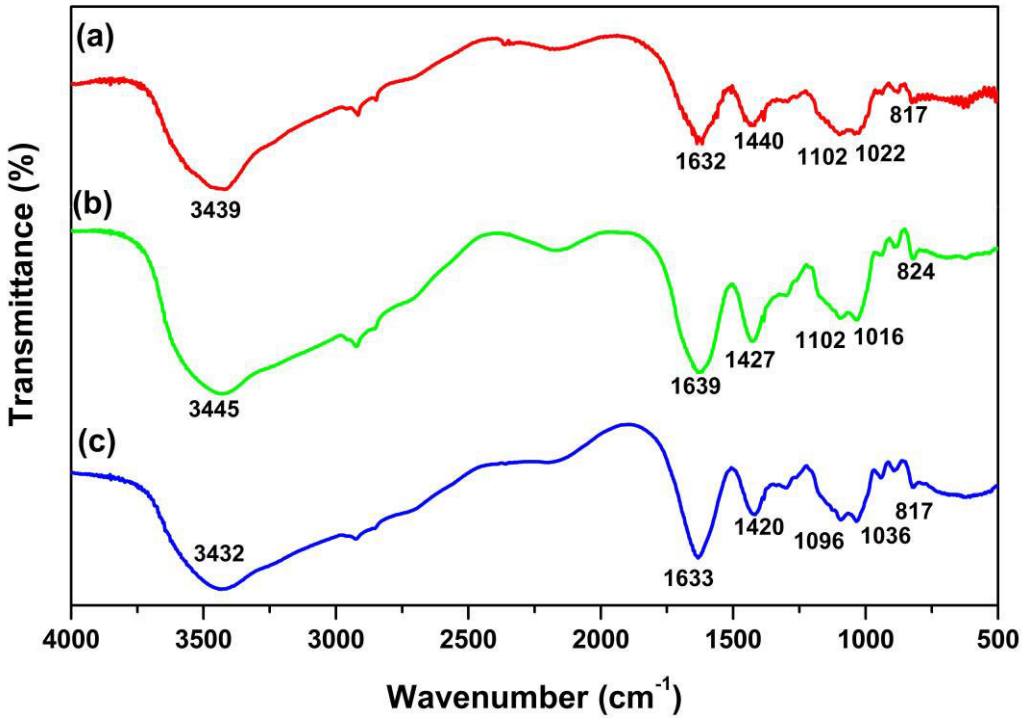

Source: Author

The diffractogram of the samples is shown in FIGURE 4. The alginate's spheres showed no diffraction peaks pronounceable, as being a polymer, it is an amorphous material, FIGURE 4(a). Samples Ag@AlgRg (FIGURE 4(b)) and Ag@AlgRm (FIGURE 4(c)), it is possible to observe the presence of characteristic peaks of silver, 37.9 ° and 44.8 °, these peaks can be attributed to the crystal planes (111), (200), respectively, which can be indexed to a face-centered cubic structure (fcc) of the nanoparticulated silver and confirms the presence of silver in crystalline form in spheres produced with AgNPs of fungal origin (CHEN et al., 2014; MOHAN et al., 2014). The peak of 54.1°, diffraction can be attributed to proteins present in AgNPs because they are of fungal origin (VERMA, KHARWAR, GANGE, 2010). When using AgNPs immersed in polymeric matrices, it is normal to observe the presence of other peaks (BOZANIC et al., 2011).

FIGURE 4- PDXRD: alginate's spheres (a); Ag@AlgRg (b) and Ag@AlgRm (c).

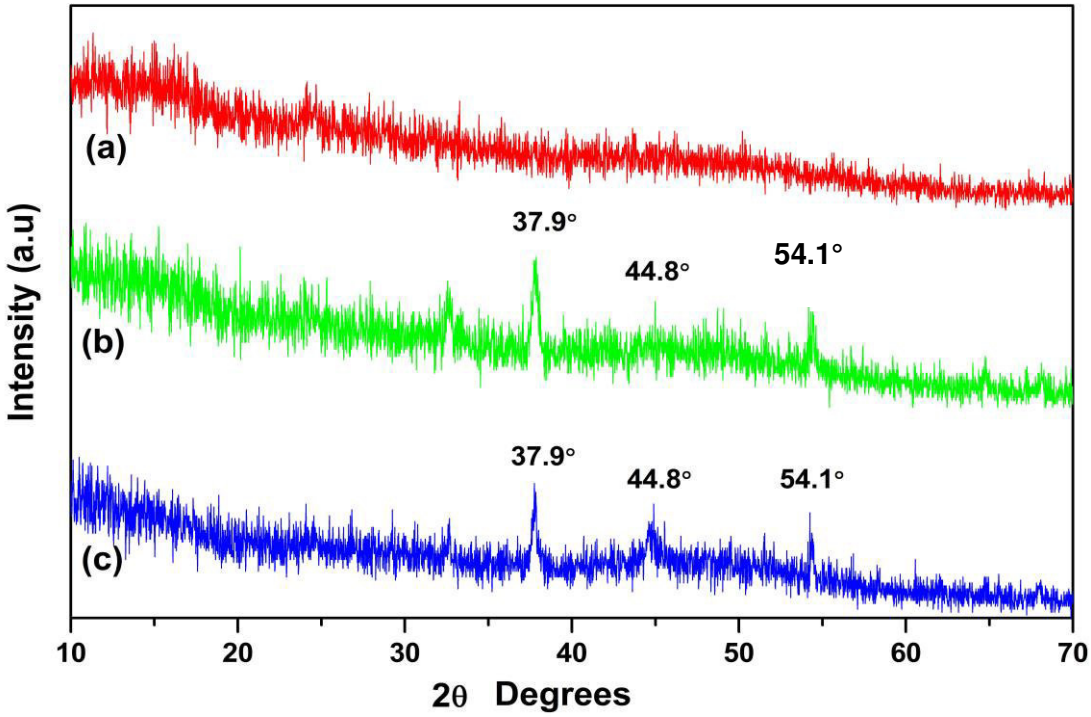

Source: Author

FIGURES 5a and 6a show the spheres in scanning electron microscopy (SEM), we can observe the spherical or oval shape. When the spheres are wet they had a similar format (see FIGURE S7 in Supporting Information Chapter 5). Ag@AlgRg measured 800 μm and Ag@AlgRm measured 1000 μm when viewed through SEM, the decrease in size when compared to the original size is due to dehydration (AI, JIANG, 2013). The structure details show that the spheres have several protrusions which may favor the catalytic activity (see FIGURE S8 in Supporting Information Chapter 5). Described studies show that this roughness may be important for catalytic activity (AI, YUE, JIANG, 2012; WANG et al., 2016).

The compositional analysis was performed using EDX and we can observe in FIGURE 5b and 6b the presence of silver, which absorbs in 3 keV (CAKIĆ et al., 2016). Other elements present are part of the constituents of the reagents used in the preparation of spheres and AgNPs. In the compositional map we can observe that AgNPs are well distributed across the surface of the spheres (see Supporting Information in FIGURE S9 Chapter 5).

Atomic Force Microscopy (AFM) is a technique used to elucidate surface of polymers (GAO et al., 2016), in FIGURES 7a and 8a the AFMs of spheres are shown, we can

see the various existing recesses which would facilitate the catalysis of reactions, because of the increasing of the contact area, the same roughness can be seen in the FIGURES 5a and 6a. The huges crypts facilitate anchoring and carrying out the reactions. In FIGURES7b and 8b, we can observe the uniform distribution of AgNPs across the surface of the spheres. In this study we evaluate the value of the AFM technique to elucidate the intimacy of the spheres and other work structures have used AFM with the same purpose (LIAO et al., 2015; LIU et al., 2015; MENG, WINTERS, YU, 2015) .

FIGURE 5- SEM (a) and EDx (b) of Ag@Alg Rg.

.

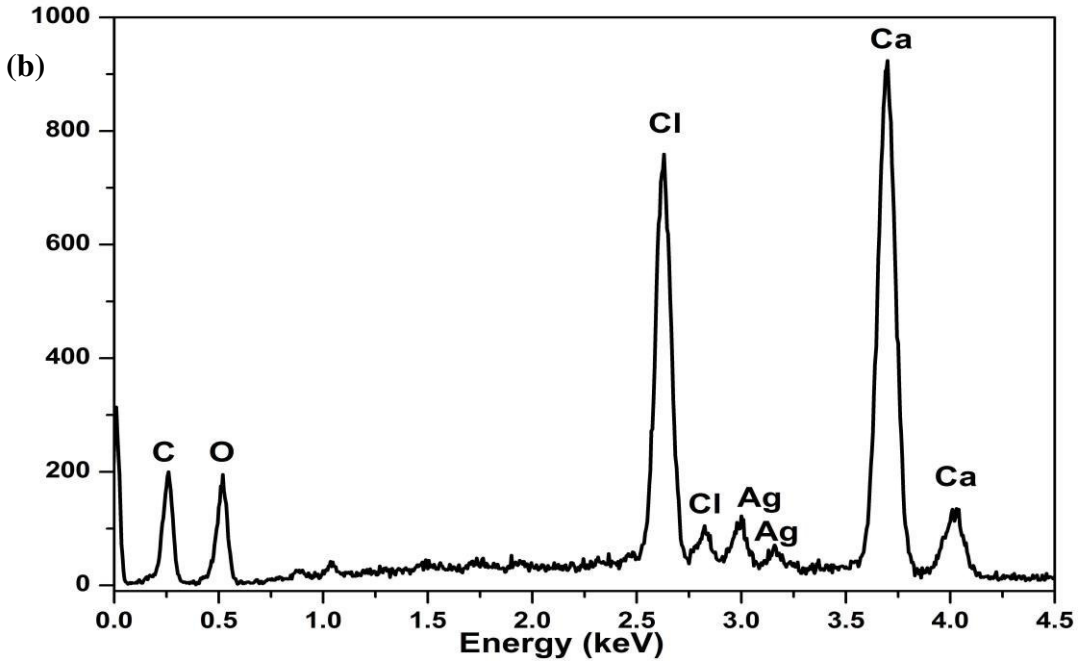

Source: Author

FIGURE 6- SEM (a) and EDx (b) of Ag@Alg Rm.

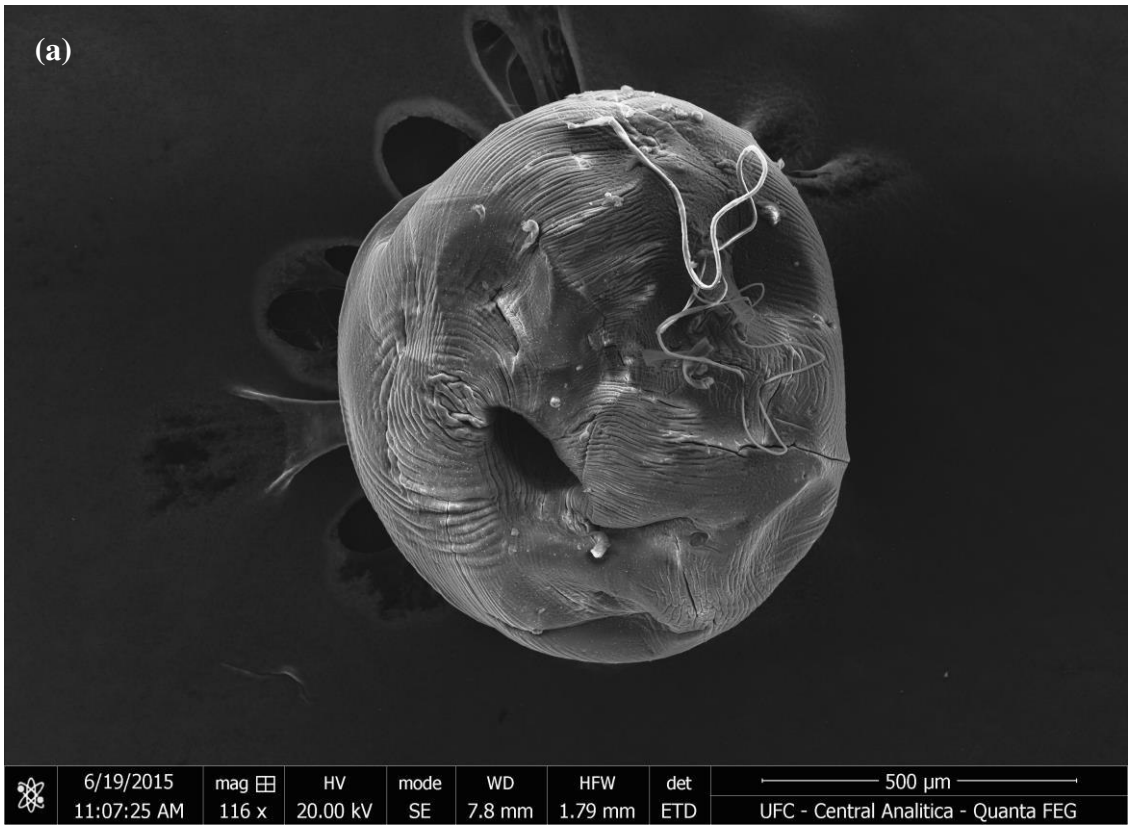

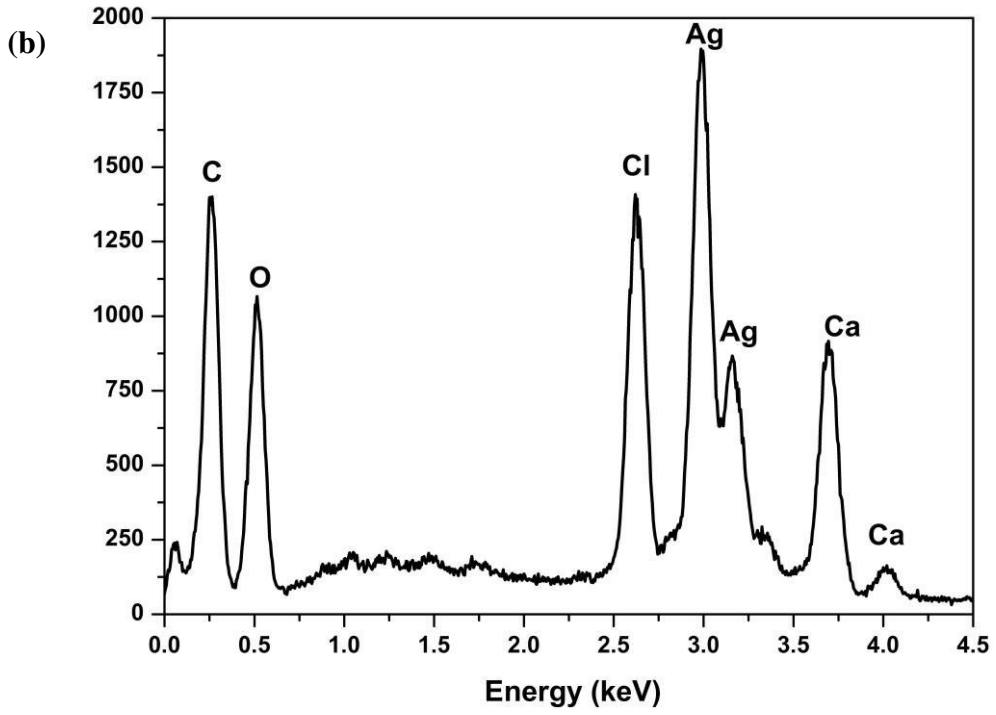

Source: Author

FIGURE 7- AFM of Ag@Alg Rg (a,b).

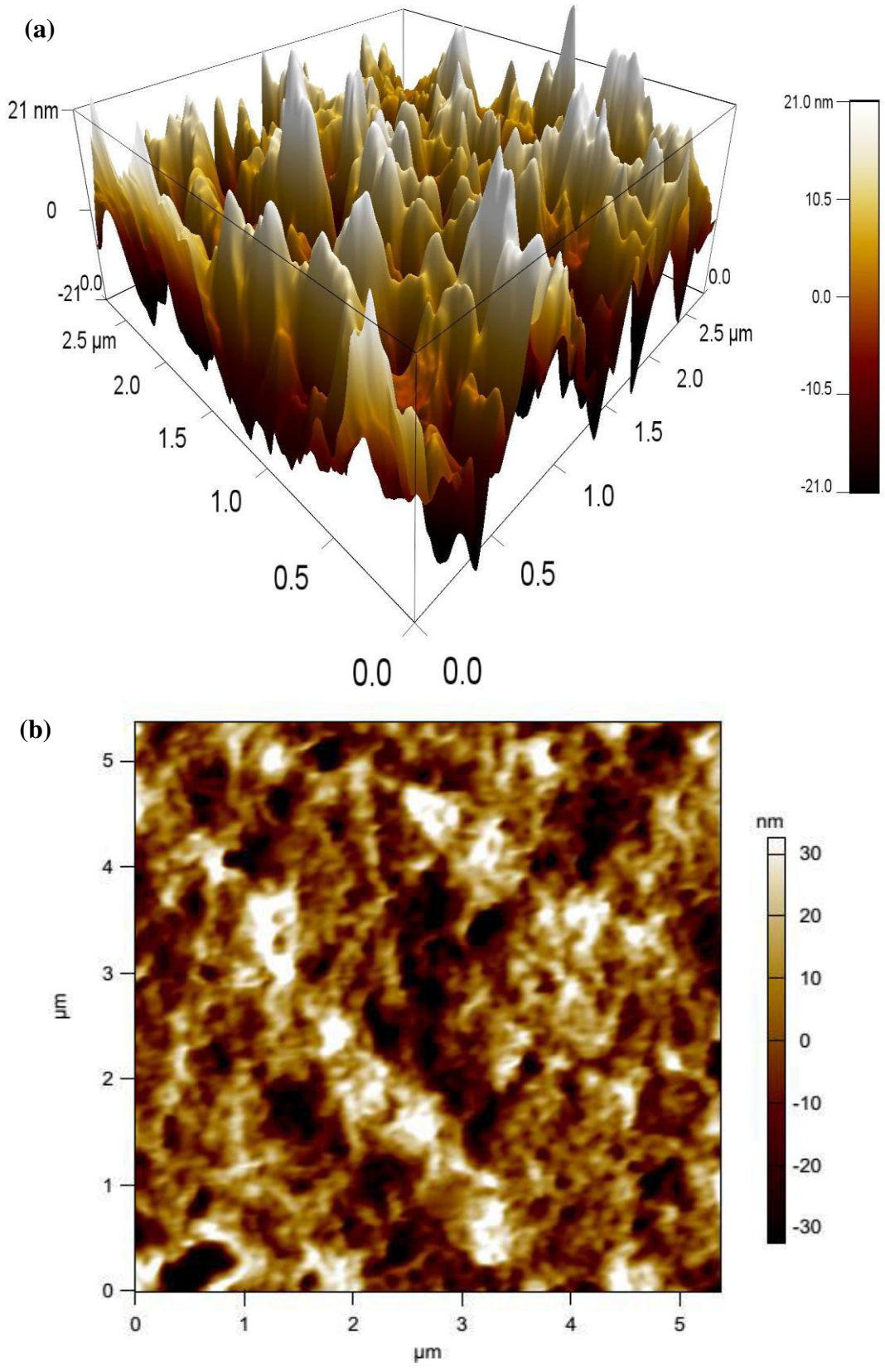

Source: Author

FIGURE 8- AFM of Ag@Alg Rm (a,b).

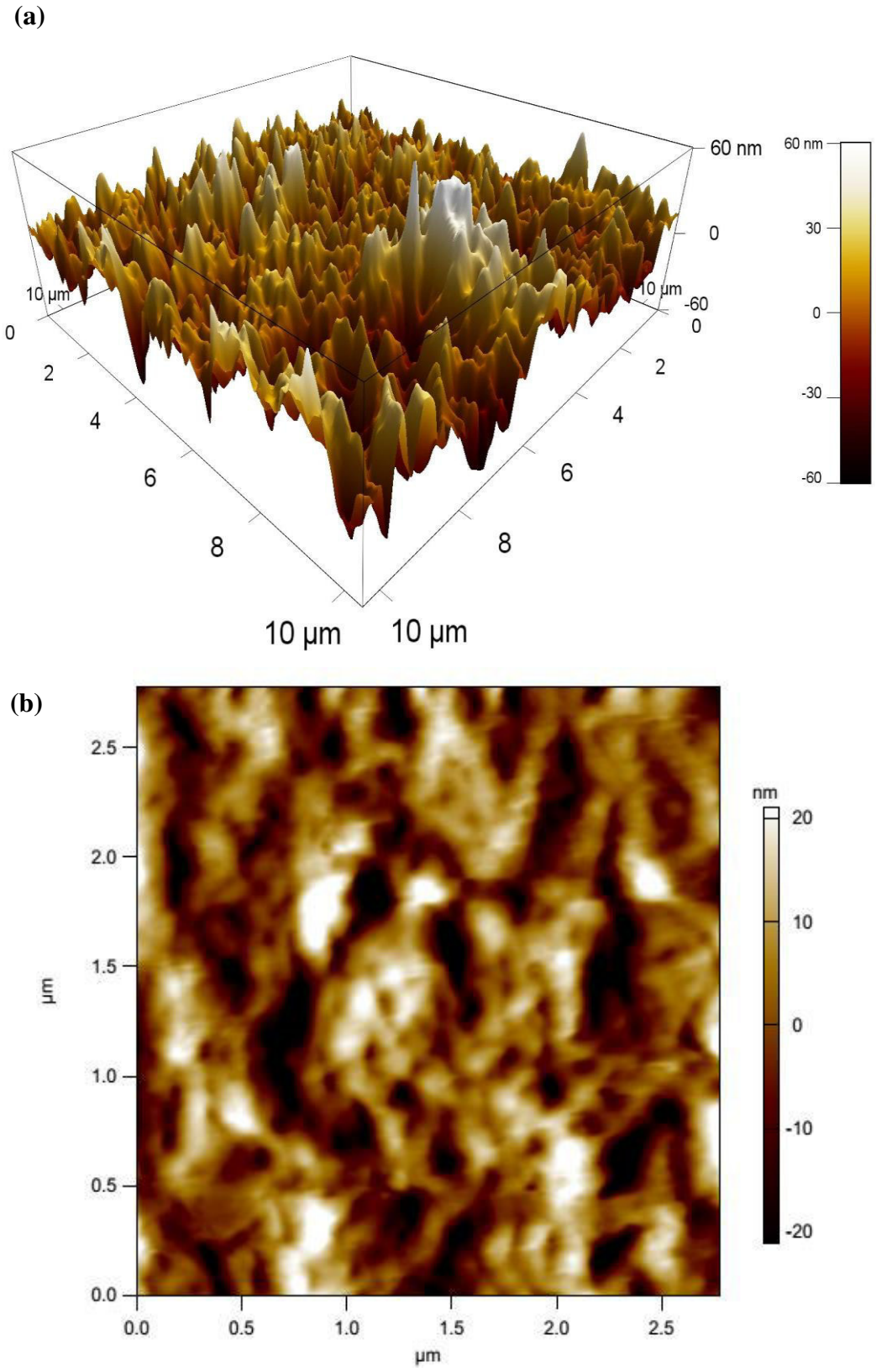

Source: Author

Heterogeneous catalysis is one of the most prominent applications of AgNPs and the used model to evaluate the efficiency of the system heterogeneous is the catalytic reduction of 4-nitrophenol (4-NP), due to its importance in the manufacturing industry (SHARMA et al., 2016; ALSHEHRI et al., 2016). In FIGURES 9a and 10a are shown the conversion of 4-NP to 4-aminophenol (4-AP), catalyzed by AgNPs present in the Ag@AlgRg and Ag@AlgRm spheres, respectively. The reduction occurs in the presence of an excess of $NaBH_4$ as the source of hydrogen and sphere being the catalysts, FIGURE 9a (1), (2) and FIGURE 10a (1), (2)), it is possible to observe that occurred the discoloration of 4-NP solution firstly yellow to white as the 4-AP in water is colorless. The presence of 4-AP is detected in the UV-Vis spectroscopy by the appearance of a band at 300 nm, FIGURES (9a (3) and 10a (3)). The band which appears at 317 nm is 4-NP, FIGURES (9a (4)) and (10a (4)), which changes to 400 nm due to the formation of the ion-4-nitrophenolato. This ion is suffering the catalytic action and it is converted to 4-AP over the course of 30 min. This finding is reported in numerous studies and coincides with our results (AJITHA et al., 2016; PARK et al., 2016).

After the reaction the spheres were easily removed from the system due to its macroscopic nature, however it was not possible to reuse them because of the fact that the crosslink structure of the alginate spheres broke up and become unusable for a reuse. To solve this problem, it could be carried out the production of new spheres with a higher content of alginate, however this was not possible in this study, which only studied the viability of process.

The FIGURES 9b and 10b show a linear relationship between ln (A/A_0) and the time "t", which indicates a reaction of pseudo-first order, pseudo because it used an excess of $NaBH_4$. The rate constant was found kapp = $2.9x10^{-3}$ s^{-1}, with correlation coefficient of R^2 = 0.9564 for Ag@AlgRg; and kapp = $2.2x10^{-3}$ s^{-1}, with correlation coefficient of R^2 = 0.8695 for Ag@AlgRm. The results compared with those described in the literature are very similar (AI, YUE, JIANG, 2012; AI, JIANG 2013) .

The removal efficiency of the pollutant of a system is an important variable when assessing the usefulness of a catalyst, in our study in FIGURES 9c and 10c are shown to 4-NP removal rate in the 30 min interval, we observed that after the time, 95% of 4-NP was converted into 4-AP, which leads us to conclude the effectiveness of Ag@AlgRg catalysts and Ag@AlgRm. The AgNPs and Ag-impregnated polymers have been effective in removing pollutants dyes (ZHENG, WANG, 2012).

The Ag@AlgRg and Ag@AlgRm spheres work as catalysts and follow a catalytic model Langmuir-Hinshelwood, similar to other metal nanoparticles (Pt, Au) in which reactants and products adhere to the surface of the nanoparticle and the dynamic adsorption and release depends on the nature of the nanoparticle (WUNDER et al., 2016) .

Ceftazidime (Ceft) is a widely used antibiotic in Brazil and in the world, once it is used in hospital infections, especially against Gram-negative bacteria (*Pseudomonas aeruginosa*, *Escherichia coli*, *Klebsiella pneumoniae*), often associated with other antibiotics (ROYER et al., 2016). However, the high consumption is accompanied by the generation of a large amount of waste because Ceft is not metabolized in the body and is excreted unchanged in the urine, urinary recovery of the drug in 24 hours reaches 83% (HARDING, HARPER, 1983).

There is currently a lack of information about the effects of these chemicals when discarded, however one of the clearest effects is the selection of resistant bacterial strains to these drugs (BAQUERO, MARTÍNEZ, CANTÓN, 2008; WATKINSON, MURBY, COSTANZO, 2007). In FIGURES 11a, 11b, we can see that the spheres are capable of degrade Ceft over a period of 30 min. It can be observed that the absorption band at 255 nm, characteristic of Ceft, disappeared at the end of the studied period. The two spheres were extremely effective in the degradation of this potent antibiotic. Ceft degradation is a process few studied and so far are few studies that describe actual degradation processes (HU, YU, SUN, 2016). Our process is simple, inexpensive and efficient. Other drugs of the same class Ceft were degraded by AgNPs, however, this is the first time that a process uses immersed fungal AgNPs in a polymer matrix (JUNEJO, GUNER, BAYKAL, 2014).

FIGURE 9- Reduction of 4-NP by Ag@Alg Rg (a); Plot of $\ln(A/A_0)$ against the time for the reduction of 4-NP (b); (%) of 4-NP Removal (c). (1) Reduction of 4-NP to 2-AP by spheres; (2) schematic reduction of 4-NP; (3) 4-aminophenol; (4) aminophenolate.

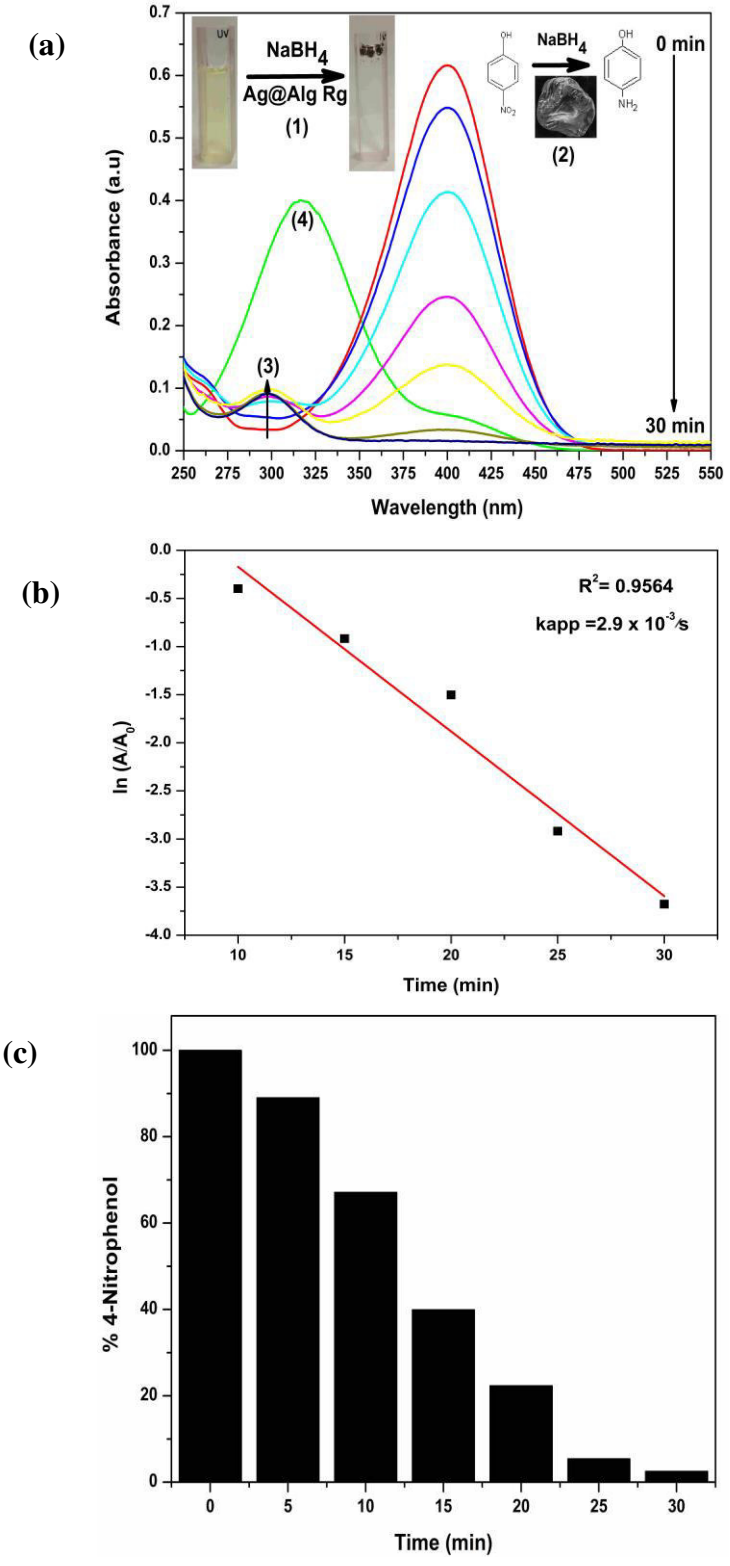

Source: Author

FIGURE 10- Reduction of 4-NP by Ag@Alg Rm (a); Plot of $\ln(A/A_0)$ against the time for the reduction of 4-NP (b); (%) of 4-NP Removal (c). (1) Reduction of 4-NP to 2-AP by spheres; (2) schematic reduction of 4-NP; (3) 4-aminophenol; (4) aminophenolate.

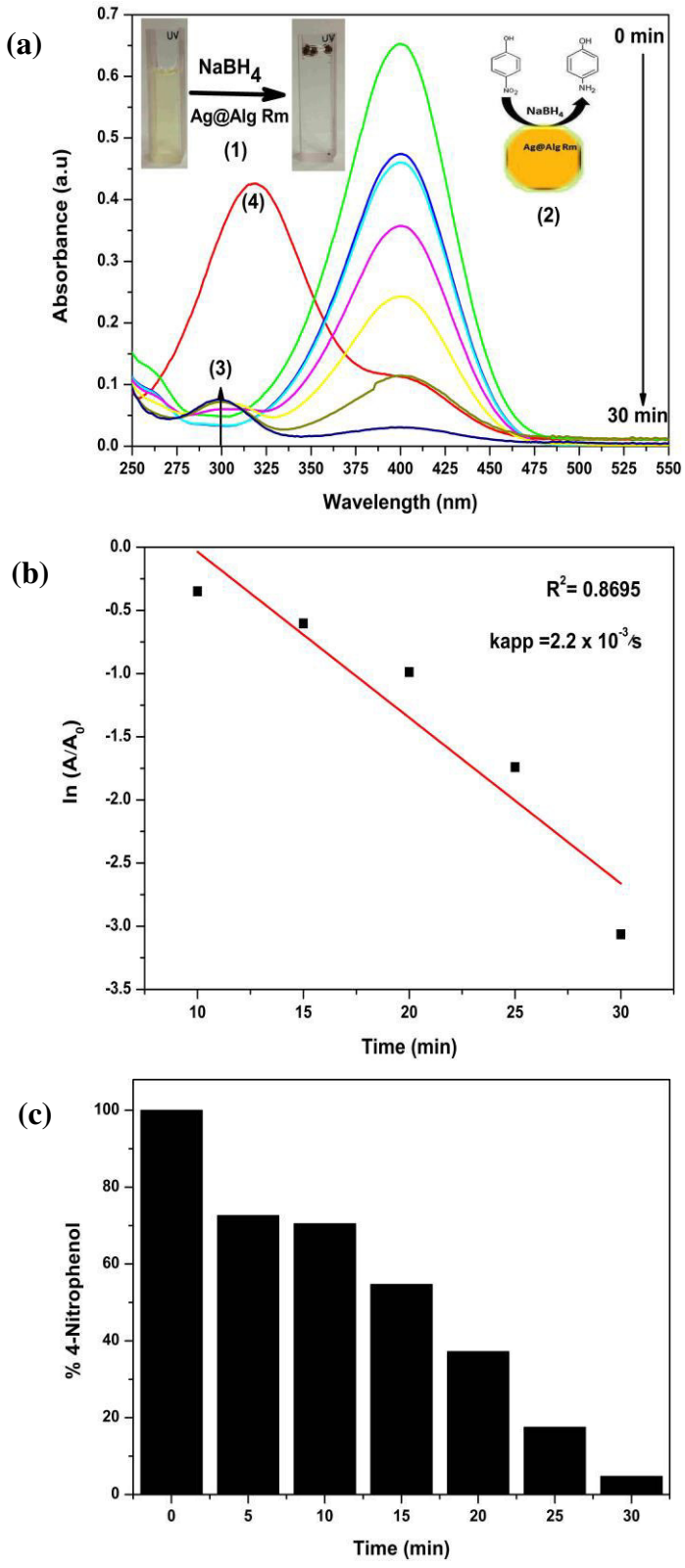

Source: Author

FIGURE 11- Ceftazidime inactivation by Ag@Alg Rg (a) and Ag@Agl Rm (b). (I) 0; (II) 10; (III) 20 and (IV) 30 min.

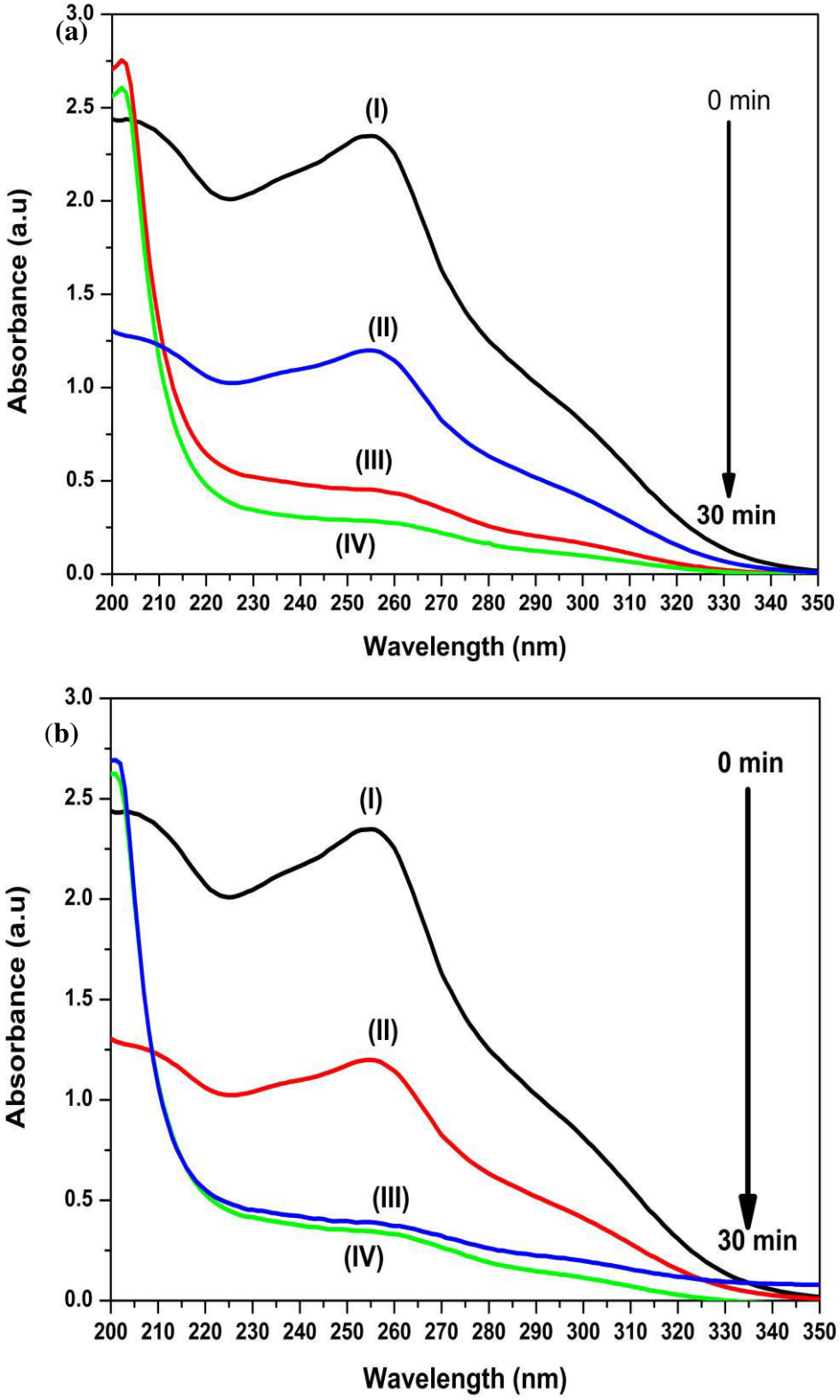

Source: Author

The chemical degradation can produce metabolites with antimicrobial activity, which selected resistant bacteria, especially when these residues achieve the sewer system, so in addition to the degradation it is necessary to ensure that the products formed do not show antimicrobial activity. In FIGURE 12, we can see that Ceft treated by spheres containing AgNPs lost all the antimicrobial activity, not exerting any effect on *Klebsiella pneumoniae* (FIGURE 12(a)) neither on *Escherichia coli* ((FIGURE 12 (b)). These two bacteria are the main microorganisms of the groups of coliform bacteria that can be found in domestic and hospital sewage (SZABO, MINAMYER , 2014) .

The practical result of this finding is that Ceft with its destroyed microbial activity, cannot exert a selective pressure on microorganisms, minimizing the problems related to bacterial resistance, which is a multifaceted global problem (MUNOZ –PRICE et al., 2013; PATEL, BONOMO , 2013) .

CONCLUSION

In summary, this present work, we have effortlessly developed an eco-friendly, green, cheap and simple method for the synthesis of spheres inlead with AgNPs produced fungi (*R. glutinis* and *R. mucilaginosa*) which itself played a dual role of stabilizing and reducing agent. The UV-vis spectral study reveals the formation of Ag@AlgRg and Ag@Alg Rm, AgNPs showing an absorption peak around 400 nm, FTIR shows the interaction between alginate and AgNPs, and the powder XRD and EDX confirmed the purity and crystalline, SEM and AFM show a nature of spheres. The prepared Ag@AlgRg/Rm spheres exhibit excellent catalytic activity towards both reduction of 4-NP and degradation of ceftazidime using $NaBH_4$. The results indicated that those spheres can be ally important in heterogeneous catalysis.

FIGURE 12- Microbiological effect of ceftazidime (Ceft) (100 uL) before and after inactivation by Ag@Alg Rg (a) and Ag@Alg Rm (b).

Klebsiella pneumoniae

(a)

Escherichia coli

(b)

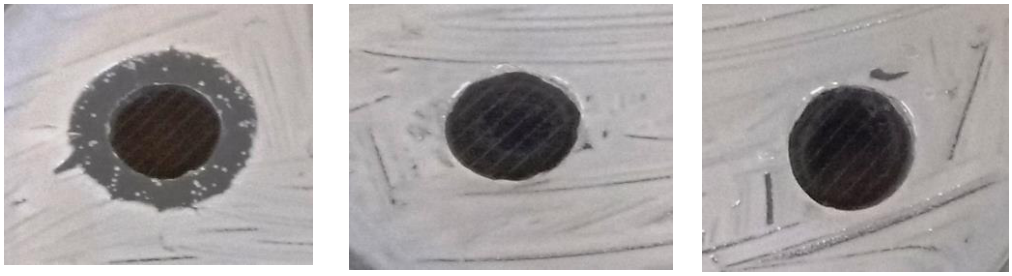

Source: Author

REFERENCES

1. AI, L.; JIANG, J. Catalytic reduction of 4-nitrophenol by silver nanoparticles stabilized on environmentally benign macroscopic biopolymer hydrogel. **Bioresource Technology**, v. 132, p. 374–377, 2013. Disponível em: http://linkinghub.elsevier.com/retrieve/pii/S0960852412016707 . Acesso em: 22 mai. 2014.
2. AJITHA, B. et al. Instant biosynthesis of silver nanoparticles *using Lawsonia inermis* leaf extract: Innate catalytic, antimicrobial and antioxidant activities. **Journal of Molecular Liquids**, v. 219, p. 474–481, 2016. Disponível em: http://linkinghub.elsevier.com/retrieve/pii/S0167732215304281 . Acesso em: 27 jul. 2016.
3. ALSHEHRI, S. M. et al. Chitosan based polymer matrix with silver nanoparticles decorated multiwalled carbon nanotubes for catalytic reduction of 4-nitrophenol. **Carbohydrate Polymers**, v. 151, p. 135–143, 2016. Disponível em: http://linkinghub.elsevier.com/retrieve/pii/S0144861716305318 . Acesso em: 27 jul. 2016.
4. BAQUERO, F.; MARTÍNEZ, J.; CANTÓN, R. Antibiotics and antibiotic resistance in water environments. **Current Opinion in Biotechnology**, v. 19, n. 3, p. 260–265, 2008. Disponível em: http://linkinghub.elsevier.com/retrieve/pii/S0958166908000591 . Acesso em: 12 abri. 2015.
5. BOŽANIĆ, D.K. *et al*. Silver nanoparticles encapsulated in glycogen biopolymer: Morphology, optical and antimicrobial properties. **Carbohydrate Polymers**, v. 83, n. 2, p. 883–890, 2011. Disponível em: http://linkinghub.elsevier.com/retrieve/pii/S0144861710007162 . Acesso em: 26 de julho de 2016.
6. CAKIĆ, M. *et al*. Synthesis, characterization and antimicrobial activity of dextran sulphate stabilized silver nanoparticles. **Journal of Molecular Structure**, v. 1110, p. 156–161, 2016. Disponível em: http://linkinghub.elsevier.com/retrieve/pii/S0022286016300400 . Acesso em: 26 jul. 2016.
7. CHEN, G. *et al*. A novel green synthesis approach for polymer nanocomposites decorated with silver nanoparticles and their antibacterial activity. **The Analyst**,

v. 139, n. 22, p. 5793–5799, 2014. Disponível em: http://www.ncbi.nlm.nih.gov/pubmed/25199560 . Acesso em: 26 de julho de 2016.

8. DESHMUKH, D. K. Removal of phenol in aqueous solution by adsorption onto green synthesized coinage nanoparticles beads. **Research on Chemical Intermediates**, v. 41, n. 11, p. 8363–8379, 2015. Disponível em: http://link.springer.com/10.1007/s11164-014-1898-9 . Acesso em: 13 mai. 2016.
9. DU, L. *et al*. Synthesis of small silver nanoparticles under light radiation by fungus *Penicillium oxalicum* and its application for the catalytic reduction of methylene blue. **Materials Chemistry and Physics**, v. 160, p. 40–47, 2015. Disponível em: http://linkinghub.elsevier.com/retrieve/pii/S0254058415300109 . Acesso em: 29 out. 2013.
10. FENG, M. *et al*. Degradation of fluoroquinolone antibiotics by ferrate(VI): Effects of water constituents and oxidized products. **Water Research**, v. 103, p. 48–57, 2016. Disponível em: http://linkinghub.elsevier.com/retrieve/pii/S0043135416305188 . Acesso em: 23 jul. 2016.
11. GAO, H. *et al*. *In vitro* and *in vivo* degradation and mechanical properties of ZEK100 magnesium alloy coated with alginate, chitosan and mechano-growth factor. **Materials Science and Engineering: C**, v. 63, p. 450–461, 2016. Disponível em: http://linkinghub.elsevier.com/retrieve/pii/S0928493116301667 . Acesso em: 27 jul. 2016.
12. GU, S. *et al*. Kinetic analysis of the reduction of 4-nitrophenol catalyzed by Au/Pd nanoalloys immobilized in spherical polyelectrolyte brushes. **Phys. Chem. Chem. Phys.**, p. 22–24, 2015. Disponível em: http://xlink.rsc.org/?DOI=C5CP00519A . Acesso em: 7 nov. 2015.
13. GULKOWSKA, A. *et al*. Removal of antibiotics from wastewater by sewage treatment facilities in Hong Kong and Shenzhen, China. **Water Research**, v. 42, n. 1-2, p. 395–403, 2008. Disponível em: http://linkinghub.elsevier.com/retrieve/pii/S0043135407005076 . Acesso em: 1 dez. 2014.
14. HARDING, S. M; HARPER, P. B. The pharmacokinetic behaviour of ceftazidime in man and the relationship between serum levels and the in vitro susceptibility of clinical isolates. **Infection**, v. 11 Suppl 1, p. S49–53, 1983. Disponível em: http://www.ncbi.nlm.nih.gov/entrez/query.fcgi?cmd=Retrieve&db=PubMed&dopt=Citation&list_uids=6339419 . Acesso em 27 jul. 2016.

15. HERVÉS, P. *et al*. Catalysis by metallic nanoparticles in aqueous solution: model reactions. **Chemical Society Reviews**, v. 41, n. 17, p. 5577, 2012. Disponível em: http://xlink.rsc.org/?DOI=c2cs35029g . Acesso em: 5 jan. 2015.
16. HU, X.; YU, Y.; SUN, Z. Preparation and characterization of cerium-doped multiwalled carbon nanotubes electrode for the electrochemical degradation of low-concentration ceftazidime in aqueous solutions. **Electrochimica Acta**, v. 199, p. 80–91, 2016. Disponível em: http://linkinghub.elsevier.com/retrieve/pii/S0013468616306302 . Acesso em: 23 jul. 2016.
17. ISLAN, G. A.; MUKHERJEE, A.; CASTRO, G. R. Development of biopolymer nanocomposite for silver nanoparticles and Ciprofloxacin controlled release. **International Journal of Biological Macromolecules**, v. 72, p. 740–750, 2015. Disponível em: http://www.sciencedirect.com/science/article/pii/S0141813014006229 . Acesso em: 6 mar. 2016.
18. JUNEJO, Y.; GÜNER, A.; BAYKAL, A. Synthesis and characterization of amoxicillin derived silver nanoparticles: Its catalytic effect on degradation of some pharmaceutical antibiotics. **Applied Surface Science**, v. 317, p. 914–922, 2014. Disponível em: http://www.sciencedirect.com/science/article/pii/S0169433214019114 . Acesso em: 5 abr. 2015.
19. LIAO, H. et al. Mechanisms of oligoguluronate modulating the calcium-induced gelation of alginate. Polymer, v. 74, p. 166–175, 2015. Disponível em: http://linkinghub.elsevier.com/retrieve/pii/S0032386115301464 . Acesso em: 27 jul. 2016.
20. LIN, S. *et al*. Silver nanoparticle-alginate composite beads for point-of-use drinking water disinfection. **Water Research**, v. 47, n. 12, p. 3959–3965, 2013. Disponível em: http://dx.doi.org/10.1016/j.watres.2012.09.005 . Acesso em: 25 jul. 2016.
21. LIU, M. et al. In vitro evaluation of alginate/halloysite nanotube composite scaffolds for tissue engineering. Materials Science and Engineering: C, v. 49, p. 700–712, 2015. Disponível em: http://linkinghub.elsevier.com/retrieve/pii/S0928493115000478 . Acesso em: 27 jul. 2016.
22. LIU, Y. *et al*. Preparation of high-stable silver nanoparticle dispersion by using sodium alginate as a stabilizer under gamma radiation. **Radiation Physics and Chemistry**, v. 78, n. 4, p. 251–255, 2009. Disponível em:

http://linkinghub.elsevier.com/retrieve/pii/S0969806X09000164 . Acesso em: 8 mai. 2014.

23. MENG, S.; WINTERS, H.; LIU. Ultrafiltration behaviors of alginate blocks at various calcium concentrations. Water Research, v. 83, p. 248–257, 2015. Disponível em: http://linkinghub.elsevier.com/retrieve/pii/S0043135415300580 . Acesso em: 27 jul. 2016.
24. MOHAMMED F. A. *et al*. Mycobased Synthesis of Silver Nanoparticles and Their Incorporation into Sodium Alginate Films for Vegetable and Fruit Preservation. **Journal of Agricultural and Food Chemistry**, v. 57, n. 14, p. 6246–6252, 2009. Disponível em: http://pubs.acs.org/doi/abs/10.1021/jf900337h . Acesso em: 11 jan. 2014.
25. MOHAN, Y. M. *et al*. Controlling of silver nanoparticles structure by hydrogel networks. **Journal of Colloid and Interface Science**, v. 342, n. 1, p. 73–82, 2010. Disponível em: http://dx.doi.org/10.1016/j.jcis.2009.10.008 . Acesso em: 29 nov. 2014.
26. MUNOZ-PRICE, L. S. *et al*. Clinical epidemiology of the global expansion of Klebsiella pneumoniae carbapenemases. **The Lancet Infectious Diseases**, v. 13, n. 9, p. 785–796, 2013. Disponível em: http://linkinghub.elsevier.com/retrieve/pii/S1473309913701907 . Acesso em: 28 jul. 2016.
27. NARAYANAN, K. B.; PARK, H. H.; SAKTHIVEL, N. Extracellular synthesis of mycogenic silver nanoparticles by *Cylindrocladium floridanum* and its homogeneous catalytic degradation of 4-nitrophenol. **Spectrochimica Acta Part A: Molecular and Biomolecular Spectroscopy**, v. 116, p. 485–490, 2013. Disponível em: http://linkinghub.elsevier.com/retrieve/pii/S1386142513008147 . Acesso em: 24 jul. 2016.
28. OTARI, S. V. *et al*. A novel microbial synthesis of catalytically active Ag–alginate biohydrogel and its antimicrobial activity. **Dalton Transactions**, v. 42, n. 27, p. 9966, 2013. Disponível em: http://www.ncbi.nlm.nih.gov/pubmed/23698554 . Acesso em: 17 ago. 2014.
29. PAL, J.; DEB, M. K.; DESHMUKH, D. K. Removal of phenol in aqueous solution by adsorption onto green synthesized coinage nanoparticles beads. **Research on Chemical Intermediates**, v. 41, n. 11, p. 8363–8379, 2015. Disponível em: http://link.springer.com/10.1007/s11164-014-1898-9 . Acesso em: 29 nov. 2014.

30. PANKONGADISAK, P. *et al*. Development of silver nanoparticles-loaded calcium alginate beads embedded in gelatin scaffolds for use as wound dressings. **Polymer International**, v. 64, n. April, p. 275–283, 2015. Disponível em: http://doi.wiley.com/10.1002/pi.4787 . Acesso em: 8 jun. 2016.
31. PANKONGADISAK, P. *et al*. Preparation and Characterization of Silver Nanoparticles-Loaded Calcium Alginate Beads Embedded in Gelatin Scaffolds. **AAPS PharmSciTech**, v. 15, n. 5, p. 1105–1115, 2014. Disponível em: http://link.springer.com/10.1208/s12249-014-0140-9 . Acesso em: 25 jul. 2016.
32. PARK, J. et al. Green synthesis of gold and silver nanoparticles using gallic acid: catalytic activity and conversion yield toward the 4-nitrophenol reduction reaction. **Journal of Nanoparticle Research**, v. 18, n. 6, p. 166, 2016. Disponível em: http://link.springer.com/10.1007/s11051-016-3466-2 . Acesso em: 27 jul. 2016.
33. PARVEEN, A. *et al*. Facile biological approach for immobilization, physicochemical characterization and antibacterial activity of noble metals nanocomposites. **Materials Letters**, v. 148, p. 86–90, 2015. Disponível em: http://linkinghub.elsevier.com/retrieve/pii/S0167577X15002566 . Acesso em: 9 set. 2016.
34. PATEL, G.; BONOMO, R. A. "Stormy waters ahead": global emergence of carbapenemases. **Frontiers in Microbiology**, v. 4, n. MAR, p. 1–17, 2013. Disponível em: http://journal.frontiersin.org/article/10.3389/fmicb.2013.00048/abstract . Acesso em: 28 jul. 2016.
35. PRADHAN, N.; PAL, A.; PAL, T. Silver nanoparticle catalyzed reduction of aromatic nitro compounds. **Colloids and Surfaces A: Physicochemical and Engineering Aspects**, v. 196, n. 2-3, p. 247–257, 2002. Disponível em: http://www.sciencedirect.com/science/article/pii/S0927775701010408 . Acesso em: 28 jun. 2014.
36. ROYER, S. *et al*. Spread of multidrug-resistant Acinetobacter baumannii and Pseudomonas aeruginosa clones in patients with ventilator-associated pneumonia in an adult intensive care unit at a university hospital. **The Brazilian Journal of Infectious Diseases**, v. 19, n. 4, p. 350–357, 2015. Disponível em: http://www.ncbi.nlm.nih.gov/pubmed/25997783 . Acesso em 27 jul. 2016.
37. SAHA, S. *et al*. Photochemical Green Synthesis of Calcium-Alginate-Stabilized Ag and Au Nanoparticles and Their Catalytic Application to 4-Nitrophenol Reduction.

Langmuir, v. 26, n. 4, p. 2885–2893, 2010. Disponível em: http://pubs.acs.org/doi/abs/10.1021/la902950x . Acesso em: 8 ago. 2014.

38. SHARMA, M. et al. Green Synthesis of Silver Nanoparticles with Exceptional Colloidal Stability and its Catalytic Activity Toward Nitrophenol Reduction. **Nano**, v. 11, n. 04, p. 1650046, 2016. Disponível em: http://www.worldscientific.com/doi/10.1142/S1793292016500466 . Acesso em: 27 jul. 2016.
39. STOJKOVSKA, J. *et al*. A comprehensive approach to in vitro functional evaluation of Ag/alginate nanocomposite hydrogels. **Carbohydrate Polymers**, v. 111, p. 305–314, 2014. Disponível em: http://linkinghub.elsevier.com/retrieve/pii/S0144861714004202 . Acesso em: 8 ago. 2014.
40. SZABO, J; MINAMYER, S. Decontamination of biological agents from drinking water infrastructure: A literature review and summary. **Environment International**, v. 72, p. 124–128, 2014. Disponível em: http://dx.doi.org/10.1016/j.envint.2014.01.031 . Acesso em: 28 jul. 2016.
41. VERLICCHI, P.; ZAMBELLO, E. Pharmaceuticals and personal care products in untreated and treated sewage sludge: Occurrence and environmental risk in the case of application on soil - A critical review**. Science of the Total Environment**, v. 538, p. 750–767, 2015. Disponível em: http://dx.doi.org/10.1016/j.scitotenv.2015.08.108 . Acesso em: 23 jul. 2016.
42. VERMA, V. C.; KHARWAR, R. N.; GANGE, A. C. Biosynthesis of antimicrobial silver nanoparticles by the endophytic fungus *Aspergillus clavatus*. **Nanomedicine (London, England)**, v. 5, n. 1, p. 33–40, 2010. Disponível em: http://www.ncbi.nlm.nih.gov/pubmed/20025462 . Acesso em: 29 nov. 2014.
43. VIENS, A. M; LITTMANN, J. Is Antimicrobial Resistance a Slowly Emerging Disaster? **Public Health Ethics**, v. 8, n. 3, p. phv015, 2015. Disponível em: http://www.ncbi.nlm.nih.gov/pubmed/26566396 . Acesso em: 23 jul. 2016.
44. WANG, Q. *et al*. In situ pore-forming alginate hydrogel beads loaded with in situ formed nano-silver and their catalytic activity. **Phys. Chem. Chem. Phys.**, v. 18, n. 18, p. 12610–12615, 2016. Disponível em: http://xlink.rsc.org/?DOI=C6CP00872K . Acesso em: 25 jul. 2016.
45. WATKINSON, A.J.; MURBY, E.J.; COSTANZO, S.D. Removal of antibiotics in conventional and advanced wastewater treatment: Implications for environmental

discharge and wastewater recycling. **Water Research**, v. 41, n. 18, p. 4164–4176, 2007. Disponível em: http://linkinghub.elsevier.com/retrieve/pii/S0043135407002539 . Acesso em 27 jul. 2016.

46. YANG, J.; PAN, J. Hydrothermal synthesis of silver nanoparticles by sodium alginate and their applications in surface-enhanced Raman scattering and catalysis. **Acta Materialia**, v. 60, n. 12, p. 4753–4758, 2012. Disponível em: http://linkinghub.elsevier.com/retrieve/pii/S1359645412003576 . Acesso em: 17 jan. 2016.
47. YIN, C. *et al*. Highly efficient degradation of 4-nitrophenol over the catalyst of Mn2O3/AC by microwave catalytic oxidation degradation method. **Journal of Hazardous Materials**, v. 305, p. 15–20, 2016. Disponível em: http://linkinghub.elsevier.com/retrieve/pii/S0304389415302284 . Acesso em: 23 jul. 2016.
48. ZAHRAN, M K; AHMED, H. B; EL-RAFIE, M. H. Alginate mediate for synthesis controllable sized AgNPs. **Carbohydrate polymers**, v. 111, p. 10–7, 2014. Disponível em: http://www.ncbi.nlm.nih.gov/pubmed/25037323 . Acesso em: 19 jan. 2016.
49. ZHAO, X. *et al*. The preparation of alginate – AgNPs composite fiber with green approach and its antibacterial activity. **Journal of Industrial and Engineering Chemistry**, v. 24, p. 188–195, 2015. Disponível em: http://dx.doi.org/10.1016/j.jiec.2014.09.028 . Acesso em: 7 fev. 2016.
50. ZHAO, X. H. *et al*. Alginate fibers embedded with silver nanoparticles as efficient catalysts for reduction of 4-nitrophenol. **RSC Adv.**, v. 5, n. 61, p. 49534–49540, 2015. Disponível em: http://www.scopus.com/inward/record.url?eid=2-s2.0-84930941544&partnerID=tZOtx3y1 . Acesso em: 17 fev. 2016.

CHAPTER SIX

Final Remarks

In the chapters discussed in this Dissertation, we were able to conclude that the synthesis of silver nanoparticles, whether chemically (using monosaccharides) or biologically (using yeasts), is a very promising field. Much remains to be elucidated when dealing with characterization of biological AgNPs. The synthesis of these structures by chemical means also needs to be better understood, so that we can control the shape and size of the kinds of particles produced.

We observed that only around 100 fungal species were used for the purpose of producing AgNPs, and when dealing with yeasts, such as those studied herein, that number drops even more, revealing that this point has hardly been explored or not explored at all. The major challenge, beyond controlling the physical–chemical conditions of the synthesis, is to understand how the elements that make AgNPs stable are selected, and what groups and molecular forces are involved in the process.

The AgNPs produced by synthetic means proved their power against bacteria and fungi, and – if the toxicity thereof is assessed – can be powerful allies against difficult-to-treat infections. We should not think only in terms of drugs for human or animal use, in injectable or oral form, but also in sanitizers of surfaces and surgical equipment/environments. The use of AgNPs in coating catheters is already a reality. Several commercial products manufactured based on nanoparticles are available on the global and Brazilian market.

The biological AgNPs studied in this dissertation showed their antimicrobial and catalytic activities, a valuable property vis-à-vis the challenges that present themselves to modern society. We have to keep growing without harming the environment.

In conclusion, Ceará soil proved to be a niche of opportunities not yet explored in this aspect. Hundreds of micro-organisms are currently inhabiting this soil and we need to get to know them and exploit them, for therein can lie the answer to many problems that afflict us and for which we need urgent and innovative solutions.

APPENDICES

Supporting Information CHAPTER ONE

FIGURE S1- Silver Nanoparticles synthesis protocol.

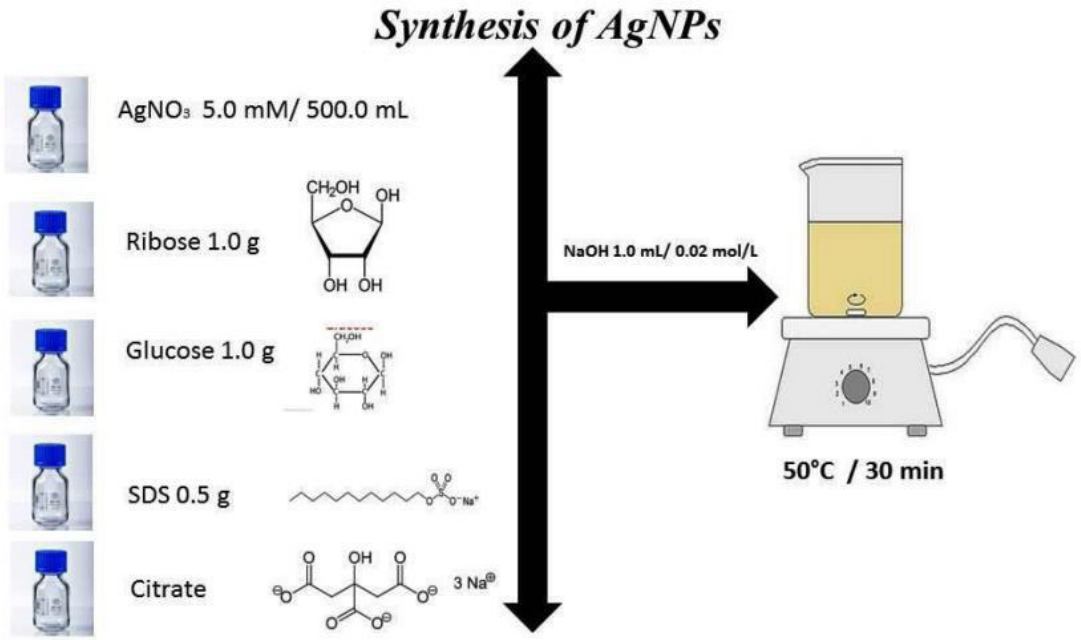

Source: Author

Supporting Information CHAPTER TWO

FIGURE S1- Ciprofloxacin.

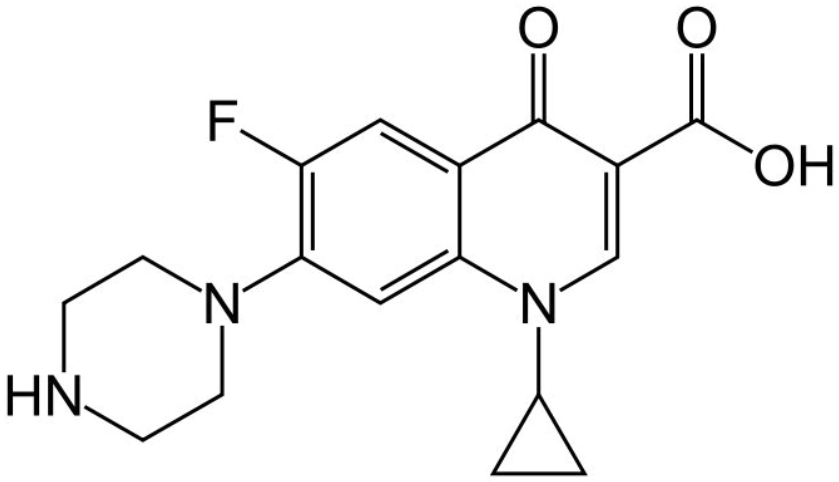

Source: Wikipedia. Disponível: https://en.wikipedia.org/wiki/File:Ciprofloxacin.svg Acesso 22 abr 2015

FIGURE S2- *Escherichia coli* on MaCkonkey agar.

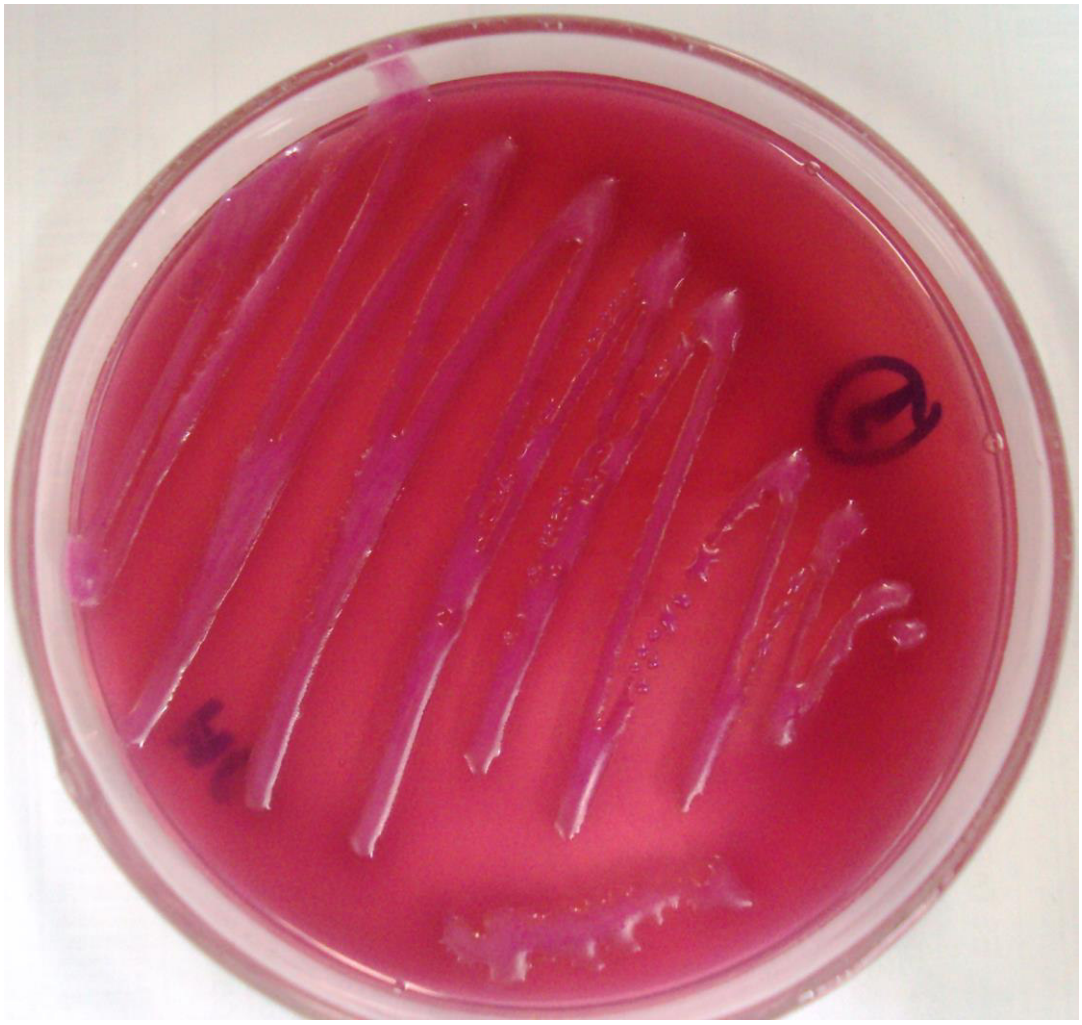

Source: Author

FIGURE S3- Cartoon of Silver Nanoparticles (AgNPs).

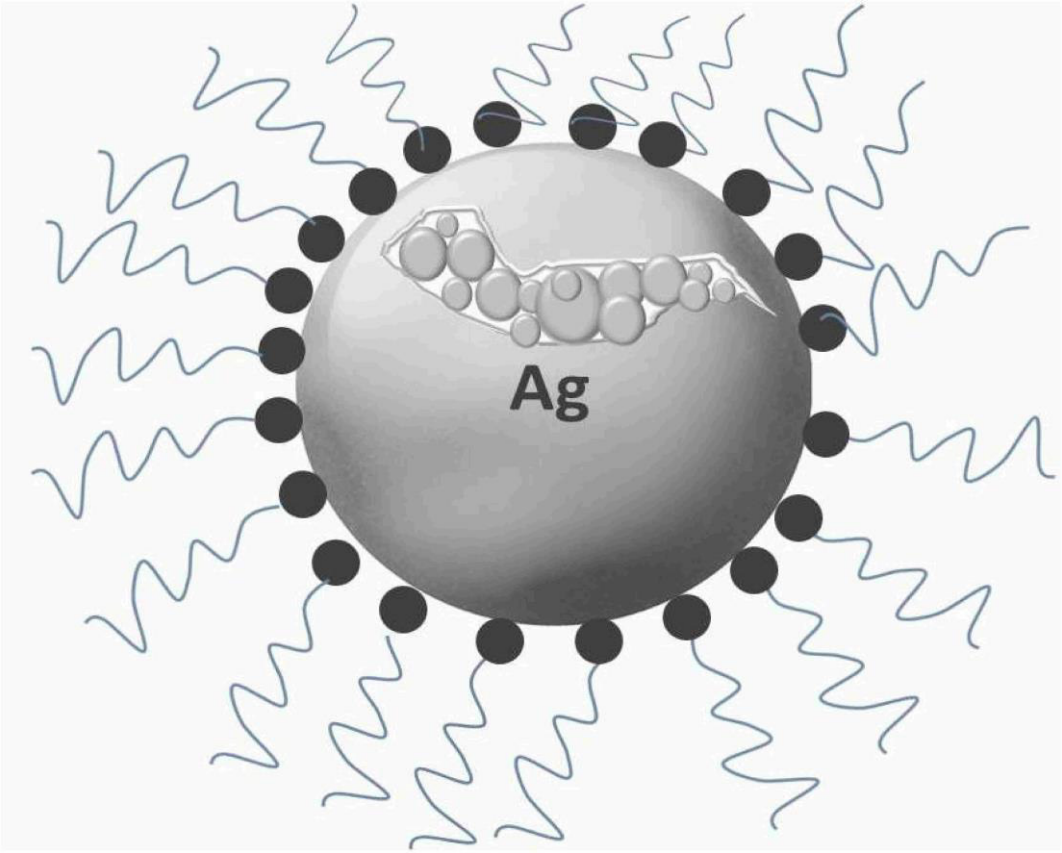

Source: Author

FIGURE S4- Full width at half maximum (FWHM) measure of AgNPs.

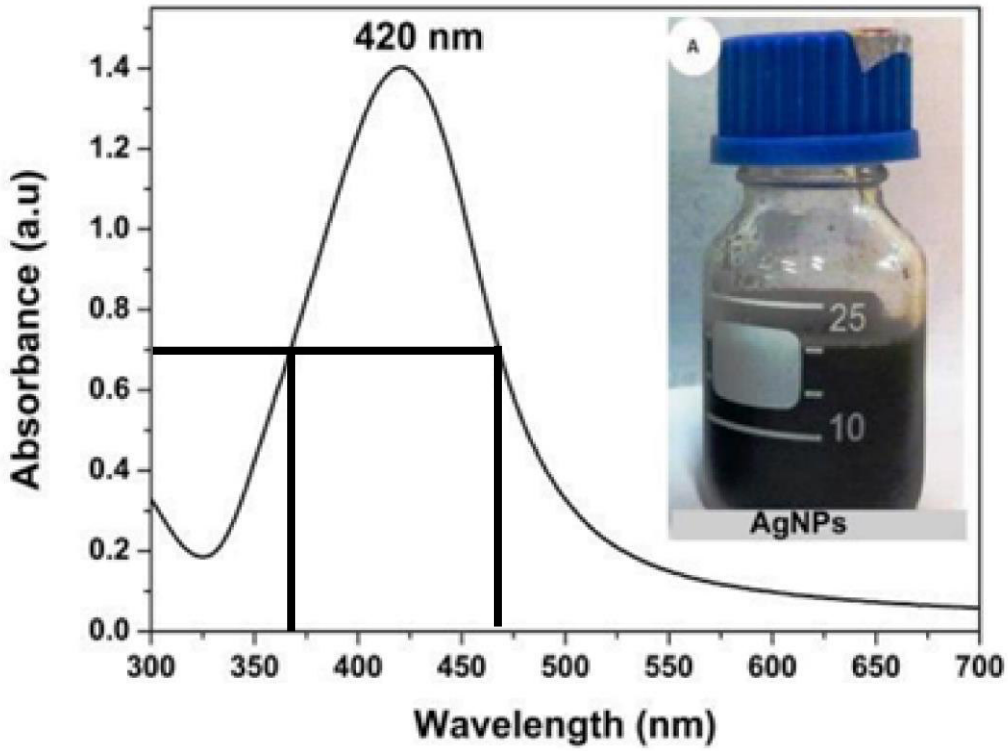

Source: Author

FWHW= 470-370 = 100 nm

FIGURE S5- Energy dispersive X-ray spectroscopy (EDX) of AgNPs.

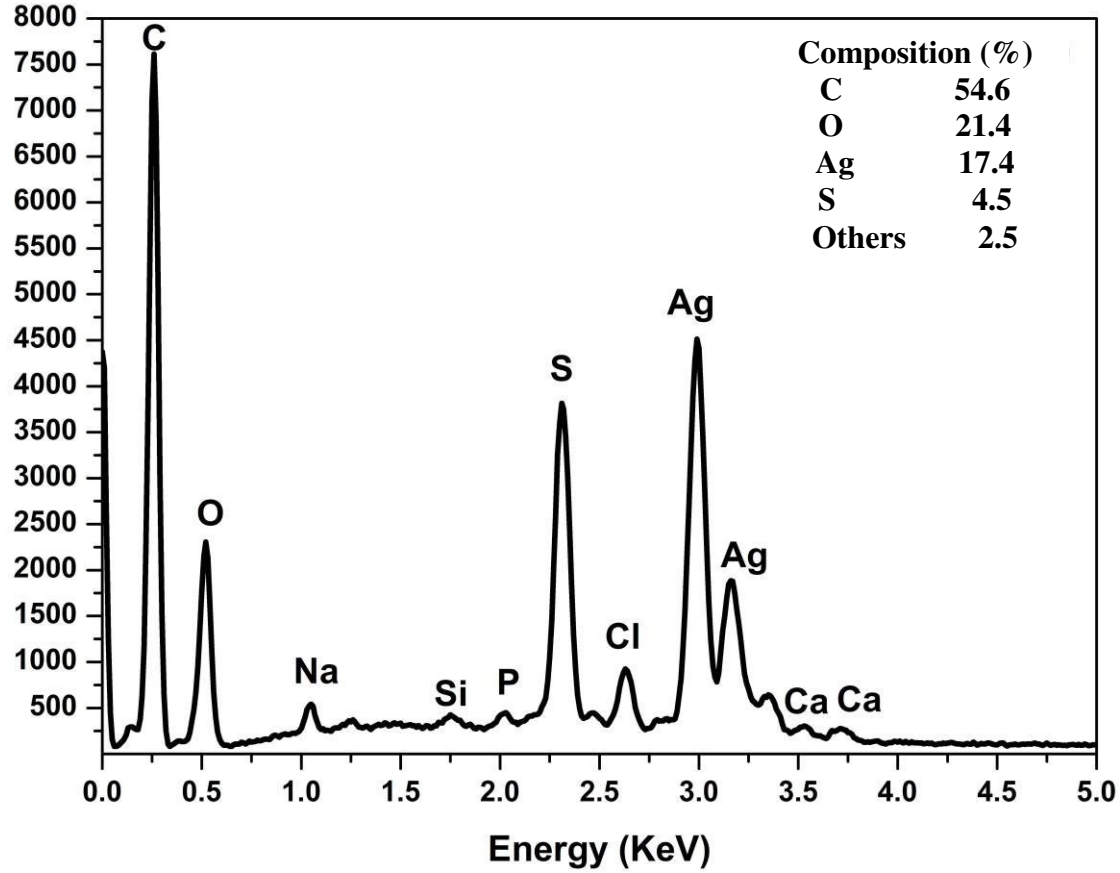

Source: Author

FIGURE S6- Summary of Effects of AgNPs on Bacteria.

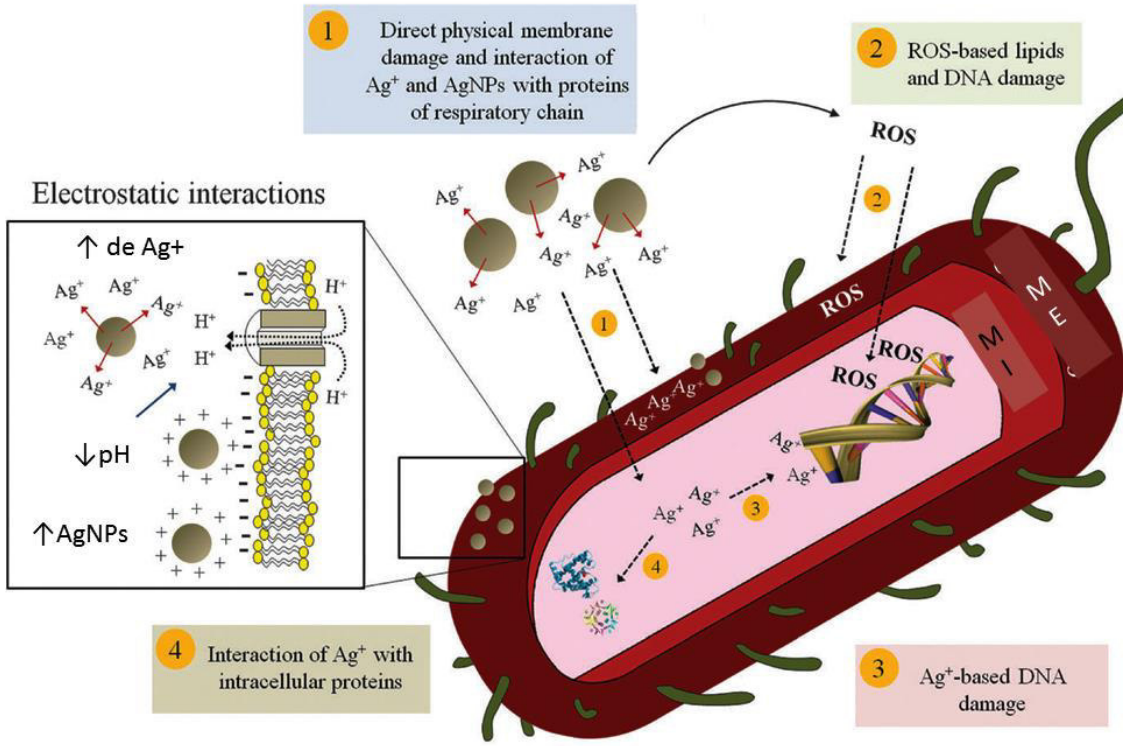

Source: Rizzello e Pompa 2014.

Supporting Information CHAPTER THREE

FIGURE S1- Amphotericin B

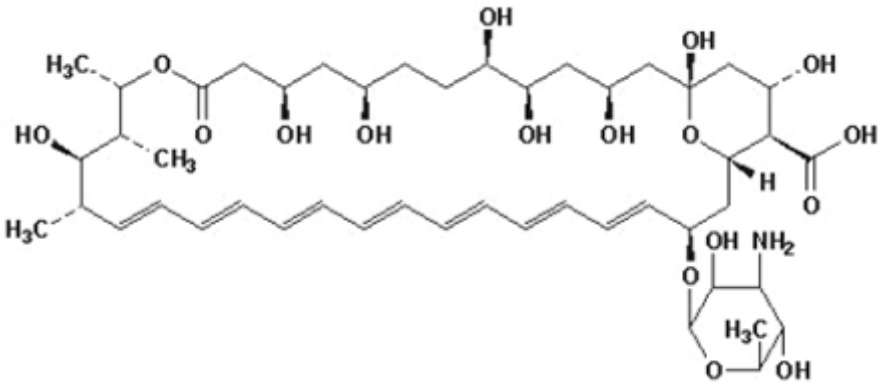

Source: https://en.wikipedia.org/wiki/Amphotericin_B. Acesso: 22 ago. 2015

FIGURE S2- Nystatin

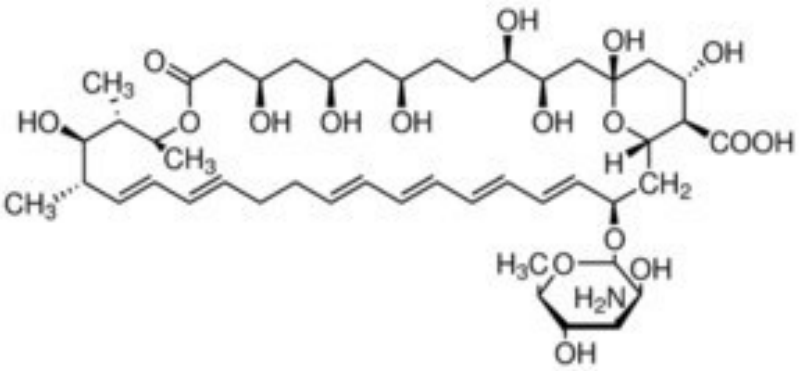

Source: https://en.wikipedia.org/wiki/Nystatin . Acesso: 22 ago. 2015

FIGURE S3- Summary of protocol Silver Nanoparticles.

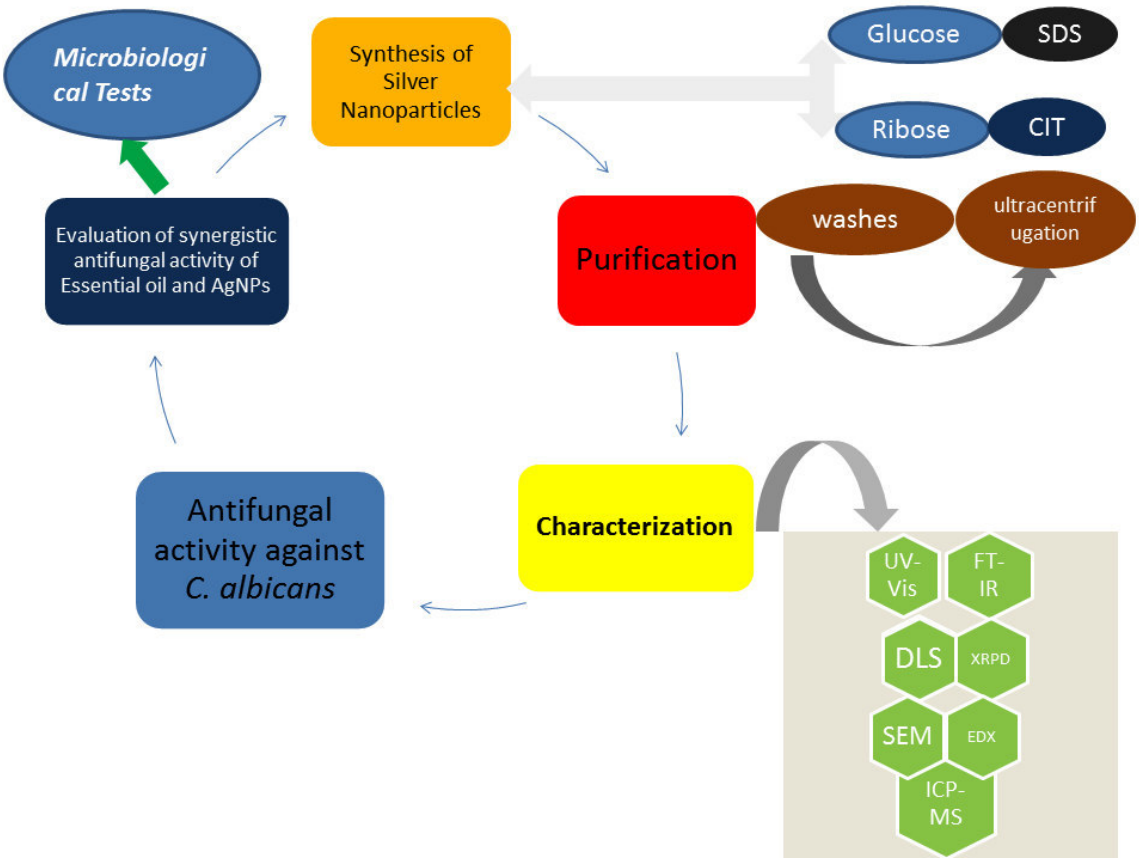

Source: Author

Supporting Information CHAPTER FOUR

FIGURE S1- Protocol of collect fungi.

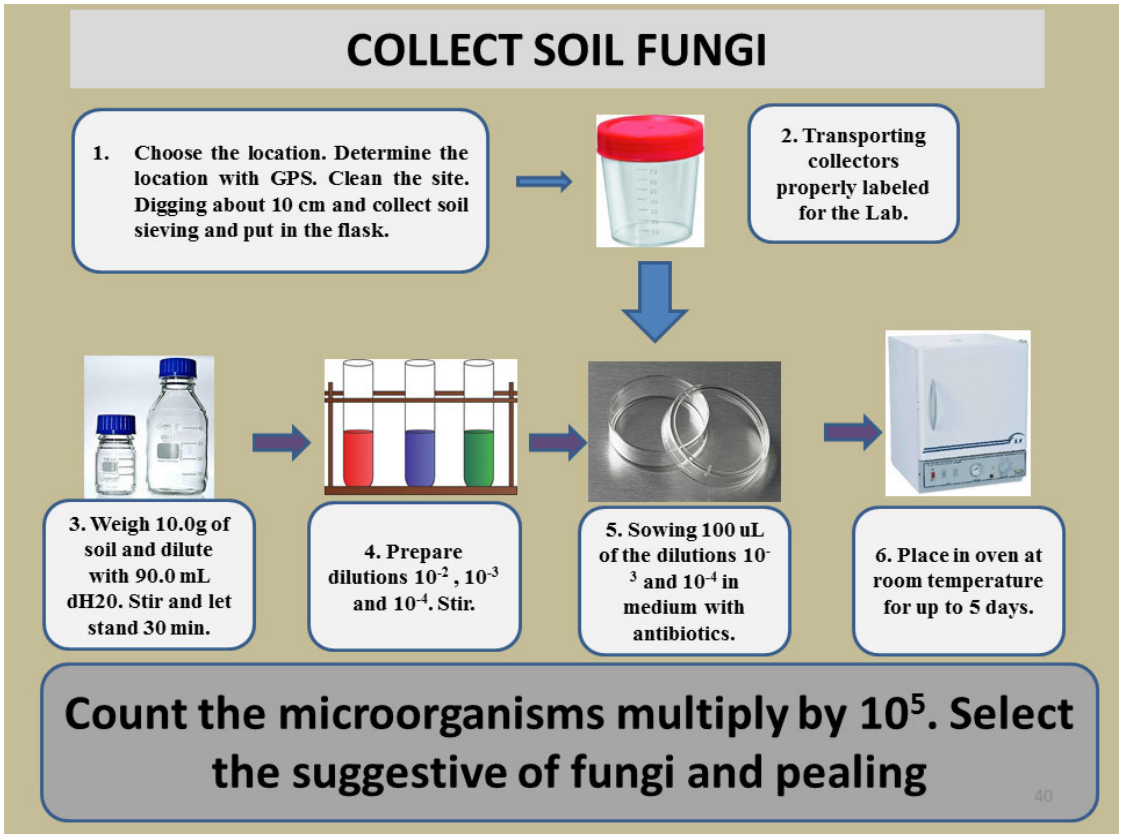

Source: Author

FIGURE S2- Protocol of Biosynthesis of AgNPs.

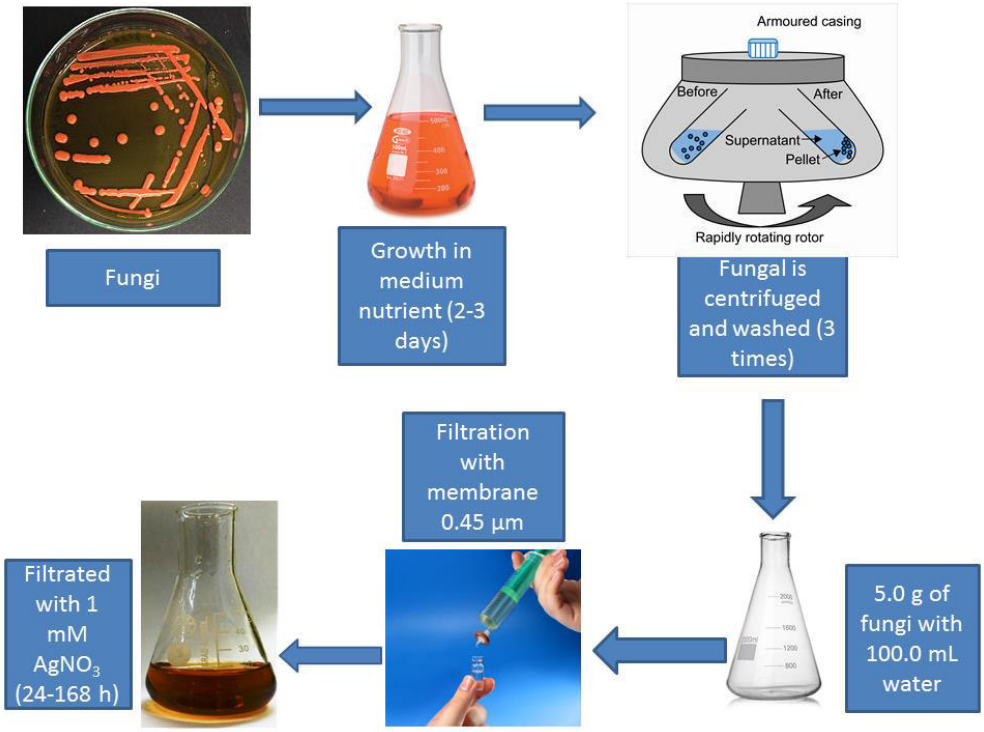

Source: Author

FIGURE S3- Dynamic Light Scattering.

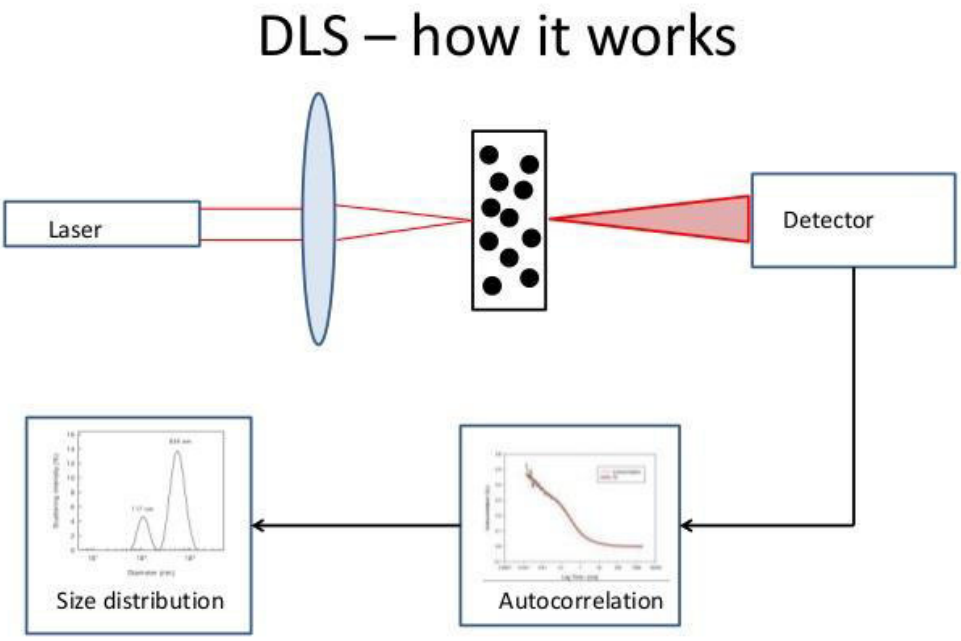

Source: http://www.slideshare.net/EdwardMansfield1/dynamic-light-scattering-48645581

FIGURE S4- *Candida parapsilosis* on Potato-glucose ágar.

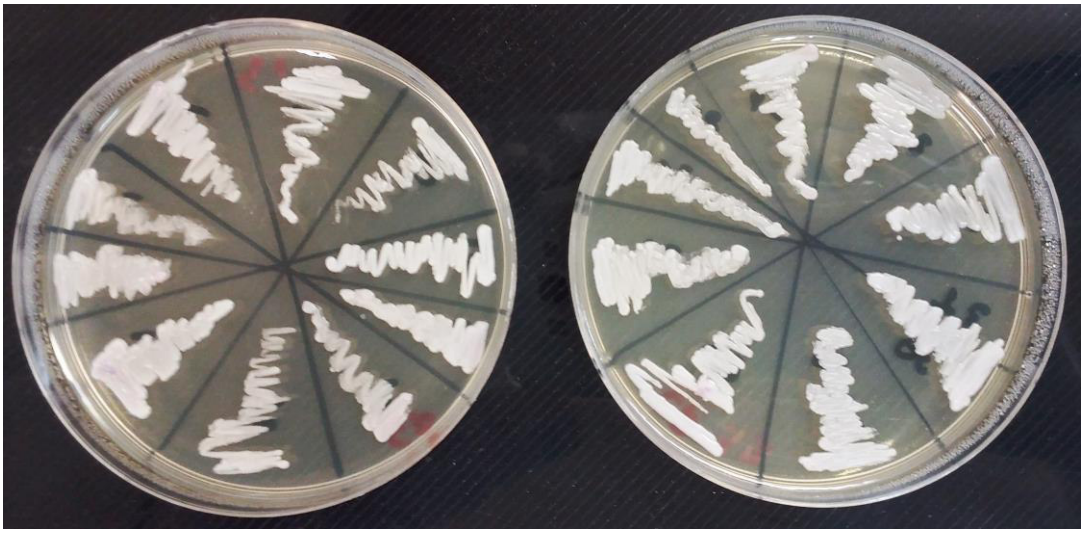

Source: Author

FIGURE S5- *Candida parapsilosis* on Chromoagar.

Source: Author

FIGURE S6- *Candida sp* (*C. tropicalis*- blue; *C. parapsilosis*- rose) on Chromoagar.

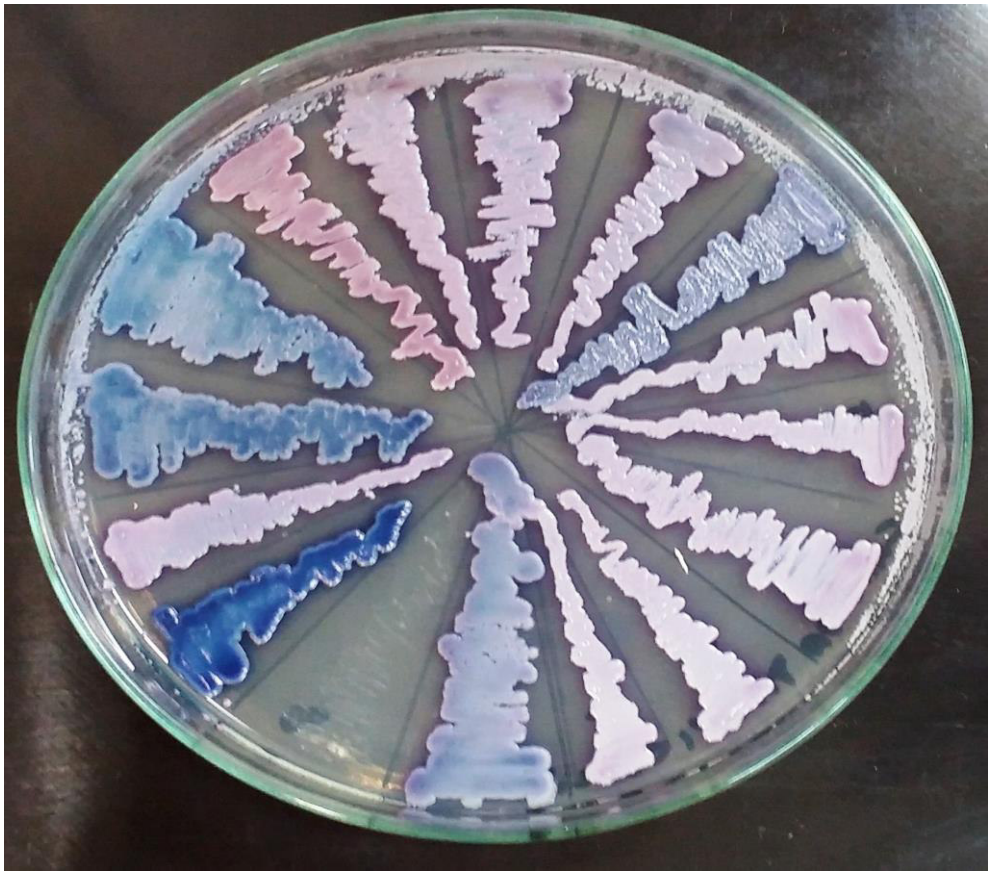

Source: Author

FIGURE S7- Broth Method Microdilution.

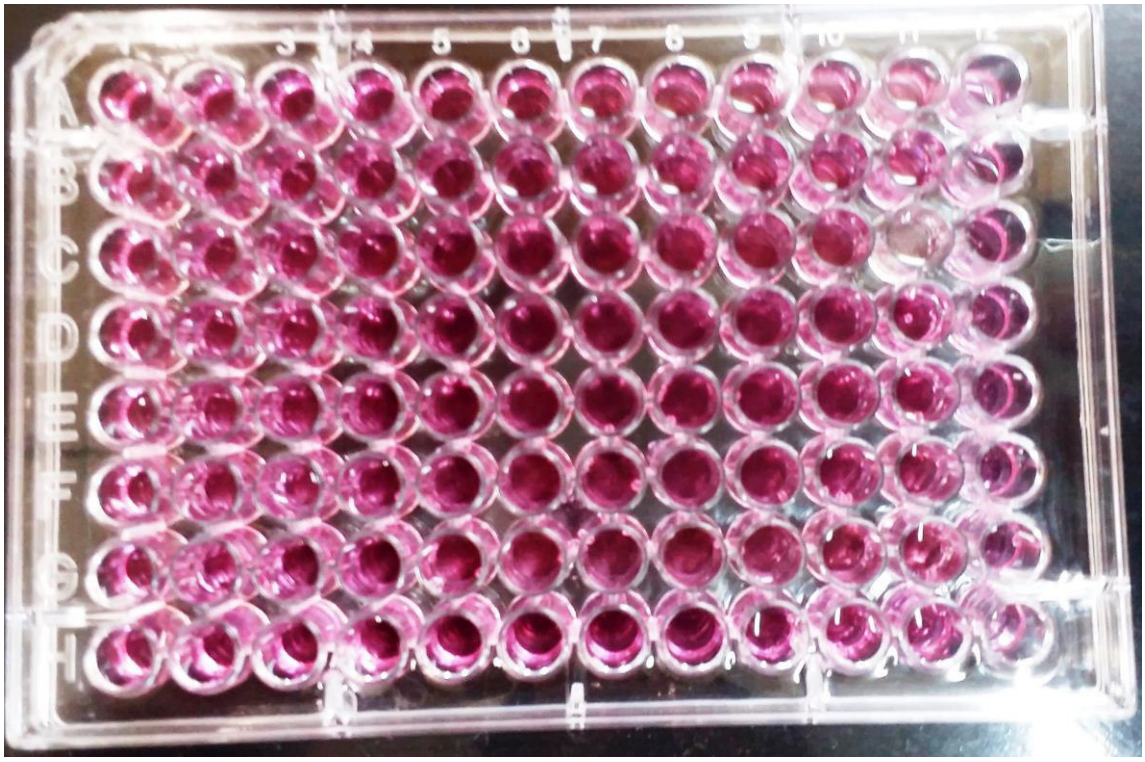

Source: Author

FIGURE S8- Tyndall effect: (a) $AgNO_3$; (b) AgNPs produced from Rg; and (c) AgNPs produced from Rm.

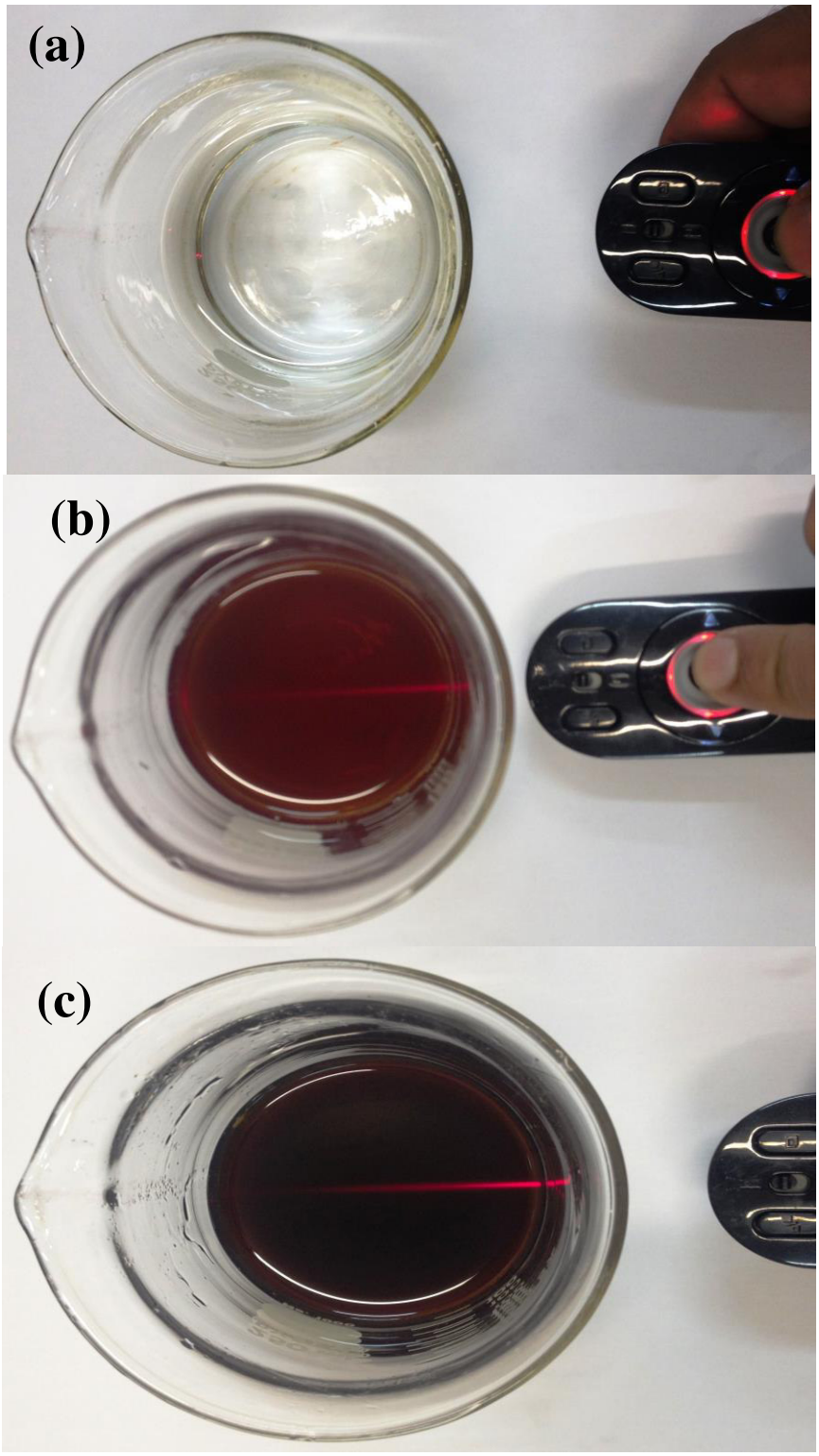

Source: Author

FIGURE S9- AgNPs aspects 15 months after, (a) AgNPs produced by Rg and (b) Rm.

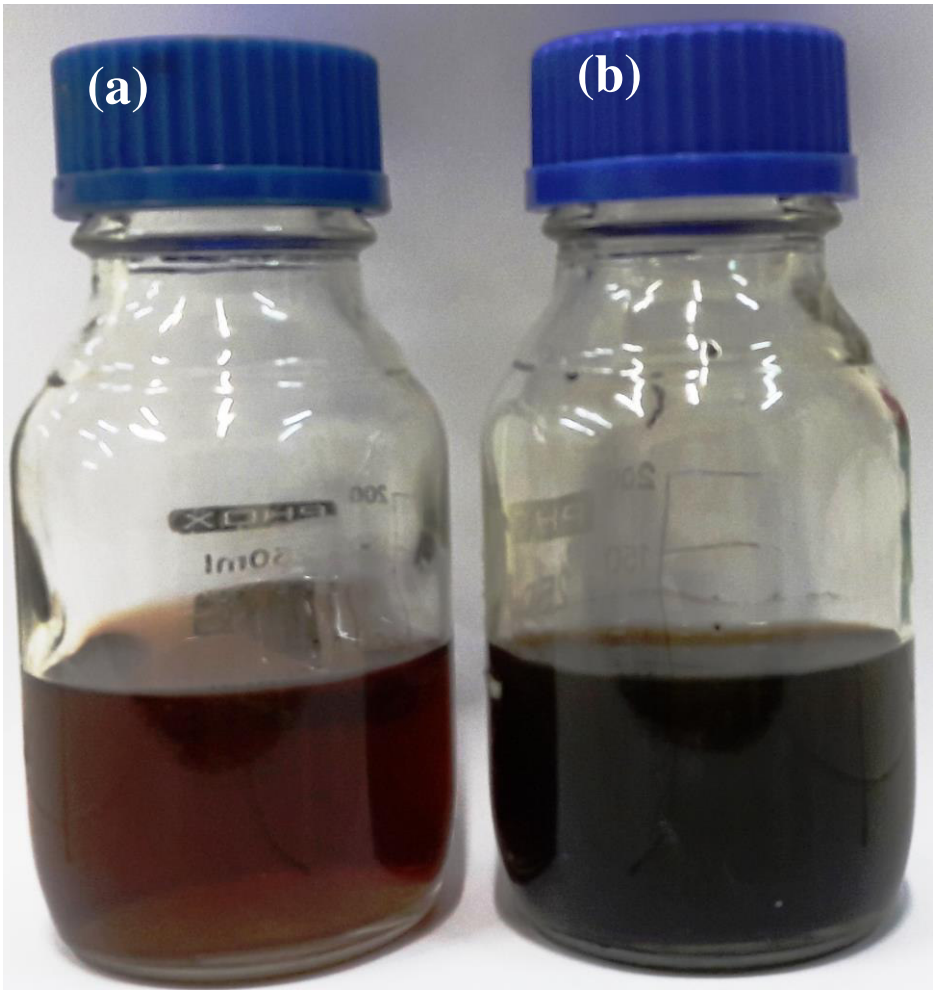

Source: Author

FIGURE S10- TEM of AgNPs produced by *R. glutinis*.

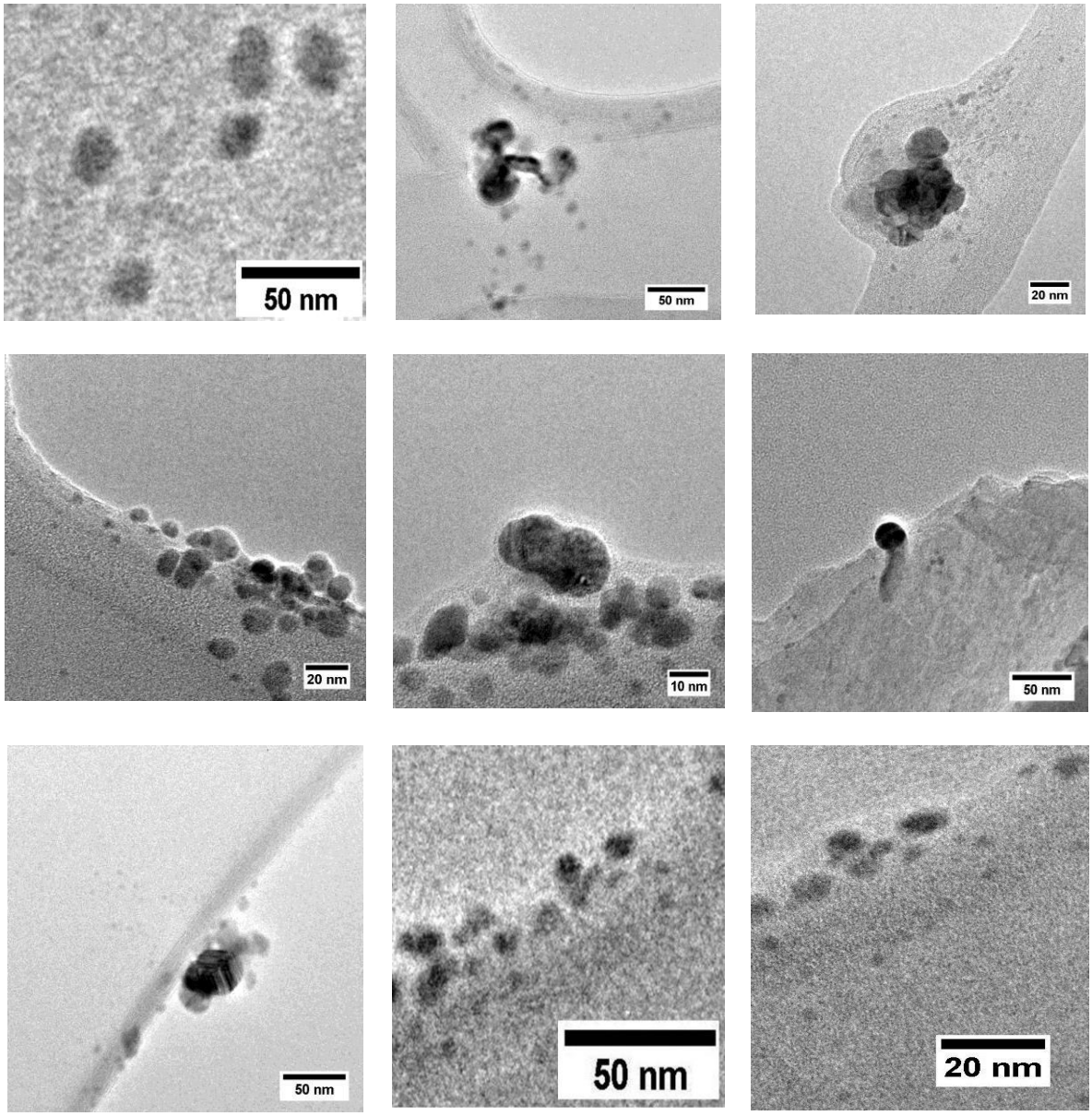

Source: Author

FIGURE S11- TEM of AgNPs produced by *R. mucilaginosa.*

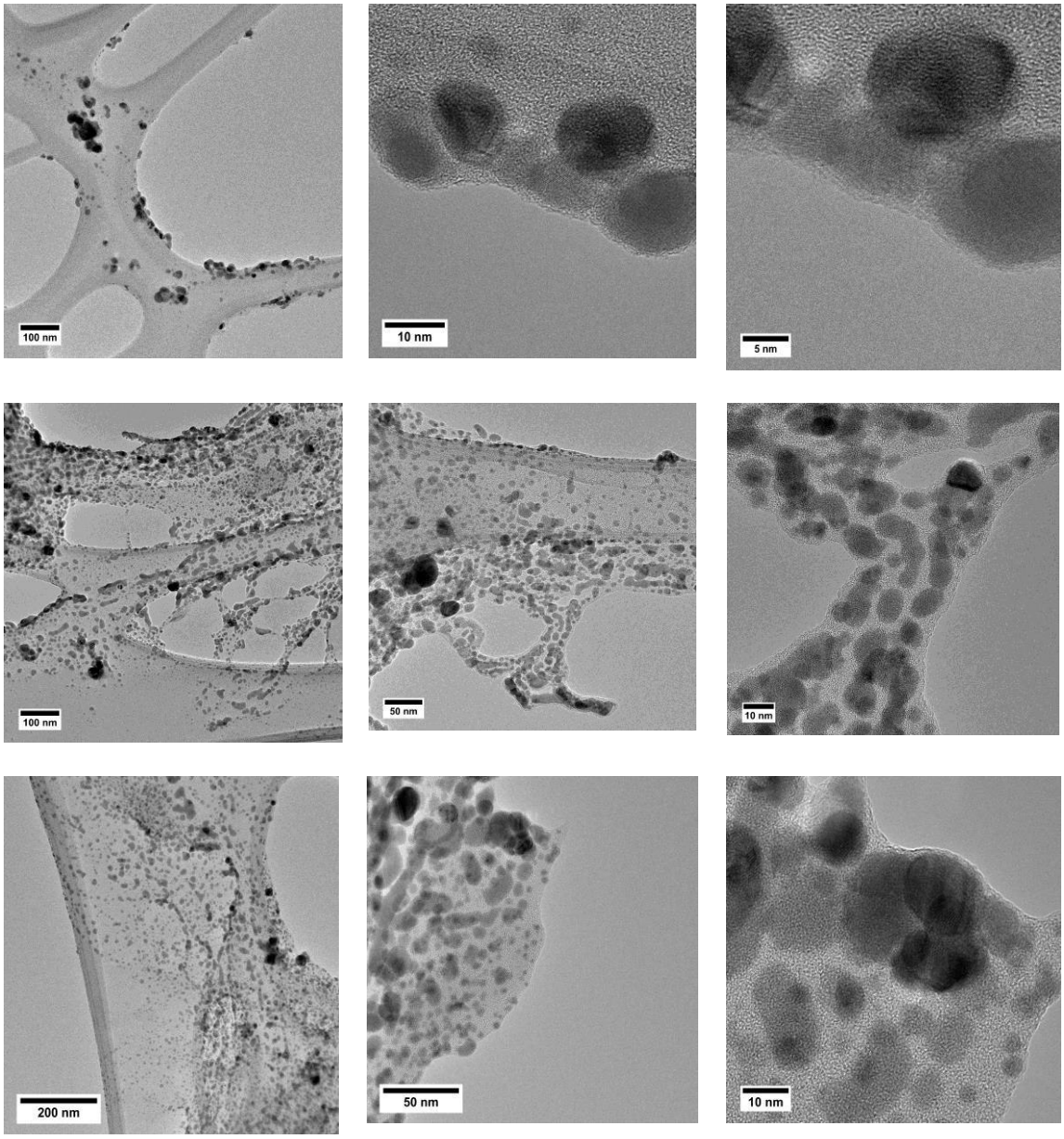

Source: Author

FIGURE S12: AFM of AgNPs produced by *R. glutinis*.

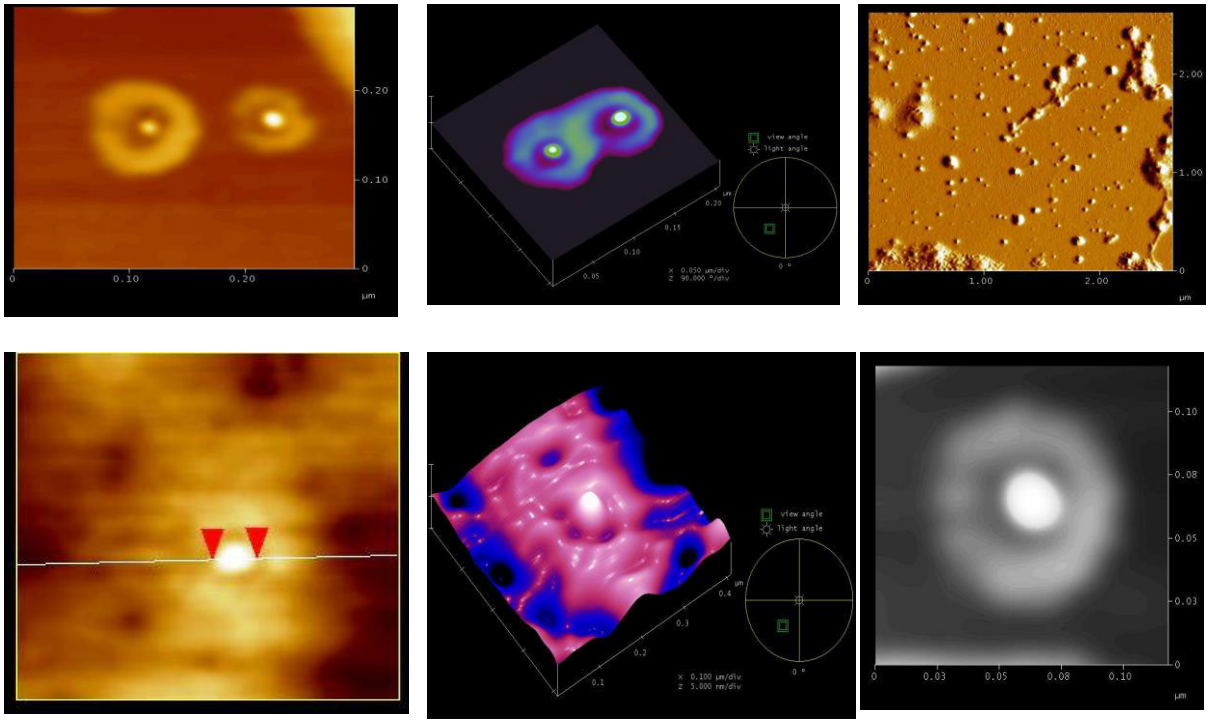

Source: Author

FIGURE S13: AFM of AgNPs produced by *R. mucilaginosa.*

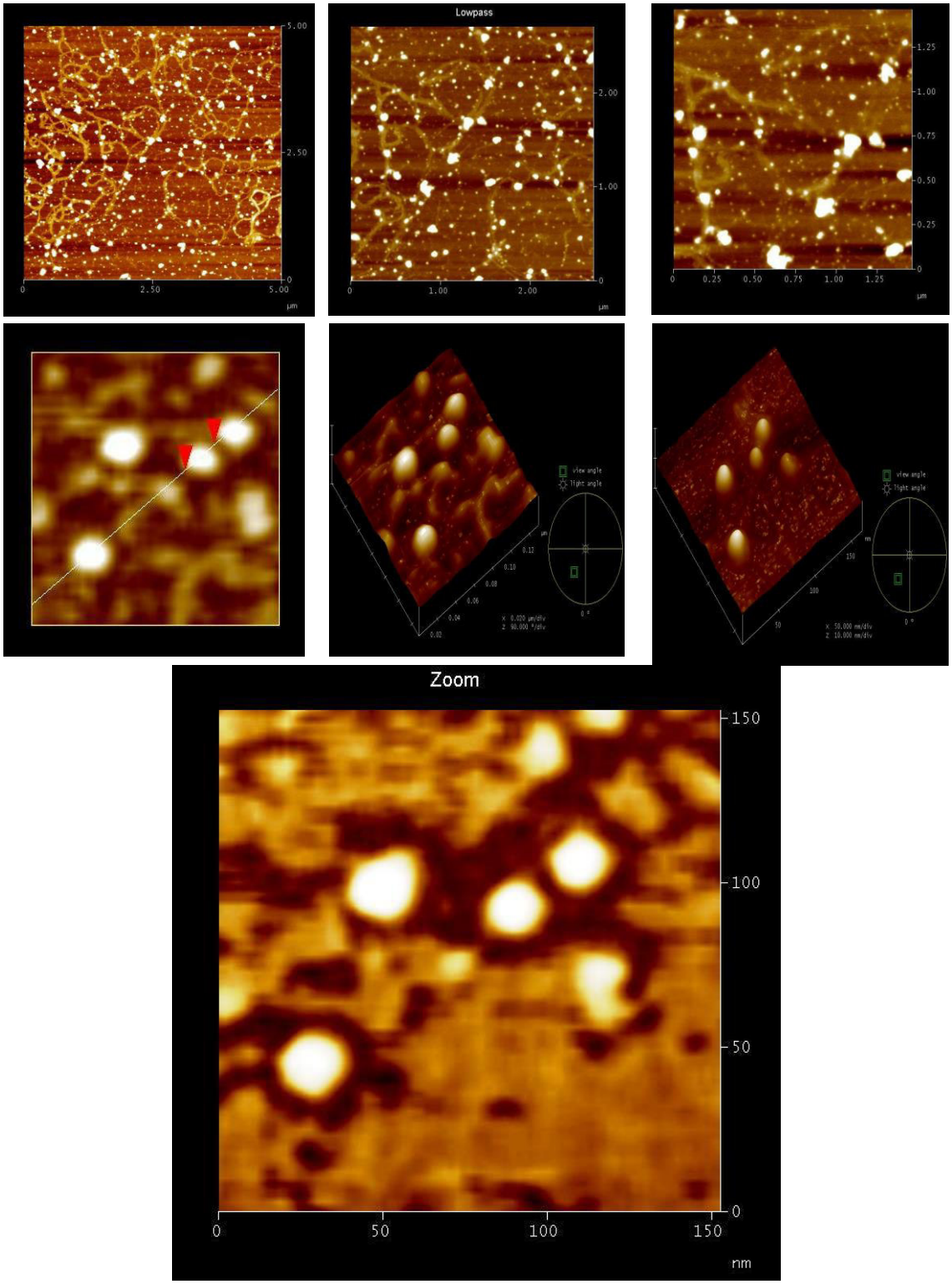

Source: Author

FIGURE S14- Langmuir-Hinshelwood model of heterogeneous catalysis of AgNPs.

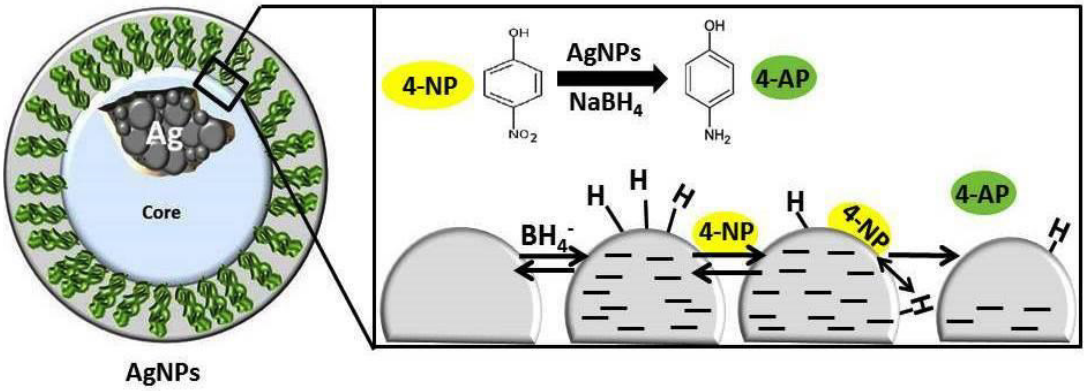

Source: Author

Supporting Information CHAPTER FIVE

FIGURE S1. Protocol of production of alginate's spheres inlead with AgNPs.

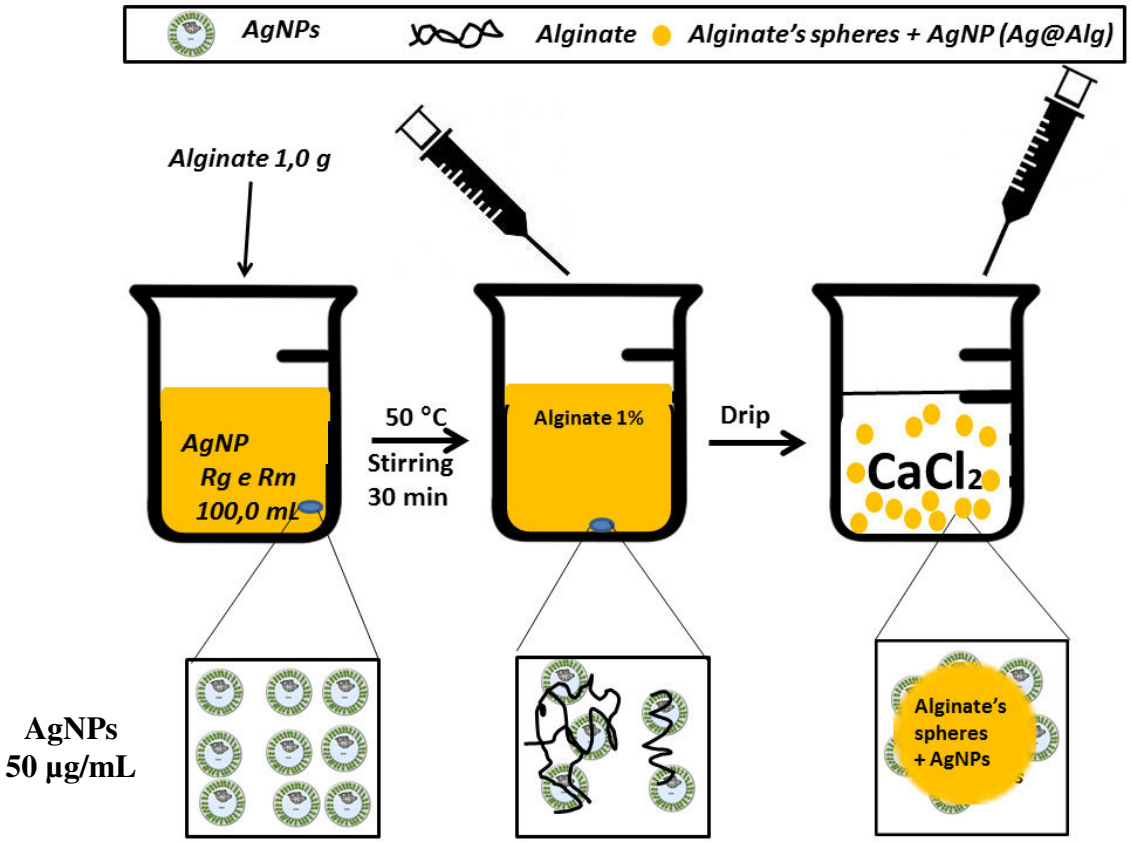

Source: Author

FIGURE S2. Reduction's 4-NP by Ag@Alg Rg and Ag@Alg Rm.

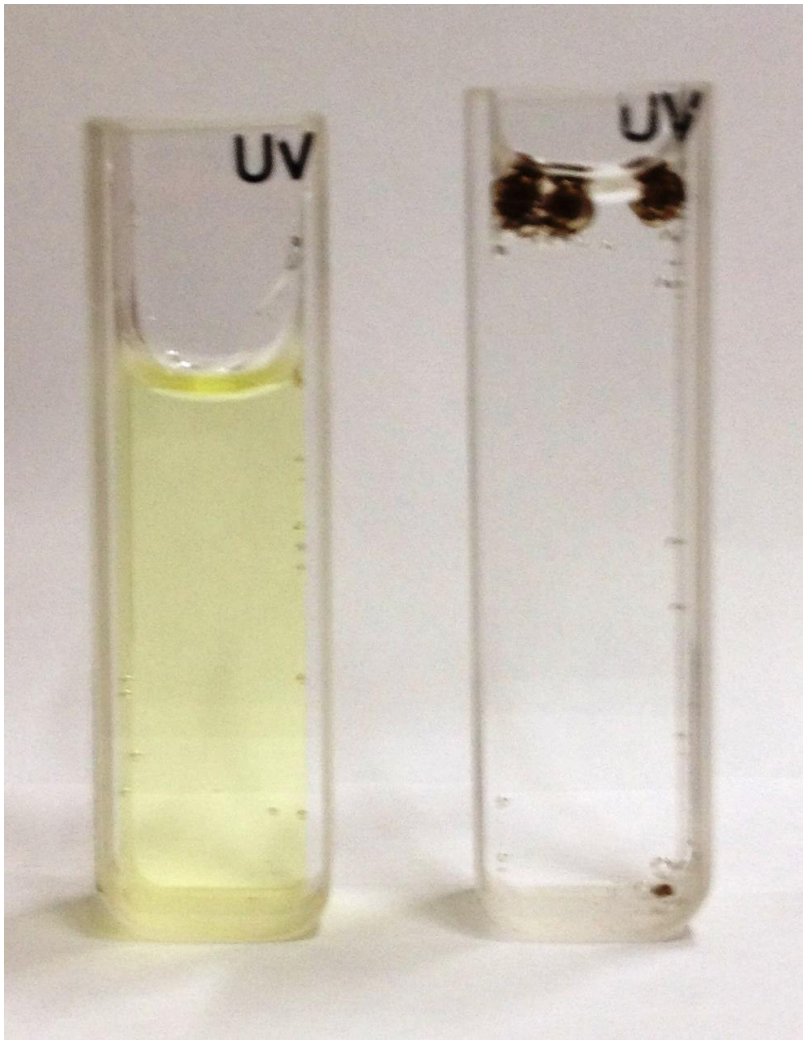

Source: Author

FIGURE S3. Ceftazidime.

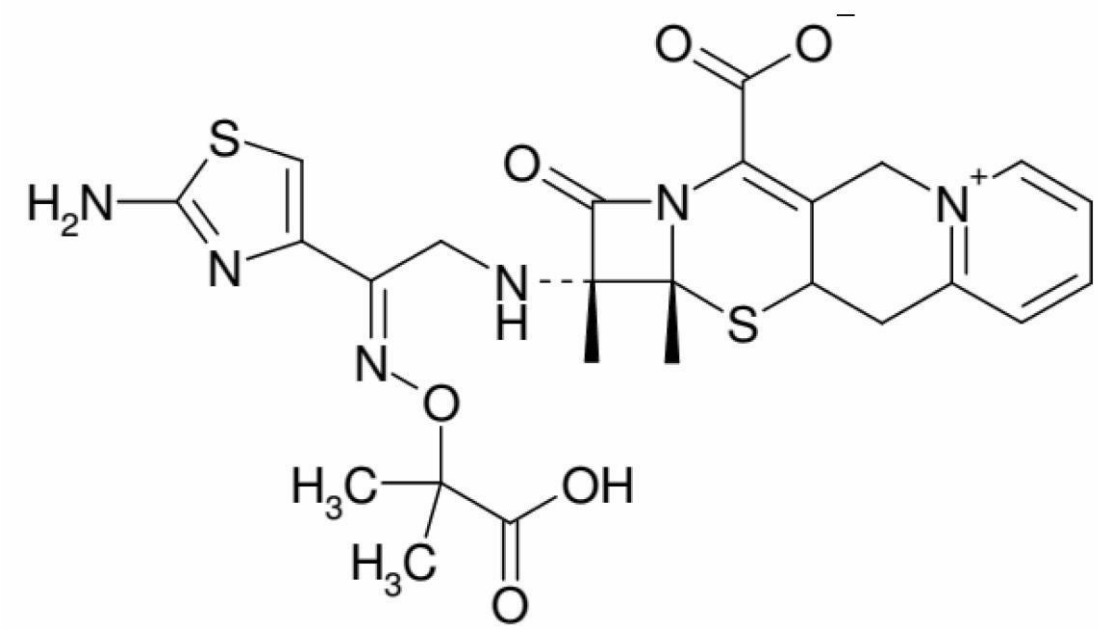

Nomenclature (IUPAC): (6R,7R,Z)-7-(2-(2-aminotiazol-4-yl)-2-(2-carboxipropano-2-iloximino) acetamido)-8-oxo-3-(piridinio-1-ilmetil)-5-tia-1-aza-biciclo[4.2.0]oct-2-ene-2-carboxilato. Molecular Formula: $C_{22}H_{22}N_6O_7S_2$ CAS: 72558-82-8. Molecular weight: 546,58 g/mol

Source: https://commons.wikimedia.org/wiki/File:Ceftazidime.png

FIGURE S4. UV-Vis of Ceftazidime.

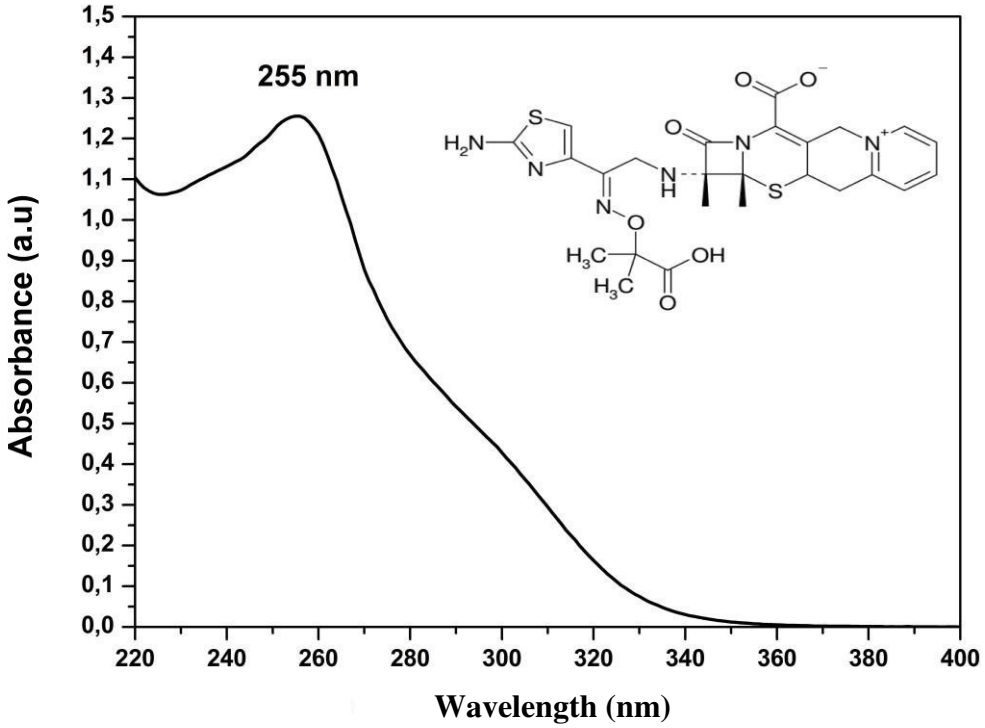

Source: Author

FIGURE S5. FTIR of Ceftazidime.

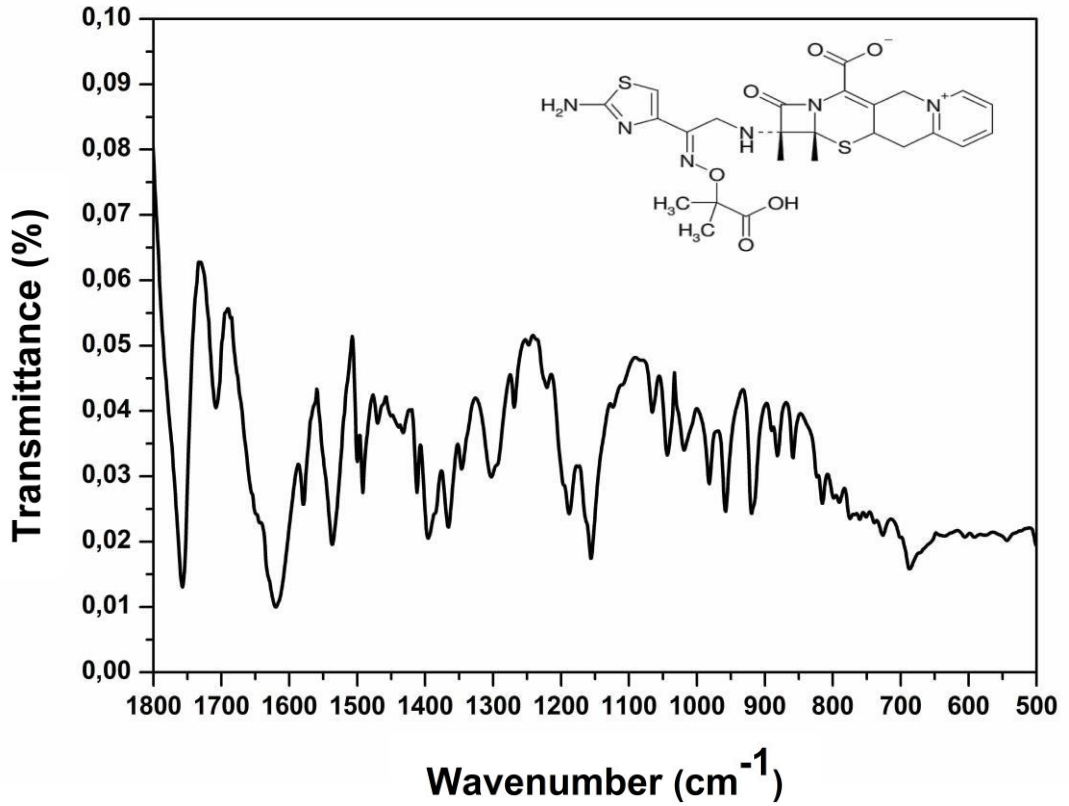

FIGURE S6. Size of spheres.

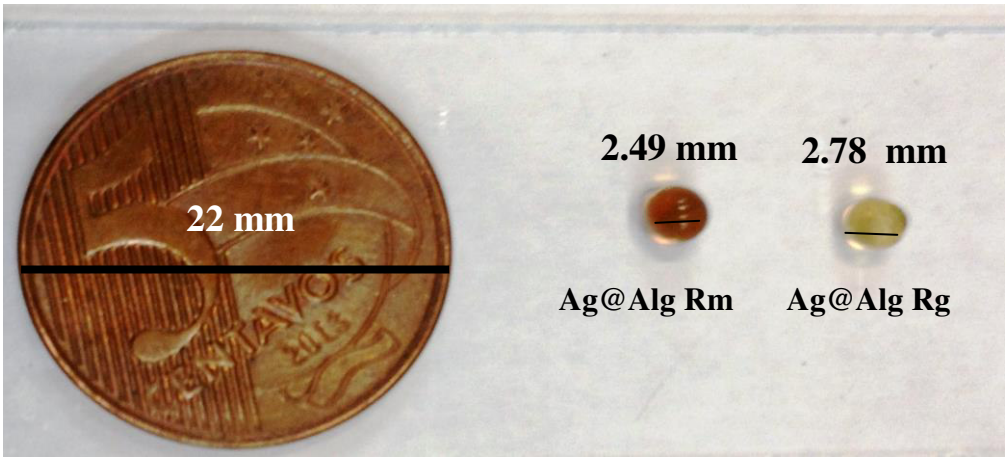

Source: Author

FIGURE S7. Wet Spheres *in natura*. Ag@Alg Rg (a) and Ag@Alg Rm.

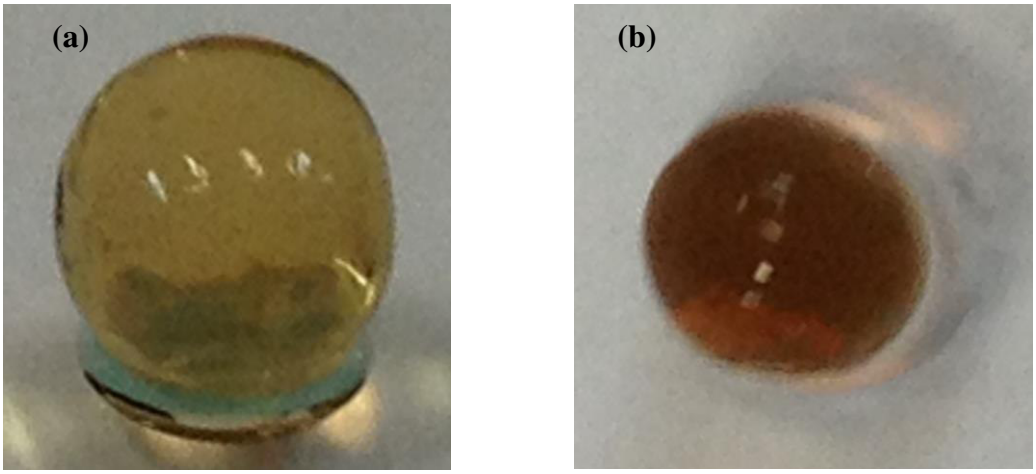

Source: Author

FIGURE S8. Details of the spheres surface by SEM. Ag@Alg Rg (a) and Ag@Alg Rm.

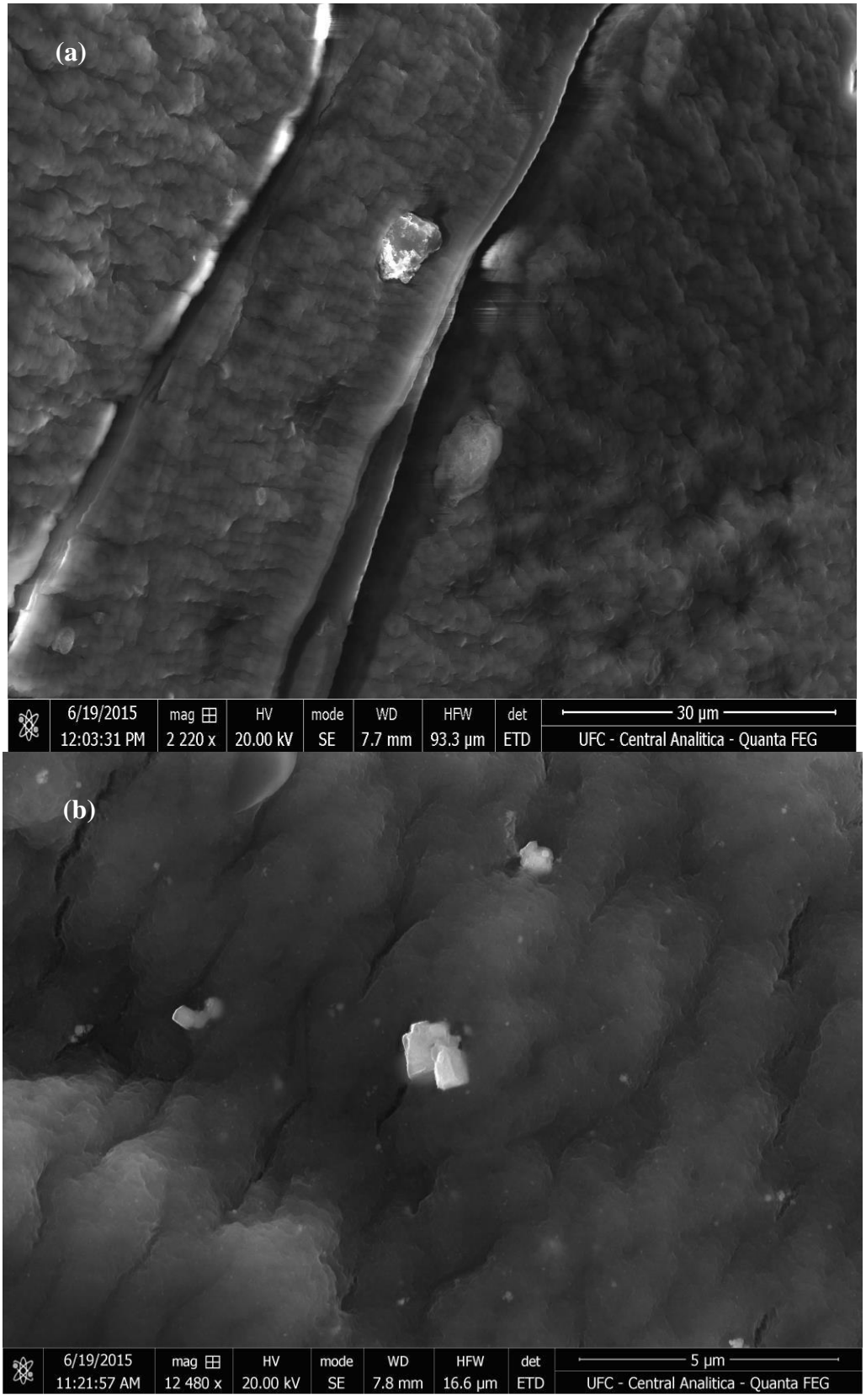

Source: Author

FIGURE S9. Microanalysis: alginate beads map of with AgNPs embedded *R. mucilaginosa.*

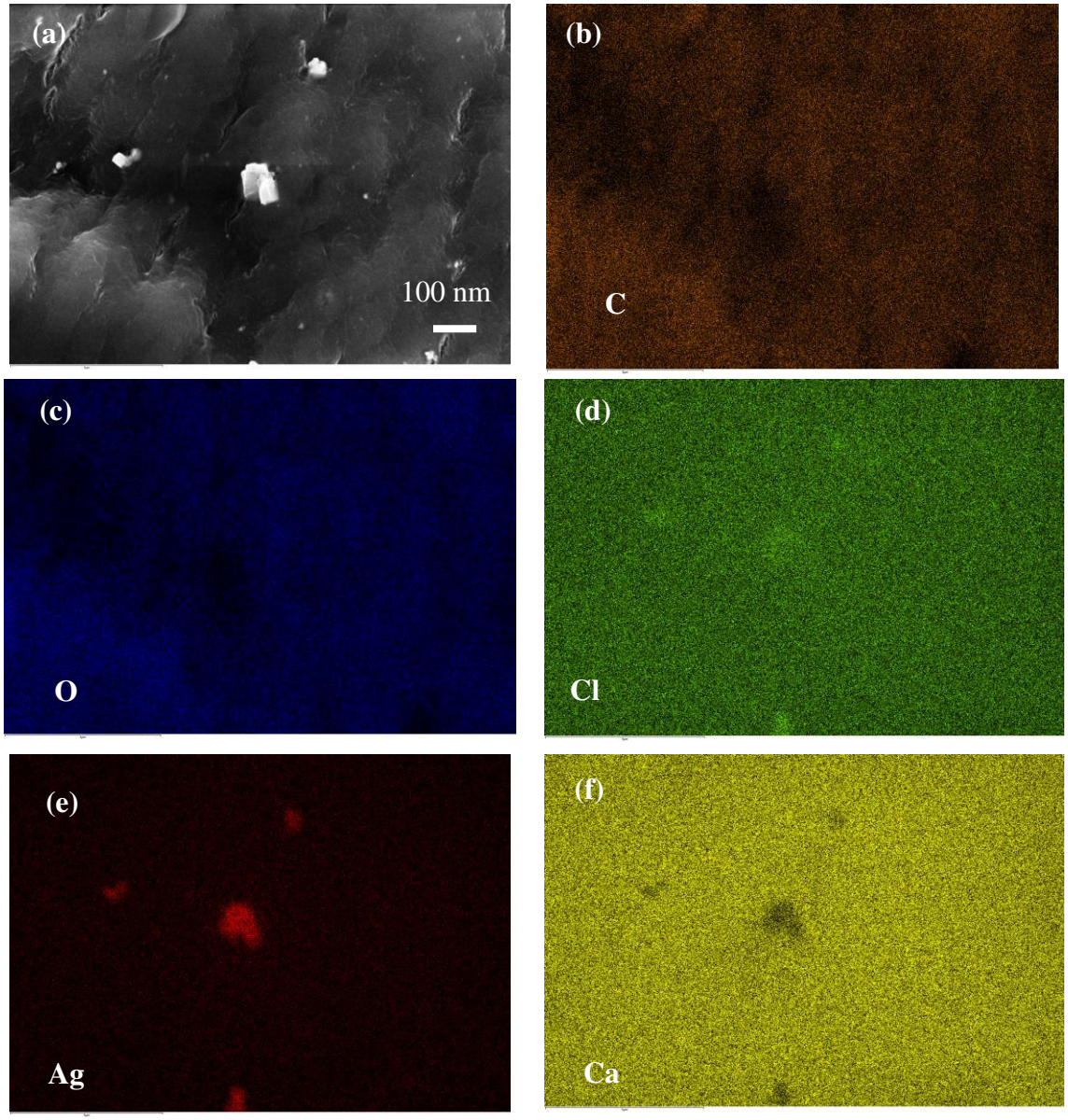

Source: Author